

## LA SALLE COUNTY POWER STATION

INSTRUCTIONS FOR UPDATING YOUR MARK II DAR

To update your copy of the LSCS-MARK II DAR, remove and destroy the following pages and figures and insert pages and figures as indicated.

REMOVECONTENTS

Pages i to xii

Chapter 1.0

All existing pages and figures

Chapter 2.0

All existing pages and figures

Chapter 3.0

All existing pages and figures

Chapter 4.0

All existing pages and figures

Chapter 5.0INSERT

POOR ORIGINAL

Pages i to xi

New Chapter 1.0, including pages 1.0-1 through 1.0-8 and 1.1-1 through 1.1-4, and Figures 1.1-1 through 1.1-4

New Chapter 2.0, including pages 2.0-1 through 2.0-3 and 2.1-1 through 2.1-4

New Chapter 3.0, including pages 3.0-1 through 3.0-4, 3.1-1 through 3.1-6, 3.2-1 through 3.2-21, Figures 3.2-1 through 3.2-5, pages 3.3-1 through 3.3-31, Figures 3.3-1 through 3.3-22, and pages 3.4-1 through 3.4-8

New Chapter 4.0, including pages 4.1-1 through 4.1-4, 4.2-1, 4.3-1 through 4.3-4, 4.4-1 through 4.4-8, Figures 4.4-1 (18 sheets) and 4.4-2 (3 sheets), and pages 4.5-1 through 4.5-4

Tab for "Chapter 5.0". New Chapter 5.0, including pages 5.1-1 through 5.1-25, Figures

REMOVEChapter 5.0 (Cont'd)Chapter 6.0Chapter 7.0Chapter 8.0Chapter 9.0Appendix A

All existing pages  
and figures

Appendix B

Appendix B remains as  
already printed except  
for the following  
deletions and insertions:

INSERT

5.1-1 through 5.1-18;  
pages 5.2-1 through 5.2-6,  
Figures 5.2-1 through 5.2-3;  
pages 5.3-1 through 5.3-12,  
Figures 5.3-1 through 5.3-4;  
page 5.4-1; and pages 5.5-1  
and 5.5-2.

Tab for "Chapter 6.0." New  
Chapter 6.0, including pages  
6.1-1 through 6.1-5; and  
pages 6.2-1 through 6.2-17 and  
Figures 6.2-1 through 6.2-8

Tab for "Chapter 7.0." New  
Chapter 7.0, including pages  
7.1-1, 7.1-2, and 7.1-3; pages  
7.2-1 through 7.2-4; page 7.3-1;  
and pages 7.4-1 and 7.4-2

Tab for "Chapter 8.0." New  
Chapter 8.0, including pages  
8.1-1 through 8.1-5; and  
pages 8.2-1 and 8.2-2

Tab for "Chapter 9.0." New  
Chapter 9.0, including pages  
9.0-1 and 9.0-2

Pages A-1 through A-7

POOR ORIGINAL

REMOVE

INSERT

Appendix B (Cont'd)

Page B.0-1  
Pages B.2-51 and B.2-52

Page B.0-1  
Pages B.2-51 and B.2-52

Appendix C

All existing pages and figures

New Appendix C, including pages C-1 through C-40 and Figures C-1 through C-15

Appendix D

All existing pages and figures

New Appendix D, including pages D-1 and D-2

Appendix E, F, and G

After new page D-2

Tab "Appendix E," pages E-1 through E-6, Figure E-1, Tab "Appendix F," pages F-1 through F-4, Tab "Appendix G," and pages G-1 and G-2

POOR ORIGINAL

TABLE OF CONTENTS

	<u>PAGE</u>
1.0 <u>INTRODUCTION</u>	1.0-1
1.1 <u>GENERAL DESCRIPTION OF PLANT</u>	1.1-1
2.0 <u>MARK II POOL DYNAMICS HISTORY</u>	2.0-1
2.1 <u>SUMMARY OF DESIGN ASSESSMENT</u>	2.1-1
3.0 <u>LOADS CONSIDERED</u>	3.0-1
3.1 <u>ORIGINAL DESIGN LOADS</u>	3.1-1
3.1.1 Loads on the Structure	3.1-1
3.1.2 Loads on Piping and Equipment	3.1-4
3.2 <u>SAFETY/RELIEF VALVE (SRV) LOADS</u>	3.2-1
3.2.1 Design-Basis SRV Loads - Rams Heads	3.2-3
3.2.1.1 Conservatism in SRV Rams Head Methods	3.2-4
3.2.1.2 Safety/Relief Valve Discharge Cases	3.2-8
3.2.1.2.1 Single Valve Actuation	3.2-8
3.2.1.2.2 Asymmetric SRV Actuation	3.2-9
3.2.1.2.3 Automatic Depressurization System (ADS)	3.2-9
3.2.1.2.4 All Valve Discharge Cases	3.2-10
3.2.1.2.5 Second Actuation	3.2-13
3.2.1.3 Safety/Relief Valve Boundary Loads	3.2-14
3.2.1.4 Submerged Structure Loads	3.2-15
3.2.2 Assessment for SRV Loads - T-Quencher	3.2-15
3.2.2.1 Conservatism of the T-Quencher Load Definition	3.2-15
3.2.2.2 SRV Quencher Discharge Cases	3.2-16
3.2.2.2.1 Single Valve	3.2-16
3.2.2.2.2 Asymmetric SRV Load	3.2-16
3.2.2.2.3 Automatic Depressurization System (ADS)	3.2-16
3.2.2.2.4 All Valve Discharge	3.2-17
3.2.2.3 Quencher Boundary Loads	3.2-17
3.2.2.4 Quencher Submerged Structure Loads	3.2-17
3.2.3 Assessment of NRC Acceptance Criteria - SRV	3.2-17
3.3 <u>LOSS-OF-COOLANT ACCIDENT (LOCA) LOADS</u>	3.3-1
3.3.1 Design-Basis LOCA Loads	3.3-4
3.3.1.1 Load Definitions	3.3-4
3.3.1.1.1 LOCA Water Jet Loads	3.3-4
3.3.1.1.2 LOCA Charging Air Bubble Load	3.3-4
3.3.1.1.3 Pool Swell	3.3-5
3.3.1.1.4 Pool Fallback	3.3-5
3.3.1.1.5 Condensation Oscillation	3.3-5
3.3.1.1.6 Chugging	3.3-6
3.3.1.1.7 Lateral Loads on Downcomers	3.3-8
3.3.1.2 LOCA Boundary Loads	3.3-11

TABLE OF CONTENTS (Cont'd)

	<u>PAGE</u>
3.3.1.2.1 LOCA Water Jet	3.3-11
3.3.1.2.2 Charging Air Bubble	3.3-11
3.3.1.2.3 Pool Swell	3.3-11
3.3.1.2.4 Pool Fallback	3.3-12
3.3.1.2.5 Condensation Oscillation	3.3-12
3.3.1.2.6 Chugging	3.3-12
3.3.1.3 LOCA Submerged Structure Loads	3.3-12
3.3.1.3.1 LOCA Water Jet	3.3-13
3.3.1.3.2 Charging Air Bubble	3.3-13
3.3.1.3.3 Pool Swell	3.3-13
3.3.1.3.3.1 Pool Swell Impact Loads	3.3-14
3.3.1.3.3.2 Pool Swell Drag Loads	3.3-16
3.3.1.3.4 Pool Fallback	3.3-16
3.3.1.3.5 Condensation Oscillation Drag Loads	3.3-16
3.3.1.3.6 Chugging Drag Loads	3.3-18
3.3.1.4 Annulus Pressurization Loads	3.3-20
3.3.2 Assessment of NRC Acceptance Criteria - LOCA	3.3-25
3.3.2.1 LOCA Water Jet Loads	3.3-26
3.3.2.2 Pool Swell	3.3-28
3.3.2.2.1 Pool Swell Velocity	3.3-28
3.3.2.2.2 Pool Swell Impact	3.3-28
3.3.2.3 Drag Load Calculations	3.3-29
3.3.2.4 Chugging Lateral Loads	3.3-29
3.3.3 References	3.3-31
3.4 <u>LSCS POSITION ON NUREG-0478 LEAD PLANT ACCEPTANCE CRITERIA</u>	3.4-1
4.0 <u>LOAD COMBINATIONS CONSIDERED</u>	4.1-1
4.1 <u>CONTAINMENT AND INTERNAL CONCRETE STRUCTURES</u>	4.1-1
4.2 <u>CONTAINMENT LINER</u>	4.2-1
4.3 <u>OTHER STRUCTURAL COMPONENTS</u>	4.3-1
4.3.1 Concrete Structures	4.3-1
4.3.2 Steel Structures	4.3-1
4.4 <u>BALANCE-OF-PLANT PIPING AND EQUIPMENT</u>	4.4-1
4.4.1 Wetwell Piping	4.4-1
4.4.2 Non-Wetwell Piping	4.4-1
4.4.2.1 Load Combination and Acceptance Criteria	4.4-1
4.4.2.2 Evaluation of Bounded Load Combination - Rams Head Definition	4.4-2
4.4.2.3 Justification of Alternative Acceptance Criteria	4.4-2
4.4.2.4 Summary	4.4-3
4.4.3 Equipment	4.4-3

TABLE OF CONTENTS (Cont'd)

	<u>PAGE</u>
4.5 <u>NSSS PIPING AND EQUIPMENT</u>	4.5-1
4.5.1 Loading Combinations and Acceptance Criteria	4.5-1
4.5.2 References	4.5-2
5.0 <u>REEVALUATION AND DESIGN ASSESSMENTS</u>	5.1-1
5.1 <u>CONTAINMENT AND INTERNAL CONCRETE STRUCTURES</u>	5.1-1
5.1.1 Structural Analysis for SRV Loads	5.1-1
5.1.2 Structural Analysis for LOCA Loads	5.1-3
5.1.2.1 Vent Clearing Analysis	5.1-3
5.1.2.2 Pool Swell Analysis	5.1-3
5.1.2.3 Condensation Oscillation Analysis	5.1-4
5.1.2.4 Chugging Analysis	5.1-5
5.1.2.5 ECCS Reflood Analysis	5.1-6
5.1.3 Downcomer Effects on the Drywell Floor	5.1-7
5.1.4 Design Assessment Margin Factors	5.1-10
5.1.4.1 Critical Design Sections	5.1-10
5.1.4.2 Design Forces and Margin Factors	5.1-11
5.1.5 References	5.1-12
5.2 <u>CONTAINMENT WALL AND BASEMAT LINER ANALYSIS</u>	5.2-1
5.2.1 Basemat Liner	5.2-1
5.2.1.1 Description of Liner and Liner Stiffeners	5.2-1
5.2.1.2 Loads for Analysis	5.2-1
5.2.1.3 Load Combinations	5.2-2
5.2.1.4 Acceptance Criteria	5.2-2
5.2.1.5 Analysis	5.2-3
5.2.2 Containment Wall Liner	5.2-3
5.2.2.1 Description of Liner	5.2-3
5.2.2.2 Loads for Analysis	5.2-4
5.2.2.3 Load Combinations	5.2-4
5.2.2.4 Acceptance Criteria	5.2-4
5.2.2.5 Analysis	5.2-4
5.3 <u>OTHER STRUCTURAL COMPONENTS</u>	5.3-1
5.3.1 Concrete Structures	5.3-1
5.3.1.1 Acceptance Criteria	5.3-1
5.3.2 Steel Structures	5.3-2
5.3.2.1 Acceptance Criteria	5.3-2
5.3.3 Downcomers and Downcomer Vent Bracing	5.3-2
5.3.3.1 General Description	5.3-3
5.3.3.2 Loads for Analysis	5.3-4
5.3.3.3 Design Load Combinations	5.3-6
5.3.3.4 Acceptance Criteria	5.3-7
5.3.3.5 Analysis	5.3-8
5.3.4 References	5.3-9

TABLE OF CONTENTS (Cont'd)

	<u>PAGE</u>
5.4 <u>BOP PIPING ANALYSIS</u>	5.4-1
5.5 <u>EQUIPMENT (BOP)</u>	5.5-1
5.5.1 Reevaluation and Design Assessment Methods	5.5-1
5.5.1.1 Analysis	5.5-1
5.5.1.1.1 Static Analysis	5.5-1
5.5.1.1.2 Dynamic Analysis	5.5-1
5.5.1.1.2.1 Acceptance Criteria	5.5-2
5.5.1.2 Testing	5.5-2
5.5.1.2.1 Single Frequency Testing	5.5-2
5.5.1.2.2 Random Frequency Testing	5.5-2
5.5.1.2.3 Acceptance Criteria	5.5-2
6.0 <u>SUPPRESSION POOL WATER TEMPERATURE MONITORING SYSTEM</u>	6.1-1
6.1 <u>SYSTEM DESIGN</u>	6.1-1
6.1.1 Safety Design Basis	6.1-1
6.1.2 General System Description	6.1-1
6.1.3 Normal Plant Operation	6.1-3
6.1.4 Abnormal Plant Operation	6.1-3
6.2 <u>SUPPRESSION POOL TEMPERATURE RESPONSE</u>	6.2-1
6.2.1 Introduction	6.2-1
6.2.2 Temperature Response Analysis	6.2-2
6.2.2.1 Model Description	6.2-3
6.2.2.2 General Assumptions and Initial Conditions	6.2-4
6.2.2.3 Description of Non-LOCA Events	6.2-6
6.2.2.3.1 Stuck-Open Relief Valve (SORV) Conditions	6.2-6
6.2.2.3.2 SRV Discharge During RPV Isolation Conditions	6.2-7
6.2.2.4 Description of LOCA Event	6.2-9
6.2.3 Results/Conclusions	6.2-9
7.0 <u>PLANT MODIFICATIONS AND RESULTANT IMPROVEMENTS</u>	7.1-1
7.1 <u>STRUCTURAL MODIFICATIONS</u>	7.1-1
7.2 <u>BALANCE OF PLANT PIPING AND EQUIPMENT</u>	7.2-1
7.3 <u>NSSS PIPING AND EQUIPMENT</u>	7.3-1
7.4 <u>SRV DISCHARGE QUENCHER</u>	7.4-1
8.0 <u>PLANT SAFETY MARGINS</u>	8.0-1
8.1 <u>CONSERVATISM IN PLANT DESIGN</u>	8.1-1

TABLE OF CONTENTS (Cont'd)

	<u>PAGE</u>
8.1.1 Conservatism in Pool Dynamic Loads	8.1-1
8.1.2 Structural Conservatism	8.1-2
8.1.3 Mechanical Conservatism	8.1-3
8.1.4 Conservatism in NSSS Design	8.1-4
8.2 <u>PLANT STRUCTURAL MARGINS DURING MAXIMUM TRANSIENT CONDITIONS</u>	8.2-1
9.0 <u>CONCLUSIONS</u>	9.0-1
A.0 <u>COMPUTER PROGRAMS</u>	A-1
A.1 <u>DYNAX</u>	A-1
A.2 <u>FAST</u>	A-2
A.3 <u>KALSHEL</u>	A-2
A.4 <u>TEMCO</u>	A-3
A.5 <u>PIPSYS</u>	A-5
A.6 <u>RSG</u>	A-6
A.7 <u>SRVA</u>	A-6
B.0 <u>RESPONSES TO NRC QUESTIONS</u>	B.0-1
B.1 <u>QUESTIONS OF JUNE 23, 1976</u>	B.1-1
B.2 <u>QUESTIONS OF JANUARY 19, 1977</u>	B.2-1
B.3 <u>QUESTIONS OF JUNE 30, 1978</u>	B.3-1
C.0 <u>SUBMERGED STRUCTURE METHODOLOGY</u>	C-1
C.1 <u>INTRODUCTION</u>	C-1
C.2 <u>DRAG AND LIFT COEFFICIENTS FOR UNSTEADY FLOW</u>	C-3
C.2.1 General Considerations	C-3
C.2.2 LOCA Charging Air Bubble	C-8
C.2.3 Pool Swell	C-10
C.2.4 Fallback	C-12
C.2.5 SRV Air Bubbles	C-14
C.3 <u>INTERFERENCE EFFECTS ON ACCELERATION DRAG</u>	C-15
C.3-1 Method of Analysis	C-15
C.3.2 Two Stationary Cylinders (Real Cylinders)	C-16

TABLE OF CONTENTS (Cont'd)

	<u>PAGE</u>
C.3.3 Stationary Cylinders Near a Plane Boundary (Real and Imaginary Cylinders)	C-18
C.3.4 Total Acceleration Drag Force	C-19
C.3.5 Practical Application	C-20
C.3.6 Model/Data Comparisons	C-22
C.4 <u>INTERFERENCE EFFECTS ON STANDARD DRAG</u>	C-23
C.4.1 Interference Between Two Cylinders of Equal Diameter	C-23 C-23
C.4.2 Interference Between More Than Two Cylinders of Equal Diameter	C-24
C.4.3 Drag on Small Cylinder Upstream of Large Cylinder	C-28
C.4.4 Standard Drag on Smaller Cylinder Downstream of Large Cylinder	C-31
C.4.5 Standard Drag on the Large Cylinder	C-32
C.4.6 Structures of Non-Circular Cross Section	C-32
C.4.7 Interference Between Non-Parallel Cylinders	C-32
C.5 <u>UNIFORM VELOCITY AND ACCELERATION EVALUATED AT THE GEOMETRIC CENTER OF A STRUCTURE</u>	C-33
C.6 <u>LA SAMP-SPECIFIC PARAMETERS</u>	C-37
C.7 <u>REFERENCES</u>	C-38
D.0 <u>NSSS OPERABILITY ASSURANCE</u>	D-1
E.0 <u>RPV INTERNALS LUMPED-MASS MODEL ANALYSIS METHODS</u>	E-1
F.0 <u>NSSS PIPING SYSTEMS ANALYSIS METHODS</u>	F-1
G.0 <u>CALCULATION OF PRESSURE TIME HISTORIES IN THE ANNULUS</u>	G-1

LIST OF TABLES

<u>NUMBER</u>	<u>TITLE</u>	<u>PAGE</u>
1.0-1	Mark II Containment Supporting Program: LOCA-Related Tasks	1.0-4
1.0-2	Mark II Containment Supporting Program: SRV-Related Tasks	1.0-6
1.0-3	Mark II Containment Supporting Program: Miscellaneous Tasks	1.0-7
1.1-1	Primary Containment Principal Design Para- meters and Characteristics	1.1-2
3.1-1	Functional Capability Acceptance Criteria (Equation 9 of NB-3652 and NC-3652)	3.1-6
3.2-1	SRV Discharge Line Clearing Transient Para- meterization	3.2-18
3.2-2	SRV Bubble Dynamics Parameterization	3.2-19
3.2-3	Second Actuation Assumptions	3.2-20
3.2-4	Second Actuation Results	3.2-21
3.4-1	Conformance of the LSCS Design to NUREG-0478 Criteria	3.4-2
4.1-1	Design Load Combinations	4.1-4
4.3-1	LOCA and SRV Design Load Combinations - Reinforced Concrete Structures Other Than Containment	4.3-3
4.3-2	LOCA and SRV Design Load Combinations - Structural Steel Elastic Design	4.3-4
4.4-1	Load Combinations for Equipment and Piping	4.4-7
4.4-2	Load Combinations and Allowable Stress Limits for BOP Equipment	4.4-8
4.5-1	Load Combinations and Acceptance Criteria for NSSS Piping and Equipment	4.5-3
5.1-1	Margin Table for Basemat for All Valves Discharge	5.-13
5.1-2	Margin Table for Basemat for 2 Valves Discharge	5.1-14
5.1-3	Margin Table for Basemat for ADS Valves Discharge	5.1-15
5.1-4	Margin Table for Basemat for LOCA Plus Single SRV	5.1-16
5.1-5	Margin Table for Containment for All Valves Discharge	5.1-17
5.1-6	Margin Table for Containment for 2 Valves Discharge	5.1-18
5.1-7	Margin Table for Containment for ADS Valves Discharge	5.1-19
5.1-8	Margin Table for Containment for LOCA Plus Single SRV	5.1-20
5.1-9	Margin Table for Reactor Support for All Valves Discharge	5.1-21

LIST OF TABLES (Cont'd)

<u>NUMBER</u>	<u>TITLE</u>	<u>PAGE</u>
5.1-10	Margin Table for Reactor Support for 2 Valves Discharge	5.1-22
5.1-11	Margin Table for Reactor Support for ADS Valves Discharge	5.1-23
5.1-12	Margin Table for Reactor Support for LOCA Plus Single SRV	5.1-24
5.1-13	Margin Table for Drywell Floor and SRV and LOCA Loads	5.1-25
5.2-1	Summary of Containment Wall Liner Plate Stresses/Strains for All SRV Cases	5.2-5
5.2-2	Summary of Containment Wall Liner Anchorage Load/Displacement for All SRV Cases	5.2-6
5.3-1	LOCA and SRV Design Load Combinations Reinforced Concrete Structures Other Than Containment	5.3-10
5.3-2	LOCA and SRV Design Load Combinations Structural Steel Elastic Design	5.3-11
5.3-3	Capability of Concrete (Other Than Containment) and Steel Structures	5.3-12
6.2-1	Stuck-Open Relief Valve from Power Operation - Event A	6.2-12
6.2-2	Stuck-Open Relief Valve from Hot Standby - Event B	6.2-13
6.2-3	Isolation and Reactor Depressurization - Event C	6.2-14
6.2-4	Isolation and Reactor Depressurization - Event D	6.2-15
6.2-5	Intermediate Break Accident (Liquid) With ADS - Event E	6.2-16
6.2-6	Summary of Results Suppression Pool Temperature Response Analysis	6.2-17
7.2-1	Tested HVAC Equipment	7.2-3
8.2-1	Margin Factors for Containment During Maximum Transient Condition	8.2-2

LIST OF FIGURES

<u>NUMBER</u>	<u>TITLE</u>
1.1-1	Primary Containment
1.1-2	Suppression Chamber - Plan View
1.1-3	Suppression Chamber - Section "L-L"
1.1-4	Suppression Chamber - Section "M-M"
3.2-1	Second Actuation - ATWS Pump Trip Off
3.2-2	Second Actuation - ATWS Pump Trip On
3.2-3	Second Actuation - Mitigating Approach
3.2-4	Orientation of SRV Discharge Line Device for Automatic Depressurization System Actuation
3.2-5	Cross Section of Suppression Pool and Definition of Suppression Chamber Walls Loading Zones
3.3-1	Multiple Main Vent Chugging Load Factor
3.3-2	Downcomer Vent Clearing Jet Angle During LOCA
3.3-3	Jet Impingement Load
3.3-4	Drag Coefficients
3.3-5	Drag Load on Submerged Structures Due to Downcomer Vent Clearing
3.3-6	Maximum Impact Pressure on Small Structures
3.3-7	Maximum Impact Force on Pipes
3.3-8	Maximum Impact Force on I-Beams
3.3-9	Time History of Impact Load For Small Structures in Pool Swell Region
3.3-10	Chugging Load
3.3-11	Drywell/Wetwell Pressure Transients For a Main Steamline Break
3.3-12	Drywell/Wetwell Temperature Transients For a Main Steamline Break
3.3-13	Drywell/Wetwell Pressure Transients for Recirculation Line Break
3.3-14	Drywell/Wetwell Temperature Transients For Recircula- tion Line Break
3.3-15	Drywell/Wetwell Pressure Transients For an Inter- mediate Break
3.3-16	Drywell/Wetwell Temperature Transients For an Intermediate Break
3.3-17	Drywell/Wetwell Pressure Transients Due to SBA
3.3-18	Drywell/Wetwell Temperature Transients Due to SBA
3.3-19	Sequence of Annulus Pressurization Events
3.3-20	Acoustic Load Illustration
3.3-21	Annulus Pressurization Loading Description
3.3-22	Restricted Pipe Motion During Blowdown
4.4-1	Response Spectra Comparison Design Basis vs. Chugging
4.4-2	Restraint Load Change Distribution
5.1-1	Pool Dynamics Model with ISI Effect
5.1-2	Drywell Floor Analytical Model
5.1-3	Circumferential Variation of Moment in Drywell Floor Due to Concentrated Radial Moment Applied at Radius 23'-3"

LIST OF FIGURES (Cont'd)

<u>NUMBER</u>	<u>TITLE</u>
5.1-4	Radial Variation of Moment in Drywell Floor Due to Concentrated Radial Moment Applied at Radius 23'-3"
5.1-5	Circumferential Variation of Moment in Drywell Floor Due to Concentrated Circumferential Moment Applied at Radius 23'-3"
5.1-6	Radial Variation of Moment in Drywell Floor Due to Concentrated Circumferential Moment Applied at Radius 23'-3"
5.1-7	Base Mat Plan - Top Reinforcing Layout
5.1-8	Base Mat Plan - Bottom Reinforcing Layout
5.1-9	Containment Wall Post-Tensioning Tendon Layout
5.1-10	Containment Wall Reinforcing Layout
5.1-11	Reactor Support - Concrete Plug
5.1-12	Reactor Support - Reinforcing Layout Before Modification
5.1-13	Unit 1 Drywell Floor Reinforcing Layout
5.1-14	Unit 2 Drywell Floor Reinforcing Layout
5.1-15	Design Sections - Primary Containment and Reactor Support
5.1-16	Design Sections - Drywell Floor
5.1-17	Representative Base Mat Interaction Diagram
5.1-18	Representative Containment Interaction Diagram
5.2-1	Base Mat Liner Detail
5.2-2	Base Mat Liner Stiffener Detail
5.2-3	Containment Wall Liner Detail
5.3-1	Downcomer Vent Bracing at Elevation 721'-0"
5.3-2	Downcomer Vent Bracing at Elevation 697'-0"
5.3-3	Partial Downcomer Bracing Model Inner Rings 1 and 2
5.3-4	Partial Downcomer Bracing Model Outer Rings 3 and 4
6.2-1	Pool Temperature vs. Mass Flux - Event A: SORV from Power Operation
6.2-2	Pool Temperature Response - Event A: SORV from Power Operation
6.2-3	Pool Temperature Response - Event B: SORV from Hot Standby
6.2-4	Pool Temperature vs. Mass Flux - Event C: Isolation and Reactor Depressurization
6.2-5	Pool Temperature Response - Event C: Isolation and Reactor Depressurization
6.2-6	Pool Temperature vs. Mass Flux - Event D: Isolation and Reactor Depressurization
6.2-7	Pool Temperature Response - Event D: Isolation and Reactor Depressurization
6.2-8	Pool Temperature Response - Event E: Intermediate Break Accident with ADS (0.1 ft <sup>2</sup> Liquid Break)

LIST OF FIGURES (Cont'd)

<u>NUMBER</u>	<u>TITLE</u>
Q20.58-1	Experimental Data as Compared to Computer Code Prediction
Q20.58-2	Comparison of Computer Code with EPRI Test Data, Water Velocity vs. Time
Q20.58-3	Comparison of Computer Code with EPRI Test Data, Water Level vs. Time
Q20.58-4	Pool Surface Position vs. Time
Q20.58-5	Pool Surface Velocity vs. Time
Q20.58-6	Pool Surface Velocity vs. Position
Q20.58-7	Air Slug and Wetwell Pressure
Q20.71-1	Pool Surface Elevation - Run 36
Q20.71-2	Pool Surface Elevation - Run 37
Q20.71-3	Pool Surface Velocity - Run 36
Q20.71-4	Pool Surface Velocity - Run 37
Q20.71-5	Bubble Pressure - Run 36
Q20.71-6	Bubble Pressure - Run 37
Q20.75-1	Multiple Main Vent Chugging Load Factor
C-1	LOCA Air Clearing Velocity
C-2	LOCA Air Clearing Acceleration
C-3	Top View of 36° Sector of a Typical Mark II Suppression Pool
C-4	Schematic View of Section A-A of Typical Mark II Suppression Pool
C-5	Model/Data Comparisons
C-6	Cylinder Locations
C-7	Flow Around Unequal Cylinders
C-8	Top and Side View of Structure and Source Locations
C-9	Location of Horizontal Submerged Structure in the Suppression Pool
C-10	Top and Side View of (Second) Structure and Source Location
C-11	Location of Vertical Submerged Structure in the Suppression Pool
C-12	Horizontal Component of Velocity Along a Structure Segmented Into 4, 8 and 32 Sections
C-13	Vertical Component of Acceleration Along a Structure Segmented Into 4, 8 and 32 Sections
C-14	Radial Component of Velocity Along a Structure Segmented Into 4, 6, 8 and 32 Sections
C-15	Radial Component of Acceleration Along a Structural Segmented Into 4, 6, 8 and 32 Sections
E-1	Lumped-Mass Model of RPV, Internals and Reactor Building

## 1.0 INTRODUCTION

The purpose of this final revision of the Design Assessment Report (DAR) is to demonstrate that the La Salle County Station (LSCS) containment can accommodate all hydrodynamic load phenomena associated with the SRV discharge and LOCA in the BWR Mark II containment concept, to document conformance with the Nuclear Regulatory Commission (NRC) Lead Plant Acceptance Criteria of NUREG-0487, and to provide a response to questions posed by the NRC.

The Mark II Containment Dynamic Forcing Functions Information Report (DFFR) NEDO/NEDE 21061 has already been submitted to the NRC in September 1975.

The purpose of the DFFR was:

- a. to identify and describe the time-history of those normal and abnormal operating conditions related to both the SRV discharge and the design-basis LOCA which must be considered in plant design;
- b. to explain the generic methods of analysis used to obtain the forcing functions that are required to predict loads on structures and components in the suppression chamber region; and
- c. to justify these methods of analysis on the basis of analytical models and test data.

In some cases, the forcing function defined in the DFFR is believed to be excessively conservative. In a few other cases, it is believed that additional test data are required to confirm the conservatism of the forcing functions defined in the DFFR. Therefore, a Mark II Containment Supporting Program (NEDC

21297) was established and is being implemented. This supporting program is expected to confirm the conservatism of the forcing functions defined in the DFFR and to provide test data sufficient to allow analytical model improvements that result in design load reductions. The generic Mark II Containment Supporting Program is summarized in Tables 1.0-1 through 1.0-3.

This report (DAR) employs the analytical models, test data, and other information from the DFFR to assess the design adequacy of the La Salle County Station containment structures, piping, and equipment.

The objective of this report is to demonstrate that the NRC Lead Plant Acceptance Criteria are satisfied and to describe how results of the generic Mark II containment supporting program are being incorporated in the design reassessment. This report provides the NRC Staff with all information necessary to continue and complete the licensing of La Salle County Station as scheduled. All pertinent information related to loads, load specification, load combinations, acceptance criteria, plant modification, plant margins, and confirmation of loads that applies to the La Salle County Station has been compiled in this document. A bounding load approach has been used to permit an early evaluation and approval. Specific commitments are made to do further analysis and tests to refine and confirm loads in those cases where there is a significant licensing issue. It is expected that when these more refined loads are determined increased margins will be conclusively demonstrated.

This report, together with the DFFR (NEDO/NEDE 21061-P), Mark II Containment Supporting Program NEDO 21297, FSAR, and reports referenced in this document, constitutes a complete basis for issuance of an Operating License. In addition, an in-plant SRV test will be performed to confirm the adequacy of loads used for design assessment.

In this report the individual loads and load combinations that are being utilized in the reassessment are identified and described in the first four sections. Reports defining the individual loads and providing justification for application to the La Salle County containment are referenced rather than repeated. This is consistent with the objective of this report.

The methods used in re-evaluating the structures, piping systems and equipment are described in Section 5.0. The plant modification and resultant changes that have been completed are described in Section 7.0. The plant margins and conservatisms are summarized in Section 8.0.

It is concluded that the present evaluation of the design is completely adequate. Significant design modifications and resultant plant changes have been identified so that the LSCS plant is completely safe and does not represent any hazard to the public. In fact, it is anticipated that future results from the generic Mark II Containment Supporting Program and the LSCS in-plant SRV testing will conclusively demonstrate increased design margins in the plant. Therefore, LSCS plant startup should proceed as scheduled.

TABLE 1.0-1

## MARK II CONTAINMENT - SUPPORTING PROGRAM

## LOCA-RELATED TASKS

TASK NUMBER	ACTIVITY	ACTIVITY TYPE	TARGET COMPLETION	DOCUMENTATION	DATE DOCUMENT/SUBMITTAL	LEAD PLANT SER/ INTERMEDIATE PLANT
A.1	"4T" TEST PROGRAM	Phase I Test Report	Completed	NEDO/NEDE 13442-P-01	5/76 - 5/76	LP SER/IP
		Phase I Appl Memo	Completed	Application Memo	6/76 - 6/76	LP SER/IP
		Phase II & III Test Rpt	Completed	NEDO/NEDE 13468-P	12/76 - 1/77	LP SER/IP
		Application Memorandum	Completed	NEDO/NEDE 13678-P	1/77 - 2/77	LP SER/IP
A.2	POOL SWELL MODEL REPORT	Model Report	Completed	NEDO/NEDE 21544-P	12/76 - 2/77	LP SER/IP
A.3	IMPACT TESTS	PSTF 1/3 Scale Tests	Completed	NEDO/NEDE 13426-P	8/75 - 9/75	LP SER/IP
		Mark I 1/12 Scale Tests	Completed	NEDO/NEDE 20989-2P	9/75 - 11/75	LP SER/IP
A.4	IMPACT MODEL	PSTF 1/3 Scale Tests	Completed	NEDO/NEDE 13426P	8/75 - 9/75	LP SER/IP
		Mark I 1/12 Scale Tests	Completed	NEDO/NEDE 20989-2P	8/75 - 11/75	LP SER/IP
A.5	LOADS ON SUBMERGED STRUCTURES	LOCA/RH Air Bubble Model	Completed	NEDO/NEDE 21471-P	9/77 - 1/78	LP SER/IP
		LOCA/RH Water Jet Model	Completed	NEDO/NEDE 21472-P	9/77 - 1/78	LP SER/IP
		Ring Vortex Model	Completed	Letter Report	5/79 - 5/79	LP/IP
		2Q 80	Completed	Topical Report		IP
		Applications Methods	Completed	NEDO/NEDE 21730-P	12/77 - 1/78	LP SER/IP
		Quenc. Air Bubble Model	4Q 79	NEDO 21471 Supplement		IP
		Quencher Air Bubble	4Q 79	NEDE 21730 Supplement		IP
		Appl. Memo. Supp.				
		1/4 Scaling Tests	Completed	NEDE 23817-P	9/78 - 12/78	IP
		Steam Condensation Methods		LSCS DACR	7/78 - 7/78	SER
A.6	CHUGGING ANALYSIS AND TESTING	Single Cell Report	Completed	NEDO/NEDE 23703-P	9/77 - 11/77	LP SER
		Multivent Model	Completed	NEDO/NEDE 21669-P	2/78 - 3/78	IP
		4T FSI Report	Completed	NEDO/NEDE 23710-P	4/78 - 3/78	LP SER
A.7	CHUGGING SINGLE VENT	CREARE Report	Completed	NEDO/NEDE 21851-P	6/78 - 7/78	Info
A.9	ERPI TEST EVALUATION EPRI 1/13 SCALE TESTS EPRI SINGLE CELL TESTS	EPRI-4T Comparison	Completed	NEDO 21667	8/77 - 9/77	LP SER*
		3D Tests	Completed	EPRI NP-441	4/77 - --	LP SER*
		Unit Cell Tests	4Q 79	EPRI Report		Info
A.11	MULTIVENT SUBSCALE TESTING AND ANALYSIS	Preliminary MV Prog Plan	Completed	NEDO 23697	12/77 - 1/78	LP SER/IP
		MV Test Program Plan & Proc.	Completed	NEDO 23697 Rev 1	1/79 - 4/79	IP
		- Phase I				
		Phase I Test Report	4Q 79	Report		IP
		MV Test Prog Plan & Proc				
		- Phase II	4Q 79	NEDO 23697, Rev.1, Supp. 1		IP
		Phase II Test Report	2Q 80	Report		IP
CONMAP Tests	Completed	Report	6/79 - 8/79	Info		
MHM Verification						
1/10 Scale	Completed	NEDE 25116-P	5/79 - 7/79	Info		

1.0-4

LSCS-MARK II DAR

Rev. 7 1/80

TABLE 1.0-1 (Cont'd)

LOCA-RELATED TASKS

<u>TASK NUMBER</u>	<u>ACTIVITY</u>	<u>ACTIVITY TYPE</u>	<u>TARGET COMPLETION</u>	<u>DOCUMENTATION</u>	<u>DATE DOCUMENT/SUBMITTAL</u>	<u>LEAD PLANT SER/ INTERMEDIATE PLANT</u>
A.13	SINGLE VENT LATERAL LOAIS	Dynamic Analysis Summary Report Dynamic Analysis (Extension)	Completed Completed 4Q 79	NEDO 24106-P NEDE 23806-P Report	3/78 - 7/76 10/78 - 11/78	IP IP
A.16	IMPROVED CHUGGING LOAD DEFINITION	Impulse Evaluation Improved Chug Load Defn.	Completed 1Q 80	Letter Report Report	6/78 - 7/78	LP SER* IP
A.17	STEAM CONDENSATION OSCILL. CO LOAD DEFINITION	4T C.O. Test CO Data Evaluation	2Q 80 3Q 80	Report Report		IP LP/IP

TABLE 1.0-2

MARK II CONTAINMENT - SUPPORTING PROGRAMSRV-RELATED TASKS

<u>TASK NUMBER</u>	<u>ACTIVITY</u>	<u>ACTIVITY TYPE</u>	<u>TARGET COMPLETION</u>	<u>DOCUMENTATION</u>	<u>DATE DOCUMENT/SUBMITTAL</u>	<u>LEAD PLANT SER/ INTERMEDIATE PLANT</u>	
B.1	QUENCHER EMPIRICAL MODEL	DFFR Model	Completed	NEDO/NEDE 21061-P	9/76 - 9/76	IP	
		Supporting Data	Completed	NEDO/NEDE 21078-P	5/75 - 7/75	IP	
B.2	RAMSHEAD MODEL	DFFR Model	Completed	NEDO/NEDE 21061-P	9/76 - 9/76	LP SER	
		Supporting Data	Completed	NEDO/NEDE 21062-P	7/75 - 10/75	LP SER	
		Analysis	Completed	NEDO/NEDE 20942-P	5/75 - 7/75	LP SER	
B.3	MONTICELLO IN-PLANT S/RV TESTS	Preliminary Test Rpt.	Completed	NEDO/NEDC 21465-P	12/76 - 1/77	LP SER	
		Hydrodynamic Report	Completed	NEDO/NEDC 21581-P	8/77 - 8/77	LP SER	
B.5	S/RV QUENCHER IN-PLANT CAORSO TESTS	Test Plan	Completed	NEDM 20988 Rev. 2	12/76 - 3/77	IP	
		Test Plan Addendum 1	Completed	NEDM 20988 Rev. 2, Add 1	10/77 - 3/78	IP	
		Test Plan Addendum 2	Completed	NEDM 20988 Rev. 2, Add 2	4/78 - 7/78	IP	
		Test Summary	Completed	Letter Report	3/79 - 3/79		
		Phase I Phase II	Test Report	Completed	NEDO/NEDE-25100-P	5/79 - 6/79	IP
		Test Report	iq 80		Report		IP
B.6	THERMAL MIXING MODEL	Analytical Model	Completed	NEDO/NEDC 23689-P	3/78 - 3/78	Info	
B.10	MONTICELLO PSI	Analysis of PSI	Completed	NEDO 23834	6/78 - 7/78	LP SER	
B.11	DFFR RAMSHEAD MODEL TO MONTICELLO DATA	Data/Model Comparison	Completed	NSC-GEN 0394	9/77 - 10/77	LP SER	
B.12	RAMSHEAD SRV METHODOLOGY SUMMARY	Analytical Methods	Completed	NEDO 24070	10/77 - 11/77	LP SER	

1.0-6

ISCS-MARK II DAR

Rev. 7 1/80

TABLE 1.0-3

MARK II CONTAINMENT - SUPPORTING PROGRAMMISCELLANEOUS TASKS

<u>TASK NUMBER</u>	<u>ACTIVITY</u>	<u>ACTIVITY TYPE</u>	<u>TARGET COMPLETION</u>	<u>DOCUMENTATION</u>	<u>DATE DOCUMENT/SUBMITTAL</u>	<u>LEAD PLANT SER/ INTERMEDIATE PLANT</u>
C.0	SUPPORTING PROGRAM	Supp Prog Rpt	Completed	NEDO 21297	5/76 - 6/76	-
		Supp Prog Rpt Rev. 1	Completed	NEDO 21297 - Rev. 1	4/78 - 4/78	-
		Supp Prog Rpt Rev. 2	2Q 80	NEDO 21297 - Rev. 2		
C.1	DFFR REVISIONS	Revision 1	Completed	NEDO/NEDE 21061-P Rev. 1	9/75 - 4/76	-
		Revision 2	Completed	NEDO/NEDE 21061-P Rev. 2	9/76 9/76	-
		Revision 3	Completed	NEDO/NEDE 21061-P Rev. 3	6/78 - 6/78	-
C.3	NRC ROUND 1 QUESTIONS	DFFR Rev. 2	Completed	NEDO/NEDE 21061-P Rev. 2	9/76 - 9/76	LP SER*/IP
		DFFR Rev. 2 Amendment 1	Completed	NEDO/NEDE 21061-P Rev. 2 Amendment 1	12/76 - 2/77	LP SER*/IP
		DFFR Rev. 3 Appendix A	Completed	NEDO/NEDE 21061-P Rev. 3 Appendix A	6/78 - 5/79	LP SER*/IP
C.5	SRSS JUSTIFICATION	Interim Report	Completed	(NEDE 24010)	4/77 - 3/77	
		SRSS Report	Completed	NEDO/NEDE 24010-P	7/77 - 8/77	LP SER*/IP
		SRSS Exec. Report	Completed	Summary Report	4/78 - 5/78	LP SER*/IP
		SRSS Criteria Appl.	Completed	NEDO/NEDE 24010-P Suppl. 1	10/78 - 11/78	LP SER*/IP
		SRSS Bases	Completed	NEDO/NEDE 24010-P Suppl. 2	12/78 - 2/79	LP/IP
		SRSS Justification Sup	Completed	NEDO 24010 Suppl. 3	8/79 - 11/79	LP/IP
C.6	NRC ROUND 2 QUESTIONS	DFFR Amendment 2	Completed	NEDO/NEDE 21061-P Rev. 2 Amendment 2	6/77 - 7/77	LP SER*/IP
		DFFR Amend 2, Suppl 1	Completed	NEDO/NEDE 21061-P Rev. 2 Amendment 2 Suppl. 1	8/77 - 9/77	LP SER*/IP
		DFFR Amend 2, Suppl 2	Completed	NEDO/NEDE 21061-P Rev. 2 Amend. 2 Suppl. 2	9/77 - 11/77	LP SER*/IP
		DFFR Rev. 3, Appendix A	4Q 79	NEDO/NEDE 21061-P, Rev. 3 Appendix A		LP SER*/IP
C.7	JUSTIFICATION OF "4T" BOUNDING LOADS	Chugging Loads	Complete	NEDO/NEDE 23617-P	7/77 - 8/77	LP SER/IP
		Justification	Complete	NEDO/NEDE 24013-P	6/77 - 8/77	LP SER/IP
			Complete	NEDO/NEDE 24014-P	6/77 - 8/77	LP SER/IP
			Complete	NEDO/NEDE 24015-P	6/77 - 8/77	LP SER/IP
			Complete	NEDO/NEDE 24016-P	6/77 - 8/77	LP SER/IP
			Complete	NEDO/NEDE 24017-P	6/77 - 8/77	LP SER/IP
			Complete	NEDO/NEDE 23627-P	6/77 - 8/77	LP SER/IP
C.8	S/RV AND CHUGGING FSI	Prestressed Concrete Reinforced Concrete Steel	Completed	NEDO/NEDE 21936-P	7/78 - 7/78	LP SER/IP

1.0-7

LOGS-MARK II DAB

Rev. 7 1/80

TABLE 1.0-3 (Cont'd)

MISCELLANEOUS TASKS

<u>TASK NUMBER</u>	<u>ACTIVITY</u>	<u>ACTIVITY TYPE</u>	<u>TARGET COMPLETION</u>	<u>DOCUMENTATION</u>	<u>DATE DOCUMENT/SUBMITTAL</u>	<u>LEAD PLANT SER/ INTERMEDIATE PLANT</u>
C.9	MONITOR WORLD TESTS	Monitor Tests	2Q 80	None		
C.13	LOAD COMBINATIONS & FUNCTIONAL CAPABILITY CRITERIA	Criteria Justification	Completed	NEDO 21985	9/78 - 12/78	IP
C.14	NRC ROUND 3 QUESTIONS	Letter Report DFFR, Rev. 3, Appendix A	Completed	Letter Report NECO/NEDE 21061-P Rev. 3 Appendix A	3/78 - 6/78 6/78 - 5/79	LP SER*/IP LP SER*/IP
C.15	SUBMERGED STRUCTURE CRITERIA	NRC Question Responses	4Q 79	Letter Report		IP

\*Submitted in response to NRC question.

LP SER: Zimmer, LaSalle, Shoreham  
IP: All Other Plants

## 1.1 GENERAL DESCRIPTION OF PLANT

The La Salle County Station (LSCS) is a two unit nuclear powered electrical generating station which utilizes two General Electric Company BWR-5 (1969 product line) nuclear reactors, with an electrical power output of approximately 1100 MWe each.

The primary containment design is based on the Mark II concept (over/under, drywell/suppression chamber), as represented in Figure 1.1-1. The containment is a 1/4-inch steel-lined, post-tensioned concrete structure. The lining material in the drywell is carbon steel and in the wetwell is 304 stainless steel. Pertinent physical data on the containment is summarized in Table 1.1-1.

The drywell is connected to the suppression pool through 98 suppression vent downcomer pipes. These downcomers function as the path for pressure suppression of steam released in the drywell during a LOCA. The arrangement of the downcomers at the drywell floor is shown in Figure 1.1-2.

The arrangement of piping and structures in the suppression chamber area is shown in Figures 1.1-2, 1.1-3, and 1.1-4.

Downcomer pipes, SRV discharge lines, drywell floor support columns, ECCS piping, and other pertinent features have been identified on these drawings.

TABLE 1.1-1

PRIMARY CONTAINMENT  
PRINCIPAL DESIGN PARAMETERS AND CHARACTERISTICS

<u>II. DESIGN PRESSURE</u>		
A.	Containment Internal Design Pressure	45 psig
B.	Negative Differential Design Pressure	5 psi
C.	Drywell Floor Differential Design Pressure	
	1. downward	25 psi
	2. upward	5 psi
<u>II. VOLUMES</u>		
A.	Drywell Free Air Volume	221,500 ft <sup>3</sup>
B.	Suppression Chamber Free Air Volume	166,400 ft <sup>3</sup>
C.	Suppression Chamber Water Volume	142,160 ft <sup>3</sup>
<u>III. DOWNCOMER SUPPRESSION VENTS</u>		
A.	Number of Downcomers	98
B.	Internal Diameter	23.5 inches
C.	Wall Thickness (Nominal)	0.375 inches
D.	Material	SA-240, TP304
E.	Length	
	1. unembedded length	45.8 feet
	2. total length	49.3 feet
	3. submergence depth	12 feet
<u>IV. SAFETY/RELIEF VALVE DISCHARGE LINES</u>		
A.	Number of Discharge Lines	18
B.	Size	12 inch
C.	Drywell	Schedule 40
	Wetwell	Schedule 80 (with Schedule 160 elbows at selected locations)
D.	Material	SA-106 Grade B

TABLE 1.1-1 (Cont'd)

E. ASME Code Class	3
F. Type of Discharge Device	T-Quencher
G. Height of T-Quencher Centerline Above Base Mat	5 feet
H. Line Lengths, Location, and Valve Setpoints	

<u>Line Number</u>	<u>Valve Set Pressure (psig)</u>	<u>Line Length (ft)</u>	<u>Number of Fittings</u>	<u>Azimuth Location</u>	<u>Radius</u>
MSO4BA	1185	159	13-90° elbows 3-45° elbows	288°	20.61
MSO4BB	1175	183	11-90° elbows 1-45° elbows	72°	20.61
MSO4BC*	1205	172	12-90° elbows 2-45° elbows	230°	36.50
MSO4BD*	1205	136	8-90° elbows 2-45° elbows	50°	36.50
MSO4BE*	1195	131	9-90° elbows 2-45° elbows	310°	36.50
MSO4BF	1185	153	13-90° elbows 1-60° elbows	108°	20.61
MSO4BG	1130	182	13-90° elbows 1-45° elbows	210°	20.61
MSO4BH	1175	168	15-90° elbows 4-45°	252°	20.61
MSO4BJ	1175	160	9-90° elbows 2-45° elbows	24°	20.61
MSO4BK	1175	165	13-90° elbows 1-45° elbows	130°	36.50
MSO4BL	1185	170	12-90° elbows 3-45° elbows	330°	20.61
MSO4BM	1185	192	13-90° elbows 1-45° elbows 1-72° elbows	170°	36.50

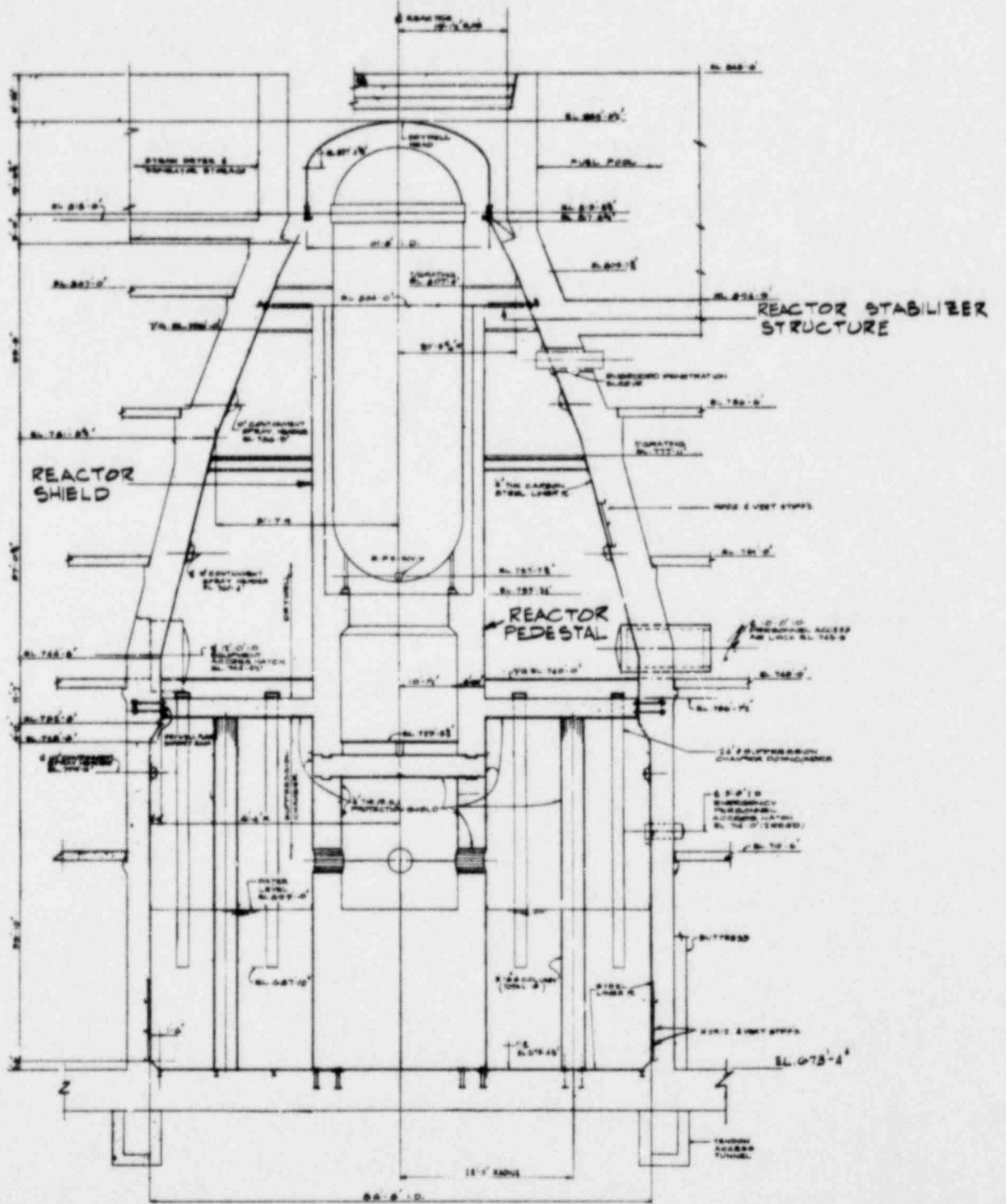
\*Indicates an ADS valve discharge.

TABLE 1.1-1 (Cont'd)

<u>Line Number</u>	<u>Valve Set Pressure (psig)</u>	<u>Line Length (ft)</u>	<u>Number of Fittings</u>	<u>Azimuth Location</u>	<u>Radius</u>
M5O4BN	1195	161	8-90° elbows 4-45° elbows	190°	36.50
M5O4BP	1130	163	11-90° elbows	10°	36.50
M5O4BR*	1195	147	10-90° elbows 2-45° elbows	264°	36.50
M5O4BS*	1195	162	11-90° elbows 4-45° elbows	150°	20.61
M5O4BU <sup>2</sup>	1205	170	11-90° elbows 4-45° elbows	350°	36.50
M5O4BV*	1205	154	10-90° elbows	84°	36.50

\*Indicates an ADS valve discharge.

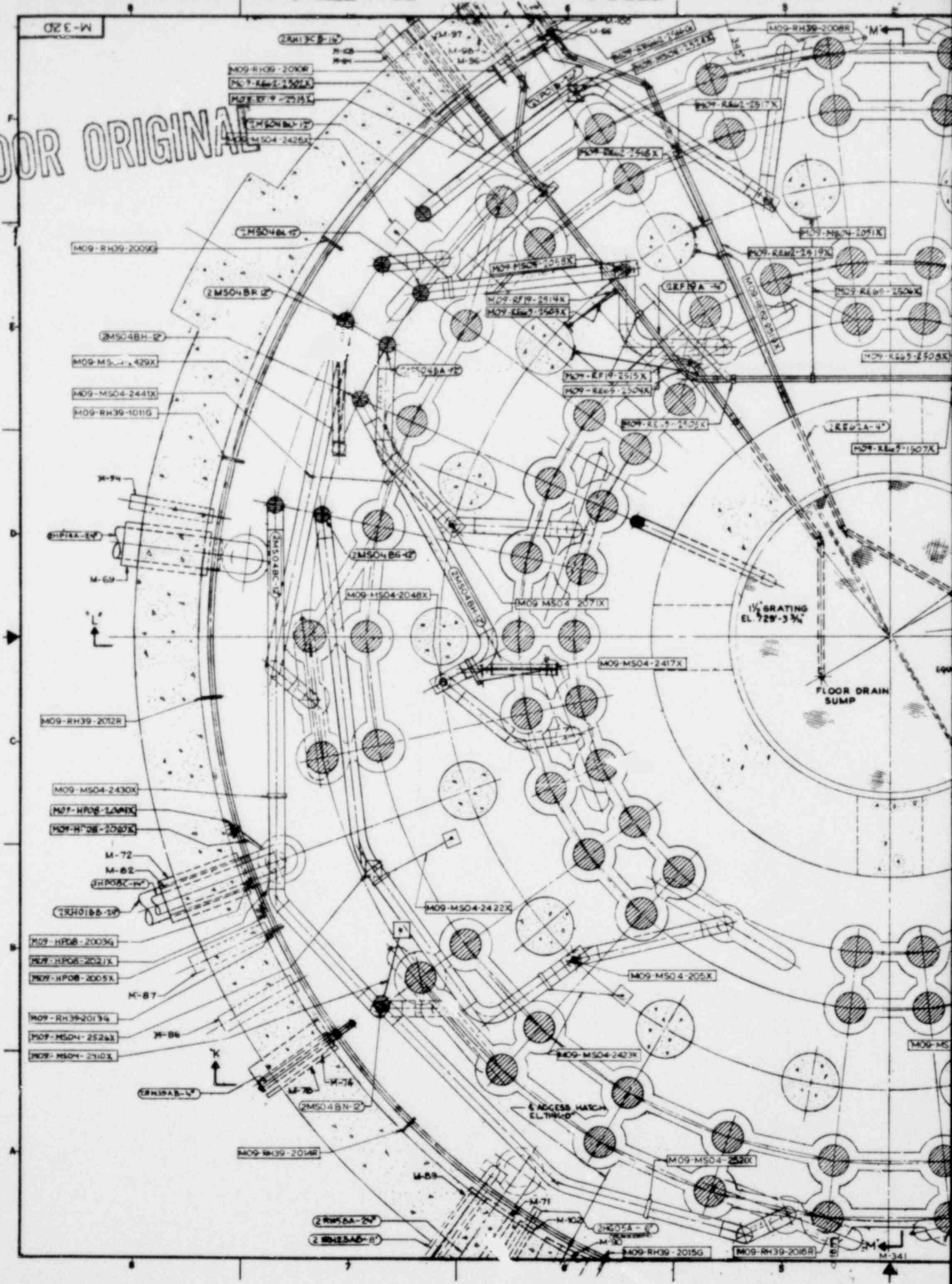
POOR ORIGINAL



LA SALLE COUNTY STATION  
MARK II DESIGN ASSESSMENT REPORT

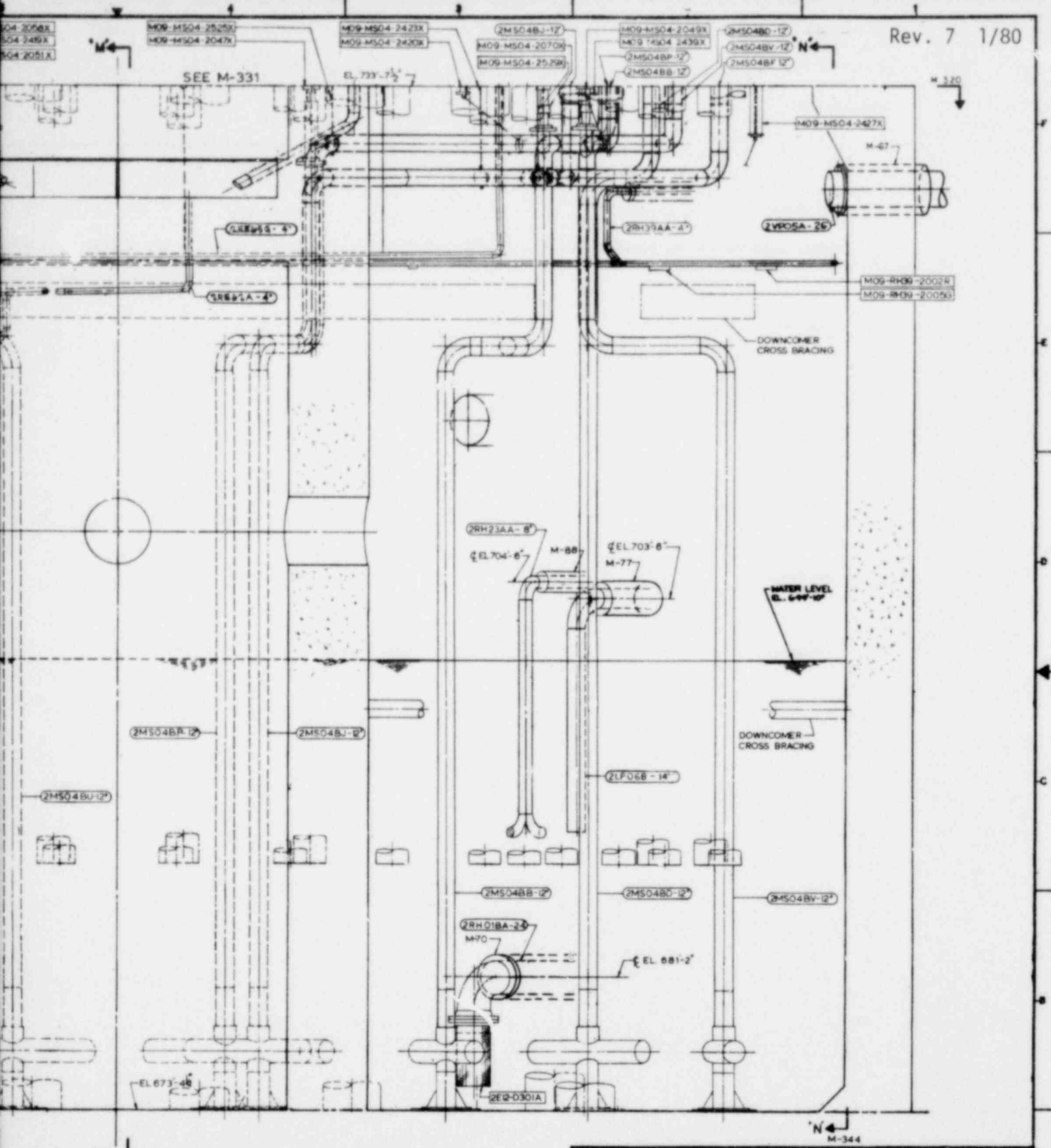
FIGURE 1.1-1  
PRIMARY CONTAINMENT

POOR ORIGINAL









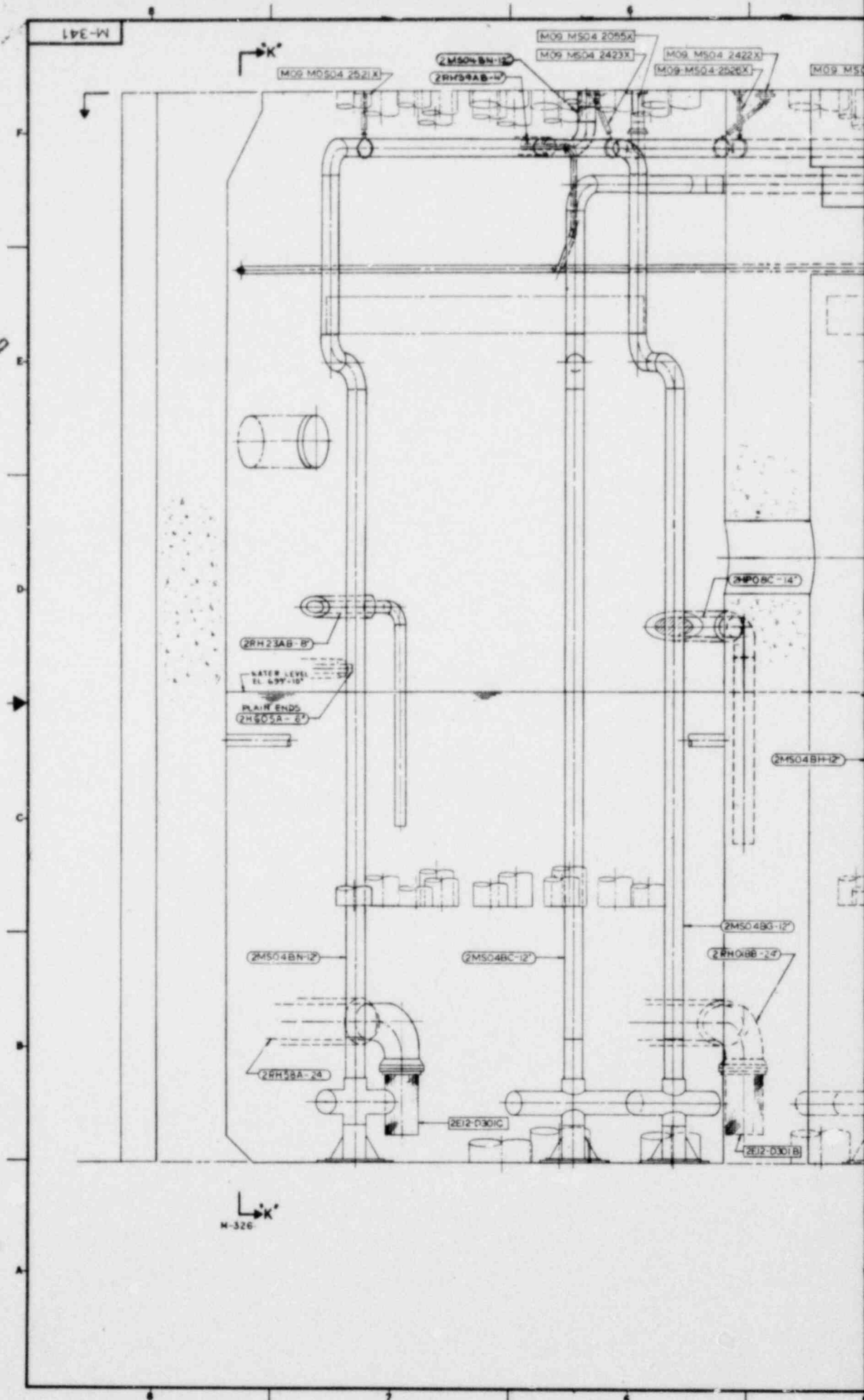
POOR ORIGINAL

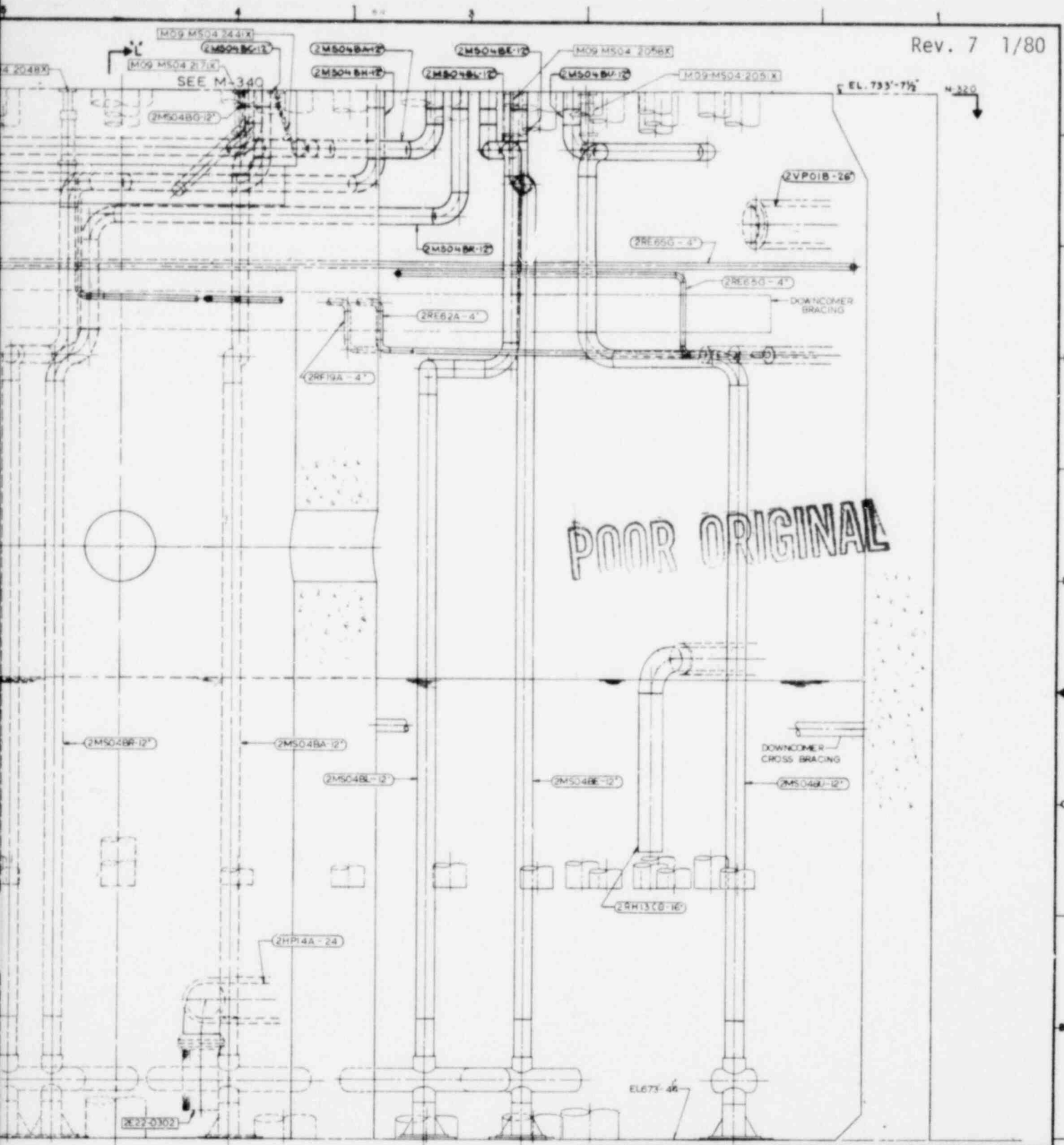
LA SALLE COUNTY STATION  
 MARK II DESIGN ASSESSMENT REPORT

FIGURE 1.1-3

SUPPRESSION CHAMBER - SECTION "L-L"

POOR ORIGINAL





POOR ORIGINAL

LA SALLE COUNTY STATION  
MARK II DESIGN ASSESSMENT REPORT

FIGURE 1.1-4  
SUPPRESSION CHAMBER - SECTION "M-M"

M-332

2.0 MARK II POOL DYNAMICS HISTORY

During the course of a General Electric testing program for the pressure suppression containment program, new containment loads associated with a postulated loss-of-coolant accident (LOCA) were identified which had not been explicitly included in the original design of the La Salle Mark II containment. These loads result from the dynamic effects of drywell air and steam being rapidly forced into the suppression pool during a postulated LOCA event. Additional pool dynamic loads which result from the actuation of safety/relief valves (SRV) were also identified in other tests.

In view of the potential significance of these loads, it was determined that a reassessment of the containment system design would be required. A letter was sent by the NRC to each domestic Mark II owner on April 11, 1975 notifying them of the need for this reassessment.

An "ad hoc" Mark II owner's group was formed which is an organization of all domestic utilities owning Mark II BWR facilities and the General Electric Company to address this containment matter. General Electric has been engaged as the program manager for resolution of the Mark II containment pool dynamic matter. A generic program was developed to establish pool dynamic forcing functions, load combinations, and acceptance criteria appropriate to the Mark II Containment. The program consists of a number of experimental and analytical tasks. These form the basis for establishing the Mark II pool dynamic forcing functions to be used to predict loads that are considered in the specific plant reassessment. They are listed in Table 1.0-1 for reference.

Information resulting from the generic load definition program is contained in the Mark II Containment Dynamic Forcing Function Report (DFFR, Report NEDO/NEDE 21061-P). Results of the specific

plant reassessment are reported in the LSCS Design Assessment Report (DAR). The DAR utilizes the analytical models and information in the DFFR to calculate loads to be used in the specific plant reassessment. A Mark II Containment Supporting Program (NEDO 21297) provides a compilation of all tasks that provide confirmation of the generic methods in the DFFR. (See Table 1.0-1 for a summary of the tasks in the Mark II Containment Supporting Program.)

Since Mark II plants have different licensing schedules, these schedule differences have been accommodated by developing a "Lead Plant Program" to facilitate a timely licensing evaluation. This program permits the licensing of lead Mark II plants, such as Zimmer, La Salle and Shoreham, to progress concurrently with the confirmatory tests and analyses of the total generic Mark II program effort.

The Lead Plant Program consists, in part, of providing conservative, "bounding load" definitions for the assessment of containment, piping, and equipment adequacy. This lead plant program provides an early definition of bounding loads derived from generic tests and analysis efforts. The "bounding load" approach is based on a technical understanding of the phenomena and is expected that to lead to very conservative load definitions. It is expected that results of the confirmatory supporting program and the results of the LSCS in-plant SRV testing will demonstrate the conservatism of the bounding loads used in the design assessment of the La Salle containment.

This Mark II Lead Plant approach was reviewed by the NRC staff, and the results of this review are documented in NUREG-0487, dated November 1978. NUREG-0487 established acceptance criteria for the Mark II Lead Plants based on the "bounding loads" approach. Several of these criteria were reviewed further by the NRC staff at the request of the Mark II Owners Group. As a result of this

further review, a limited number of Alternate Acceptance Criteria were established and presented to the ACRL in September 1979. These criteria are used in the LSCS design reassessment, and the results are reported in this document.

## 2.1 SUMMARY OF DESIGN ASSESSMENT

An analysis has been performed to determine the effect of the hydrodynamic forces due to safety/relief valve discharge and LOCA blowdown on the containment and major structures in the suppression chamber. The loading conditions considered were:

- a. SRV rams head design assessment loads,
- b. SRV KWU T-Quencher design assessment loads,
- c. dynamic LOCA loads due to vent clearing,
- d. dynamic LOCA loads due to pool swell,
- e. dynamic LOCA loads due to condensation oscillations and chugging, and
- f. the above loads combined with each other and with additional loads as described in Section 4.0.

The SRV discharge loads were evaluated for both the rams head and quencher discharge devices. The oscillating air bubble loads are generally less for the quencher than for the rams head. The rams head loads are used as the design basis to provide a greater design margin. An assessment of the quencher loads is also performed to ensure the adequacy of the design basis. This assessment is discussed in Section 4.0. An additional consideration is the potential for high loads due to unstable steam condensation with rams head steam discharges at high pool temperatures. Although analysis indicated that the rams head was acceptable as described in Section 6.0, quenchers were installed to provide additional margin.

The structures and plant components which were assessed are:

- a. containment base mat;
- b. containment wall (drywell and wetwell);
- c. reactor support pedestal (drywell and wetwell);
- d. drywell floor;

- e. containment liner (wetwell);
- f. downcomer vents and downcomer vent bracing;
- g. piping and equipment (wetwell, drywell, and reactor building); and
- h. nuclear steam supply system.

With the design modifications discussed in Section 7.0, the structures will safely handle these loads. A detailed summary of all safety margins for each structure and load combination is given in Section 8.0.

It is believed that this report satisfies the NRC request for additional information and demonstrates the capability of the LSCS structures to fully accommodate all of the NRC Lead Plant Acceptance Criteria documented in NUREG-0487 (November 1978).

TABLE 2.1-1  
SUMMARY OF LOADS

LOAD DESCRIPTION	LOAD CLASS	LOAD MAGNITUDE		REFERENCES		DESIGN CHANGES	NOTES AND COMMENTS
		DFFR	DAR	DFFR	DAR		
<b>I. LOCA RELATED</b>							
<b>A. CONTAINMENT</b>							
1. Clearing Transient	G	33 psi	33 psi	4.4.5.1	3.3.2.2.1***	No	
2. Chugging	G	+4.8/-4.0 psi	-4.8/-4.0 psi	4.3.3	3.3.4, 3.3.7***	No	Preliminary Load
<b>B. WETWELL COMPONENTS</b>							
1. Bulk Pool Swell Height**	G	1.5H	1.5H	4.4.3	3.3.2.2.1***	Yes	Components Moved
2. Pool Swell Impact							
a. Pipes	U	77 psi*	70 psi	4.4.6.1	3.3.2.2.1	Yes	Additional Supports
b. Beams	U	60 psi*	60 psi	4.4.6.1	3.3.2.2.1	Yes	Additional Supports
3. Pool Swell Drag	U	5 psi*	3.2 psi	4.4.7			
4. Pool Fallback	U	5 psi*	9.96 psi	4.4.5.4 4.4.7	3.3.2.2.4	No	
<b>C. DIAPHRAGM FLOOR</b>							
1. Bulk Pool Swell	G	2.5 psi (upward)	2.5 psi (upward)	4.4.6.6	3.3.6***	No	
<b>D. DOWNCOMERS</b>							
1. Vertical	U	-0.6 kips*	-0.55 kips	4.2.3	3.3.1***	No	
2. Lateral							
a. Single	G	8.8 kips	8.8 kips	4.3.2.3	3.3.1	Yes	Additional Floor Reinforcement
b. Multiple	U	36.5 kips* per 10 downcomers	79.2 kips per 9 downcomers	4.3.2.4	3.3.1	Yes	Additional Floor Reinforcement

G: Generic DFFR Load

U: Generic DFFR method, plant unique load value.

\* Example loads derived from the generic analytical methods presented in DFFR reference. This is not a generic numerical load value.

\*\* This includes all pool swell during LOCA transient.

\*\*\* The design assessment analysis initially performed, utilized loads which are higher than those now indicated in the DAR. Analysis completed to date indicates that additional capability exist and that this load is not design controlling.

TABLE 2.1-1 (Cont'd)

LOAD DESCRIPTION	LOAD CLASS	LOAD MAGNITUDE		REFERENCES		DESIGN CHANGES	NOTES AND COMMENTS
		DFFR	DAR	DFFR	DAR		
II. SHW RELATED							
A. RAMS HEAD DEVICE							
1. Containment (average pressure on base mat)**							
a. Single Valve	U	+4.9/-1.0 psi*	+5.0/-1.0 psi	3.2.4.1.1	3.2.1.5	No	Filled RVV Pedestal with Reinforced Concrete Below Suppression Pool Water Level and Added Additional Reinforcement and Additional Pipe Supports
b. Asymmetric	U	+6.6/-1.6 psi*	+6.6/-1.6 psi	3.2.4.1.3	3.2.1.3	Yes	
c. ADS	U	+14.3/-4.3 psi*	14.3/-4.3 psi	3.2.4.1.2	3.2.1.4	Yes	
d. All Valves							
i) Symmetric	U	+24.6/-3.6 psi*	+24.6/-8.6 psi	3.2.4.1.4	3.2.1.2***	Yes	
ii) Resonant	U	+23.6/-6.5 psi	+23.6/-6.5 psi	3.2.4.1.4	3.2.1.2	Yes	
2. Submerged Structures							
a. Pipes	U	0.5 psi*	1.9 psi		3.2.3	Yes	Additional Pipe Supports may be required
b. Support Column	U	2.5 psi*	2.3 psi		3.2.2	No	
3. Tiedown Loads							
a. Horizontal	U	100 kips*	100 kips*	3.2.5	4.5	Yes	Additional pipe supports may be required
b. Vertical	U	70 kips*	50 kips*	3.2.5	4.5	Yes	Additional pipe supports may be required

\* Example loads derived from the generic analytical methods presented in DFFR reference. This is not a generic numerical load value.

\*\* These are pressure differential loads. Therefore, air pressure above the pool and hydrostatic water pressure must be added to these values to obtain the absolute pressure for design assessment.

\*\*\*The design assessment analysis initially performed, utilized loads which are higher than those now indicated in the DAR. Analysis completed to date indicates that additional capability exist and that this load is not design controlling.

2.1.4

LSCS-MARK II DAR

Rev. 7 1/89

### 3.0 LOADS CONSIDERED

In this section, it is intended to identify all the loads that are being considered in the LSCS design reassessment. In the next section, load combinations are identified and discussed. This section includes a brief summary of the original design loads, safety/relief valve discharge loads, and loss-of-coolant accident loads. Loads caused by safety/relief valve discharge and loss-of-coolant accidents are listed below for reference:

#### a. Safety/Relief Valve (SRV) Actuation

1. Original design loads such as weight, thermal, pump trip, valve closure, pipe internal pressure, and reaction loads are always considered (as appropriate) in addition to the other SRV loads.
2. Bubble-induced loads:
  - a) on containment structures;
  - b) on submerged structures; and
  - c) on piping, equipment, RPV, and internals.
3. Water jet loads:
  - a) on submerged structures, and
  - b) on wetted containment surfaces.
4. Second actuation loads.
5. Quencher SRV support loads.

b. Loss-of-Coolant Accident (LOCA) Loads

1. Original design loads such as weight, thermal, pump trip, valve closure, pressure and temperature transient in wetwell/drywell, subcompartments, pipe jet loads, and pipe reaction loads are always considered (as appropriate) in addition to the LOCA loads.
2. Water clearing loads:
  - a) on submerged structures;
  - b) on containment structures; and
  - c) on piping, equipment, RPV, and internals.
3. Air clearing loads:
  - a) on submerged structures;
  - b) on containment structures; and
  - c) on piping, equipment, RPV, and internals.
4. Pool swell loads:
  - a) drag loads,
  - b) impact loads, and
  - c) fallback loads.
5. Condensation oscillation loads:
  - a) on submerged structures;
  - b) on containment structures; and
  - c) on piping, equipment, RPV, and internals.
6. Chugging loads:
  - a) on submerged structures;

- b) on containment structures; and
  - c) on piping, equipment, RPV, and internals.
7. Downcomer lateral loads:
- a) static equivalent load, and
  - b) dynamic load.
8. Loads on drywell floor:
- a) downward differential pressure,
  - b) upward differential pressure, and
  - c) loads due to forces on downcomers and main vent bracing.
9. Annulus pressurization:
- a) on sacrificial shield,
  - b) on RPV and internals, and
  - c) on piping and equipment.

The original design loads, of course, are always considered to occur in combination, as appropriate, with the pool dynamic loads. It should be noted that these pool dynamic loads are relatively small compared to the original containment and reactor pressure vessel (RPV) design basis. Therefore, the original design contains adequate margin to accommodate these pool dynamic loads. These conservatisms are discussed in Section 8.0 of this report.

These additional pool dynamic loads are significant, however, when compared to the original design basis for the piping and equipment. Therefore, design modifications are being implemented in these areas which will allow these additional loads to be safely accommodated by meeting all code requirements. These modifications are discussed in Section 7.0 of this report.

This section provides the most recent load compilation and "road map" of the pool dynamic loads used for the reassessment. In some cases, this reassessment has not been completed, and in these cases, this section describes the methods that will be followed in the reassessment evaluation. This report together with the DFFR, FSAR, and the referenced reports constitute a complete basis for the design reassessment evaluation.

### 3.1 ORIGINAL DESIGN LOADS

The design basis of the LSCS structure, piping, and equipment was established before all pool dynamic loads were identified. Hence, this design basis must be reassessed for these newly identified pool dynamic loads in addition to the original design loads. The original design-basis loads for the structure, piping, and equipment are summarized in the following.

#### 3.1.1 Loads on the Structure

The following loads were used in the original design of the plant:

##### Operating-Basis Loads

- D - dead loads
- F - prestressing loads
- L - live loads
- T<sub>O</sub> - operating temperature loads
- R<sub>O</sub> - operating pipe reactions
- P<sub>O</sub> - operating pressure loads
- P<sub>t</sub> - containment test pressure
- E<sub>O</sub> - operating-basis earthquake
- W - wind load
- H - hydrostatic flood load

##### Safe Shutdown and Design-Basis Loads

- E<sub>SS</sub> - safe shutdown or design-basis earthquake
- W<sub>t</sub> - design-basis tornado
- H' - probable maximum flood load
- P<sub>a</sub> - accident pressure loads
- T<sub>a</sub> - accident temperature loads
- R<sub>a</sub> - pipe break temperature reaction loads
- R<sub>r</sub> - reactions and jet forces due to pipe break
- H<sub>a</sub> - postaccident flooding of the containment

Details of the above loads are given in Table 3.8-11 of the FSAR. A brief description of the loads is given below:

- D = Dead load of the structure, permanent equipment, soil, or hydrostatic pressure. Construction loading is considered as dead load for the construction combination.
- F = Loads resulting from the application of pre-stress.
- L = Live loads including any movable equipment loads, roof loads, and crane loads. Appropriate impact factors are included for moving loads.
- $T_o$  = Transient or steady-state thermal load on the structure at normal operation or shutdown conditions.
- $R_o$  = Pipe, cable pan, and duct reactions due to D,  $T_o$ , and unbalanced pressure.
- $P_o$  = Normal operating pressure differentials.
- $P_t$  = Containment test pressure.
- $E_o$  = Seismic excitation effects from the operating-basis earthquake (see FSAR Section 3.7), dynamic soil pressures, hydrodynamic pressures, and sloshing.
- W = Design wind velocity loads (see FSAR Section 3.3).
- H = Hydrostatic effects from the flood of record (see FSAR Section 3.4).

- $E_{ss}$  = Seismic excitation effects from the safe shut-down earthquake (see FSAR Section 3.7). including dynamic soil pressure, hydrodynamic pressures, and sloshing.
- $W_t$  = Design-basis tornado loads, including wind velocity pressure, atmospheric pressure change, and missile impact effects (see FSAR Section 3.3).
- $H'$  = Hydrostatic effects from the probable maximum flood or precipitation (see FSAR Section 3.4 and Subsection 2.4.3.1).
- $P_a$  = Maximum differential pressure defined by a postulated pipe break.
- $T_a$  = Effects of transient thermal load following a postulated pipe break. This includes  $\tau_o$  for all other areas not affected by the pipe break.
- $R_a$  = Effects of  $T_a$  on pipe and equipment reactions generated by a postulated pipe break. This includes  $R_o$  for all other areas not affected by the pipe break.
- $R_r$  = Local effects on the structure generated by a postulated pipe break. These loads include reactions from pipe supports and whip restraints, jet impingement, and missile impact.
- $H_a$  = Postaccident flooding of the containment.

### 3.1.2 Loads on Piping and Equipment

The following loads on the piping and equipment were considered in the original design bases. These loads and load combinations are generally consistent with current codes such as ASME B&PV III, Division 1, and Regulatory Guide 1.92. All loads are applied to the piping and analyzed to assure compliance to Section III of the ASME Boiler and Pressure Vessel Code, therefore assuring the pressure integrity of the piping. Functional capability of the piping will be evaluated in accordance with NRC Interim Technical Position provided in Table 3.1-1 and the additional criteria discussed in Subsection 3.9.3.1 of the LSCS-FSAR.

#### Weight

The sustained load consisting of the weight of pipe, contents, and insulation.

#### Thermal

A secondary, self-limiting load resulting from the constraint of the free end displacement of the piping system imposed by its rigid restraints.

#### Seismic

A dynamic load caused by the excitation of the piping by its restraints during an earthquake event. A more detailed explanation of the methodology used in this analysis can be found in FSAR Subsection 3.7.3.

#### Pressure

Stress induced in the pipe by the internal pressure on the pipe wall.

### Hydraulic Transient

A dynamic load on applicable systems due to appreciable and sudden changes in the mass flow rate in the piping system caused by sudden valve opening or closure, pump trip or pump startup.

### Pool Slosh Loads

The dynamic response of suppression pool water due to rigid body horizontal motion of the pool boundary resulting from a seismic event. The water velocities and accelerations induce hydrodynamic forces on submerged structures. These forces are composed of a pressure force on the pipe walls, velocity drag loads, and water inertia loads. The seismic loads used in design include all expected pool slosh loads. For a more detailed discussion of pool slosh loads, see Subsection 3.9.1.1.3.4 of the LSCS-FSAR.

TABLE 3.1-1

FUNCTIONAL CAPABILITY ACCEPTANCE CRITERIA  
(EQ. 9 OF NB-3652 AND NC-3652)

For all piping and classes,

$$D/t \leq 50,$$

where D = Outside Diameter

t = Wall Thickness

Class 1 Piping

for tees and branch connections,

Service Level D\*

all other piping,

Service Level C\*

Class 2, 3 Piping

for tees and branch connections,

Service Level C

for elbows,

Service Level B

or Service Level C when  $.8B_2$  is substituted for  $.75i$  and the lower of  $1.8 S_h$  or  $1.5 S_y$  is used for Service Level C allowable.

for curved and straight pipe, and all other piping

Service Level B

\*For austenitic steel use  $1.5 S_y$  for Service Level C limit and  $2.0 S_y$  for Service Level D limit.

### 3.2 SAFETY/RELIEF VALVE (SRV) LOADS

Actuation of safety/relief valves (SRV) produces direct transient loads on components and structures in the suppression chamber region and the associated structural response produces transient loadings on piping systems and equipment in the drywell region and reactor building. These transient SRV loadings are discussed in the following subsections.

Prior to actuation, the discharge piping of an SRV line contains atmospheric air and a column of water corresponding to the line submergence. Following SRV actuation, pressure builds up inside the piping as steam compresses the air in the line. The resulting high-pressure air bubble that enters the pool oscillates in the pool as it goes through cycles of overexpansion and recompression. The bubble oscillations resulting from SRV actuation and discharge cause oscillating pressures throughout the pool, resulting in dynamic loads on pool boundaries and submerged structures. These dynamic loads cause a dynamic structural response sufficient to affect piping systems and equipment in the containment and reactor buildings. The assessment of the affected systems for these responses is discussed in Section 5.0.

Steam condensation vibration phenomena can occur if high-pressure, high-temperature steam is continuously discharged at high-mass velocity into the pool, when the pool is at elevated temperatures. These steam quenching vibrations may result in loads on pool boundaries and submerged structures. This phenomenon is mitigated by maintaining a low pool temperature as discussed in Section 6.0.

The characteristics of the SRV actuation load vary depending on the piping configuration and the discharge device (rams head or quencher) located at the exit of the SRV line. Typically, the quencher device produces lower dynamic loads.

La Salle County Station utilizes a bounding load calculated for a rams head device as a design basis for structures, equipment, and piping systems which are not submerged in the suppression pool. A bounding quencher load is used for components submerged in the pool. To provide increased plant safety margins for containment SRV loads and to increase the threshold temperature for steam condensation vibration, SRV quencher devices will be installed in the plant.

Pool temperature transients for several postulated cases involving a stuck-open safety/relief valve are presented in Section 6.2. The calculated maximum pool temperature is a few degrees below the temperature threshold for steam condensation instability for a rams head discharge device.

In order to increase the margin between the calculated maximum temperature and this temperature threshold, it was decided to install a quencher device having a higher suppression pool temperature limit as reported in NEDE 21078, October 1975, rather than to perform additional testing with the rams head discharge device. The quencher device provides an additional benefit, since the peak amplitude of the containment structural load due to the oscillating air bubble are reduced below the corresponding design-basis values for the rams head device. Therefore, it was concluded that a quencher discharge device not only provides an increased margin for the pool temperature threshold limit, but that the plant will generally experience lower loads than those used in the rams head design basis.

The quencher device being used is the two-arm "T" quencher developed for the Mark II Susquehanna Plant by KWU. This device has been tested in a full-scale, single-cell facility as reported in Chapter 8 of the Susquehanna Design Assessment Report. The test facility is prototypical of the Mark II Susquehanna Plant. Parameters were varied to include a range of initial conditions and the longest and shortest lines at

the Susquehanna Plant. The tests were conducted to duplicate expected operating conditions, including first and subsequent actuations. The geometries and conditions tested closely resemble those for LSCS. These tests showed that the device will condense steam without high loads at pool temperatures above 200° F. In addition, the tests showed that the actual quencher loads are bounded by the design loads given in Chapter 4 of the Susquehanna DAR. Since LSCS is being assessed for these design loads, this again demonstrates the conservatism of the LSCS design.

Quenchers with four arms (X-quenchers) have been installed and tested at Caorso, a Mark II plant in Italy. This test included single valve first and subsequent actuations, multiple-valve actuations (up to eight valves), and an extended blowdown thermal mixing test. The results of these tests are reported in NEDE-25100 P, "Mark II Containment Supporting Program Caorso Safety Relief Valve Discharge Tests, Phase I Test Report" (May 1979), and by GE letter MFN-090-79 (L. J. Sobon to J. F. Stoly, March 1979). The measured loads were much less than those predicted by the analytical models in the DFFR. The increase in load from single to multiple valve discharge was less than that predicted. The extended blowdown indicated good mixing, with a final bulk to local temperature differential of about 10° F.

In the following subsections several current topics of licensing interest are discussed and the methods used to predict loads for the LSCS reassessment are summarized.

### 3.2.1 Design-Basis SRV Loads - Rams Heads

The design basis for reassessment of the structure, attached piping systems, RPV, and equipment is based upon dynamic loads calculated for a rams head discharge device. The SRV analytical model is described in NEDO-21061, Rev. 2 (Sept. 1976). The method

of application of this model is described in the following sections. These analytical models have been compared to results obtained from in-plant tests in the Mark I Monticello plant, and it has been demonstrated that these models conservatively bound the measured load magnitudes (NSC-GEN-0394, September 1977). This subsection is concerned only with the rams head design basis. A description of the T-quencher design method and a discussion of how it has been applied is in Subsection 3.2.2.

#### 3.2.1.1 Conservatism in SRV - Rams Head Methods

This subsection contains a summary of additional conservatisms in the suppression pool dynamic load definition for SRV discharge. The methodology is explained and summarized in NEDO 24070, October 1977.

First, it is important to recognize that a number of different SRV actuation cases have been investigated in order to select the conservative design cases used for plant reassessment. The SRV actuation cases investigated are identified and defined in Subsection 3.2.1.2. It was concluded from this investigation that the all-valve case, SRV-ALL, was the governing case. Furthermore, five cases were investigated in greater detail to select the maximum SRV-ALL loading condition which provides an adequate, conservative design-basis load. The all-valve cases are explained further in Subsection 3.2.1.2.4.

Second, since the SRV discharge loadings are of a dynamic nature, three separate key characteristics were bounded by appropriate definition of input assumptions for each load case. The three key characteristics are:

- a. load magnitude and its spatial distribution,
- b. frequency content for forcing function, and
- c. load duration.

As an aid in selecting the bounding input assumptions, sensitivity of the several dependent variables to the independent variables involved in both the SRV vent clearing and oscillating air bubble dynamics aspects of the problem were investigated. Tables 3.2-1 and 3.2-2 delineate the independent and dependent variables considered in these investigations.

Third, in order to define a conservative forcing function for each SRV discharge case, four major steps were applied for each case. A bounding, conservative approach was adopted for each of these steps. Thus, the resulting final forcing functions include the compounded conservatisms utilized in each step of their definition. The SRV discharge line clearing transient was determined such that the maximum discharge pressure was obtained. Maximizing the vent clearing discharge pressure produces bounding air bubble pressures, and hence, maximized wall loads. The analysis in each step in the load definition process was bounded and then used as input to the next step. In this manner the final load definition contains the multiplicative effects of several degrees of conservatism. The four major steps and the conservatisms used in each of the load definitions are listed below. The conservatisms for the structures are discussed in Subsection 8.1.2, and the conservatisms for the piping are discussed in Subsection 8.1.3.

a. Discharge Line Clearing Transient

1. The SRV mass flow rate was maximized by utilizing the spring setpoint instead of the relief setpoint ( $P_{\text{SPRING}} > P_{\text{RELIEF}}$ ) even in cases where this was physically not possible. Further, the ASME rated capacity was increased to 122.5% based on the most conservative selection of flow characteristic tolerances.

2. All friction losses in both the air/steam and water leg portions of the piping were included. A bounding value of the rams head discharge coefficient was also included. Thus, the resulting SRV discharge line pressures were maximized.
3. The rams head submerged depth, i.e., water column leg, was maximized by using the suppression pool high water level in the analysis.
4. In the asymmetric discharge case, the maximum predicted water column recovery height was utilized to maximize the water column leg for the valve undergoing the second actuation. The normal maximized water column height was utilized for the adjacent valve.

b. Oscillating Air Bubble Dynamics

1. Each rams head was assumed to form a pair of single, spherical bubbles. No interaction with piping or structures was considered, hence only bubble escape through the pool surface terminated the loading condition. This increased the load duration.
2. Individual SRV discharge line characteristics were considered to maximize the load duration and frequency content.
3. Dissipation of bubble energy was not allowed.
4. A 15%-20% variation of bubble frequency due to changing hydrostatic pressure during bubble rise was included in the analyses.

c. Pool Geometry

1. The effects of the rigid boundaries on the pressure loading in the pool were included. This produces enhancement of the loads, especially near the containment wall.
2. The effects of the free surface on the pressure distribution were included.
3. The vertical translation and the resulting time-dependent spatial distribution of the wall loads were included in the analyses.

d. SRV Actuation Load Case

1. Four SRV actuation conditions were used in the containment design, and each load condition was investigated separately to maximize loads on structures and components. The SRV actuation conditions (i.e., SRV load combinations) used for containment design are listed as follows for convenience: (1) SRV(ALL), (2) SRV(ADS), (3) SRV(ASY), and SRV(1). Several load definitions were studied for SRV(ALL), and the most severe loading case was selected for containment design.
2. For each load case the load magnitude, frequency content, and load duration were maximized. This ensured that the dynamic nature of the forcing function was addressed and that a limiting set of its characteristics was selected.
3. The selected forcing functions were defined to ensure that both the vertical and horizontal load components were maximized.

4. For all multiple SRV actuation cases, the contribution to the loading from each SRV line was linearly summed.

Since there are a number of conservatisms in the bounding load definition in addition to the conservatisms in the application of this bounding load, it is concluded that dynamic loads caused by SRV discharge from a rams head provide a conservative design basis for plant reassessment.

Results from the KTG full-scale tests (Section 8, Susquehanna DAR) have demonstrated that increased plant safety margins will be achieved if a quencher device is installed in the containment: (1) a higher suppression pool temperature limit, as reported in NEDE 21078, will provide increased plant safety margin for postulated transients such as a stuck-open-relief valve; and (2) reduced bubble pressure loads on containment structures and submerged piping will also result in increased plant safety margin for SRV actuation during postulated plant transients. Therefore, SRV quencher devices are installed and an in-plant SRV test will be performed. This provides sufficient timely resolution of all licensing issues related to SRV actuation.

#### 3.2.1.2 Safety/Relief Valve Discharge Cases

A large number of potential rams head SRV discharge cases were considered in the process of selecting a set of realistic bounding load cases. These cases and the assumptions and conditions associated with them are described here. The corresponding quencher discharge cases are described in Subsection 3.2.2.1.

##### 3.2.1.2.1 Single Valve Actuation

The single SRV discharge loading case is required to account for the actuation of an SRV. Since it is conservatively assumed that any of the 18 SRV's may discharge, the line which produces the largest structural load was chosen to define the load

magnitude. This load magnitude is conservatively assumed to apply to any single SRV. This load condition is provided for use in the required load combinations specified in Section 4.0.

#### 3.2.1.2.2 Asymmetric SRV Actuation

The asymmetric loading case is described in Section 3.2.4.1.3 of the DFFR. The asymmetric SRV discharge loading for LSCS involves the actuation of two lines whose discharge devices are adjacent. The loading situation is constructed by first considering a low-setpoint SRV which is cycling. Then, it is assumed that, coincident with the second actuation of the cycling SRV, an adjacent SRV line is actuated. Specific line characteristics were considered for both discharge lines. A vacuum breaker system for the discharge line was evaluated to determine the water column recovery height in the line with the cycling SRV. A partial vacuum resulting from steam condensation in that vent line permits the water column to rise momentarily in the vent line to a height greater than the submergence depth of the vent line. Even though the vacuum breaker system is sized to minimize the recovery height of the water column, this conservative assumption (using the maximum water column recovery height) results in a bounding load for asymmetric SRV actuation.

#### 3.2.1.2.3 Automatic Depressurization System (ADS)

The ADS valve loading case is described in Section 3.2.4.1.2 of the DFFR.

The automatic depressurization system consists of seven valves which discharge at the rams head locations shown in Figure 3.2-4. The seven ADS valves are located nearly symmetrically and actuate simultaneously at the same system pressure. A conservative upper bound for the system pressure of 1250 psig was selected. This pressure corresponds to the highest spring

setpoint and maximizes the SRV mass flow rate. The specific individual line characteristics (length, friction factor, etc.) were used in the load evaluation.

The all-valve case produces a larger containment load than the ADS actuation. The ADS actuation loading is provided for load combinations which include IBA and SBA line breaks.

#### 3.2.1.2.4 All Valve Discharge Cases

When multiple SRV vent lines discharge into a suppression pool, the relative timing among the air bubbles' dynamics depends on individual characteristics of the valves and lines involved. In the calculation of dynamic loads, the following factors may be taken into account for various postulated discharge cases:

- a. Main steam supply pressure transient.
- b. SRV pressure setpoint.
- c. Vent line characteristics (length, diameter, equivalent friction factors, etc.).
- d. Initial conditions in the line.

The supply pressure (including its time rate of increase) and SRV setpoint determine the actuation time for each valve. The line characteristics and initial conditions determine line clearing time as well as bubble formation times and dynamics (bubble pressure, radius and depth versus time). Appropriate vent clearing times are calculated by using the vent clearing model provided in Reference 1. The line clearing time is accurately calculated as demonstrated by a predicted clearing time of 240 ms compared to a range of 200-300 ms indicated by test data (Reference 2) for the same clearing transient. The valve flow rate was calculated using a conservative method which gives flow 22.5% higher than expected. A conservatively short valve opening time is also used which will maximize the bubble pressures.

The bounding load approach taken in design assessment calculations is to postulate a number of conceivable discharge situations, then mechanistically calculate the suppression pool loading functions for each case, and finally select the bounding case on the basis of the load function or its structural response. The bounding discharge case usually varies depending on the configuration of the loaded structure. That is, major structural loads on the pedestal, base mat and containment are often bounded for a different discharge case than are loads on submerged structures, such as support columns, downcomers, and SRV vent lines themselves. The discharge cases must also include bounding structural loads for forces in the vertical and horizontal directions as well as bounding "rocking" moments. Mechanistic calculations include individual vent line transients, air bubble dynamics, and the load factors which relate bubble dynamics to pressure or drag forces on specific structures. Each calculation is unique to each plant, structure and discharge case.

The following discharge cases have been considered in design reassessment as reported in this section:

a. Simultaneous Bubble Discharge

A single pressure-time history corresponding to the SRV line giving the maximum bubble pressure is used. All 18 bubble pairs are identical. SRSS is used to simultaneously combine the effect of all the bubbles.

b. Symmetric Discharge

Simultaneous firing of all 18 valves. The bubble pairs are all unique and are not in phase. The effect of each bubble pair is combined by the SRSS method and the effect of each line is then added linearly.

c. Ganged Sequential Discharge

All 18 lines are discharged in accordance with their

given pressure relief setpoints for a linear RPV pressure transient. The maximum anticipated RPV pressure ramp rate of 136.4 psi/sec is used. The bubble pairs are all unique and out of phase. The effects of the bubbles are combined as in (b) above.

d. Continuous Sequential Discharge

All 18 lines are discharged in accordance with 18 different relief setpoints which could occur due to setpoint drift. The "drift" is assumed to cause all 18 setpoints to be equally spaced (in pressure) over the duration of SRV discharge. A linear RPV pressure transient is used. The maximum anticipated RPV pressure ramp rate of 136.4 psi/sec is used. The bubble pairs are all unique and out of phase. Their effects are combined as in (b) above.

e. Resonant Sequential Symmetric Discharge

All 18 lines are discharged in accordance with their given pressure relief setpoints for a linear RPV pressure transient. This case is reported in Subsection 3.2.1.2.2. These setpoints are equally spaced in pressure. The period of oscillation of the first bubble pair in the pool is determined. The RPV pressure ramp rate is then chosen such that the period between actuation of adjacent relief setpoints equals the oscillation period of the bubbles in the pool. In this manner, an effort is made to cause the discharge of subsequent relief valves to be in "resonance" with the bubbles in the suppression pool. Variations of the pressure ramp rate or value setpoint will generally result in bubbles further out of phase, since these variables have been chosen within an allowable range to be as closely phased as possible. The effects of bubble pairs are combined as in (b) above.

As described above, five all-valve discharge cases were considered before selecting the one (symmetric discharge) that is judged to

to produce the most severe structural response.

Thus, several mechanistic methods were used to determine five all-valve load trials. By considering five SRV<sub>(ALL)</sub> discharge cases which utilize worst-case mechanistic assumptions and conservative load methodology, it is judged that this procedure results in a conservative and appropriate SRV load for design reassessment. SRV<sub>(ALL)</sub> Case b referenced above gives a loading condition that is judged to produce the most severe structural response.

#### 3.2.1.2.5 Second Actuation

On October 11, 1977, the NRC was notified by General Electric of a reportable condition involving the transient analysis prediction of the sequence and number of relief valves expected to operate following a reactor isolation event.

To investigate the effects of second actuation, a plant-unique analysis was performed. Table 3.2-5 lists the assumptions used in the analysis, and Table 3.2-6 shows the number of valves actuated on each lift. Since the initial pressure falls in the range of the ATWS high-pressure recirculation pump trip (1135 to 1165 psia), cases with and without the pump trip are given. Note that the case with the pump trip is more severe and that the pressure on the second and third peaks is within 1 psi of actuating another group of valves. Figure 3.2-1 is a pressure versus time plot without the recirculation pump trip, and Figure 3.2-2 is a similar plot with the pump trip.

For further information, the transient model used in this analysis assumes a single, spatially uniform pressure in the vessel. The fluid in the vessel is divided into five homogeneous nodes. Four nodes contain liquid or liquid vapor mixture, with two inside the shroud and two outside. A steam dome of saturated vapor fills the remainder of the vessel. There are

two sources of heat: (1) the stored and decay heat from the fuel, and (2) the stored heat from the metal within the vessel. The relief valve modeling includes the following for each group of relief valves: opening and closing setpoint, opening and closing relief valve delay times, opening and closing relief valve stroke times, and the flow rate at the opening pressure. The water level within the vessel is tracked, and the auxiliary systems such as HPCS and RCIC are activated when their level setpoints are reached.

In addition, the following two mitigating approaches were also investigated: (1) varying of relief valve setpoint, and (2) the setdown of relief valve closure to assure only one relief valve is actuated for a second time. The results of this analysis are shown in Table 3.2-4 and Figure 3.2-3.

With the incorporation of SRV quencher devices, the loads are reduced sufficiently to eliminate concern over multiple subsequent actuation. As described in Section 3.2.2.1, the KWU/SRV load definition includes the effect of subsequent actuation. Furthermore, the "GE Low-Low Setpoint Logic" (FSAR Subsection 7.3.1.1.1.2.10, Amendment 48) is used to prevent multiple valve subsequent actuation from occurring following a reactor isolation event.

### 3.2.1.3 Safety/Relief Valve Boundary Loads

The submerged portion of the suppression pool is divided into nine zones for analysis purposes. The specific pool geometry and the definition of the nine zones are shown in Figure 3.2-5. The forcing functions for the containment walls and base mat are specified by determining the time history of the spatially averaged pressure for each zone. For example, the forcing function for Zone 4 (on the base mat) was calculated by determining the point pressures for a grid of several hundred points on the entire submerged structure.

Next, the integral from a radius of 15 feet to a radius of 2.45 feet for a full  $2\pi$  radians of the pressure distribution is evaluated for a series of points in time.

#### 3.2.1.4 Submerged Structure Loads

The oscillating SRV bubble will cause fluid motion in the suppression pool, causing structures in the pool to be subjected to drag loads. Standard and acceleration drag are calculated using the analytical methods documented in Reports NEDO/NEDE 21471-P, NEDO/NEDE 21472, and NEDE 21730. Loads are calculated for all structures in the pool by subdividing the structure and evaluating the characteristics of the flow at the center point of each segment.

#### 3.2.2 Assessment For SRV Loads - T-Quencher

Although the loads expected with quencher are lower in magnitude than those predicted with the rams head, changes in the discharge device locations and differences in the applicable load definitions required an assessment to confirm the adequacy of the design.

##### 3.2.2.1 Conservatism of the T-Quencher Load Definition

A T-quencher load definition has been developed by KWU. This load definition is documented in Chapter 4 of the Susquehanna DAR. This load definition is based on actual pressure-time histories of single valve discharges. These pressure time histories include subsequent actuations. Conservatism is added by increasing the amplitude (by using a 1.5 multiplier) and expanding the frequency range (to include all significant frequencies from 3.4 to 10 hertz). The KTG single cell tests (reported in Chapter 8 of the Susquehanna DAR) confirm the conservatism of this load definition. Additional conservatism is added when the spatial load distribution for the SRV

cases (as discussed in Section 3.2.2.2) is also applied conservatively.

The T-quencher methodology includes cases corresponding to the rams head cases described in Section 3.2.1.2. A specific subsequent actuation case is not defined, since the data used to form the load definition includes subsequent actuation cases.

#### 3.2.2.2.1 Single Valve

The load distribution on the containment walls for a single valve actuation is shown in Figure 4-26 of the Susquehanna DAR. This load is better described as a subsequent actuation of a single valve.

#### 3.2.2.2.2 Asymmetric SRV Load

The asymmetric quencher load is defined as a three-valve discharge rather than the two-valve discharge used in the rams head asymmetric load. Although this condition is not realistic, it gives a maximized asymmetric distribution as depicted in Figure 4-25 of the Susquehanna DAR.

#### 3.2.2.2.3 Automatic Depressurization System (ADS)

Figure 4-27 of the Susquehanna DAR shows the ADS pressure distribution. This distribution was constructed by combining single-valve discharge loads at typical quencher locations. This would yield the expected distribution of more or less evenly spaced peaks, but because of a conservative increase in the azimuthal angle of the single valve load, this results in an almost uniform distribution. For conservatism and simplicity, the all-valve distribution is used.

#### 3.2.2.2.4 All-Valve Discharge

The all valve T-quencher discharge case is defined as the single valve discharge load applied uniformly throughout 360°. The physical interpretation of this load would be a subsequent actuation of all valves, with all bubbles entering the pool simultaneously and oscillating in phase.

#### 3.2.2.3 Quencher Boundary Loads

The above described quencher load definitions have been applied to the suppression pool wetted boundaries to assess the structure, piping and equipment. This assessment is documented in Subsection 4.4.2.3.

#### 3.2.2.4 Quencher Submerged Structure Loads

Submerged structure loads are affected by geometry changes in the pool because these loads are basically local loads. The change in discharge device location was assessed by using the rams head submerged structure methodology with appropriate quencher pressure amplitude, frequencies and bubble locations corresponding to the new locations of the KWU quencher. The bubble pressure amplitude is determined for both first and subsequent actuation using the correlation in NEDO 21061 Rev. 3 (DFFR). The bubble frequency range is reported in Subsection 3.2.2.1.

#### 3.2.3 Assessment of NRC Acceptance Criteria - SRV

The original design methods and the design reassessments described in the above sections address all the NRC concerns in the Lead Plant Acceptance Criteria (NUREG-0487). An itemized list of the LSCS response to the NRC Acceptance Criteria is contained in Subsection 3.4.

TABLE 3.2-1

SRV DISCHARGE LINE CLEARING TRANSIENT PARAMETERIZATIONINDEPENDENT PARAMETERS CONSIDERED

SRV pressure setpoint  
SRV opening time  
SRV mass flowrate  
Discharge line length  
Discharge line submergence depth  
Discharge line diameter  
Equivalent friction factor  
Initial line pressure and density

DEPENDENT VARIABLES CONSIDERED

Pressure at SRV exit  
Pressure at discharge line exit  
Density at discharge line exit  
Water velocity at discharge line exit  
Vent clearing time

TABLE 3.2-2

SRV BUBBLE DYNAMICS PARAMETERIZATIONINDEPENDENT PARAMETERS CONSIDERED

Initial pressure  
Initial density  
Air inflow rate  
Duration of air discharge  
Initial bubble radial velocity  
Initial bubble radius

DEPENDENT PARAMETERS CONSIDERED

Bubble pressure  
Bubble radius  
Bubble frequency  
Bubble duration

TABLE 3.2-3

SECOND ACTUATION ASSUMPTIONS\*

1. The initiating event is a 3-second closure of all MSIV's with position scram at 105% NB rated steamflow.
2. Nominal relief valve opening setpoints are used:  
2 valves @ 1091 psia, 4 valves @ 1101 psia, 4 valves @ 1111 psia, 4 valves @ 1121 psia, and 4 valves @ 1131 psia.
3. The maximum expected relief capacity of 122.5% ASME rated is used.
4. The delay from reaching the relief valve opening pressure to start of valve motion is 0.4 second for Crosby type valves. The 0.4 second includes the pressure sensor delay.
5. The relief valve opening stroke time is 0.15 second.
6. The pressure differential between relief valve opening and closing setpoints is 50 psi.\*\*
7. ANS 5 + 20% decay heat is used.
8. If applicable, the effect of the ATWS high pressure recirculation pump trip is considered.

---

\* These assumptions were used for this preliminary conservative bounding analysis.

\*\* For Case 3 of Table 3.2-4, the pressure differential between opening and closing setpoints is 100 psi for all valves.

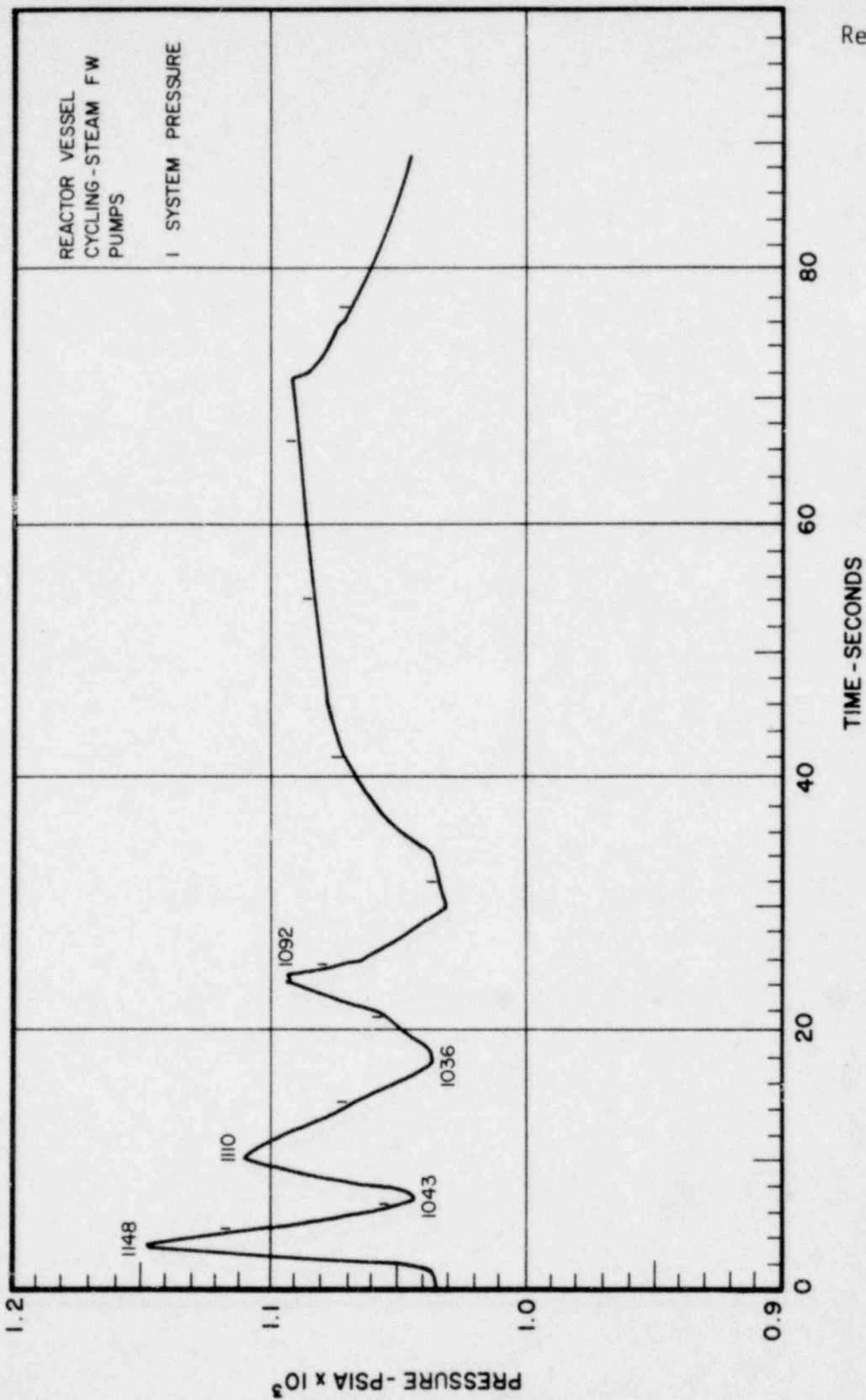
TABLE 3.2-4

SECOND ACTUATION RESULTS\*

<u>CASE</u>	FIRST POP		SECOND POP		THIRD POP		
	<u>Peak Pressure (PSIA)</u>	<u>Number of Valves</u>	<u>Peak Pressure (PSIA)</u>	<u>Number of Valves</u>	<u>Peak Pressure (PSIA)</u>	<u>Number of Valves</u>	
ATWS RPT off	1	1148	18	1110	6	1092	2
ATWS RPT on	2	1148	18	1120	10	1100	2
Mitigating Approach**	3	1148	18	1102	6	1093	2

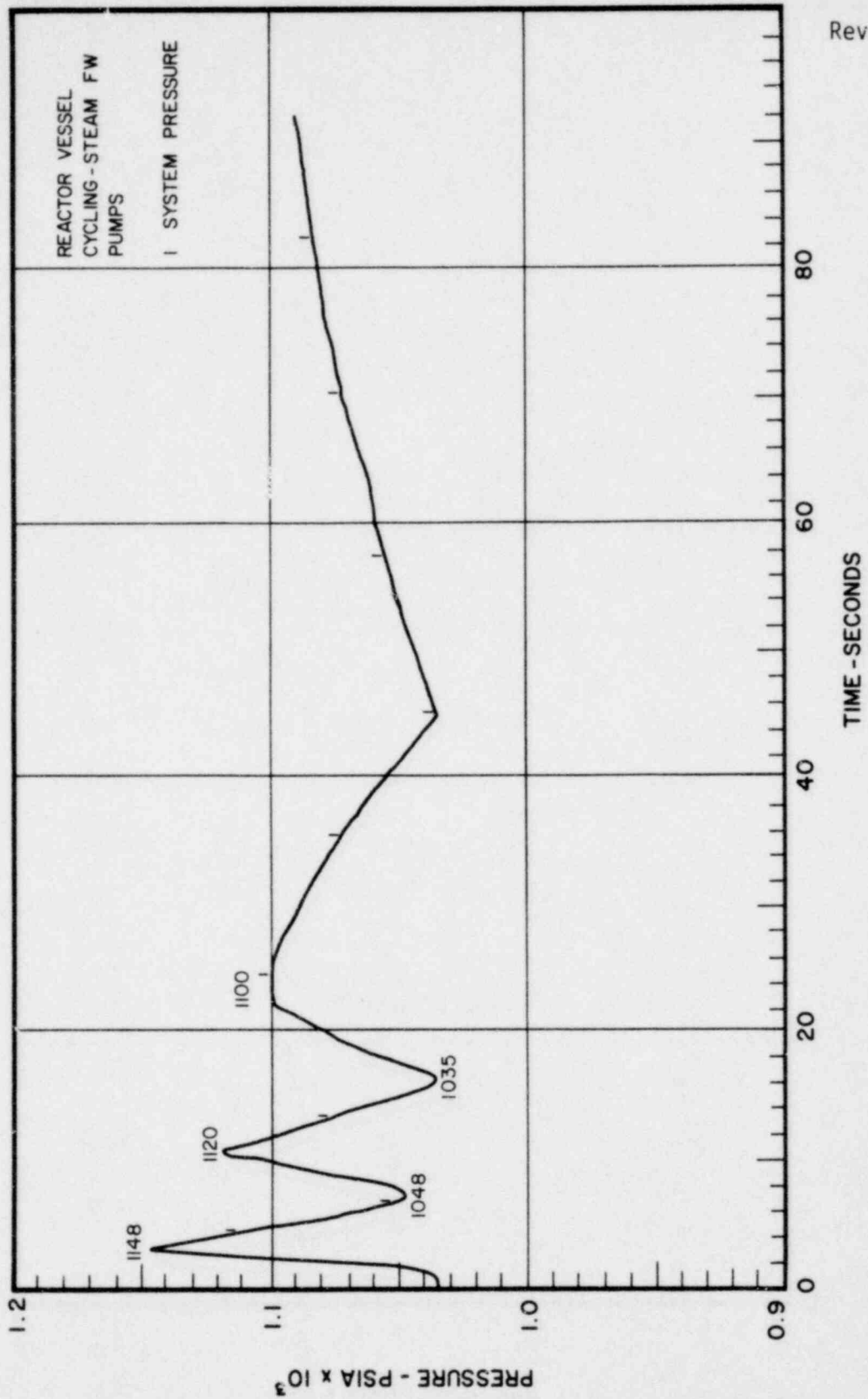
\* These are for information only and not for design purposes.

\*\* The pressure differential between opening and closing setpoints is 100 psi for all valves.



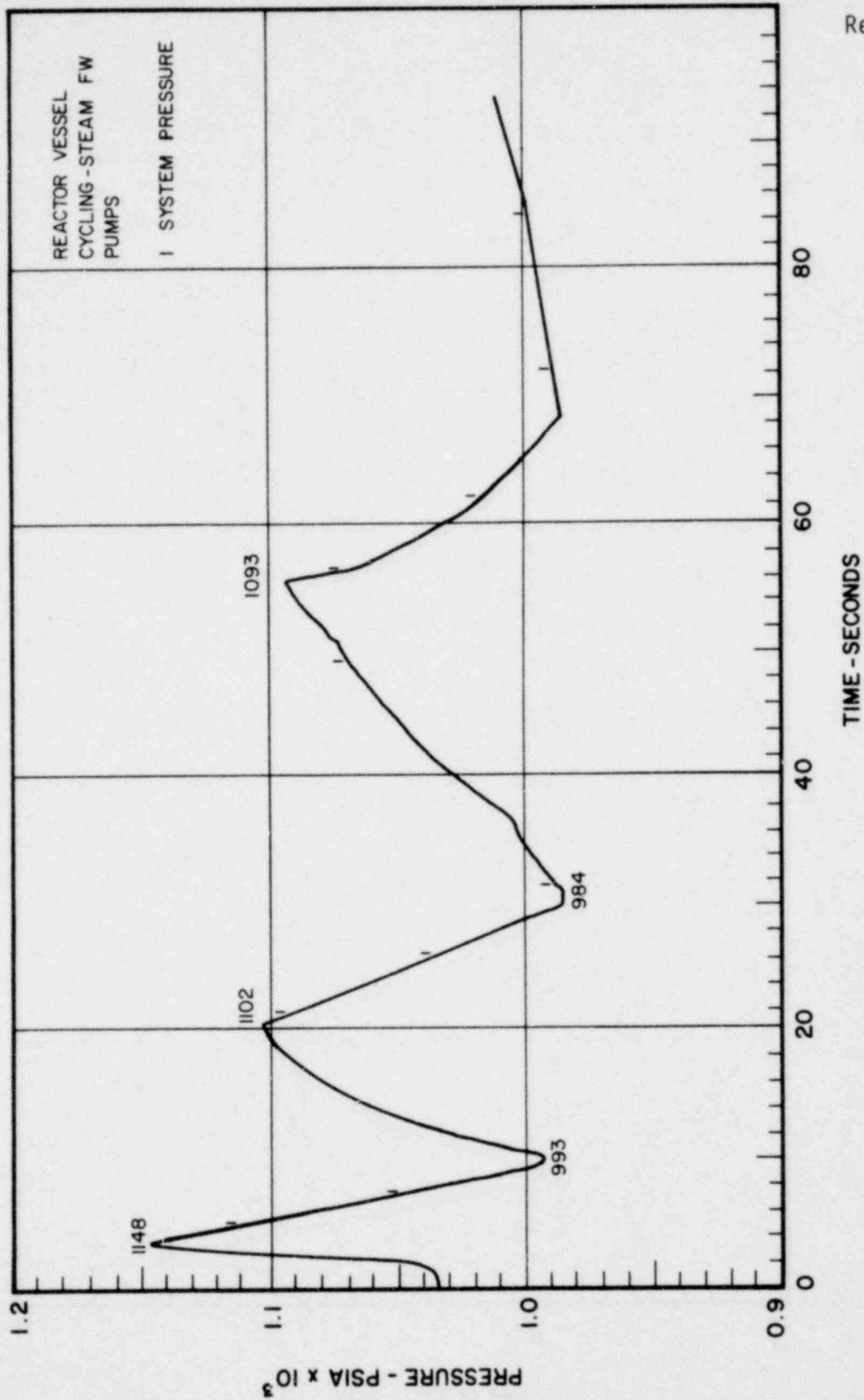
LA SALLE COUNTY STATION  
MARK II DESIGN ASSESSMENT REPORT

FIGURE 3.2-1  
SECOND ACTUATION - ATWS PUMP TRIP OFF



LA SALLE COUNTY STATION  
MARK II DESIGN ASSESSMENT REPORT

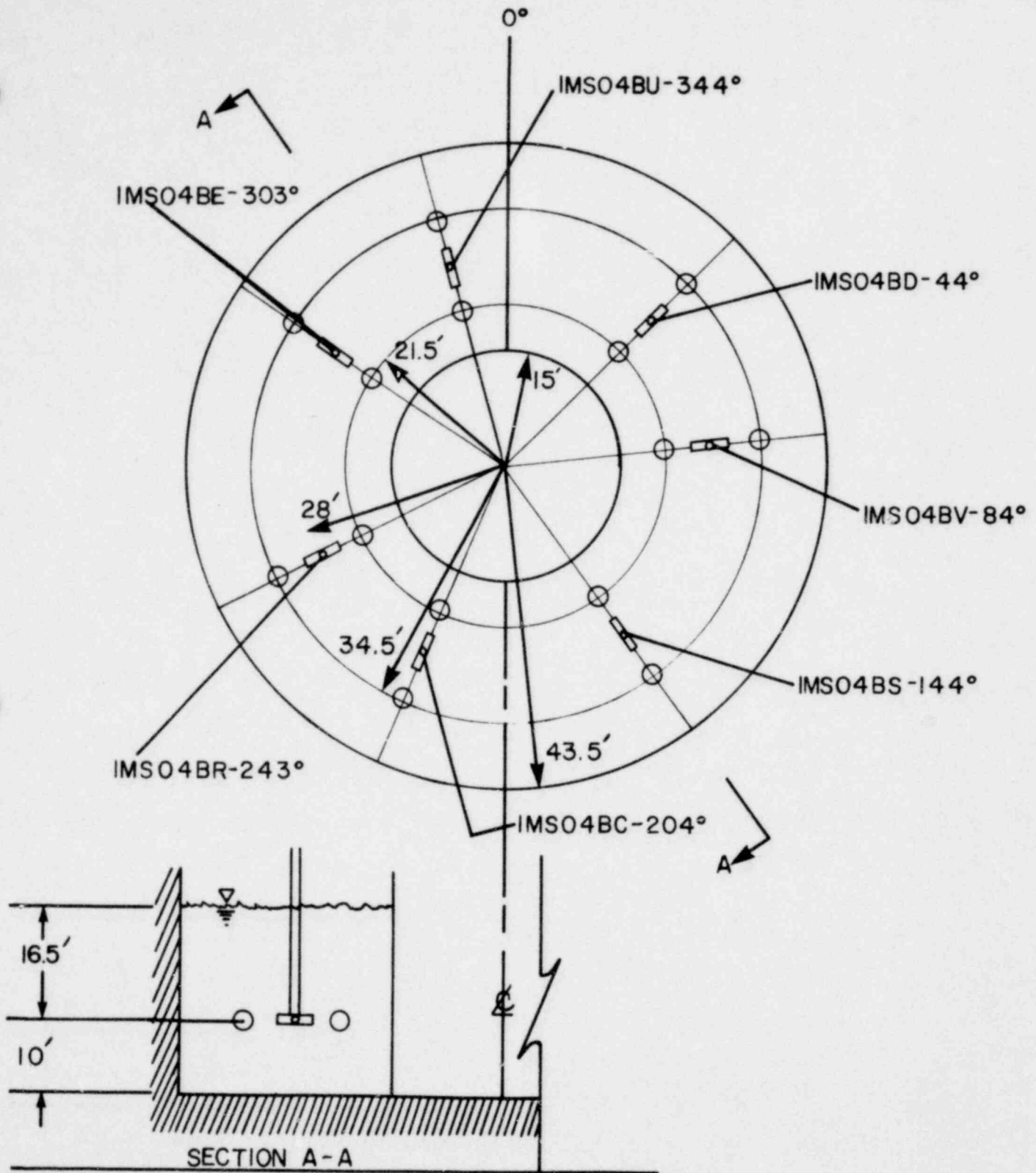
FIGURE 3.2-2  
SECOND ACTUATION - ATWS PUMP TRIP ON



LA SALLE COUNTY STATION  
MARK II DESIGN ASSESSMENT REPORT

FIGURE 3.2-3

SECOND ACTUATION - MITIGATING APPROACH



NOTES:

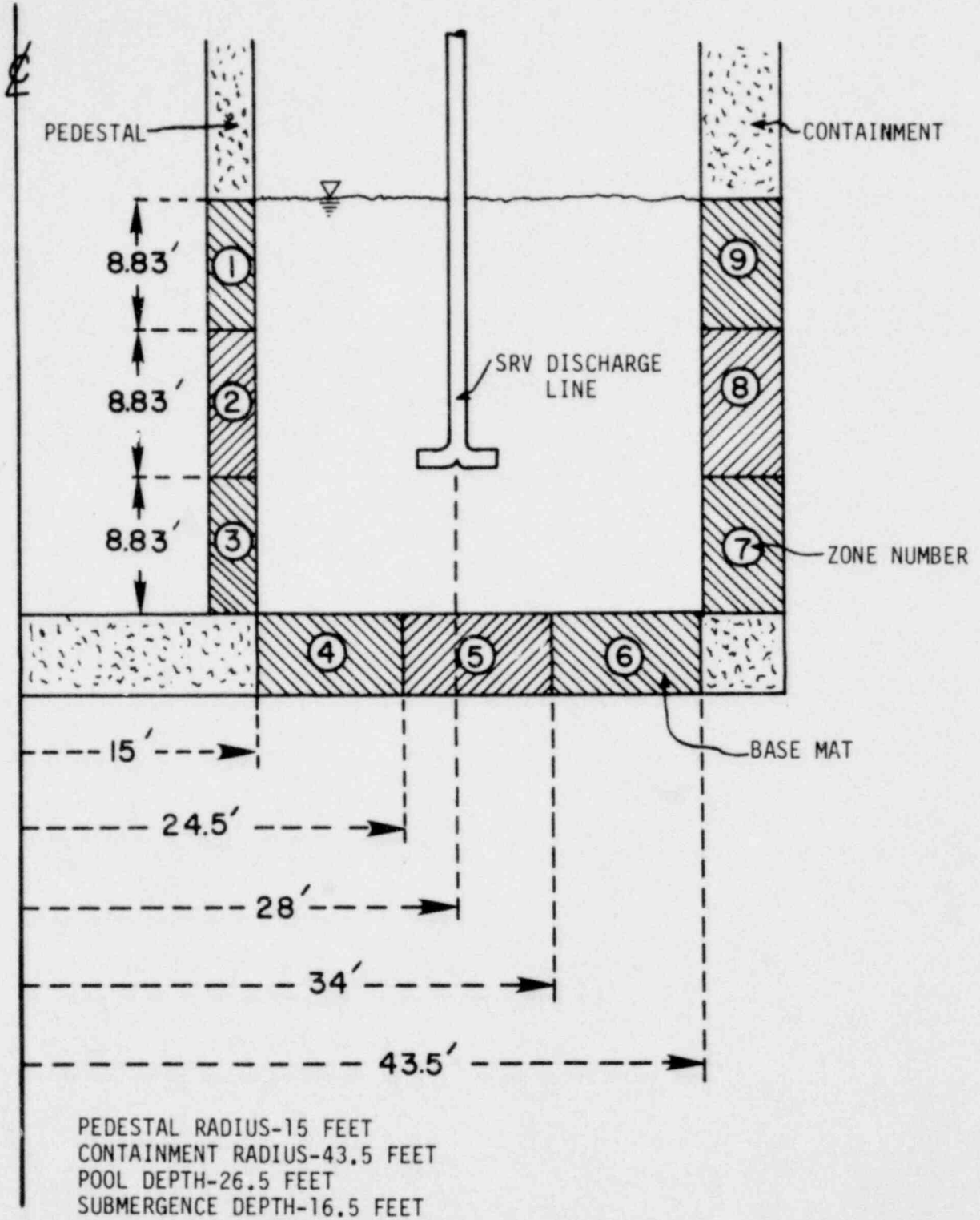
1. NOT TO SCALE.
2. RAMS HEADS ARE ORIENTED RADIALLY.
3. AUTOMATIC DEPRESSURIZATION SYSTEM ACTUATION (7 SRVs SIMULTANEOUS DISCHARGE).

LA SALLE COUNTY STATION

MARK II DESIGN ASSESSMENT REPORT

FIGURE 3.2-4

ORIENTATION OF SRV DISCHARGE LINE  
DEVICE FOR AUTOMATIC DEPRESSURIZATION  
SYSTEM ACTUATION



NOTE: DRAWING NOT TO SCALE

<b>LA SALLE COUNTY STATION</b> MARK II DESIGN ASSESSMENT REPORT
FIGURE 3.2-5 CROSS-SECTION OF SUPPRESSION POOL AND DEFINITION OF SUPPRESSION CHAMBER WALLS' LOADING ZONES

### 3.3 LOSS-OF-COOLANT ACCIDENT (LOCA) LOADS

Depending upon the rate of mass release into the drywell, LOCA events may be classified as design-basis accidents (DBA), intermediate break accidents (IBA), or small break accidents (SBA). In all cases, the wetwell and drywell will become pressurized. Typical temperatures and pressure transients are given in Figures 3.3-11 through 3.3-18. The original containment design adequately withstands loading due to these pressure and temperature transients.

In addition to the pressure and temperature transients that were considered in the original design bases, certain pool dynamic loads have also been identified to occur during a postulated LOCA. These loads are described in the following subsections.

Following a postulated LOCA, the drywell pressure increases due to blowdown of the reactor system. Pressurization of the drywell causes the water initially in the vent system to be accelerated out through the vents. During this water expulsion process, the resulting water jets cause impingement and drag loads on local containment structures.

Following vent clearing, an air/steam bubble forms at the vent exit which causes a hydrostatic pressure increase in the pool water resulting in a loading condition on the pool boundaries. The steam condenses in the pool. However, the continued addition and expansion of the drywell air causes the pool volume above the elevation of the vent exit to rise, resulting in a rise of the pool surface. This phenomenon is referred to as pool swell. Upward motion of this slug of water creates a drag load on structures submerged in the pool and impact loads on unsubmerged structures located just above the initial pool surface. Before the pool has risen 1.5 times the initial submergence of the main vents, the rising

slug of water breaks apart. Subsequent pool swell involves a two-phase air/water froth which may produce further structural-impingement loads near the elevation of the maximum pool swell height. This entire process affects only those structures between the pool surface and a maximum height of 1.5 times the initial submergence of the main vents. A gravity-induced fallback of the pool returns the pool surface to the original elevation. At the time of maximum pool swell height, the drywell floor can be subjected to an upward load due to an imbalance in pressure between the compressed air in the wetwell free air space and the air-purged drywell volume. The capability of the drywell diaphragm floor to withstand these pressure transients is discussed in Section 5.1 of this report.

Following the pool swell transient, there will be a period of high steam flow through the main vent system. At these high steam flow conditions, the water/steam condensation interface oscillates due to bubble growth and collapse. These condensation oscillations result in an oscillatory load on the pool boundary. At low vent flow rates, the water/steam condensation interface can oscillate back and forth in the vents, causing "chugging." The chugging action results in loads on both the downcomer vents and the containment boundaries.

The major Mark II-related experimental programs which confirm the design-basis load include the 4T full-scale, EPRI 1/13-scale, and PSTF 1/3-scale tests as referenced in Table 1.0-1.

The temporary tall test tank (4T) facility consists of a single cell representative of a typical Mark II containment. The test facility utilized a single full-size vertical downcomer in a tank. A total of 46 steam blowdown tests were conducted by GE in this full-scale facility during a test program consisting of three phases (NEDE 13442-P-01 and NEDE 13468-P). These tests provided the primary data source from the DFFR LOCA pool dynamic loads, including those related to pool swell (NEDE

21544-P), wetwell pressurization, vent flow, pool thermal response, condensation, and chugging (NEDE 23617-P). The test matrix included a range of vent submergence, break size, vent size, blowdown fluid, vent bracing, and initial conditions to reflect Mark II plant-to-plant differences.

Test results from the General Electric pressure suppression test facility (PSTF) supplied the data base for pool impact loads on representative small containment structures, including pipes, I-beams, and grating. Impact pressures versus pool velocity correlations were developed from these data, which are used in combination with calculated pool swell velocities and 4T data to establish the Mark II impact loads. The impact load data were obtained from PSTF test series 5805.

The Electric Power Research Institute (EPRI) Mark II test facility consists of a 1/13-scale model of a typical Mark II containment system. The facility contains 21 vents and represents a 90° sector of the suppression chamber, including the pedestal region. The EPRI tests consisted of air-charged tests in contrast to the 4T steam blowdown tests. About 90 tests were performed by Stanford Research Institute for EPRI to provide data related to Mark II pool swell phenomena (EPRI NP-441). Specifically, data from these tests were used to verify the adequacy of the 4T unit cell approach to study pool swell phenomena, validate the 4T air/steam tests, and validate the DFFR pool swell analytical model.

In addition to the above test programs, the Mark II owner's group has provided information relating to tests conducted outside the scope of the Mark II program to support some of the loads specified in the DFFR. This includes data for steam blowdown tests from the Marviken test facility and data resulting from tests in GE foreign licensee single and multivent, large-scale facilities. Data from these tests were used in

the Mark II program to support the conservatism of single-vent tests for vent lateral loads and pool boundary chugging loads.

### 3.3.1 Design-Basis LOCA Loads

The loads described in this section are those used to design the containment structure, piping and equipment. Section 3.3.2 describes assessments made to ensure that the design is adequate when the NRC Lead Plant Acceptance Criteria (NUREG-0487) are applied.

#### 3.3.1.1 Load Definitions

This section describes the load definitions which comprise the original LSCS design basis.

##### 3.3.1.1.1 LOCA Water Jet Loads

Structures located near the projected area of the downcomer vent, which is about 2 feet in diameter, will experience a water jet impingement load acting along the jet axis during the vent clearing process. The jet will flow around structures less than 2 feet wide and cause drag load. For larger structures, the significant load will be due to impingement. The maximum velocity of the jet is 60 ft/sec; its dispersion angle is given in Figure 3.3-2 (Reference 1).

##### 3.3.1.1.2 LOCA Charging Air Bubble Load

As the drywell air is forced into the wetwell, bubbles will grow at the vent exits. These bubbles will grow until they touch and pool swell begins. Submerged structures and boundary loads calculated during this portion of the event are generally much less than loads during other phases.

### 3.3.1.1.3 Pool Swell

The pool swell transient is conservatively predicted by MKII-SWELL (Sargent & Lundy implementation of PSAM described in Reference 1). During pool swell, structures initially above the vent exit and below the maximum pool swell height (1.5 times vent submergence) will be loaded by drag loads. Structures initially above the pool may experience impact loads. The compression of the wetwell air space will result in an upward force on the drywell floor.

### 3.3.1.1.4 Pool Fallback

During fallback, the air mixes with the pool water slug and greatly reduces or eliminates drag loads. However, it is conservatively assumed that the slug remains intact and falls back into the pool under the force of gravity, causing drag loads.

### 3.3.1.1.5 Condensation Oscillation

Following the pool swell transient, steam flows through the main vent system into the suppression pool, where it condenses. Evaluation of the steam-condensation phase of the 4T test results revealed the existence of a dynamic load during high steam mass flux into the suppression pool. This load, called condensation oscillation, is a low-amplitude, symmetric, pseudo-sinusoidal pressure fluctuation occurring over a range of frequencies.

The LSCS containment and piping and equipment in the containment and reactor building have been evaluated for the following load definition:

Magnitude  $\pm 3.75$  psi

Frequency 2 to 7 hertz

### 3.3.1.1.6 Chugging

Condensation oscillation occurs during the high mass flux phase of a transient. At later times (or for smaller breaks), the steam mass flux will be lower. Under these conditions, the water/steam condensation interface can oscillate in the vents, causing "chugging." The chugging action results in lateral loads on downcomer vents and also in dynamic pressure loads on the wetted containment boundary. These boundary loads produce structural responses in the containment and in the reactor building.

The application of bounding chugging loads is described in the "Mark II Phase I - 4T Tests Application Memorandum," submitted to the NRC in June 1976. This application memorandum is currently being used for LSCS containment assessment to expedite licensing review.

A study of chugging impulse was made to demonstrate that containment response to chugging using the load specification in the 4T Bounding Loads Report (NEDO 23617, July 1977) is greater than the response obtained using a realistic definition for chugging loads which does not include the system response of the 4T test tank.

The present Mark II chugging load specification is based on the application of chug pressure histories measured at the wetted boundary of the 4T test facility. These chug pressure histories were applied in a conservative manner directly to the suppression pool boundary of the Mark II containment. These 4T boundary pressures include both the chug excitation and the system response of the 4T system.

To provide a realistic chugging load definition, 4T boundary pressure histories have been reviewed to identify the chug source impulse, i.e., the impulse forcing function at the

vent exit. This chug impulse is then confirmed using a coupled fluid-structure model of the 4T facility. The response (total pressure at water/tank interface) of the 4T is calculated by applying the chug source impulse at the vent in the 4T model and comparing this response with actually recorded 4T test data. The results from this study have indicated that the chug impulse and not the detailed chug pressure history are important in determining the 4T wall pressure response. The chug impulse used was a triangular shape underpressure, with a duration of 5 to 10 msec. For example, a triangular pressure pulse at the 4T vent, 10 msec in duration and -28 psi in amplitude, will produce a wall pressure response of  $\pm 5$  psi. This is consistent with the impulse obtained from integration of the chug wall pressure traces of this amplitude.

From the impulse chug source defined at the 4T vent, an incident wall pressure chug source has been obtained. This is the wall pressure which produces the same response at the 4T wall as obtained when the chug source is applied at the vent.

The containment structure response are obtained for an axisymmetric application of the improved chugging load (incident pressure) definition which is consistent with the axisymmetric load specification in the 4T bounding load definition.

The response of the containment structures for the two chugging load definitions (present/bounding and improved) presented to the NRC on May 17, 1978, indicate the conservatism inherent in the present/bounding load specification which includes both the chugging excitation and the 4T response. For the La Salle containment, the improved chugging load definition produces a maximum displacement wall response which is less than that obtained from the present 4T bounding chug load specification.

### 3.3.1.1.7 Lateral Loads on Downcomers

This Section describes the application of lateral loads to the original design configuration of the downcomer vents and bracing. The revised design (including an additional lower bracing system) is discussed in Section 3.3.2.4.

The NRC Staff has questioned the direct application of the data reported in NEDO 21078 to the Mark II plants. Accordingly, they have requested that 4T test data also be considered in justifying the load definition. These questions have been thoroughly reviewed. It is concluded that the design lateral load of 8800 lbf applied as a static equivalent load at the tip of each downcomer represents an upper bound load. The drywell floor is assessed for all the downcomers simultaneously loaded as defined in the probability curve as per NRC criteria.

In the original design, the downcomers were braced at elevation 721 feet, which is well above the pool swell impact zone. The free length of the downcomer below the bracing is 32 feet 2 inches. The natural frequency of the empty downcomer is less than 7 hertz. If the hydrodynamic mass is considered, the frequency would be even lower. Thus the 8800 lbf bounding lateral load is applicable for the original LSCS design configuration.

This load is more conservative for design than a dynamic lateral load definition.

Based on the structural response data measured on the 4T downcomer during Phases I, II, and III, NEDE 23806-P defines the dynamic lateral load on the downcomer as follows.

The lateral chugging load can be represented by a half sine wave of duration ranging from 3 to 6 msec for high and low intensities, respectively. The maximum load amplitude ranges

from 10,000 lbf to 30,000 lbf and 's considered to be uniformly distributed over i- to 4-foot length of the downcomer end.

This transient load is represented by:

$$F(t) = A \sin \frac{\pi t}{\tau}, \text{ lateral load (lbf)}$$

where:

$$10^4 < A < 3 \times 10^4, \text{ maximum aplitude (lbf), and}$$

$$3 < \tau < 6, \text{ application period (msec).}$$

The comparison of maximum design forces from a dynamic analysis of the downcomer subjected to the transient load and from the application of 8800 lbf (static) is given below:

<u>LOAD</u>	<u>MAX VENT MOMENT</u>	<u>MAX VENT SHEAR</u>
8800 lbf (static)	301.0 ft-kip	< 0.5 ksi
10,000 - 30,000 lbf 6 msec - 3 msec (dynamic)	64.6 ft-kip	< 1.0 ksi

The above comparison demonstrates that the design downcomer lateral load of 8800 lbf represents an upper bound for LSCS.

The NRC also recently questioned lateral loads on the downcomer vent at the instant of vent clearing. It should be noted that in the 4T test series, no significant lateral loads were observed between the start of the test and the onset of chugging. However, in the referenced tests (Table 3.3 of NEDE 21078), static equivalent measurements of lateral loads up to 3.5 kips were observed. These loads are thought to be unique to the test setup (Figures 3-1, 3-1A, 3-2, and 3-3 of NEDE 210 8)

and not applicable to either the 4T facility or the Mark II containment.

In the test facility where the 3.5 kip static equivalent loads were measured, there is effectively no drywell volume except the air occupying the vent line. In contrast to the 4T facility or a Mark II containment, in the referenced tests only a very small quantity of noncondensable gas is vented to the pool, after which steam condensation occurs immediately. In these tests without a drywell, the vent pressure typically rose to approximately 1 to 1.5 atm while the small air volume cleared. It then dropped approximately 2 atm from this point as condensation of the steam commenced. This reduction in vent pressure is evidence of the collapse of the bubble at the vent exit and an attendant reentry of water into the vent.

The bubble collapse (similar to a chugging event) causes the lateral load (during vent clearing), which would not have occurred if a drywell were present as in the 4T facility and the Mark II containment. In this case continuous air flow to the bubble at the vent exit would gradually be diluted with a larger flow of steam (which in itself is capable of maintaining a positive bubble pressure at the vent exit). In the absence of a collapsing vent exit bubble, significant lateral loads would not be expected to occur during the 4T or Mark II vent clearing transients, and this was confirmed in the 4T tests.

Nevertheless, since the 8.8 kip load used to evaluate the downcomer and drywell floor is greater than the 3.5 kip load postulated to occur at the instant of vent clearing, it is clearly demonstrated that the governing design case for the containment has been considered.

The drywell floor is loaded by the chugging lateral loads. The procedure used for evaluating the structural adequacy of the downcomer and drywell floor is explained in detail in Section 5.1.3.

The current downcomer and bracing configuration has been assessed in accordance with the requirements of NUREG 0487. This assessment is described in Section 3.3.2.4.

#### 3.3.1.2 LOCA Boundary Loads

Boundary Loads caused by LOCA are analyzed using the same nodalization technique as SRV boundary loads (Section 3.2.1.3). The boundary loads described here are those used in the LSCS design basis. The load definitions are discussed in greater detail in Section 3.3.1.1. Reanalysis to meet the requirements of NUREG 0487 is discussed in Section 3.3.2.

##### 3.3.1.2.1 LOCA Water Jet

The impingement due to water jet is 33.0 psi overpressure added to local hydrostatic pressure below the vent exit, walls and base mat. Attenuation to the pool surface is assumed to be linear. This load is treated as a static load.

##### 3.3.1.2.2 Charging Air Bubble

The boundary loads during vent clearing have been assessed for the time of bubble growth at the vent exit. This load is less than the containment design capability.

##### 3.3.1.2.3 Pool Swell

The containment wall, pedestal wall, and the base mat do not experience any boundary load due to pool swell phenomena. However, the drywell floor is subjected to an uplift force

during pool swell as a result of the compression of the wetwell air space. This load is computed by comparing the transient pressure history of the wetwell air space with the drywell pressure history during pool swell. The maximum load for LSCS is 2.5 psi. This is verified by 4T test results.

#### 3.3.1.2.4 Pool Fallback

This phase of the transient causes no significant pool boundary loads.

#### 3.3.1.2.5 Condensation Oscillation

The condensation oscillation load is applied to the containment boundary walls assuming that the load occurs in phase at all vents. The load is described in Section 3.3.1.1.5.

#### 3.3.1.2.6 Chugging

Symmetric and asymmetric loads are applied to the containment boundary loads as shown in Figure 3.3-10. The asymmetric load is defined by assuming that the maximum load occurs on one side of the containment while the load is minimized on the other side. This conservative assumption results in the bounding horizontal loading due to chugging. The load is uniform below the vent exit and attenuates linearly to zero at the pool surface.

#### 3.3.1.3 LOCA Submerged Structure Loads

Submerged structure drag loads result when the LOCA-related phenomena cause fluid motion in the suppression pool. All initially submerged structures and those in the pool swell zone will potentially experience submerged structure loads. The LOCA submerged structure loads described here are those

used in the LSCS design basis. The load definitions are discussed in greater detail in Section 3.3.1.1. Reanalysis to meet the requirements of NUREG 0487 is discussed in Section 3.3.2.

#### 3.3.1.3.1 LOCA Water Jet

The drag load due to water jet is ( $C_D \times 24.06$ ) psi based on the jet velocity of 60 ft/sec (Reference 1). The duration of this load is also 0.85 sec (Reference 3).

The time history of the drag load due to water jet is given in Figure 3.3-5. The total force can be determined by multiplying ( $C_D \times 24.06$ ) by the projected area in square inches. This drag load acts on any structure located between the vent exit and the base mat. The direction of application of this load will be either in the horizontal or in the vertical directions, i.e., all structures experiencing this load must be designed to withstand the load if applied from these directions (Reference 1).

#### 3.3.1.3.2 Charging Air Bubble

The vent clearing transient results in submerged structure loads of relatively low magnitude which are bounded by loads during the steam condensation events.

#### 3.3.1.3.3 Pool Swell

During pool swell, structures are loaded by impact and by drag loads. Impact loads occur only above the initial pool surface up to the maximum pool swell elevation. Drag loads affect structures above the vent exit and below the maximum pool swell elevation.

### 3.3.1.3.3.1 Pool Swell Impact Loads

The impact load depends upon the size and shape of the structure and the velocity of the pool surface at the elevation of the structure. During design, effort was made to exclude structures from the pool swell zone. Because of this, relatively few structures are affected by impact loads.

The impact force due to pool swell occurs over a time period  $t_I$ . The typical force versus time profile is such that the force increases to a maximum value during the first half of the time period and then decreases to a value of the drag force during the second half. The duration,  $t_I$ , varies from about 7 msec for small structures to about 100 msec for large structures. These impact loads are based on the assumption that the pool surface velocity vector is perpendicular to the longitudinal axis of the body. The load in any other direction will be the vector component in that direction.

For design purposes, small structures would mean pipes, I-beams, and other similar structures having any one dimension less than or equal to 20 inches (Reference 1). All structures in the La Salle pool swell zone are classified as "small structures" for impact load design. The loads on small structures have been determined from tests conducted by the General Electric Company (Reference 1). The data reduced from these tests are plotted as average peak pressure,  $P_{max}$ , experienced by the structure versus elevation. Figure 3.3-6 is the plot of measured impact pressures for pipes and I-beams versus elevation. These results include a design margin of 50% (Reference 1), i.e., the measured impact values have been increased by 50%.

The results shown in Figure 3.3-6 can be used to determine the maximum force per unit length,  $F_{max}/L$ , on pipes and I-beams of different sizes located at different elevations

above the initial pool surface. Figure 3.3-7 gives the maximum impact force on pipes, and Figure 3.3-8 gives the force on I-beams.

The foregoing results give the maximum pressure and force experienced by a structure during impact. Knowing this maximum value, the transient profile can be constructed by using the normalized profile shown in Figure 3.3-9. The abscissa in Figure 3.3-9 is the duration of the impact load,  $t_I$ . This duration is the same for all small structures; its value is  $t_I = 7$  msec. The ordinate in Figure 3.3-9 is normalized pressure or normalized force. The normalization in the former case is done with respect to  $P_{\max}$ , Figure 3.3-6, and in the latter case with respect to  $F_{\max}/L$ , Figures 3.3-7 and 3.3-8. The conversion from pressure to force is based on the projected area at the diameter in the case of pipes, and on the area of the bottom surface in the case of I-beams.

To summarize, the following procedure is outlined for determining the impact loads on small structures:

- a. Determine the elevation at which the structure, for which the impact load is to be calculated, is located.
- b. For this elevation, the maximum impact pressure,  $P_{\max}$ , is obtained from Figure 3.3-6, or the maximum impact force per unit length,  $F_{\max}/L$ , is obtained from Figures 3.3-7 and 3.3-8.
- c. The pressure and/or force profiles are then determined using Figure 3.3-9.

The results given for the impact loads are based on pipes and I-beams. These results should also be used along with engineering judgment to determine impact loads on other similar structures.

#### 3.3.1.3.3.2 Pool Swell Drag Loads

Structures above the vent exit elevation and below the maximum pool swell elevation will experience drag loads. The velocity and acceleration history at the elevation of the structures, as predicted by pool swell analytical models, is used to calculate the drag load magnitude. The duration of the load will depend upon the pool swell velocity history and the elevation of the structure.

#### 3.3.1.3.4 Pool Fallback

Drag loads during fallback are calculated in a similar manner to the pool swell calculation. The pool slug velocity and acceleration time history are calculated assuming that a slug of water of thickness equal to the submergence depth of the downcomer falls freely under the influence of gravity only.

#### 3.3.1.3.5 Condensation Oscillation Drag Loads

The submerged structure loads due to steam condensation are calculated making use of the analytical methods developed to predict transient water jet loads and oscillating air bubble loads. These methods have been documented in reports NEDO/NEDE 21471-P, 21472-P, and 21730.

The same basic approach and fundamentals that are applied to air bubble-induced loads are applied to steam bubbles (see NEDE-21471 and NEDE-21730). The steam bubbles are treated as stationary, finite-sized multiple sources. The resulting potential gradient distribution within the bounded pool is determined by utilizing the method of images. The total drag loads due to both standard and acceleration drag are determined for each submerged structure as follows:

$$\text{Standard drag, } F_S = \frac{C_D A_x \rho U |U|}{2g_c} \quad (1)$$

$$\text{Acceleration drag, } F_A = \frac{\rho V_A \dot{U}}{g_c} \quad (2)$$

where:

$\rho$  = pool water density

$A_x$  = area of structure normal to flow direction,

$C_D$  = standard drag coefficient,

$V_a$  = acceleration drag volume,

$U$  = fluid velocity, and

$\dot{U}$  = fluid acceleration.

The source strength for steam condensation oscillation loads is derived from the 4T data (NEDE-13468P). The maximum pressure oscillations for this phenomenon were observed on the bottom of the tank and are bounded by a  $\pm 3.75$ -psi value. The load history is considered to be sinusoidal, with an amplitude of  $\pm 3.75$  psi and a possible frequency range of 2-7 hertz. An equivalent source strength at the downcomer exit is derived from the maximum observed load on the bottom of the tank. The derivation considers the finite size of the steam bubble and the 4T tank and downcomer vent configuration. This derived source strength is then used directly in the LSCS-specific submerged structure load determinations. Condensation oscillation is treated as occurring simultaneously and in phase at all the downcomer vents.

### 3.3.1.3.6 Chugging Drag Loads

The submerged structure loads due to chugging are computed on the basis of source strengths derived from 4T data in a manner analogous to that described in Subsection 3.3.1.3.5. Again, the maximum observed loads on the tank bottom are used to establish bounding source strengths. The bounding positive load used is 20 psi and the bounding negative load is -14 psi. The equivalent source strength at the downcomer exit for each of these loads is derived as in the case of the condensation oscillation loads. The frequency range used for chugging loads is 20 through 30 hertz. Main vent chugging is a stochastic phenomenon in both occurrence (timing) and load magnitude. Thus, the number of possible permutations for multiple main vent chugging combinations considering relative timing and load magnitude is immense. The relative location and orientation of the source and the submerged structure of interest are major considerations in defining the forcing functions on that structure. This consideration is complicated when multiple sources are present, since their relative phasing is important. This results directly from the fact that the load on a submerged structure is produced by the differential pressure that exists across that structure. Hence, when multiple sources are considered, the situation where sources on opposite sides of the submerged structure are out of phase will produce a larger load than the situation where the sources are in phase. The following conservative approach is being utilized as an interim method for the La Salle plant. The randomness in multiple source timing and phasing is accommodated by considering the worst case. The worst case is defined for each specific application such that the pressure gradient across the given structure is maximized. It is recognized that as the number of main vents considered to be participating in the chugging event increases, the probability of the assumed bounding source configuration decreases rapidly and soon becomes incredibly

small. Thus, as the number of participating main vents increases, the source strength for each is diminished by a factor as shown in Figure 3.3-1.

For example, if five main vents are being considered, the derived 4T source strength for each vent is reduced by multiplying by the factor 0.57. The curve in Figure 3.3-1 is based on Figure 4-10b of NEDE-21061-P, which has been extended to range from 1 to 100 downcomers and then normalized. The source strengths are thus specified as a function of the number of main vents considered to be contributing to the loading on the given structure. This procedure is applied by initially considering only the main vent of closest approach to the given structure to be chugging. The load is determined for that configuration. Next, the bounding combination of the two closest main vents is used to define the load. This procedure is repeated and each time one additional downcomer is considered in the load determination. Each successive downcomer is farther (spatially) from the given submerged structure and, hence, after the third or fourth downcomer, the increment of load increase is small. At the same time, the likelihood of each specific configuration decreases as the number of vents increases so the source strengths also decrease. Hence, the load on the submerged structure goes through a maximum as the number of main vents is increased. The combination which produces the largest load on the given structure is used for the design assessment.

The procedure described above is conservative and, hence, is considered to only be an interim procedure. Nevertheless, in an effort to expedite the LSCS licensing schedule, this interim procedure is being used to evaluate steam condensation loads on submerged structures in the suppression pool.

#### 3.3.1.4 Annulus Pressurization Loads

Loading on the shield wall and reactor vessel may be caused by a postulated pipe rupture at the reactor pressure vessel nozzle safe-end to pipe weld. This phenomenon, called "annulus pressurization," results in an asymmetric differential pressure between the reactor vessel and shield wall.

The transient asymmetric differential pressures resulting from the annulus pressurization event are caused by the mass and energy released during postulated pipe ruptures. There are two types of loadings resulting from annulus pressurization:

- a. A rapid asymmetric decompression acoustic loading of the annular region between the vessel and shroud from a recirculation inlet pipe break at the pipe to reactor pressure vessel nozzle safe-end weld.
- b. A transient asymmetric differential pressure event within the annular region between the biological shield wall and the reactor pressure vessel (annulus pressurization) from postulated pipe breaks at the pipe to reactor pressure vessel nozzle safe-end weld. Associated with this postulated event are:
  1. a jet stream release of the reactor pressure vessel inventory, and
  2. impact of the ruptured pipe against the whip restraint attached to the biological shield wall.

Figure 3.3-1 shows the time sequencing of these events. Each of the transient loading conditions is discussed in the following paragraphs.

#### Acoustic Loading

The acoustic loading results from a postulated recirculation pipe rupture at any location as shown in Figure 3.3-20. Because the boiling water reactor (BWR) system is a two-phase system that operates at or close to a saturation pressure of approximately 1000 psig, the differential pressure across the reactor shroud is of short duration, and the BWR system is not subjected to a significant shock type load with respect to structural supports. This short-duration acoustic load is confined to a bending moment and shear force on the reactor pressure vessel reactor shroud support. Typical results of the integrated force acting on the reactor pressure vessel shroud are:

<u>TIME (msec)</u>	<u>ACOUSTIC LOAD (kips)</u>
0	0
1.2	0
1.6	150
2.0	320
2.5	650
2.8	250
3.0	100
3.2	0

#### Annulus Pressurization - Design Considerations

The annulus pressurization event results from a postulated feedwater or recirculation pipe rupture at the reactor pressure vessel nozzle safe-end to pipe weld. The pipe is assumed

to have instantaneous guillotine rupture allowing mass-energy release into the drywell and annular region between the biological shield wall and reactor pressure vessel as shown in Figure 3.3-21. However, in the case of the recirculation line, the energy absorbing pipe whip restraint restricts the pipe separation to less than one full pipe diameter, see Figure 3.3-22. (Jet reaction and pipe whip restraint loads are calculated as described in ANSI 176 (draft), "Design Basis for Protection of Nuclear Power Plants Against Effects of Postulated Pipe Ruptures," January 1977.) This restricted separation, which occurs after the assumed instantaneous guillotine rupture, is accounted for as a finite break opening time in the mass/energy release calculation. The mass/energy methodology additionally accounts for the effects of the subcooled inventory initially present in the line. The feedwater line is conservatively assumed to fully separate, and the mass/energy release is calculated as described in Section 6.2 of the LSCS-FSAR (Reference 3).

The short-term (first few seconds) mass/energy release calculational method (Attachment 6.A to Reference 3) is intended for use only during the first few milliseconds of the line break transient and conservatively assumes that no vessel depressurization occurs. For calculation of the remainder of the line break transient, which involves vessel depressurization, the methods described in Reference 1 are employed. Development of the 0.5 multiplier utilized on the pipe side discharge flow during the inventory period is described in Appendix B of Reference 3.

For the case of reactor shield wall annulus pressurization, the short-term mass/energy release methodology has been separately applied to obtain break flow rates, including credit for finite break opening time in the case of the recirculation line.

## Annulus Pressurization - Design Analysis

Design analysis has been performed to reassess the plant for the effects due to annulus pressurization. There are three basic steps required to perform this analysis:

(1) calculation of mass and energy flow rates; (2) calculation of force-time histories; and (3) generation of acceleration time-histories and response spectra.

### a. Calculation of mass and energy flow rates

The assumptions and methods used in the calculation are presented in Attachment 6.A of the LSCS-FSAR. LSCS-FSAR Section 6.2 describes the short-term mass energy release calculations used for the recirculation and the feedwater line breaks.

Because the NRC has questioned the method for computing mass and energy flow rates following a postulated LOCA from long lines containing subcooled fluid, a program was developed to expedite the licensing of La Salle by performing RELAP analyses with appropriate assumptions and by comparing the results with those obtained using General Electric's method. The assumptions to be applied to these analyses are as follows:

#### Feedwater Line

1. La Salle RELAP deck as basis.
2. Use Henry-Fauske-Moody flow model.
3. Instant break opening.
4. Eliminate mass flux terms between vessel and break (short side).

Recirculation Line

1. La Salle RELAP deck as basis.
2. Allow for finite break opening time.
3. Use Henry-Fauske-Moody flow model.
4. Eliminate momentum flux terms in RELAP between vessel and break (short side).

b. Calculation of force-time histories

The mass/energy releases for the reactor recirculation and feedwater line breaks are used in calculating the force-time histories on the shield wall and reactor pressure vessel. The model used for this analysis and the assumptions are presented in FSAR Section 6.2. For convenience the method of calculating the force-time history is presented in Appendix H of this report.

c. Generation of acceleration time-histories and response spectra

The force-time histories were applied to a composite lumped-mass model of the pedestal, shield wall, and a detailed representation of the reactor pressure vessel complex, shown in Figure E-1 (Appendix E of this report). This analysis produced acceleration time histories at all nodes for use in evaluating the attached piping and reactor pressure vessel for the effects of annulus pressurization of either a feedwater or reactor recirculation system postulated rupture. Response spectra at all nodes were also generated.

The reactor pressure vessel and the attached piping were evaluated using these acceleration time-histories in performing a dynamic time-history analysis or response spectra.

The annulus pressurization loads were conservatively combined with the SSE using SRSS methods (absolute sum method for the containment structure). The following is a brief explanation of why combination of these two loads is extremely conservative. Mark II plants are designed for the loads associated with a LOCA in combination with the vibratory motion of the SSE. This loading combination, though not mechanically expected, is considered in response to regulatory requirements and also provides design margin for Seismic Category I components. Annulus pressurization loads do not occur for loss-of-coolant accidents in general, but only for those due to the instantaneous rupture of large pipes at the vessel safe-end to pipe weld inside the shield wall. The probability of a LOCA at these unique locations is significantly lower than the probability of a LOCA in general, and its combination with the SSE is well beyond the lower limit of probability established as appropriate for design-basis load combinations.

A detailed study of the probability of simultaneous occurrence of SSE and annulus pressurization was made. The probability of their simultaneous but independent occurrence was considered and found not to be an appropriate assumption. The probability of an SSE causing a LOCA in the unique location resulting in annulus pressurization loads was also examined in detail. For this case, the associated combined probability was found to be beyond the limits established for design-basis load combinations. Therefore, the simultaneous occurrence of SSE and annulus pressurization loads is not considered appropriate as a design-basis load combination; however, to facilitate the licensing schedule, this load combination has been considered.

### 3.3.2 Assessment of NRC Acceptance Criteria - LOCA

Section 3.4 provides the response to NUREG-0487, NRC Lead Plant Acceptance Criteria (September 1978). It contains a detailed description of how the intent of NUREG-0487 has been met.

The following subsections describe areas where reanalysis has been done to meet the acceptance criteria.

#### 3.3.2.1 LOCA Water Jet Loads

The NRC Lead Plant Acceptance Criteria required LOCA water jet loads to include the effects of a spherical vortex of fluid traveling with the jet front predicted by the Moody jet model (Reference 4). This procedure is expected to yield conservative results because the Moody model predicts jet penetrations much greater than those observed in tests.

In response to criterion III.A.1, the LOCA water jet loads have been reassessed by several methods. The first is essentially Acceptance Criterion III.A.1, incorporating a modification to the Moody methodology to overcome mathematical difficulties. The second is an adaptation of the method described by Abramovich and Solan (Reference 5). This method conforms to the intent of the acceptance criteria, but describes the vortex motion by applying conservation of momentum rather than using the Moody model. A final method that has been examined on a preliminary basis is the ring vortex model which is proposed by the Mark II Generic Program.

The NRC Acceptance Criteria utilizing the Moody jet model result in a vortex with a motion described by a locus of points. These points are found by tracking a number of constant velocity particles exiting from the downcomer and locating the points where a particle is overtaken by the one exiting after it. This calculation is easily done for a jet with constant acceleration but causes difficulties when applied to a jet of increasing acceleration. When the Moody method is rigorously applied, depending upon the coordinate system chosen, the jet is predicted to reverse and move back to the vent, or time at the jet front reverses. This result is unacceptable.

An alternate method has been applied which resolves these problems while conforming to the intent of the original NRC Acceptance Criteria. If the jet front position and velocity are described at any time by the particle having traveled the farthest, the jet motion is well behaved until the jet is terminated. High accelerations are experienced near the end of the transient that are overly conservative.

The vortex motion after vent clearing can be calculated assuming it continues through the pool. The water jet is, in fact, dissipated in the turbulence caused by flow of air into the pool. Calculations show that, until vent clearing, LOCA water jet loads on submerged structures in the La Salle suppression pool are negligible (less than 10% of design values). Higher loads are calculated on the quencher arms if the vortex is allowed to continue until it impacts the quencher arm. However, these loads are also within the design capability of the quencher. The calculations conservatively used direct jet impingement on the quencher arms (the arms are offset in the actual plant), and no interchange of mass between the jet and pool. The vortex was considered a rigid sphere in determination of the drag load which retards its motion.

The second method is similar to that described above but uses a different method to describe the vortex motion. Following Abramovich and Solan (Reference 2), the motion and size of the vortex may be described assuming that momentum and mass are conserved as the jet forms the vortex. Momentum is lost only through drag on the fluid sphere.

The resulting motion of the vortex is similar to that calculated previously, but without the unrealistic high accelerations noted above. The loads are lower throughout the transient. This result is again conservative because interaction between the vortex and pool (other than rigid body drag) has been ignored.

The Mark II Generic Program has proposed a ring vortex model of the LOCA water jet. Preliminary results indicate this model predicts existing experimental data well (Reference 6) and will result in lower loads than the methods described above.

Based on the above evaluations, it is judged that the LOCA water jet loads for La Salle have been evaluated in accordance with the intent of the NRC criteria. As indicated, additional evaluations were done which demonstrate the conservatism of the evaluations. The results of these evaluations were that the loads on the quencher were negligible relative to the controlling quencher design loads.

#### 3.3.2.2 Pool Swell

The acceptance criteria suggested several changes in the method of calculating pool swell loads. In the following sections, the changes are discussed and compared with the original methods.

##### 3.3.2.2.1 Pool Swell Velocity

The pool swell velocity has been increased by 10%. This change increases all pool swell drag and impact loads. Reassessment shows that the design is adequate for this load.

##### 3.3.2.2.2 Pool Swell Impact

The acceptance criteria furnished an alternative method of impact load calculation based on the premise that the methodology presently used is not necessarily conservative for all structural sizes and ranges of natural frequency. Although the method in NUREG-0487 seems overly conservative for structures in the larger size range and for those with higher natural frequency, it was found that the structures

in the LSCS pool swell zone are not in this range of size and frequency. An assessment showed that the original method in the DFFR (Reference 1) gives higher loads than the method in NUREG-0487. Therefore the design is adequate.

NUREG-0487 also included impact load criteria for large structures (no dimension less than 20 inches) and gratings. The LSCS pool swell zone contains no large structures and no grating.

#### 3.3.2.3 Drag Load Calculations

NUREG-0487 pointed out that under certain flow conditions, the standard and acceleration drag coefficients used (Figure 3.3-4) may not give conservative results. This has been investigated and the loads have been reassessed using refined drag coefficients. Relatively few calculations showed load increases. A detailed description of the methods used for reanalysis is included in Appendix C.

#### 3.3.2.4 Chugging Lateral Loads

The original configuration of the LSCS downcomers included a bracing system near the downcomer floor and a long unsupported length of vent. The natural frequency of this system is very low. As described in Subsection 3.3.1.1.7, the 8800-lbf lateral load was used in the design. Because of the low natural frequency of the vent, this load meets the requirements of NUREG-0487.

An additional bracing system is now installed. This bracing is located below the suppression pool surface but more than 8 feet above the vent exit. The natural frequency of the braced downcomers is between 7 and 14 hertz. These conditions meet the requirements of NUREG-0487 if the 8800-lbf load is increased by the ratio of the vent frequency to 7 hertz.

This is the method being used for the reassessment of the chugging lateral loads.

Because of the location of the lower bracing system in the pool, it must be capable of accommodating submerged structure loads as well as lateral loads. The bracing system has been designed for LOCA and SRV submerged structure drag loads as described in Subsections 3.2.2.4 and 3.3.1.3 incorporating the comments in NUREG-0487 as described in Appendix C.

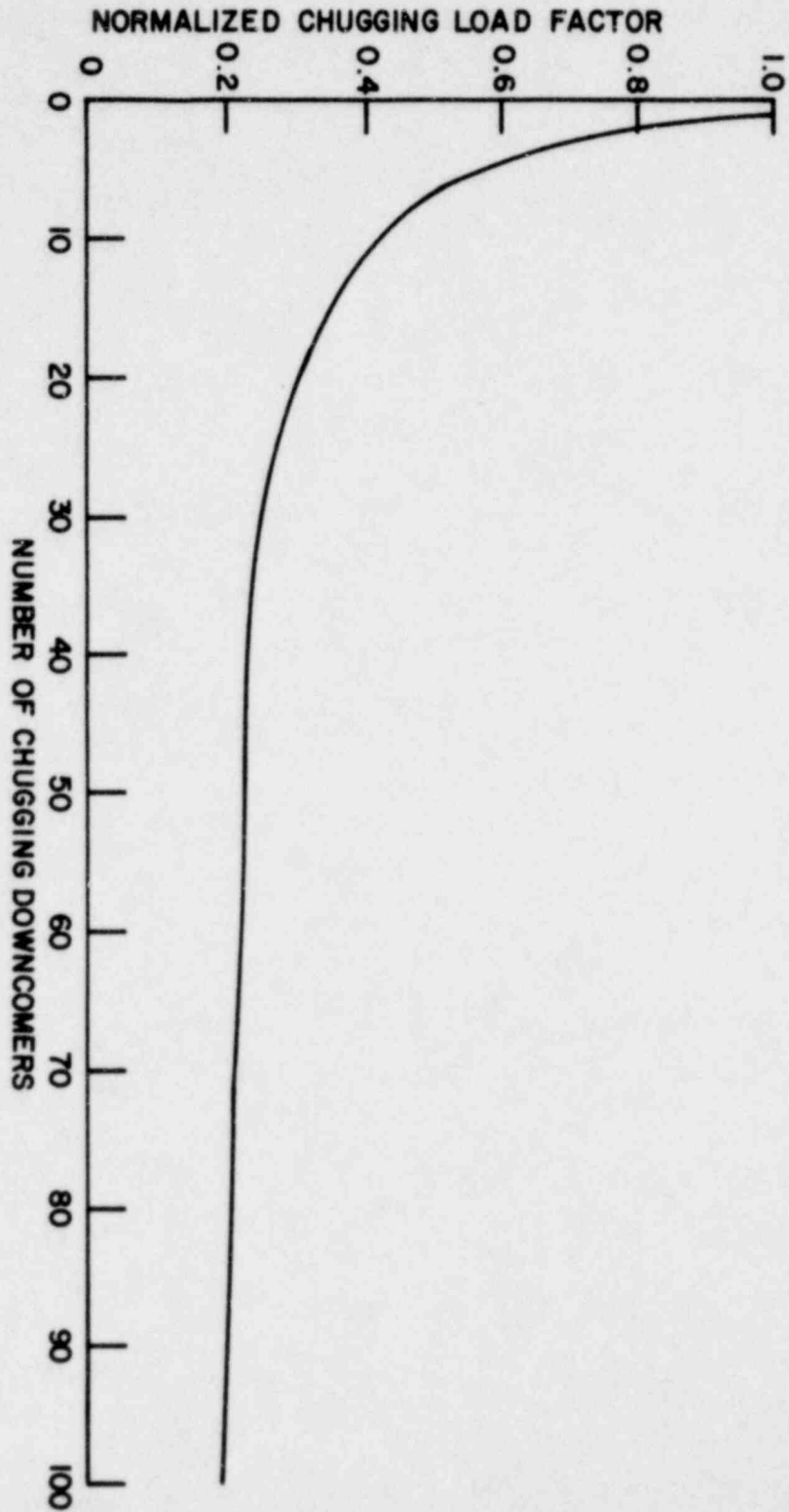
### 3.3.3 References

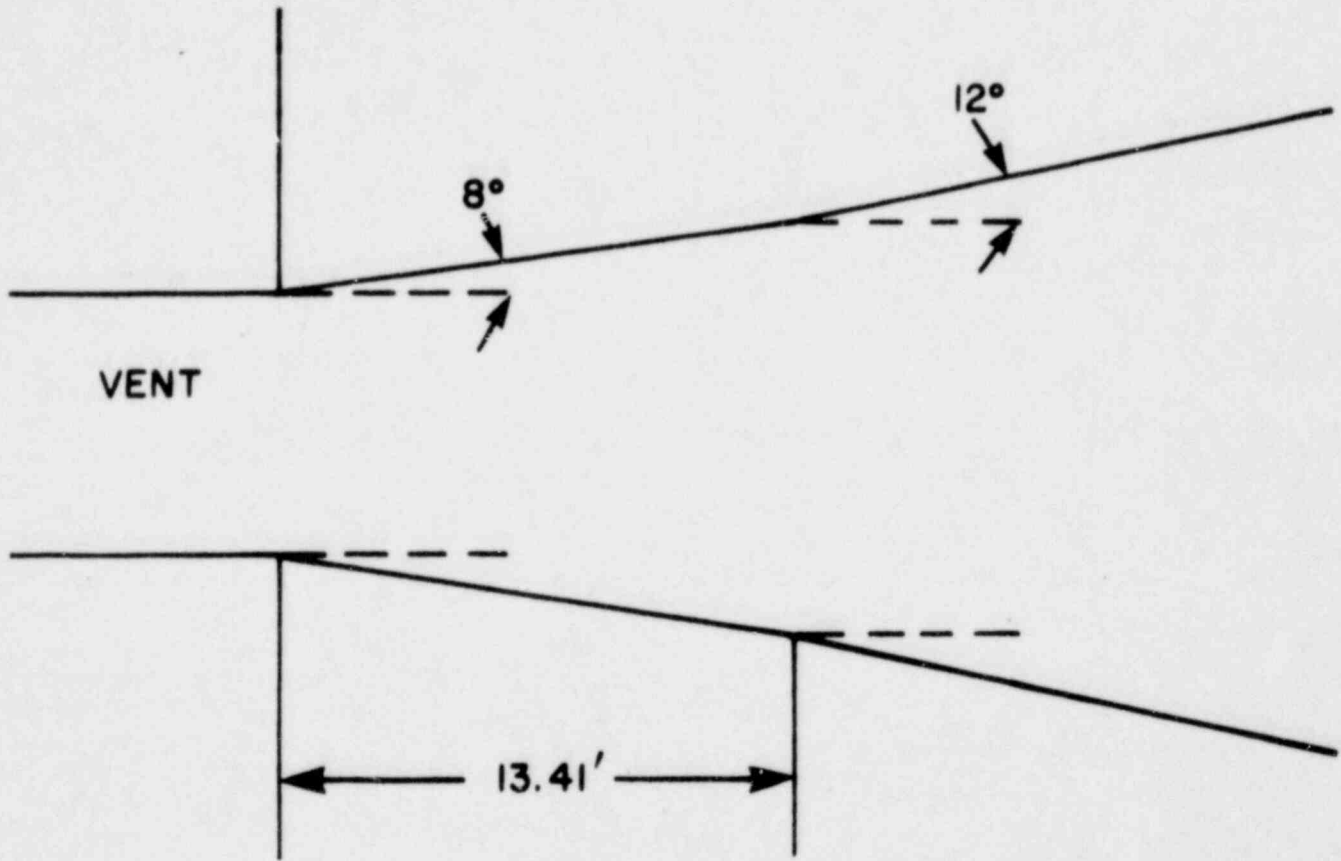
1. "Mark II Containment Dynamic Forcing Functions Information Report," General Electric Company and Sargent & Lundy Engineers, NEDO-21061, September 1976, Revision 2.
2. "Mark II Containment Dynamic Forcing Functions Information Report," Proprietary Supplement, General Electric Company and Sargent & Lundy Engineers, NEDE-21061-P, September 1976, Revision 2.
3. Final Safety Analysis Report, La Salle County Station, Chapter 6.0.
4. "Analytical Model for Liquid Jet Properties for Predicting Forces on Rigid Submerged Structures" NEDE-21472, September 1977.
5. S. Abramovich and A. Solan, "The Initial Development of a Submerged Laminar Round Jet," Journal Fluid Mechanics, Vol. 59, Part 4, pp. 791-801, 1978.
6. "Mark I Containment Program 1/4 Scale Test Report Loads on Submerged Structures due to LOCA Air Bubbles and Water Jets," NEDE-23817-P, September 1978.

MULTIPLE MAIN VENT CHUGGING  
LOAD FACTOR

FIGURE 3.3-1

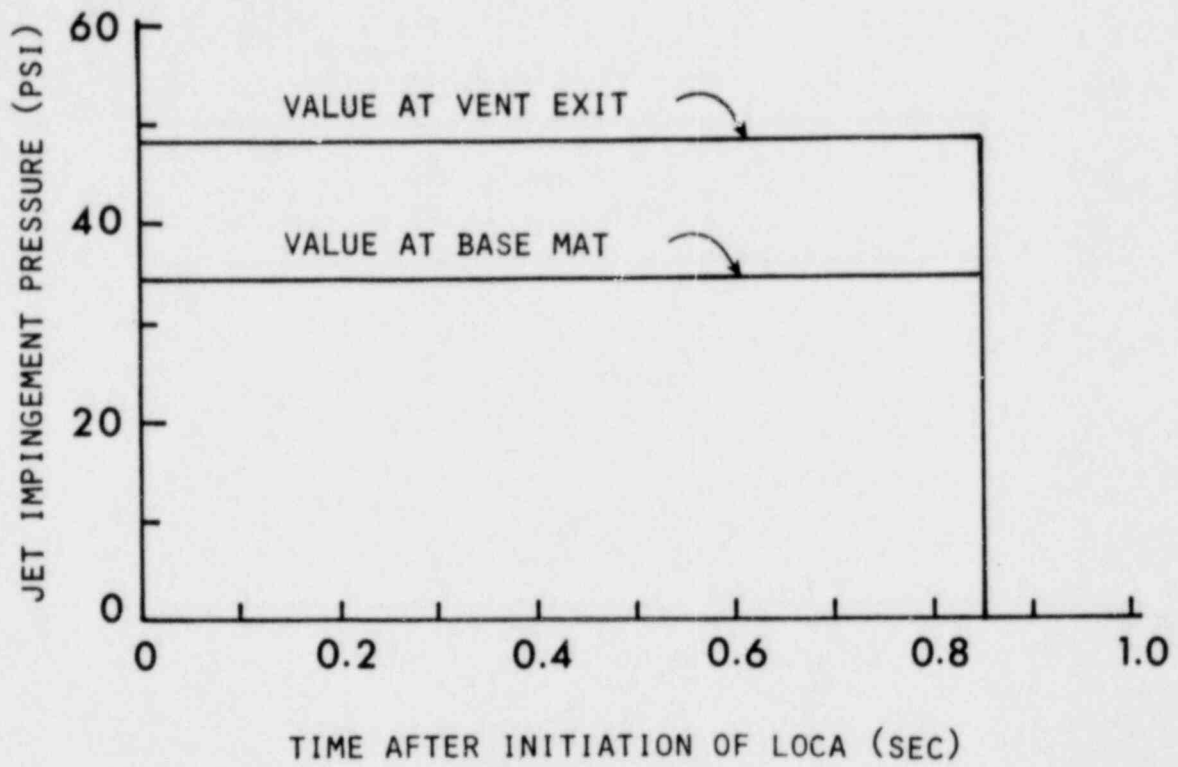
LA SALLE COUNTY STATION  
MARK II DESIGN ASSESSMENT REPORT





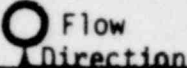
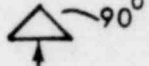
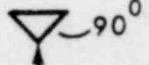
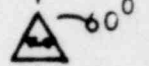
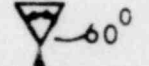
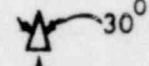
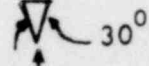
NOT TO SCALE

LA SALLE COUNTY STATION MARK II DESIGN ASSESSMENT REPORT
FIGURE 3.3-2 DOWNCOMER VENT CLEARING JET ANGLE DURING LOCA

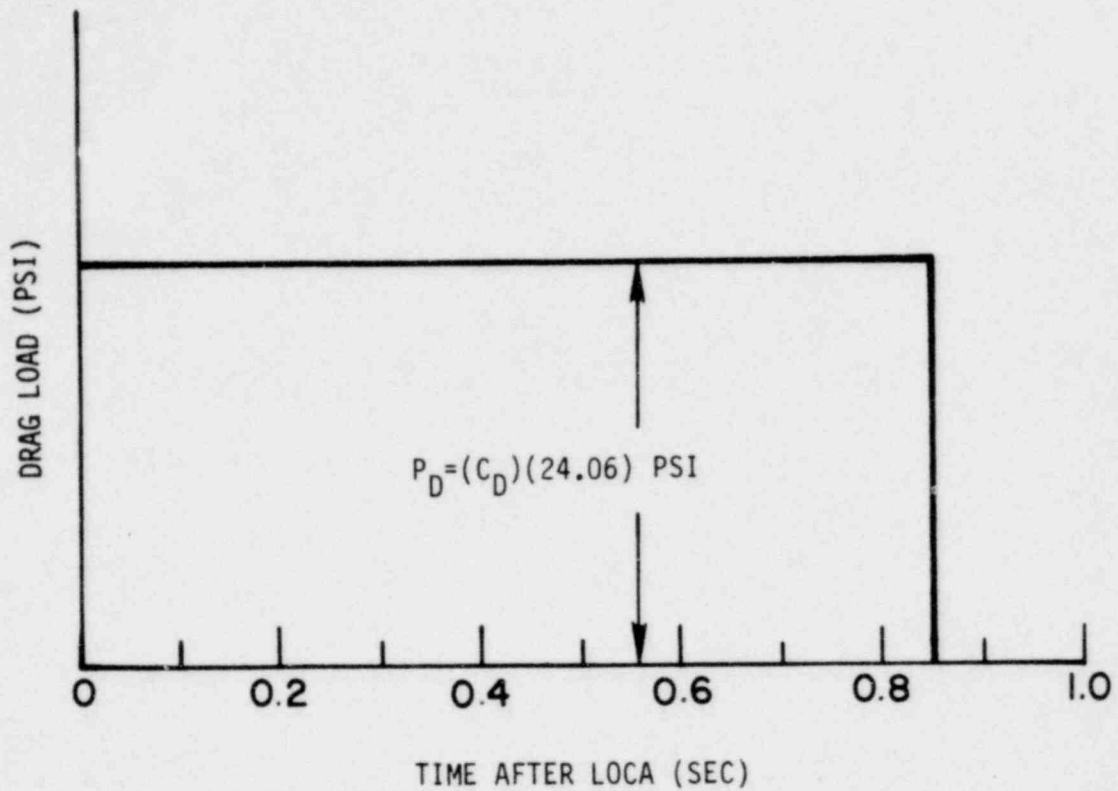


LA SALLE COUNTY STATION  
MARK II DESIGN ASSESSMENT REPORT

FIGURE 3.3-3  
JET IMPINGEMENT LOAD

Body Shape		$C_D$
Circular Cylinder		1.2
Elliptical Cylinder	 2:1	0.6 - 0.46
	 4:1	0.32
	 8:1	0.20 - 0.29
Square		2.0
Triangle	 120°	2.0
	 120°	1.72
	 90°	2.15
	 90°	1.60
	 60°	2.20
	 60°	1.39
	 30°	1.8
	 30°	1.0
Semitubular		2.3
		1.12

**LA SALLE COUNTY STATION**  
 MARK II DESIGN ASSESSMENT REPORT  
 FIGURE 3.3-4  
 DRAG COEFFICIENTS



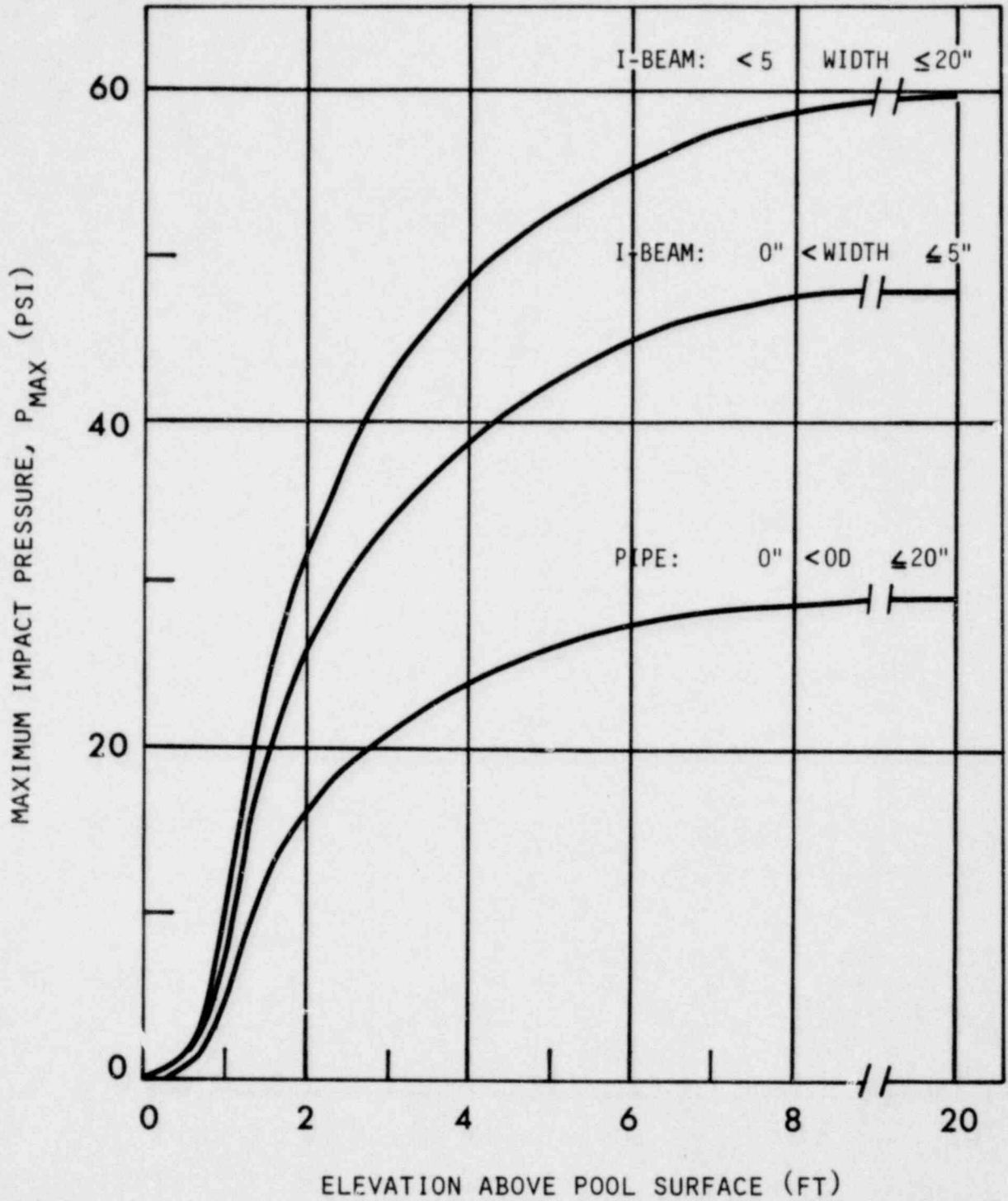
NOTE:

1. OBTAIN VALUE OF  $C_D$  FROM FIGURE 3.3-4.

LA SALLE COUNTY STATION  
MARK II DESIGN ASSESSMENT REPORT

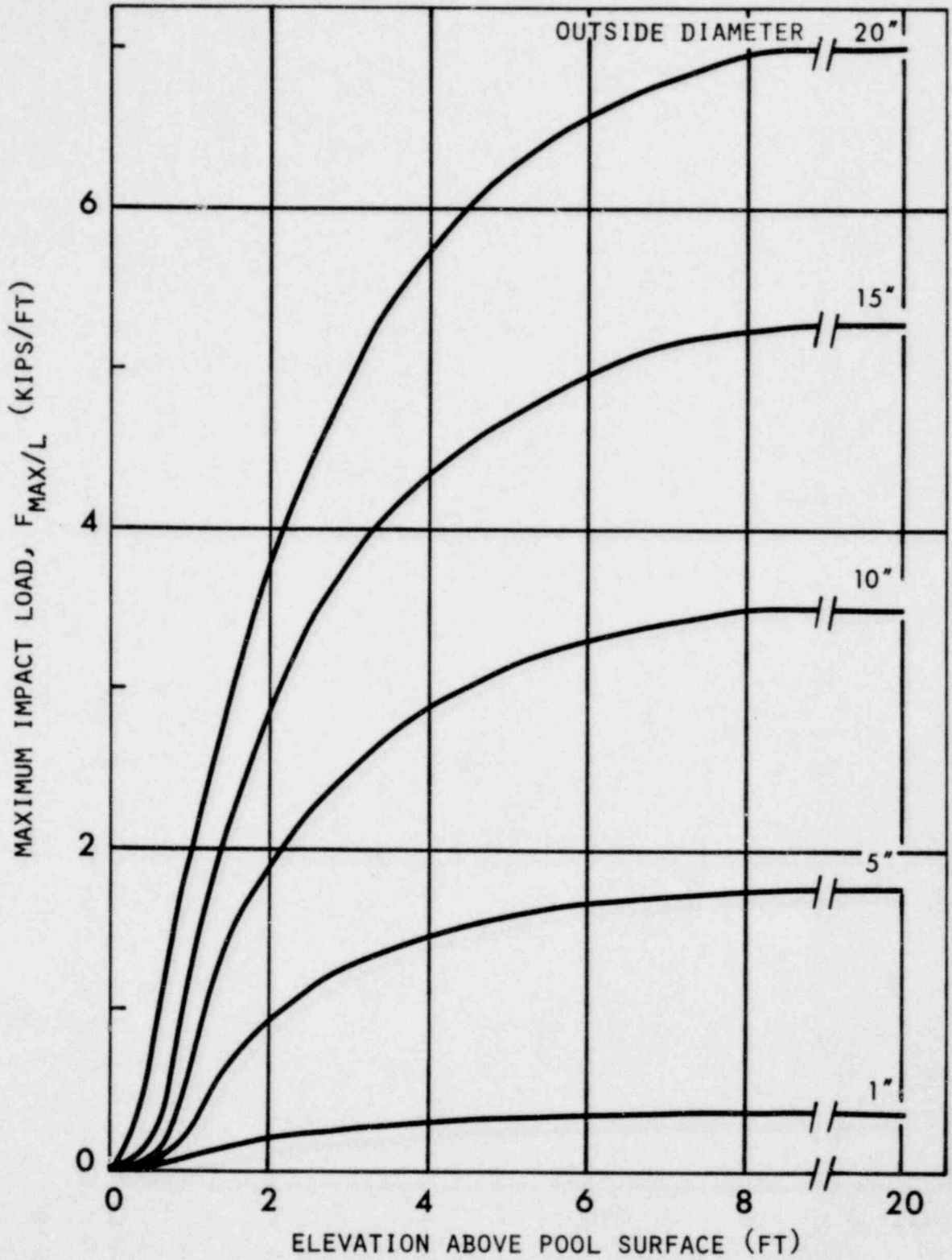
FIGURE 3.3-5

DRAG LOAD ON SUBMERGED STRUCTURES DUE  
TO DOWNCOMER VENT CLEARING



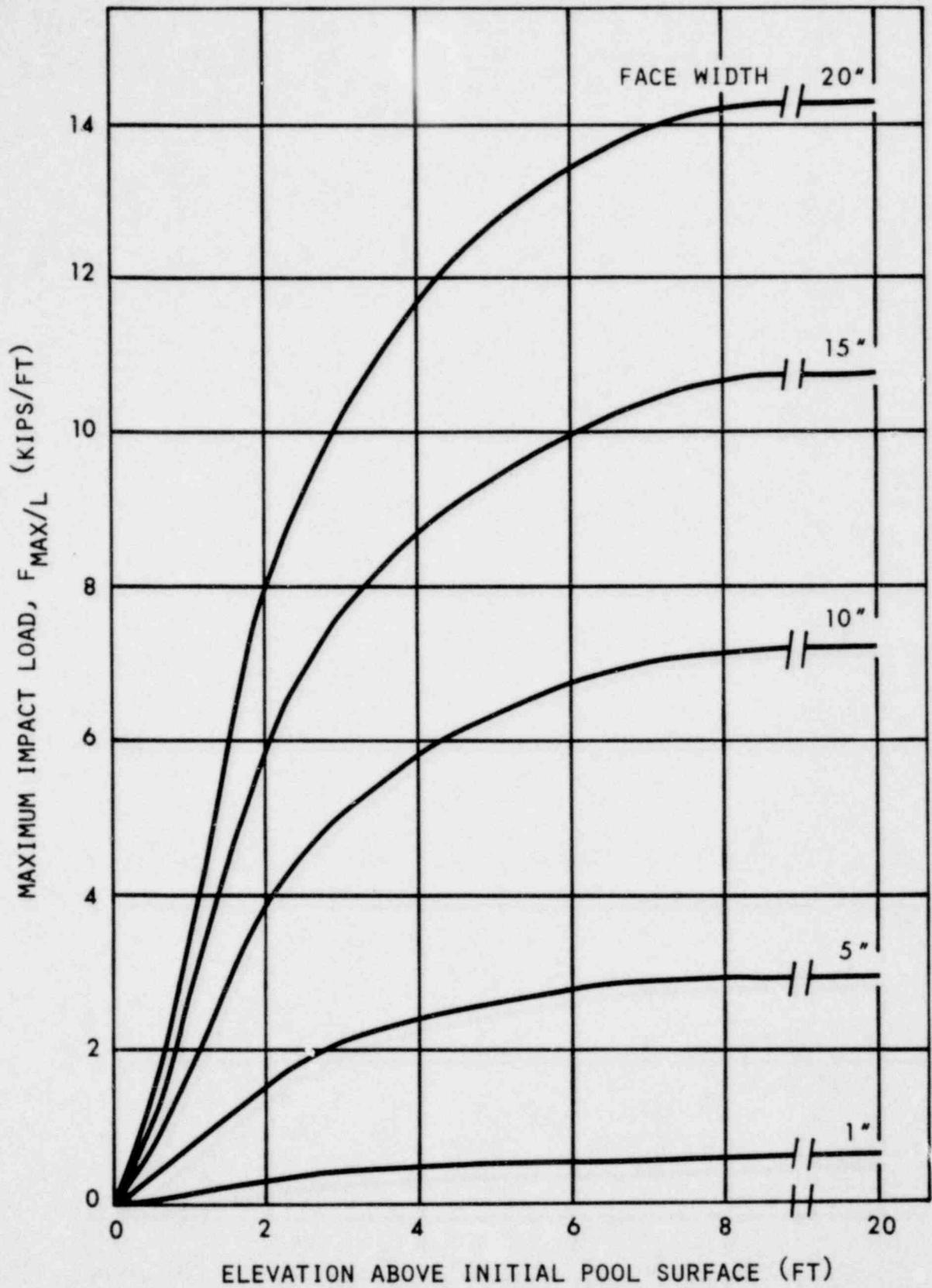
**LA SALLE COUNTY STATION**  
MARK II DESIGN ASSESSMENT REPORT

FIGURE 3.3-6  
MAXIMUM IMPACT PRESSURE ON  
SMALL STRUCTURES

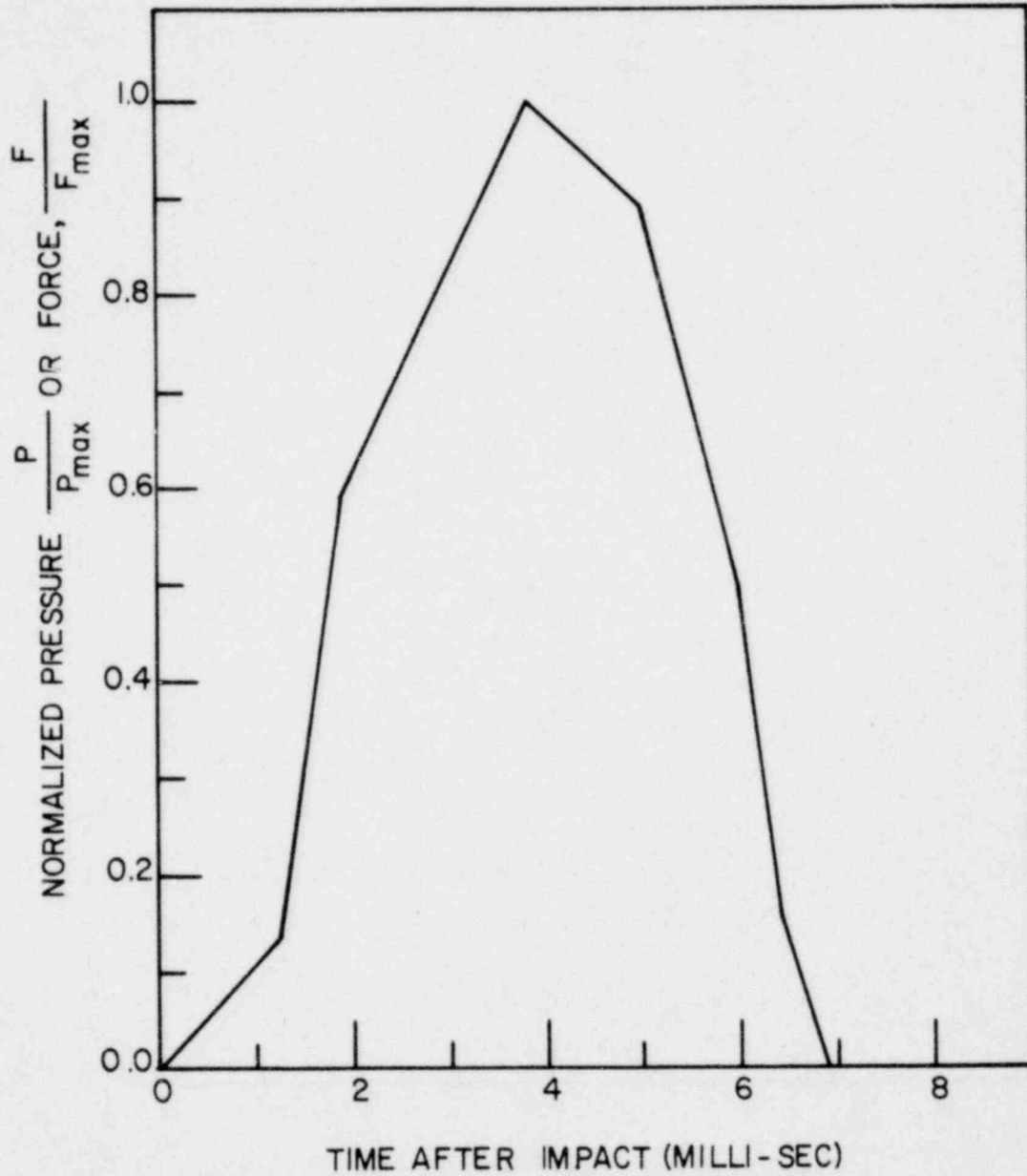


LA SALLE COUNTY STATION  
MARK II DESIGN ASSESSMENT REPORT

FIGURE 3.3-7  
MAXIMUM IMPACT FORCE ON PIPES

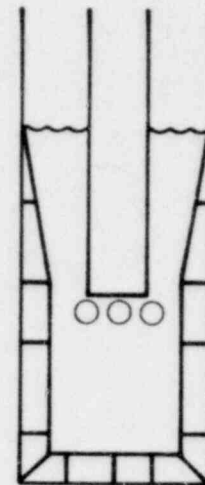
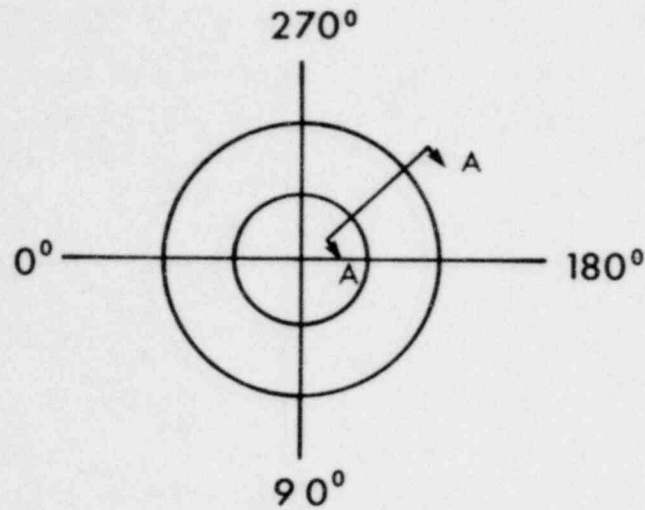


LA SALLE COUNTY STATION  
MARK II DESIGN ASSESSMENT REPORT  
FIGURE 3.3-8  
MAXIMUM IMPACT FORCE ON I-BEAMS



LA SALLE COUNTY STATION  
MARK II DESIGN ASSESSMENT REPORT

FIGURE 3.3-9  
TIME HISTORY OF IMPACT LOAD FOR SMALL  
STRUCTURES IN POOL SWELL REGION



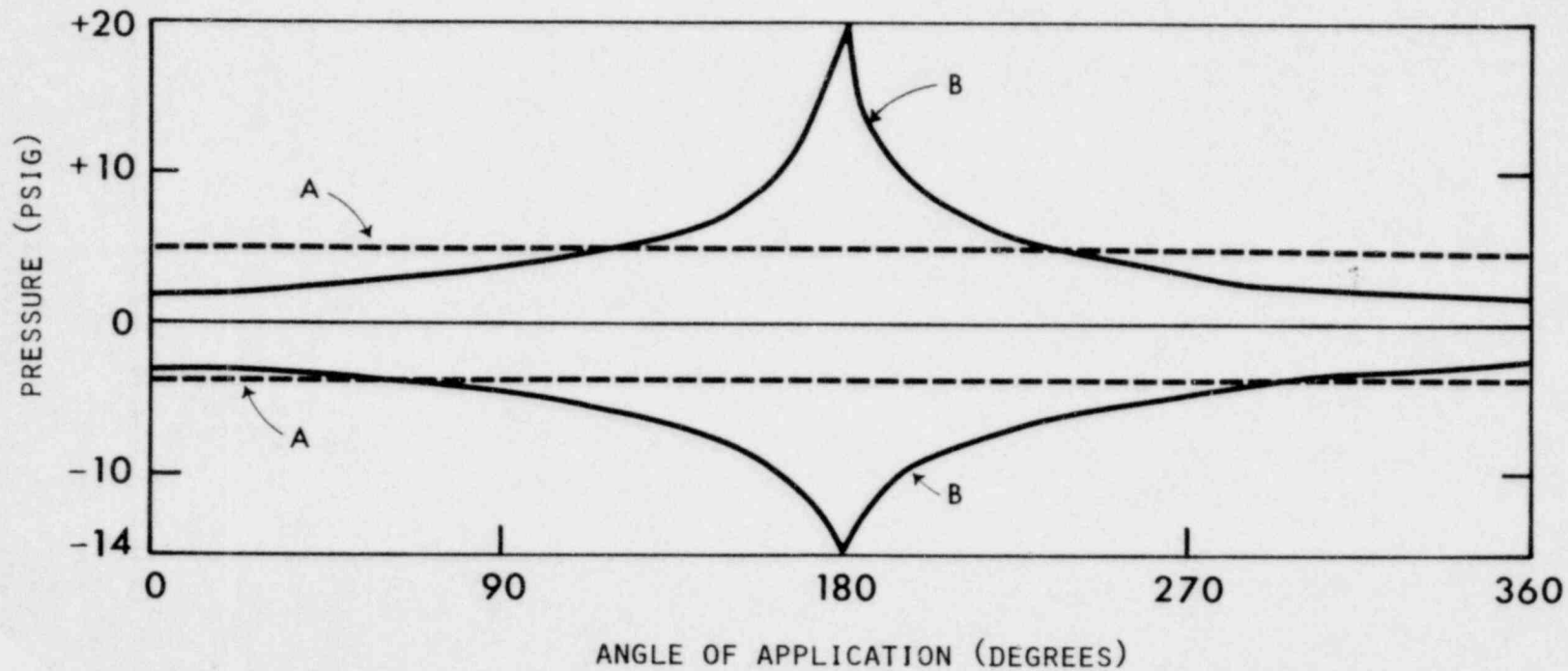
A-A

A. UNIFORM LOAD

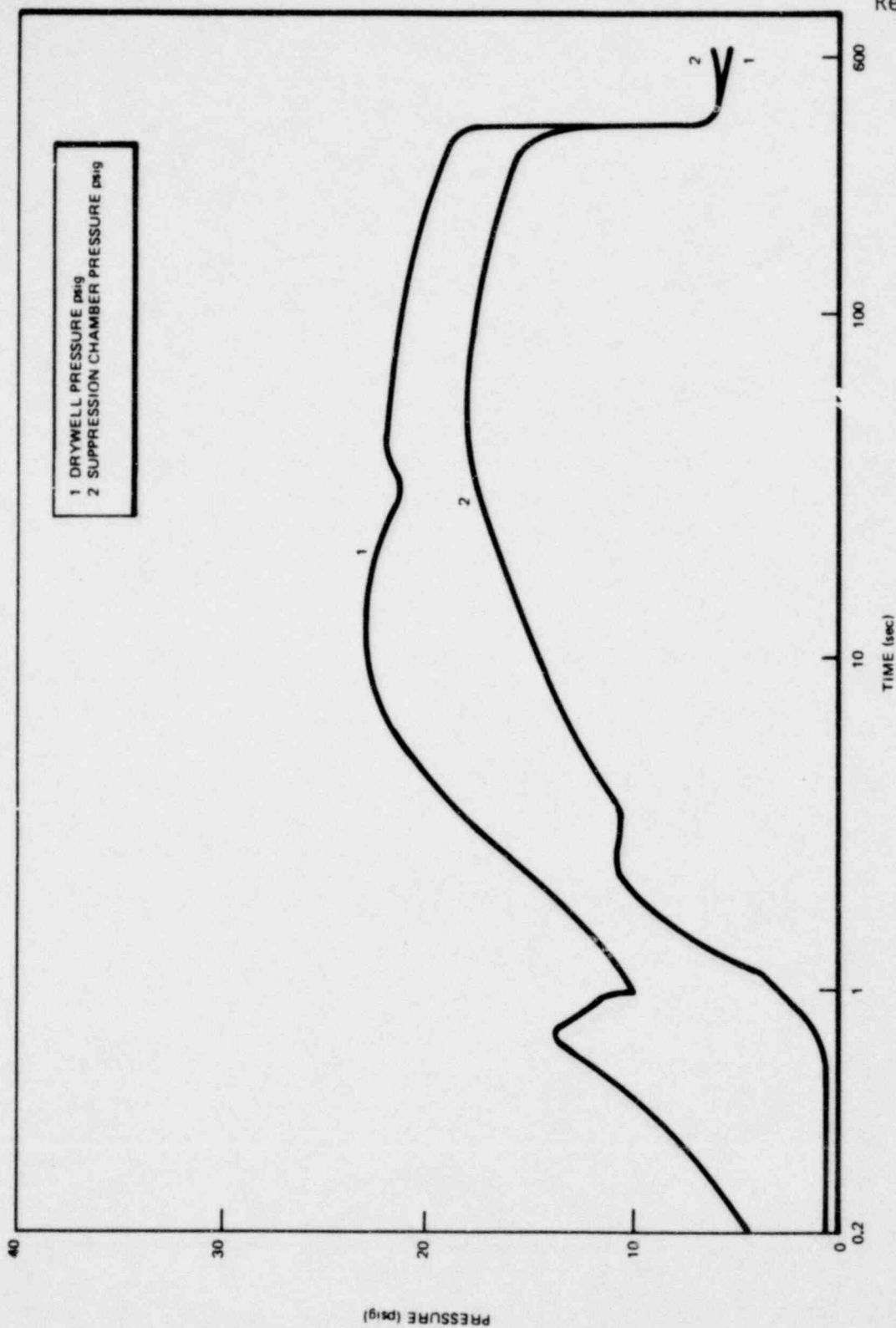
+4.8/-4.0 psig, 0°-360°

B. ASYMMETRIC LOAD

MAXIMUM +20/-14 psig

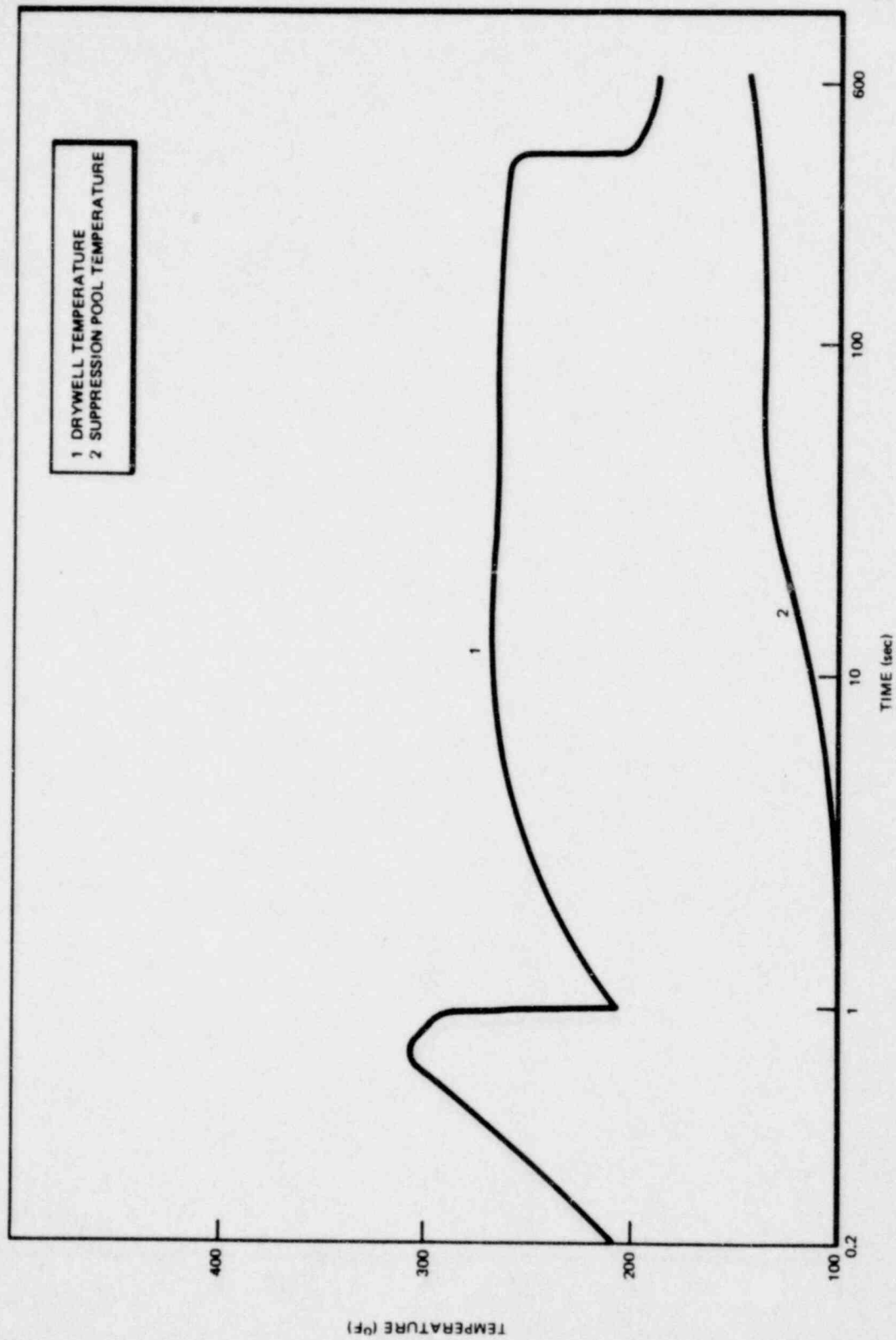


LA SALLE COUNTY STATION  
 MARK II DESIGN ASSESSMENT REPORT  
 FIGURE 3.3-10  
 CHUGGING LOAD



LA SALLE COUNTY STATION  
MARK II DESIGN ASSESSMENT REPORT

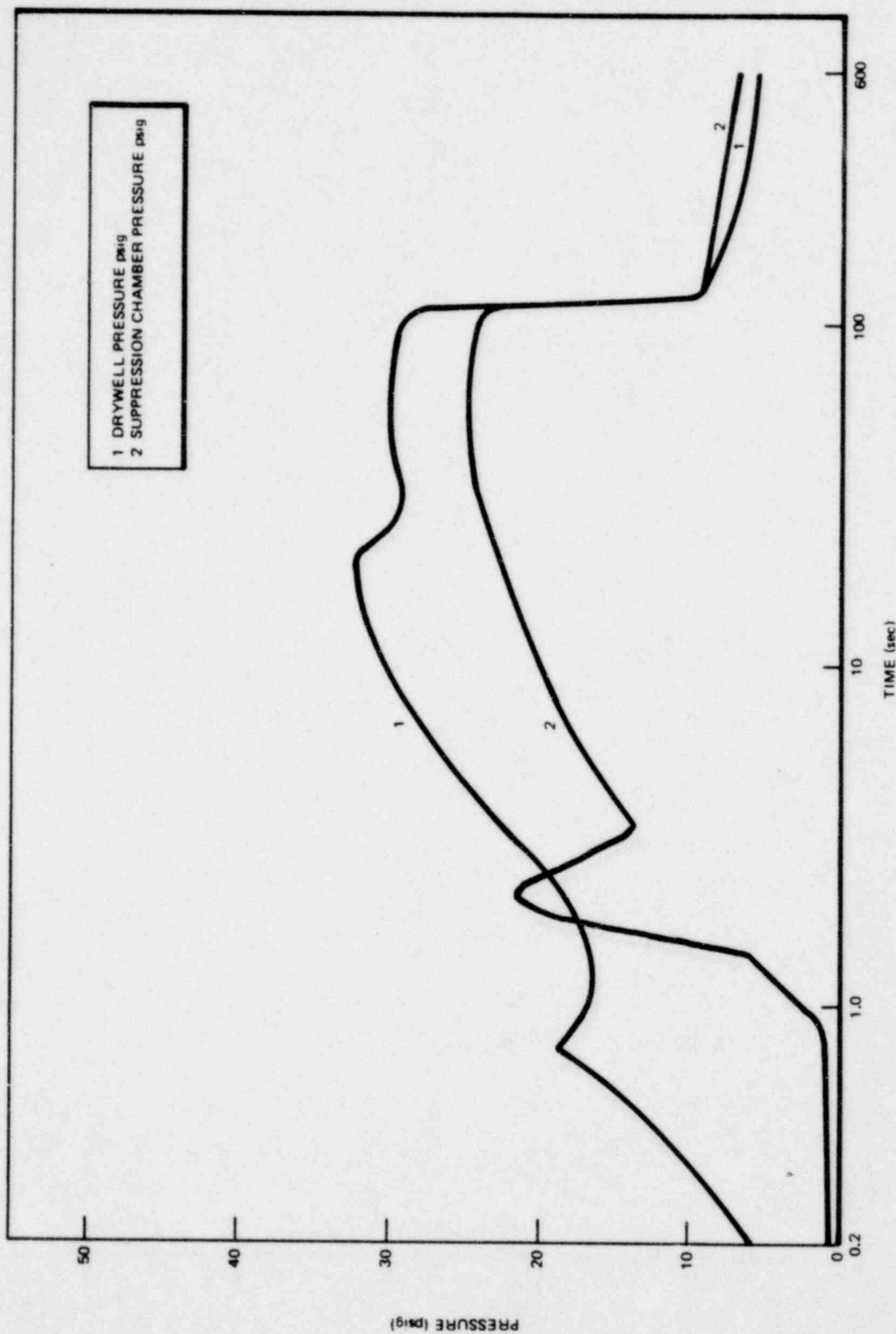
FIGURE 3.3-11  
DRYWELL/WETWELL PRESSURE TRANSIENTS  
FOR A MAIN STEAMLIN BREAK



1 DRYWELL TEMPERATURE  
2 SUPPRESSION POOL TEMPERATURE

LA SALLE COUNTY STATION  
MARK II DESIGN ASSESSMENT REPORT

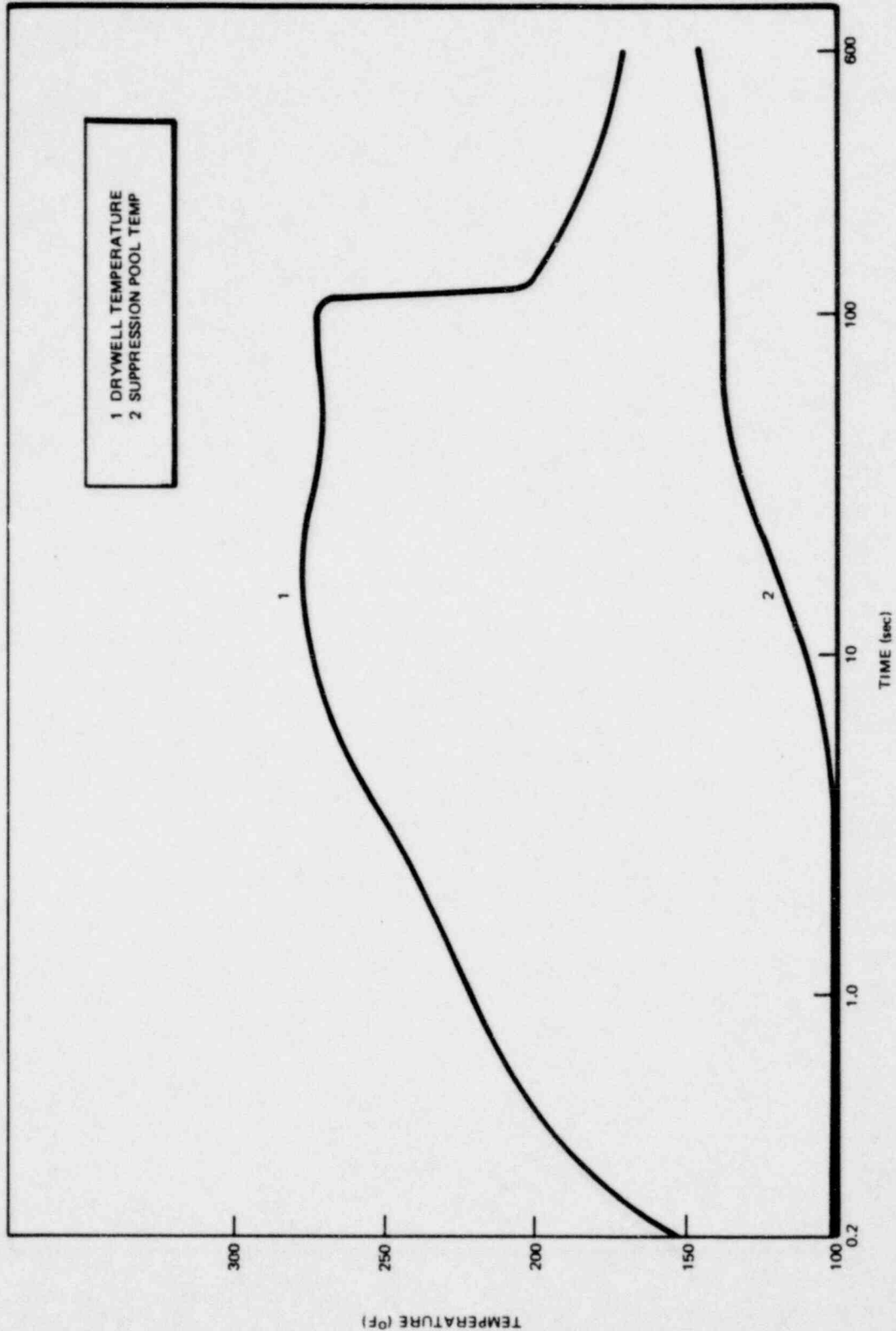
FIGURE 3.3-12  
DRYWELL/WETWELL TEMPERATURE TRANSIENTS  
FOR A MAIN STEAMLIN BREAK



LA SALLE COUNTY STATION  
MARK II DESIGN ASSESSMENT REPORT

FIGURE 3.3-13

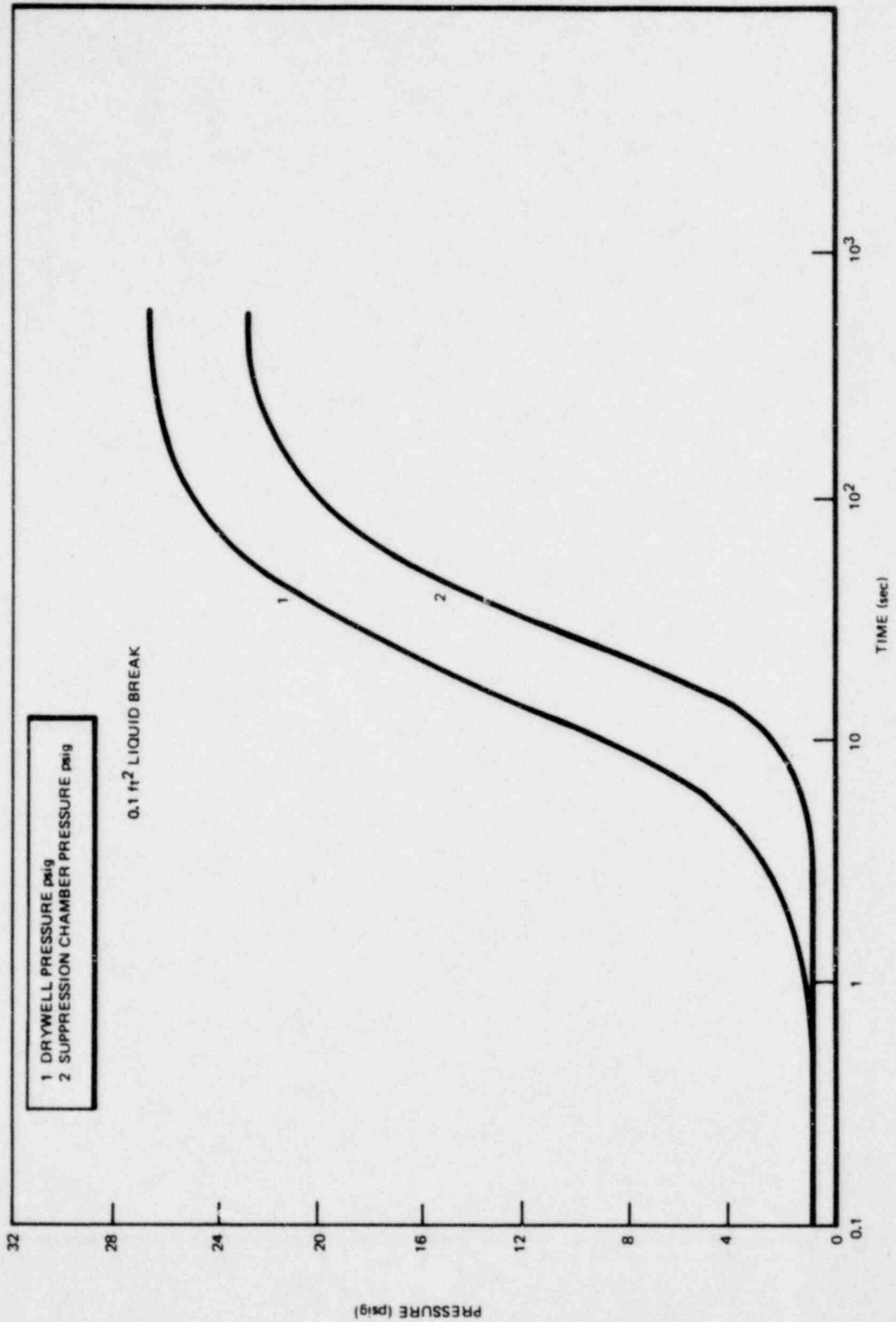
DRYWELL/WETWELL PRESSURE TRANSIENTS  
FOR RECIRCULATION LINE BREAK



1 DRYWELL TEMPERATURE  
2 SUPPRESSION POOL TEMP

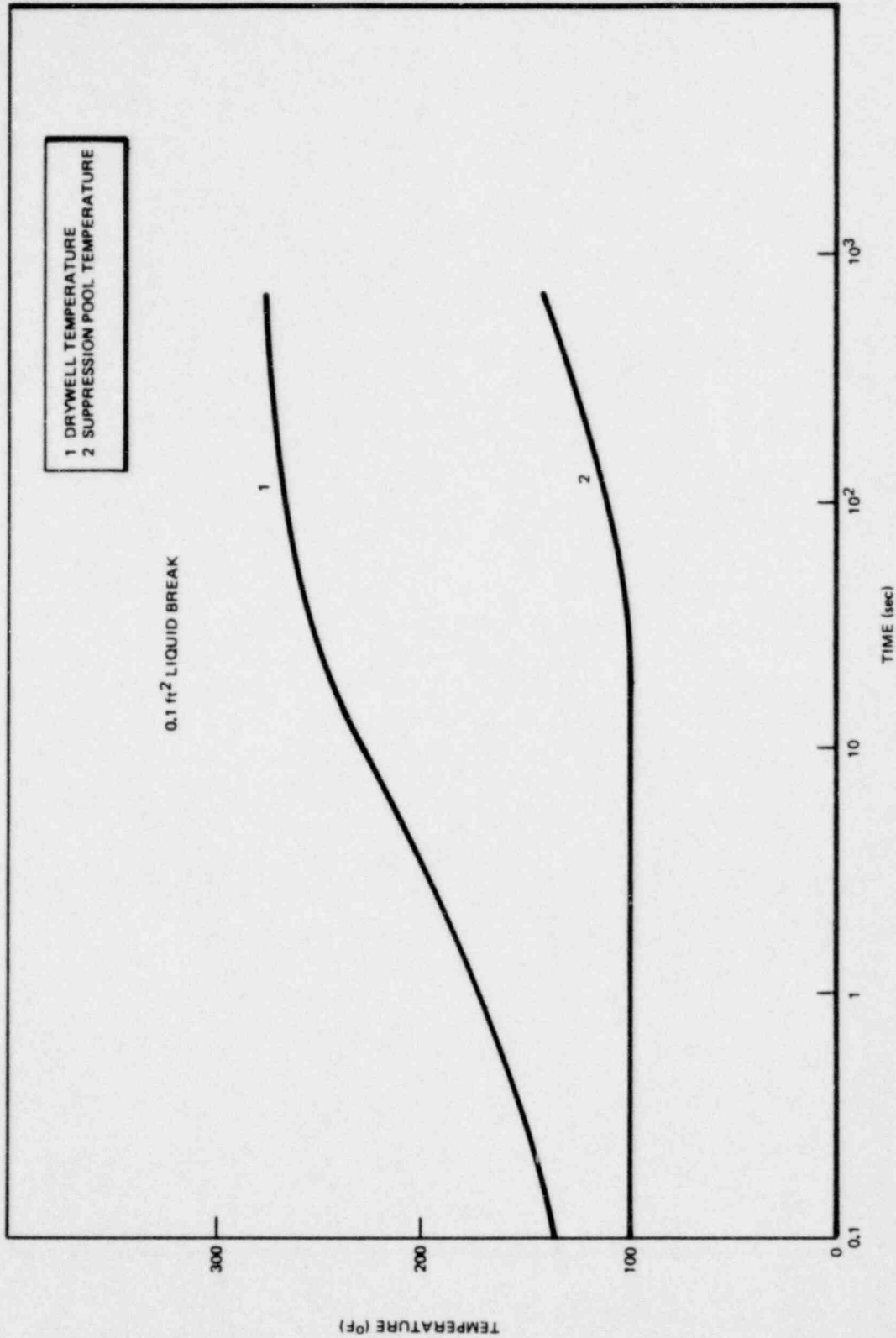
LA SALLE COUNTY STATION  
MARK II DESIGN ASSESSMENT REPORT

FIGURE 3.3-14  
DRYWELL/WETWELL TEMPERATURE TRANSIENT  
FOR RECIRCULATION LINE BREAK



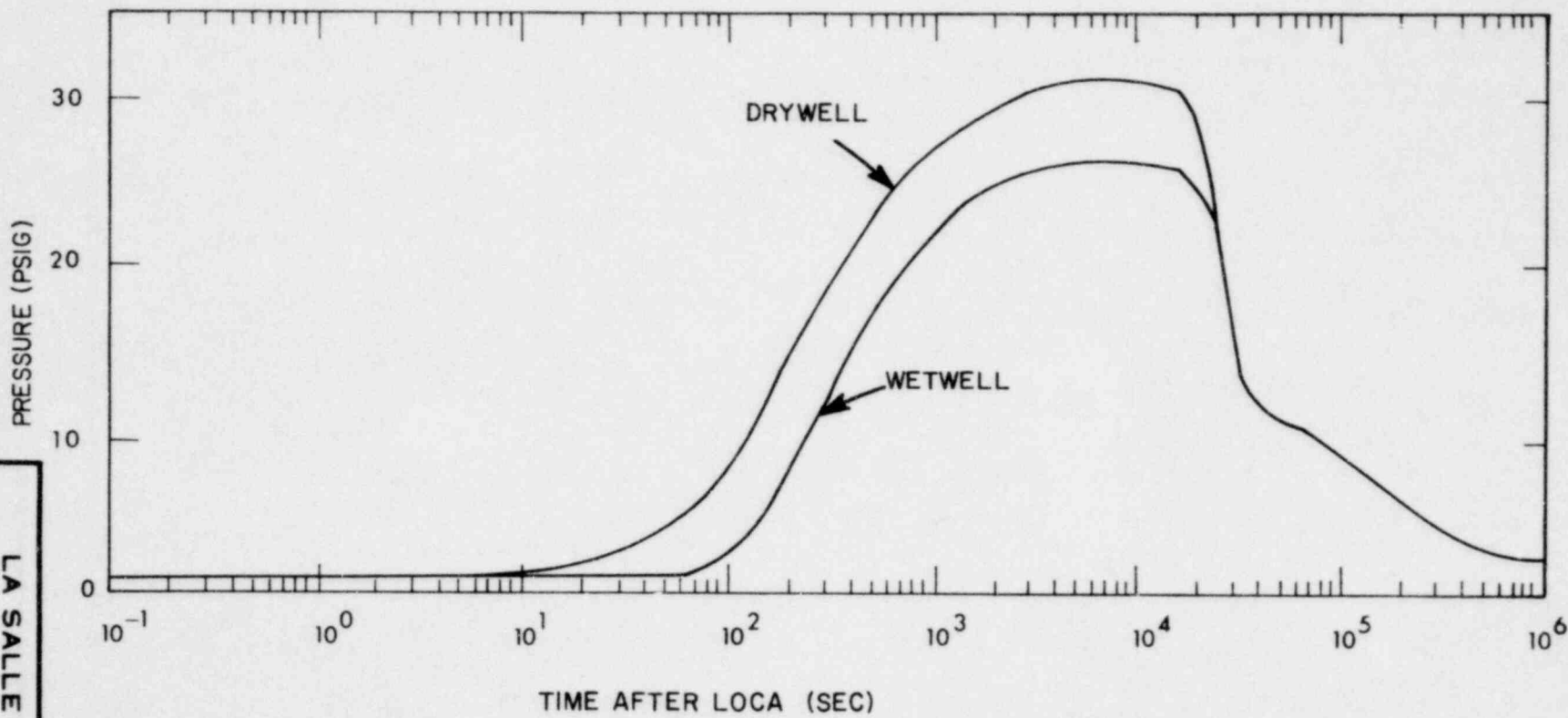
LA SALLE COUNTY STATION  
MARK II DESIGN ASSESSMENT REPORT

FIGURE 3.3-15  
DRYWELL/WETWELL PRESSURE TRANSIENTS  
FOR AN INTERMEDIATE BREAK

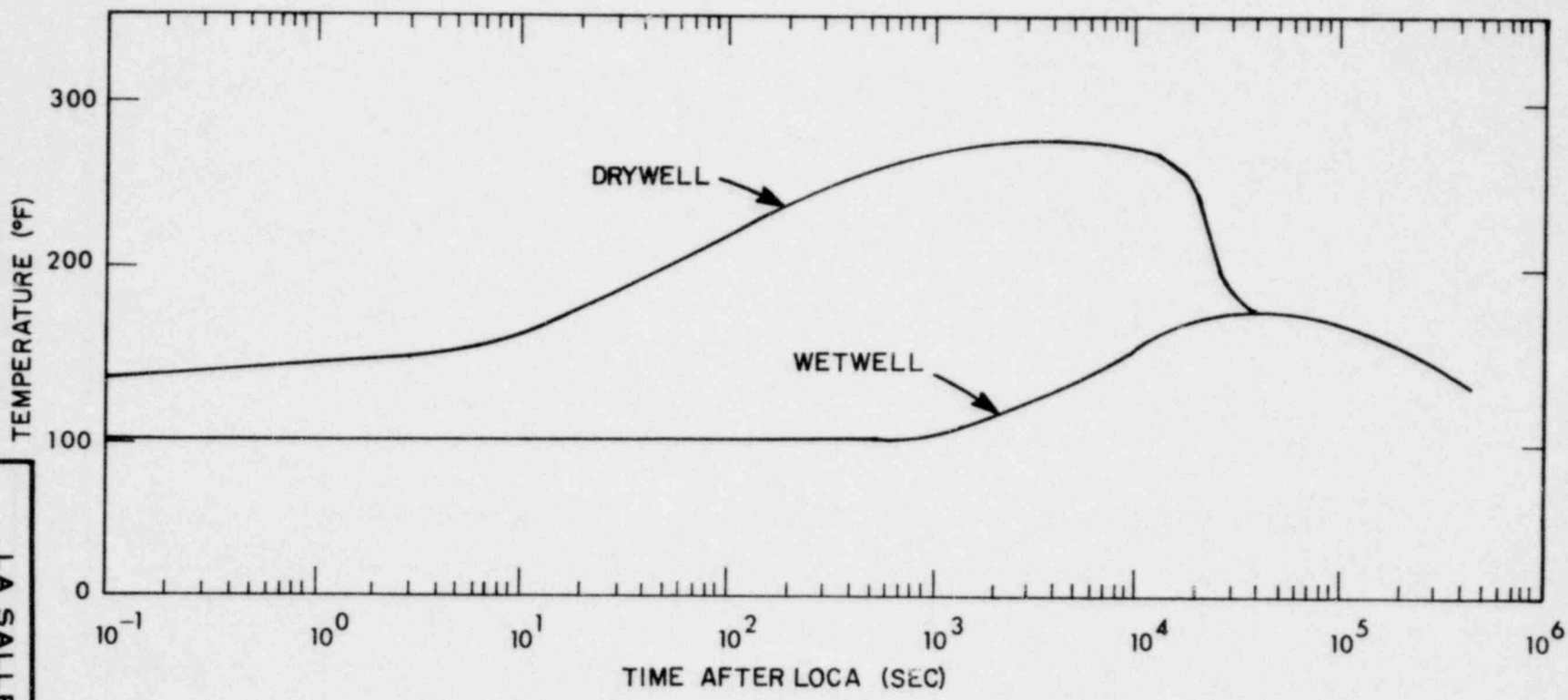


LA SALLE COUNTY STATION  
MARK II DESIGN ASSESSMENT REPORT

FIGURE 3.3-16  
DRYWELL/WETWELL TEMPERATURE TRANSIENTS  
FOR AN INTERMEDIATE BREAK

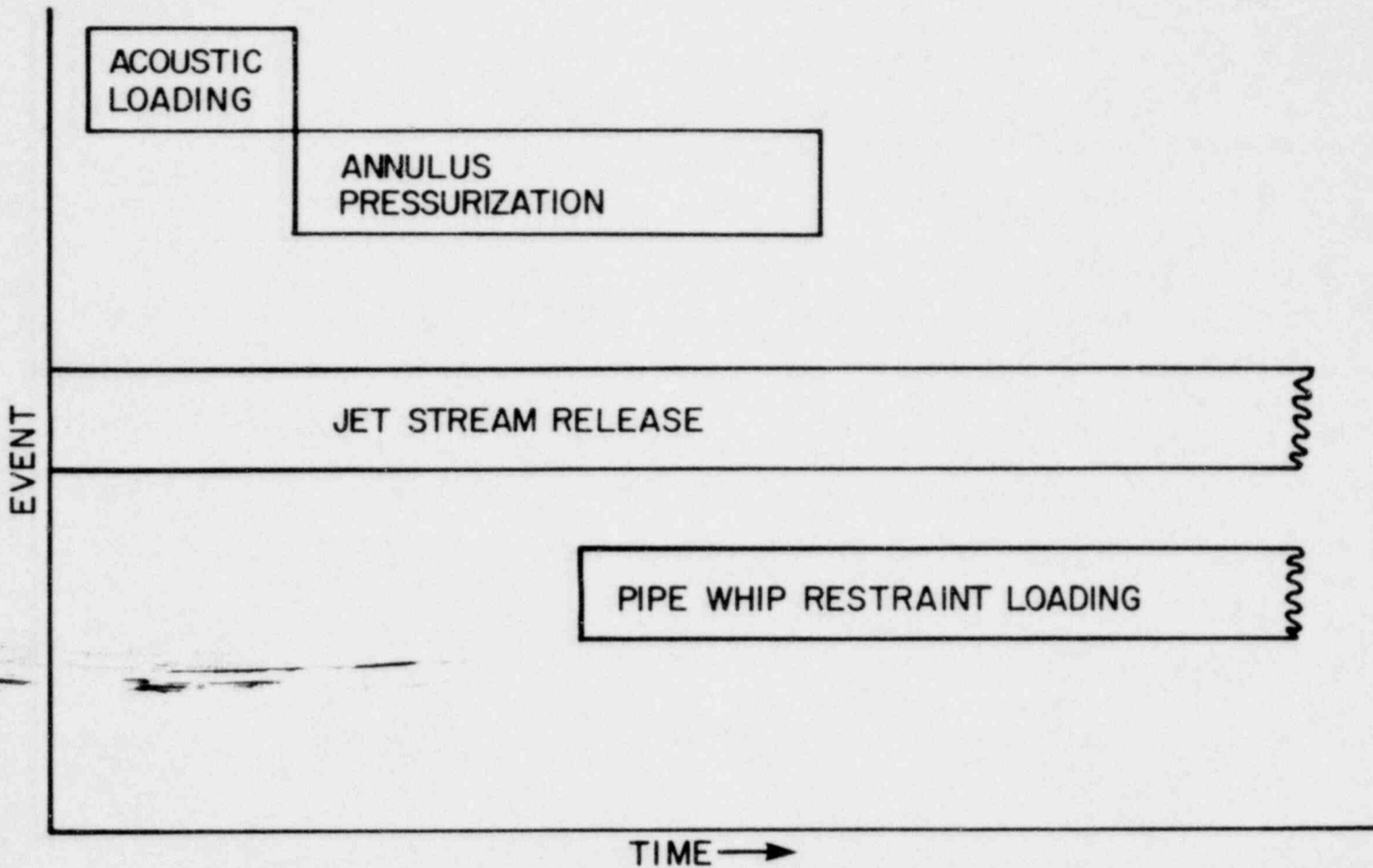


LA SALLE COUNTY STATION  
 MARK II DESIGN ASSESSMENT REPORT  
 FIGURE 3.3-17  
 DRYWELL/WETWELL PRESSURE  
 TRANSIENTS DUE TO SBA

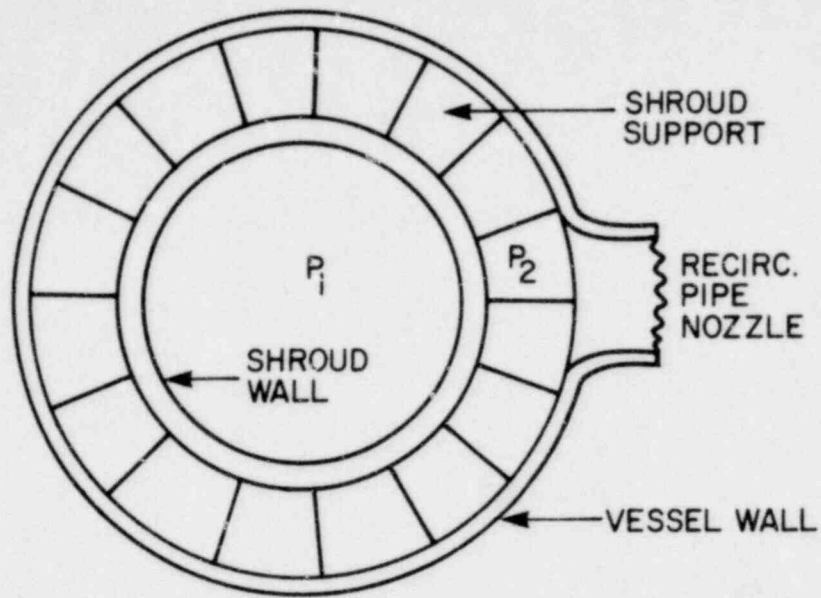


**LA SALLE COUNTY STATION**  
 MARK II DESIGN ASSESSMENT REPORT  
 FIGURE 3.3-18  
 DRYWELL/WETWELL TEMPERATURE  
 TRANSIENTS DUE TO SBA

INITIAL  
INSTANTANEOUS  
RUPTURE

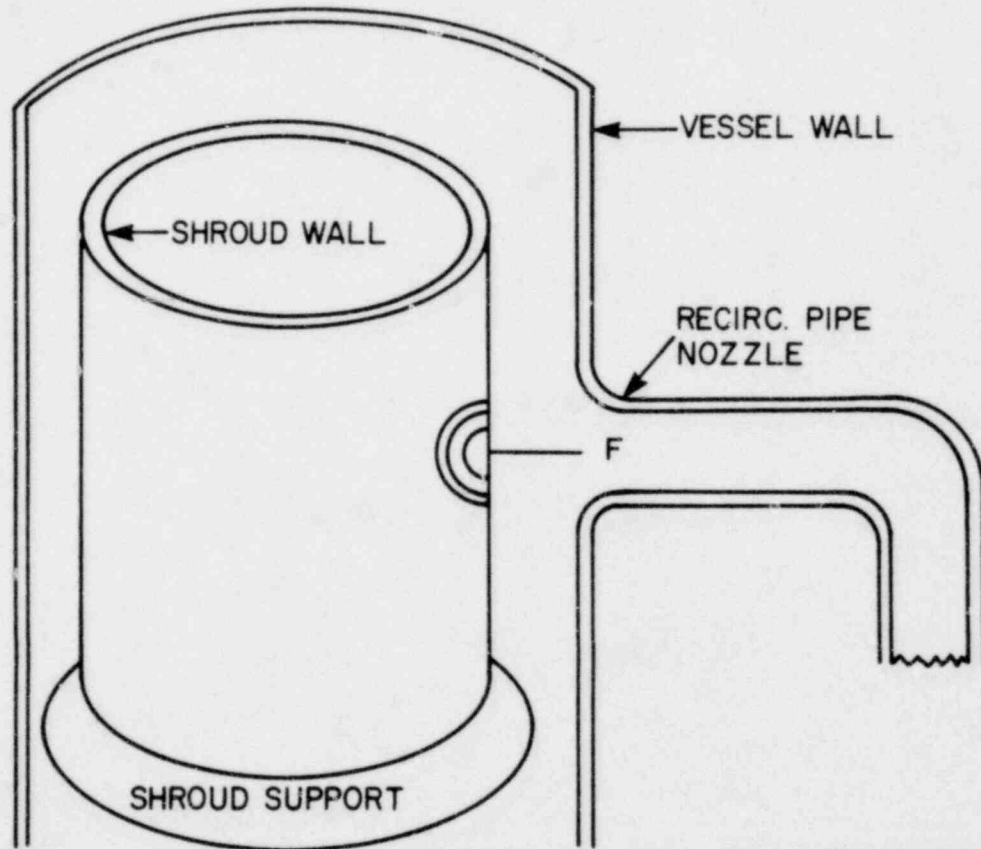


LA SALLE COUNTY STATION
MARK II DESIGN ASSESSMENT REPORT
FIGURE 3.3-19
SEQUENCE OF ANNULUS PRESSURIZATION EVENTS



$P_1$  - OPERATION PRESSURE ~ 1000 PSI

$P_2$  - SATURATION PRESSURE ~ 900 PSI

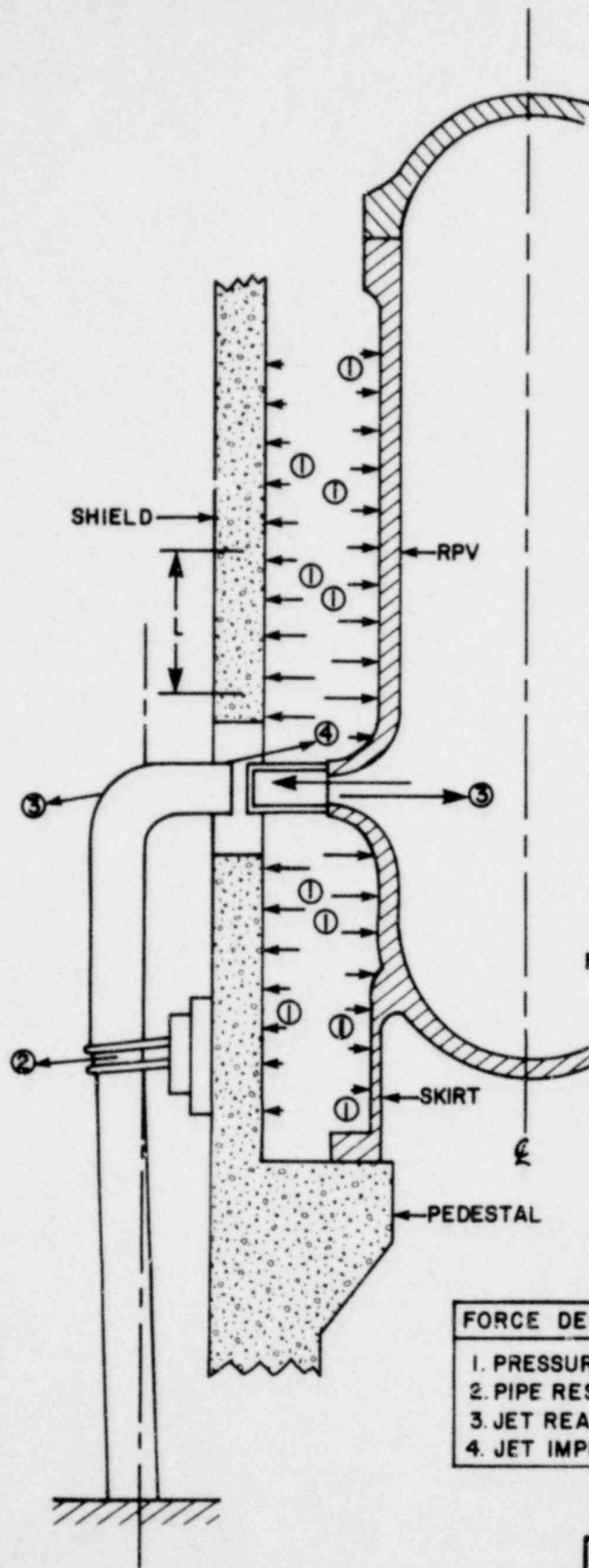


VESSEL CUTAWAY

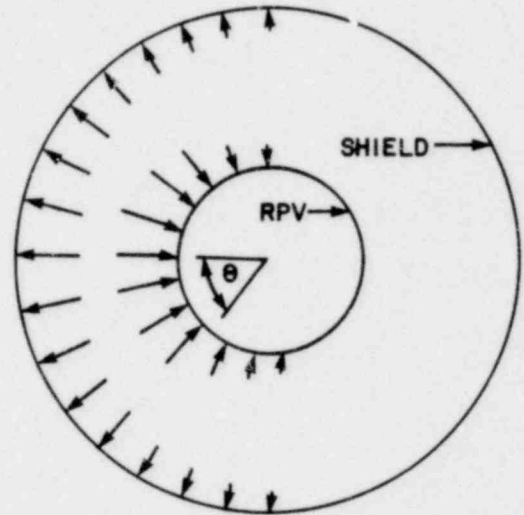
LA SALLE COUNTY STATION  
MARK II DESIGN ASSESSMENT REPORT

FIGURE 3.3-20

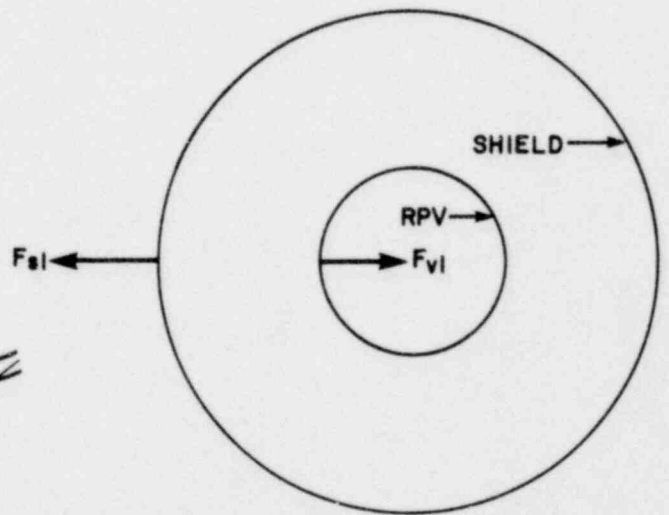
ACOUSTIC LOAD ILLUSTRATION



CALCULATION OF FORCE I



A. PRESSURE DISTRIBUTION



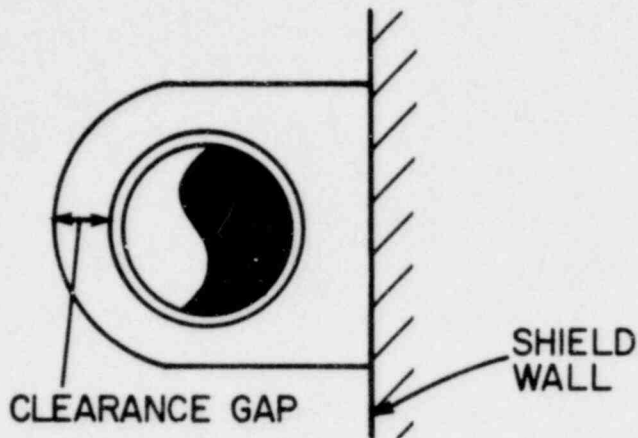
B. RESULTANT FORCES

FORCE DESCRIPTION (ALL FUNCTIONS OF TIME)
1. PRESSURE LOADS
2. PIPE RESTRAINT LOAD
3. JET REACTION FORCE
4. JET IMPINGEMENT FORCE

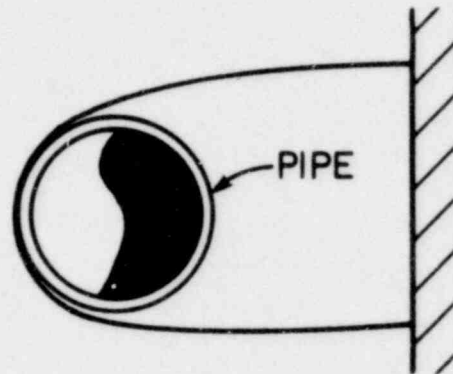
<p><b>LA SALLE COUNTY STATION</b>                  MARK II DESIGN ASSESSMENT REPORT</p>
<p>FIGURE 3.3-21                  ANNULUS PRESSURIZATION                  LOADING DESCRIPTION</p>

THE PIPE WHIP RESTRAINT RESTRICTS PIPE MOTION AND ABSORBS BLOWDOWN ENERGY,

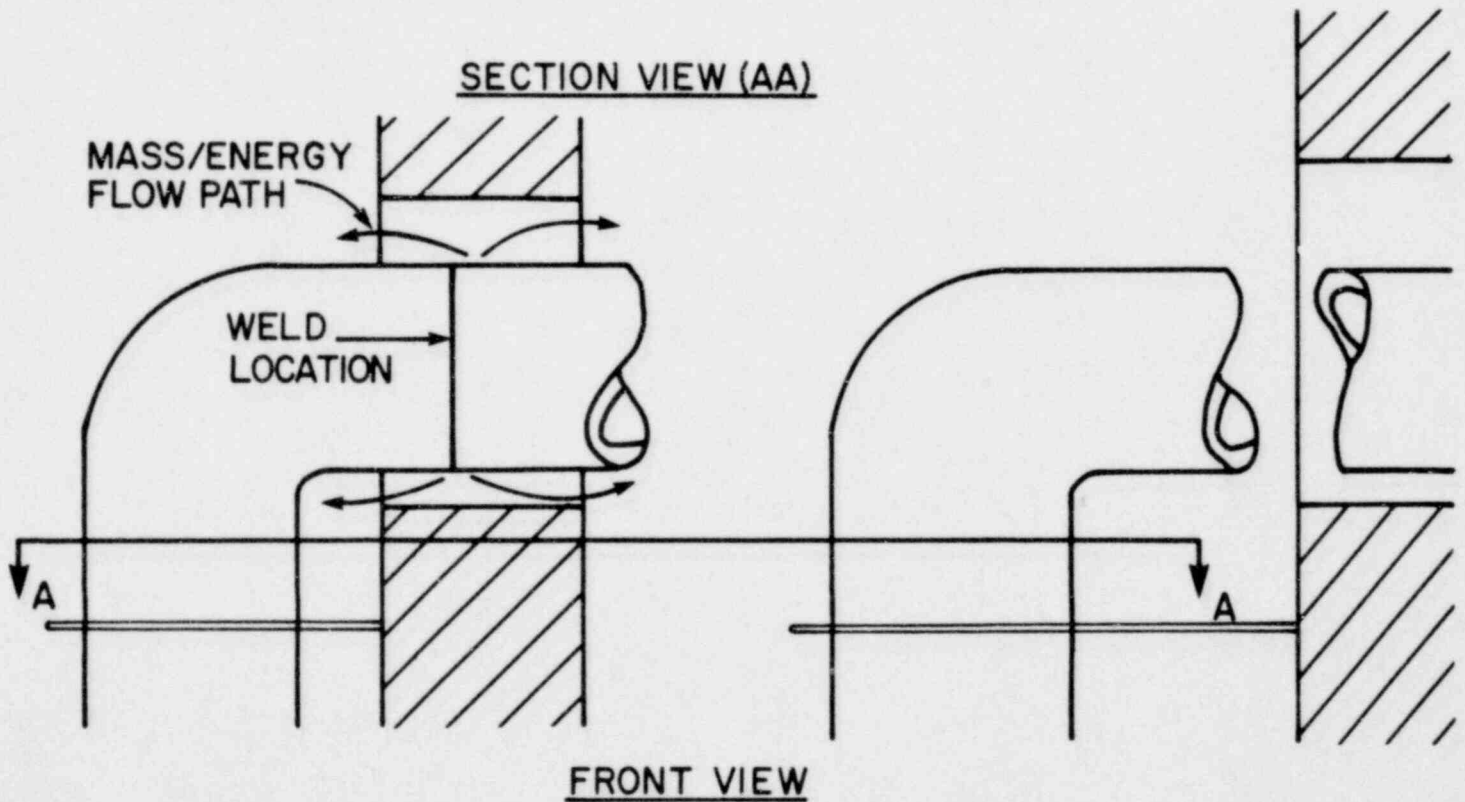
THE RUPTURED PIPE TRAVELS FREELY THROUGH THE CLEARANCE GAP AND THE RESTRAINT DEFORMS TO ABSORB THE KINETIC ENERGY,



PIPE WHIP RESTRAINT AND PIPE IN NORMAL OPERATION POSITION



YIELDED PIPE WHIP RESTRAINT AND PIPE AT REST AFTER POSTULATED RUPTURE



<p>LA SALLE COUNTY STATION MARK II DESIGN ASSESSMENT REPORT</p>
<p>FIGURE 3.3-22</p>
<p>RESTRICTED PIPE MOTION DURING BLOWDOWN</p>

### 3.4 LSCS Position On NUREG 0487 Lead Plant Acceptance Criteria

Table 3.4-1 summarizes the extent to which the LSCS design conforms to the NRC Lead Plant Acceptance Criteria. This table demonstrates that all NRC concerns as addressed in NUREG-0487 have been addressed in the LSCS design reassessment.

TABLE 3.4-1

CONFORMANCE OF THE LSCS DESIGN TO NUREG-0475 CRITERIA

<u>LOAD OR PHENOMENON</u>	<u>MARK II OWNERS GROUP LOAD SPECIFICATION</u>	<u>NRC REVIEW STATUS</u>	<u>LA SALLE POSITION ON ACCEPTANCE CRITERIA</u>
<u>I. LOCA-Related Hydrodynamic Loads</u>			
A. Submerged Boundary Loads During Vent Clearing	33 psi over-pressure added to local hydrostatic below vent exit (walls and basemat) - linear attenuation to pool surface.	Acceptable	Acceptable. The Mark II program has provided a realistic assessment of wall loads based on 4T results (General Electric letter MFN-080-79, Mr. Sobon to Mr. Stolz, March 20, 1979).
<u>B. Pool Swell Loads</u>			
<u>1. Pool Swell Analytical Model</u>			
a) Air Bubble Pressure	Calculated by the Pool Swell Analytical Model (PSAM) used in calculation of submerged boundary loads.	Acceptable	-----
b) Pool Swell Elevation	1.5 x submergence.	NRC Criteria 1.A.1	Acceptable
c) Pool Swell Velocity	Velocity history vs. pool elevation predicted by the PSAM used to compute impact loading on small structures and drag on gratings between initial pool surface and maximum pool elevation and steady-state drag between vent exit and maximum pool elevation. Analytical velocity variation used up to maximum velocity. Maximum velocity applies thereafter up to maximum pool swell.	NRC Criteria 1.A.2	Acceptable  The impact of a 10% increase in pool swell velocity will be assessed. Although the assumptions used in the Pool Swell Analytical Model are already very conservative and eliminate the need for any additional factors, the resulting calculated load increase should not require design changes since there are only a minimum of components in the pool swell region of the wetwell.
d) Pool Swell Acceleration	Acceleration predicted by the PSAM. Pool acceleration is utilized in the calculation of acceleration drag loads on submerged components during pool swell.	Acceptable	
e) Wetwell Air Compression	Wetwell air compression is calculated by the PSAM. Defines the pressure loading on the wetwell boundary above the pool surface during pool swell.	Acceptable	-----

TABLE 3.4-1 (Cont'd)

<u>LOAD OR PHENOMENON</u>	<u>MARK II OWNERS GROUP LOAD SPECIFICATION</u>	<u>NRC REVIEW STATUS</u>	<u>LA SALLE POSITION ON ACCEPTANCE CRITERIA</u>
f) Drywell Pressure History	Plant unique. Utilized to PSAM to calculate pool swell loads.	Acceptable if based on NEDM-10320. Otherwise plant unique reviews required.	Acceptable.
2. Loads on Submerged Boundaries	Maximum bubble pressure predicted by the PSAM added uniformly to local hydrostatic below vent exit (wells and basemat) linear attenuation to pool surface. Applied to walls up to maximum pool swell elevation.	Acceptable	-----
3. Impact Loads			
a) Small Structures	1.5 x Pressure-Velocity correlation for pipes and I beams. Constant duration pulse.	NRC criteria I.A.6	Acceptable. Although the criteria is unnecessarily conservative investigations indicate that, due to the size and frequency of structures in the La Salle pool swell zone, the design loads used are conservative with respect to the NRC Acceptance Criteria. It should be noted that analytical work performed by Sargent & Lundy utilizing the PSTF (Pressure Suppression Test Facility) data for circumferential targets indicates that the DFFR specification is conservative for the size and frequency of structures in the La Salle Pool Swell Zone. Tests performed by EPRI (EPRI No. NP-798, May 1978) to determine flat pool impact on rigid and flexible cylinders are also in good agreement with DFFR. The NRC Acceptance Criteria utilized an assumption (I-beam impact duration is inversely proportional to velocity) which is inconsistent with theory and experimental evidence. Nevertheless, the NRC Criteria have been used to assess structures in the pool swell zone and these structures can withstand the conservative criteria.
b) Large Structures	None - Plant unique load where applicable.	Plant unique review where applicable	Acceptable. La Salle has no large structures in the pool swell zone.
c) Grating	No impact load specified. $P_{drag}$ vs. open area correlation and velocity vs. elevation history from the PSAM.	NRC Criteria I.A.3	Acceptable. La Salle has no grating in pool swell area.

3.4-3

LSCS-MARK II DAR

Rev. 7 1/80

TABLE 3.4-1 (Cont'd)

<u>LOAD OR PHENOMENON</u>	<u>MARK II OWNERS GROUP LOAD SPECIFICATION</u>	<u>NRC REVIEW STATUS</u>	<u>LA SALLE POSITION ON ACCEPTANCE CRITERIA</u>
4. Wetwell Air Compression			
a) Wall Loads	Direct application of the PSAM calculated pressure due to wetwell compression.	Acceptable	_____
b) Diaphragm Upward Loads	2.5 psid	NRC Criteria I.A.4	Acceptable
5. Asymmetric Load	None	NRC Criteria I.A.5	La Salle was assessed for an asymmetric load of the vent clearing pressure (22 psig) applied over a 180° sector of the wetwell wall. This load was applied from the base mat to the wetwell floor. The pool hydrostatic load (1? psig at the base mat with linear decrease to zero at water surface) was superimposed on the asymmetric load. The La Salle design can accommodate this conservative load. General Electric has provided an analysis showing that this asymmetric load will actually be less than 10% of the maximum vent clearing pressure (GE letter MFN-076-79, March 16, 1979). Based on a subsequent analysis by Brookhaven National Laboratories, the NRC revised this criterion to 20% of the maximum vent clearing pressure (NRC/MK II Owners Meeting, July 24-25, 1979, Bethesda, Maryland). La Salle has been assessed for an asymmetric load five times greater than the present criterion.
C. Steam Condensation and Chugging Loads			
1. Downcomer Lateral Loads			
a) Single Vent Loads	8.8 KIP static	NRC Criteria I.B.1	Acceptable
b) Multiple Vent loads	Prescribes variation of load per downcomer vs. number of downcomers.	NRC Criteria I.B.2	Acceptable
2. Submerged Boundary Loads			
a) High Steam Flux Loads	Sinusoidal pressure fluctuation added to local hydrostatic. Amplitude uniform below vent exit-linear attenuation to pool surface. 4.4 psi peak-to-peak amplitude. 2, 6, 7 Hz frequencies.	Acceptable	_____

ISCS-MARK II DAR

Rev. 7 1/80

TABLE 3.4-1 (Cont'd)

LOAD OR PHENOMENON	MARK II OWNERS GROUP LOAD SPECIFICATION	NRC REVIEW STATUS	LA SALLE POSITION ON ACCEPTANCE CRITERIA
II. <u>SRV-Related Hydrodynamic Loads</u>			
A. Pool Temperature Limits for KWU and GE four arm quencher	None specified	NRC Criteria II.1 and II.3	Acceptable
B. Quencher Air Clearing Loads	Mark II plants utilizing the quencher use an interim load specification consisting of the rams head calculational procedure. Mark II plants utilizing the four arm quencher use quencher load methodology described in DFFR.	NRC Criteria II.2	La Salle can accommodate these loads. The first four SRV discharge cases listed in the NRC Acceptance Criteria have been assessed. In addition, a simultaneous valve actuation case is considered. The cases considered and the phasing involved were discussed with the NRC in the December 12, 1978 meeting. This material is documented in Section 3.2.1.2.  Analytical models have been used to predict forcing function frequencies for the load cases considered. Because of the wide range of discharge conditions considered the frequency range used exceeds the 4-11 Hz. range specified. A range used exceeds the 4-11 Hz. range specified. A presentation on the impact of modifications to the SRV frequency range was given in the February 13, 1979 meeting. Results of an assessment of the SRV T-quencher frequency range were presented at the July 26, 1979, meeting. Documentation of these results is being provided.  An additional demonstration of the conservatism of the lead plant approach has been documented by Long Island Lighting Co. (SNRC-374, March 30, 1979, Mr. Novarro [LILCO] to Mr. S. A. Varga NRC transmitting a report entitled, "Justification of Mark II Lead Plant SRV Load Definition.")  In-plant tests will be run to demonstrate the adequacy and conservatism of the design loads.
C. Quencher Tie-Down Loads			
1. Quencher Arm Loads			
(a) Four Arm Quencher	Vertical and lateral arm loads developed on the basis of bounding assumptions for air/water discharge from the quencher and conservative combinations of maximum/minimum bubble pressure acting on the quencher.	Acceptable	-----

3.4-5

LSCS-MARK II DAR

Rev. 7 1/89

TABLE 3.4-1 (Cont'd)

LOAD OR PHENOMENON	MARK II OWNERS GROUP LOAD SPECIFICATION	NRC REVIEW STATUS	LA SALLE POSITION ON ACCEPTANCE CRITERIA
(b) KWU T Quencher	KWU "T" quencher not included in Mark II O.G. Program. T quencher arm loads not specified at this time.	Review Continuing	Acceptable. These loads will be calculated using the methodology and assumptions described in DFFR for four arm quencher, as recommended in the Acceptance Criteria. The KWU T-quencher methodology was used to verify the conservatism of this approach.
2. Quencher Tie-Down Loads			
(a) Four-Arm Quencher	Includes vertical and lateral arm load transmitted to the base-mat via the tie downs. See II.C.1.a above plus vertical transient wave and thrust loads. Thrust load calculated using a standard momentum balance. Vertical and lateral moments for air or water clearing are calculated based on conservative clearing assumptions.	Acceptable	-----
(b) KWU "T" Quencher	KWU "T" quencher not included in Mark II O.G. program. T quencher tie-down loads not specified at this time.	Review Continuing	Acceptable. These loads will be calculated using the methodology and assumptions described in DFFR for four arm quencher and assumptions described in DFFR for four arm quencher. The KWU T-quencher methodology was used to verify the conservatism of this approach.
III. <u>LOCA/SRV Submerged Structure Loads</u>			
A. <u>LOCA/SRV Jet Loads</u>			
1. LOCA/Rams head SRV Jet Loads	Methodology based on a quasi-one-dimensional model.	NRC Criteria III.A.1	See Section 3.3.2.1 for LOCA Jet Loads; SRV Ramshead - NA
2. SRV-Quencher Jet Loads	No loads specified for lead plants. Model under development in long-term program.	NRC Criteria III.A.2	The spherical zone of influence defined in the Acceptance Criteria is not appropriate for the two arm quencher. A zone of influence for each arm will be defined as a cylinder with an axis coincidental with the quencher arm. The length of the cylinder will be equal to the length of the quencher arm plus 10 end cap hole diameters. The radius of the cylinder is expected to be quite small. However, because no structures are within 5 feet of the quencher arm, 5 feet will be assumed. Since no structures are located within 5 feet of the quencher, the NRC Criterion III.A.2 is now satisfied.

TABLE 3.4-1 (Cont'd)

<u>LOAD OR PHENOMENON</u>	<u>MARK II OWNERS GROUP LOAD SPECIFICATION</u>	<u>NRC REVIEW STATUS</u>	<u>LA SALLE POSITION ON ACCEPTANCE CRITERIA</u>
B. LOCA/SRV Air Bubble Drag Loads			
1. LOCA Air Bubble Loads	The methodology follows the LOCA air carryover phase from bubble charging, bubble contract, pool rise and pool fallback. The drag calculations include standard and acceleration drag components.	NRC Criteria III.B.1.	<p>The NRC Acceptance Criteria required modification to the present methodology in several areas. The lead plants have addressed these concerns. Generic documentation will be provided in a Mark II Owners Group submittal. For La Salle County Station, these items have been addressed as follows:</p> <p>a. Bubble asymmetry - The NRC acceptance criterion recommends a 10% increase in velocity and acceleration to accommodate potential asymmetries in the LOCA and SRV air bubbles. La Salle feels that this added factor is unnecessary given the available data and the conservatism already included in the calculations. In support of this position, it is best to discuss LOCA and SRV air bubbles separately.</p> <p>The LOCA charging air bubble transient is driven by the pressurization of the drywell. The limiting case is a double-ended guillotine break of a recirculation line. In spite of the low probability of this type of break, additional conservatisms are included in the calculation of the mass-energy release rate. After the bubble begins to form, observations from tests indicate no significant asymmetries when the bubble expands (EPRI report NP-441, April 1977). Drag coefficients are also conservatively determined as outlined in Appendix B.5. Loads measured in tests show that LOCA air bubble loads are greatly over-predicted by analytical models.</p> <p>The SRV air bubble loads have been demonstrated to be very conservative by the Caora in-plant tests (GE letter MFN-090-79 to Mr. J. F. Stolz, March 28, 1979) and the ETC full-scale, single-cell tests in Germany (as reported by Pennsylvania Power &amp; Light). In addition, multiple valve phasing has been assessed for very conservative unrealistic conditions. Finally, as noted for the LOCA air bubble, drag coefficients have been determined conservatively.</p> <p>In view of the conservatisms identified here and the conservatism of the current methods when compared to test data, no additional multipliers are being applied to velocities and accelerations to simulate postulated bubble asymmetries.</p>

3.4-7

LSGS-MARK II DAR

Rev. 7 1/80

TABLE 3.4-1 (Cont'd)

<u>LOAD OR PHENOMENON</u>	<u>MARK II OWNERS GROUP LOAD SPECIFICATION</u>	<u>NRC REVIEW STATUS</u>	<u>LA SALLE POSITION ON ACCEPTANCE CRITERIA</u>
2. SRV-Rams Head Air Bubble Loads	The methodology is based on an analytical model of the bubble charging process including bubble rise and oscillation. Acceleration drag alone is considered.	NRC Criteria III.B.2	<ul style="list-style-type: none"> <li>b. Standard Drag in Accelerating Flows - Addressed in Section B.5.</li> <li>c. Nodalization of Structures - Addressed in Section B.5.</li> <li>d. Interference Effects - Addressed in Section B.5.</li> <li>e. Interference in Downcomer Bracing - Does not apply to La Salle.</li> <li>a. Neglecting Standard Drag - Standard drag is calculated and included for all submerged structure load calculations.</li> <li>b. LOCA Bubble Criteria - See Section B.5.</li> </ul>
3. SRV-Quencher Air Bubble Loads	No quencher drag model provided for lead plants. Lead plants propose interim use of rams head model (See III.B.2 above). Model will be developed in long-term program.	NRC Criteria III.B.3.	The bubble location and radius will be defined appropriately for T-quencher. Bubbles are located near the arms. The bubble size is predicted from the line air volume.
C. Steam Condensation Drag Loads	No generic load methodology provided. Generic model under development in long-term program.	Lead plant load specification and NRC review will be conducted on a plant unique basis with confirmation in long-term program using generic model.	Described in Subsections 3.3.1.3.5 and 3.3.1.3.6.

LSCS-MARK II DAR

Rev. 7 1/80

3.4-8

#### 4.0 LOAD COMBINATIONS CONSIDERED

##### 4.1 CONTAINMENT AND INTERNAL CONCRETE STRUCTURES

The containment and internal concrete structures were assessed for the load combinations presented in Table 4.1-1. These combinations include the forces due to pool dynamic loads as reported in DFFR Table 5-2.

The loading categories considered in Table 4.1-1 are consistent with those specified in Article CC-3000 of the ASME B&PV Code, Section III, Division 2 and include the following categories:

- a. normal operating load: with and without thermal loads,
- b. normal operating loads with severe environmental loads,
- c. normal operating loads with extreme environmental loads,
- d. abnormal loads,
- e. abnormal loads with severe environmental loads, and
- f. abnormal loads with extreme environmental loads.

The time sequence of occurrence of the LOCA and SRV transient loads presented in the DFFR Figures 5-1 through 5-6 were used in determining these design load combinations with pool dynamic loads.

All combinations of SRV and LOCA loads with other design loads required by the NRC have been considered, including the hypothetical combination of LOCA with one SRV valve actuation.

As shown in Table 4.1-1, the various modes of SRV actuation considered (with the rams head discharge) are:

- |         |  |
|---------|--|
| SRV-ALL | 1. Symmetric actuation of all valves                     |
|         | 2. Resonant sequential symmetric actuation of all valves |

SRV-ADS	Automatic depressurization actuation of seven valves.
SRV-Asymmetric	Actuation of two adjacent valves.
SRV-Single	Actuation of one valve.

The LOCA loads are denoted by  $P_A$  and  $P_B$  in the load combination table and represent three possible pipe break accidents:

- a. DBA - design-basis large break accident
- b. IBA - intermediate break accident, and
- c. SBA - small break accident.

Wherever applicable, the following loads associated with LOCA are included wherever  $P_A$  or  $P_B$  occur in the load combinations:

- a. LOCA pressure,
- b. accident temperature,
- c. pipe break reactions,
- d. vent clearing and pool swell,
- e. condensation-oscillation, and
- f. chugging.

Even though the SRV and LOCA loads used for design are bounding loads as discussed in Section 3.0, additional load factors are applied to these loads (see load combination Table 4.1-1) to assure conservatism for hypothetical overloads.

The load factors adopted are based upon the degree of certainty and probability of occurrence for the individual loads as discussed in the DFFR. The relation between the different times of occurrence of various time-dependent loads as presented in the DFFR were combined and accounted for to determine the most critical loading conditions. In any load combination, if the effect of any load other than dead load (such as thermal

loads) reduces the net design forces, it is deleted from the combination to maximize the design loads.

The reversible nature of the structural responses due to the pool dynamic loads and seismic loads is accounted for by considering for each the peak positive and negative magnitudes of the response forces and maximizing the total positive and negative forces and moments governing the design.

Seismic and pool dynamic load effects are combined by summing the peak responses of each load by the ABS method. The SRSS method is more appropriate than this conservative approach, since the peak effects of all loads do not occur simultaneously. However, the conservative ABS method is used in the design assessment of the containment and internal concrete structure to expedite licensing review.

Re-evaluation of the containment structure for these loads is described in Section 5.1.

#### Acceptance Criteria

The acceptance criteria used in the reassessment of the containment and internal concrete structures for these additional loads and load combinations are the same as those reported in LSCS-FSAR Subsection 3.8.1. These criteria meet or exceed the requirements of Article CC-3000 of the ASME B&PV code, Section III, Division 2. For example, the ASME Code permits yielding of the containment reinforcing steel when thermal loads are present, whereas the criteria used in the reassessment do not permit yielding of the reinforcing steel.

TABLE 4.1-1  
DESIGN LOAD COMBINATIONS

<u>EQN</u>	<u>LOAD COND</u>	<u>D</u>	<u>L</u>	<u>F</u>	<u>P<sub>O</sub></u>	<u>T<sub>O</sub></u>	<u>R<sub>O</sub></u>	<u>E<sub>O</sub></u>	<u>ESS</u>	<u>P<sub>B</sub></u>	<u>P<sub>A</sub></u>	<u>T<sub>A</sub></u>	<u>R<sub>A</sub></u>	<u>R<sub>R</sub></u>	<u>SRV</u>	<u>ADS</u>	<u>ALL</u>	<u>ASYMMETRICAL</u>	<u>SINGLE</u>
1	Normal w/o Temp	1.4	1.7	1.0	1.0	-	-	-	-	-	-	-	-	-	1.5	0	X	X	
2	Normal w/Temp	1.0	1.3	1.0	1.0	1.0	1.0	-	-	-	-	-	-	-	1.3	0	X	X	
3	Normal Sev. Env.	1.0	1.0	1.0	1.0	1.0	1.0	1.25	-	-	-	-	-	-	1.25	0	X	X	
4	Abnormal	1.0	1.0	1.0	-	-	-	-	-	1.25	-	1.0	1.0	-	1.25	X	0	X	
4a		1.0	1.0	1.0	-	-	-	-	-	-	1.25	1.0	1.0	-	1.0	0	0	0	X
5	Abnormal Sev. Env.	1.0	1.0	1.0	-	-	-	1.1	-	1.1	-	1.0	1.0	-	1.1	X	0	X	
5a		1.0	1.0	1.0	-	-	-	1.1	-	-	1.1	1.0	1.0	-	1.0	0	0	0	X
6	Normal Ext. Env.	1.0	1.0	1.0	1.0	1.0	1.0	-	1.0	-	-	-	-	-	1.0	0	X	X	
7	Abnormal Ext. Env.	1.0	1.0	1.0	-	-	-	-	1.0	1.0	-	1.0	1.0	1.0	1.0	X	0	X	
7a		1.0	1.0	1.0	-	-	-	-	1.0	-	1.0	1.0	1.0	1.0	1.0	0	0	0	X

4.1-4

LSCS-MARK II DAR

LOAD DESCRIPTION

D = Dead Loads  
L = Live Loads  
F = Prestressing Loads  
T<sub>O</sub> = Operating Temperature Loads  
R<sub>O</sub> = Operating Pipe Reactions  
P<sub>V</sub> = Operating Pressure Loads  
SRV = Safety/Relief Valve Loads  
E<sub>O</sub> = Operating Basis Earthquake

ESS = Safe Shutdown Earthquake  
P<sub>B</sub> = SBA and IBA LOCA Loads  
T<sub>A</sub> = Pipe Break Temperature Load  
R<sub>A</sub> = Pipe Break Temperature Reactions Loads  
P<sub>A</sub> = DBA LOCA Loads  
R<sub>R</sub> = Reactions and Jet Forces Due to Pipe Break

Rev. 7 1/80

#### 4.2 CONTAINMENT LINER

The load combinations used for the design of the suppression pool liner and its anchorage system are the same as given in Table 4.1-1 except that all load factors are equal to unity. The use of unity loads factors is in accordance with Article CC-3000 of the ASME B&PV Code, Section III, Division 2.

##### Acceptance Criteria

The self-limiting thermal loads, the strains in the liner plate and the displacements of the liner anchorage system are limited to the values allowed in Article CC-3000 of the ASME B&PV Code, Section III, Division 2.

For mechanical loads such as any net negative pressure from pool dynamic load, the liner stresses are limited to the values specified in Subsection NE-3211 of the ASME B&PV Code, Section III, Division 1.

Fatigue evaluation of the liner is based on Subsection NE-3222-4 of the ASME B&PV Code, Section III, Division 1.

### 4.3 OTHER STRUCTURAL COMPONENTS

#### 4.3.1 Concrete Structures

The load combinations, including pool dynamic loads, considered in the reassessment of concrete structures (other than containment concrete structures) such as shear walls, slabs, and beams are shown in Table 4.3-1.

For concrete structures, the peak effects resulting from seismic and pool dynamic loads were combined by the conservative ABS method even though the SRSS method is more appropriate, since the probability of all peak effects occurring at the same time is very small.

#### Acceptance Criteria

The acceptance criteria used in the reassessment of reinforced concrete structures other than containment and internal concrete structures are the same criteria defined in Subsection 3.8.4.5 of the LSCS-FSAR and are identified in Table 4.3-1 for each load combination. The stresses and strains are limited to those specified in ACI 318-1971. As indicated in Table 4.3-1, ultimate strength design method has been used for all load combinations. No overstress is allowed for seismic loads. As stated in the FSAR, when a LOCA occurs outside the containment, as in load combinations 4, 4a, 5, 5a, 7, and 7a, yield line theory is used to design reinforced concrete walls and slabs.

#### 4.3.2 Steel Structures

The load combinations including pool dynamic loads considered in the reassessment of steel structures such as framing, containment galleries, embedments, hangers for cable trays, conduits, and ducts are listed in Table 4.3-2.

For steel structures such as containment and reactor building galleries, framing and their embedments, the peak effects resulting from seismic and pool dynamic loads were combined by the conservative ABS method, whereas for the design of hangers for cable trays, conduits and HVAC ducts, the peak effects from seismic and pool dynamic loads were combined by the SRSS method.

#### Acceptance Criteria

For steel structures, stresses and strains in accordance with the 1969 AISC specifications are used for load combinations 1 through 3 defined in Table 4.3-2. No overstress is allowed for seismic loads. For load combinations involving abnormal or extreme environmental loads, as in load combinations 4 through 7a of Table 4.3-2, the steel stresses were conservatively limited to  $0.95 F_y$ . No plastic deformations were allowed.

TABLE 4.3-1

LOCA AND  
SRV DESIGN LOAD COMBINATIONS  
REINFORCED CONCRETE STRUCTURES OTHER THAN CONTAINMENT

<u>EQN</u>	<u>LOAD COND</u>	<u>D</u>	<u>L*</u>	<u>F</u>	<u>P<sub>O</sub></u>	<u>T<sub>O</sub></u>	<u>R<sub>O</sub></u>	<u>E<sub>O</sub></u>	<u>E<sub>SS</sub></u>	<u>P<sub>B</sub></u>	<u>P<sub>A</sub></u>	<u>T<sub>A</sub></u>	<u>R<sub>A</sub></u>	<u>R<sub>R</sub></u>	<u>SRV**</u>	<u>ADS</u>	<u>ALL</u>	<u>ASYM- MET- RICAL</u>	<u>SINGLE</u>	<u>DESIGN STRENGTH</u>
1	Normal w/o Temp	1.4	1.7	1.0	1.0	-	-	-	-	-	-	-	-	-	1.5	0	X	X		ACI 318-71
2	Normal w/Temp	1.0	1.3	1.0	1.0	1.0	1.0	-	-	-	-	-	-	-	1.3	0	X	X		ACI 318-71
3	Normal Sev. Env.	1.0	1.0	1.0	1.0	1.0	1.0	1.25	-	-	-	-	-	-	1.25	0	X	X		ACI 318-71
4	Abnormal	1.0	1.0	1.0	-	-	-	-	-	1.25	-	1.0	1.0	-	1.25	X	0	X		Yield Limit
4a		1.0	1.0	1.0	-	-	-	-	-	-	1.25	1.0	1.0	-	1.0	0	0	0	X	
5	Abnormal Sev. Env.	1.0	1.0	1.0	-	-	-	1.1	-	1.1	-	1.0	1.0	-	1.1	X	0	X		Yield Limit
5a		1.0	1.0	1.0	-	-	-	1.1	-	-	1.1	1.0	1.0	-	1.0	0	0	0	X	
6	Normal Ext. Env.	1.0	1.0	1.0	1.0	1.0	1.0	-	1.0	-	-	-	-	-	1.0	0	X	X		ACI 318-71
7	Abnormal Ext. Env.	1.0	1.0	1.0	-	-	-	-	1.0	1.0	-	1.0	1.0	1.0	1.0	X	0	X		Yield Limit
7a		1.0	1.0	1.0	-	-	-	-	1.0	-	1.0	1.0	1.0	1.0	1.0	0	0	0	X	

LOAD DESCRIPTION

D	=	Dead Loads	E <sub>SS</sub>	=	Safe Shutdown Earthquake
L	=	Live Loads	P <sub>B</sub>	=	SBA and IBA LOCA Loads
F	=	Prestressing Loads	T <sub>A</sub>	=	Pipe Break Temperature Load
P <sub>O</sub>	=	Normal Operating Pressure Differential Load	R <sub>A</sub>	=	Pipe Break Temperature Reactions Loads
T <sub>O</sub>	=	Operating Temperature Loads	P <sub>A</sub>	=	DBA LOCA Loads
R <sub>O</sub>	=	Operating Pipe Reactions	R <sub>R</sub>	=	Reactions and Jet Forces Due to Pipe Break
P <sub>V</sub>	=	Operating Pressure Loads	*	=	Varies in Magnitude and Intensity
SRV	=	Safety/Relief Valve Loads	**	=	Only One SRV Load should be Combined at One Time
E <sub>O</sub>	=	Operating Basis Earthquake			

TABLE 4.3-2

LOCA AND  
SRV DESIGN LOAD COMBINATIONS  
STRUCTURAL STEEL ELASTIC DESIGN

<u>EQN</u>	<u>LOAD COND</u>	<u>D</u>	<u>L*</u>	<u>F</u>	<u>P<sub>O</sub></u>	<u>T<sub>O</sub></u>	<u>R<sub>O</sub></u>	<u>E<sub>O</sub></u>	<u>E<sub>SS</sub></u>	<u>P<sub>B</sub></u>	<u>P<sub>A</sub></u>	<u>T<sub>A</sub></u>	<u>R<sub>A</sub></u>	<u>R<sub>R</sub></u>	<u>SRV**</u>	<u>ADS</u>	<u>ALL</u>	<u>ASYM-MET-RICAL</u>	<u>SINGLE</u>	<u>DESIGN STRESS</u>
1	Normal w/o Temp	1.0	1.0	1.0	1.0	-	-	-	-	-	-	-	-	-	1.0	0	X	X		AISC Allowable
2	Normal w/Temp	1.0	1.0	1.0	1.0	1.0	1.0	-	-	-	-	-	-	-	1.0	0	X	X		AISC Allowable
3	Normal Sev. Env.	1.0	1.0	-	1.0	1.0	1.0	1.0	-	-	-	-	-	-	1.0	0	X	X		AISC Allowable
4	Abnormal	1.0	1.0	1.0	-	-	-	-	-	1.0	-	1.0	1.0	-	1.0	X	0	X		1.6 AISC Allowable
4a		1.0	1.0	1.0	-	-	-	-	-	-	1.0	1.0	1.0	-	1.0	0	0	0	X	≤ .95 Fy
5	Abnormal Sev. Env.	1.0	1.0	-	-	-	-	1.0	-	1.0	-	1.0	1.0	-	1.0	X	0	X		1.6 AISC Allowable
5a		1.0	1.0	-	-	-	-	1.0	-	-	1.0	1.0	1.0	-	1.0	0	0	0	X	≤ .95 Fy
6	Normal Ext. Env.	1.0	1.0	-	1.0	1.0	1.0	-	1.0	-	-	-	-	-	1.0	0	X	X		1.6 AISC Allowable
7	Abnormal Ext. Env.	1.0	1.0	-	-	-	-	-	1.0	1.0	-	1.0	1.0	1.0	1.0	X	0	X		1.6 AISC Allowable
7a		1.0	1.0	-	-	-	-	-	1.0	-	1.0	1.0	1.0	1.0	1.0	0	0	0	X	≤ .95 Fy

LOAD DESCRIPTION

D =	Dead Loads	E <sub>SS</sub> =	Safe Shutdown Earthquake
L =	Live Loads	P <sub>B</sub> =	SBA and IBA LOCA Loads
S =	Stability Loads	T <sub>A</sub> =	Pipe Break Temperature Load
P <sub>O</sub> =	Operating Pressure Differential Load	R <sub>A</sub> =	Pipe Break Temperature Reactions Load
R <sub>O</sub> =	Operating Pipe Reactions	P <sub>A</sub> =	IBA LOCA Loads
P <sub>V</sub> =	Operating Pressure Loads	R <sub>R</sub> =	Reactions and Jet Forces Due to Pipe Break
SRV =	Safety/Relief Valve Loads	** =	Only One SRV Should be Combined at One Time
E <sub>O</sub> =	Operating Basis Earthquake		
* =	Varies in Magnitude and Intensity		

NOTE: In loading Combinations 2 and 3, the design stress is 1.5 AISC Allowable when T<sub>O</sub> is considered.

#### 4.4 BALANCE-OF-PLANT PIPING AND EQUIPMENT

##### 4.4.1 Wetwell Piping

The load combinations considered for piping located in the wetwell are shown in Table 4.4-1. The combinations include the loads described in Section 3 resulting from building response, loads on submerged structures due to the surrounding fluid motion, and pool swell and fallback loads. Where certain load combinations are bounded by another load combination, the bounding combination was considered. The loads were combined using the SRSS method, with the exception of condensation oscillation loads, which were added absolutely.

##### 4.4.2 Non-Wetwell Piping

###### 4.4.2.1 Load Combination and Acceptance Criteria

For piping not submerged in the wetwell, all loads described in Section 3 are applied to piping through the building response. These loads were considered in the combinations and for the acceptance criteria shown in Table 4.4-1. Of these load combinations, number 2 and 3 were considered to be the bounding combinations, and piping was analyzed for these two combinations. As the other load definitions and combinations became more clearly defined, it became possible to verify the adequacy of load combinations 2 and 3 with respect to the others. Studies were performed and are described in the following subsection. Loads were combined using the SRSS method with the exception of condensation oscillation loads which were added absolutely.

#### 4.4.2.2 Evaluation of Bounded Load Combination - Rams Head Definition

##### a. SSE + SRV<sub>ADS</sub> + CHUG vs. DESIGN BASIS

To evaluate the adequacy of the design basis relative to this load combination, spectra for various points in the containment and reactor building were combined SRSS and compared with the design-basis spectra at these points. The plots are shown in Figure 4.4-1. The spectra show that in the piping frequencies the chugging load combination is bounded by the design basis.

##### b. SSE + Co vs. DESIGN BASIS

Eighty-six subsystems were analyzed for this combination and 1,132 restraint loads compared with the design-basis loads. Of the loads for this combination, 91.3% were lower than the design basis.

Approximately 8.7% of the restraints increased in load, and of these, three restraints (or 0.3%) increased sufficiently to require redesign. Figure 4.4-2, Sheet 1, shows the complete distribution of the load changes. The CO load used was the 7.5-psi peak to peak definition with fluid-structure interaction.

#### 4.4.2.3 Justification of Alternative Acceptance Criteria

##### a. Quencher vs. Rams Head

The switch to a quencher discharge device caused a change in building response spectra which was evaluated to ensure the continued adequacy of the design basis. The study described in

Subsection 4.4.2.2b was performed for this load combination and a distribution of load changes is shown in Figure 4.4-2, Sheet 2. Of these loads, 98.2% are lower than the design basis. The 1.8% that are increases are caused by the fact that although the quencher spectra peaks are lower in amplitude than the rams head spectra peaks, the frequency of the peaks shifts in the low-frequency direction, causing a small number of restraints on low-frequency systems to increase. None of the increases would require redesign, since the fundamental frequencies of the piping are larger than these low frequencies.

b. SSE + SRV<sub>ADS</sub> + CHUGGING vs. DESIGN BASIS

Because SRV<sub>ALL</sub> loads are used instead of SRV<sub>ADS</sub> for the quencher load definition, this load combination must be reevaluated for the quencher device. It now becomes equivalent to SSE + SRV<sub>ALL</sub> + CHUGGING. The same study as described in Subsection 4.4.2.2 was done for this load combination, and the load change distributions are shown in Figure 4.4-2, Sheet 3. Approximately 90.4% of the loads are lower, and one restraint (or 0.09%) would require redesign.

4.4.2.4 Summary

Based on the evaluations outlined above, the current rams head design basis can be considered an acceptable design basis for the plant. The results of the piping analyses for the rams head design basis are in Tables 3.9-34 through 3.9-36 of the LSCS-FSAR.

#### 4.4.3 Equipment

All loading combinations shown in Table 4.4-1 were considered. The following bounding load cases were used for the re-evaluation:

<u>Load Combination</u>	<u>Acceptance Criteria</u>
a. Normal operating loads + OBE Seismic + SRV <sub>all</sub> (1% damping) (1% damping)	Upset
b. Normal operating loads + SSE Seismic + SRV <sub>all</sub> (2% damping) (2% damping)	}  Emergency
c. Normal operating loads + SSE Seismic + CO <sub>2-7</sub> hz (2% damping) (2% damping)	

The seismic loads were combined with the pool dynamic loads by the SRSS method except for case (c), where the absolute sum method was used.

The acceptance criteria used for BOP equipment are given in Table 4.4-2 for both active and nonactive equipment and for fluid and nonfluid systems.

SQRT Forms have been completed for all pieces of equipment located in the reactor building (except for valves). Equipment reevaluation for loads combination case (c) is not documented in SQRT Form because of one of the following reasons:

- a. Equipment does not possess any natural frequencies in the dominant frequency range of 2-8 Hz.

- b. Equipment possess natural frequencies in the dominant frequency range of 2-8 Hz with insignificant participation to the equipment total response.

- I. Nonactive fluid system equipment has been checked for the same loading combinations and the corresponding ASME Section III design limits.

Operability of all active components was established by an elastic deflection analysis if the combined stresses were below the yield stress and by an exact deflection analysis if combined stresses exceeded the yield stress.

- II. The piping reaction on mechanical equipment will be maintained within the equipment vendor's nozzle allowables by providing additional pipe restraints if needed.

If the nozzle load cannot be maintained within the vendor-supplied equipment allowables, the following additional checks will be performed:

- a. Local nozzle stress analysis using WRC Bulletin 107 as a guide.
- b. Evaluation of the equipment supporting structure.

- III. The seismic qualification reports for all equipment and components mounted to the floor will be reviewed and checked using the new loading combinations. Additional calculation and/or test shall be made where necessary. In addition, foundation loads will be checked for acceptability.

- IV. For Seismic Category I valves, the dynamic coefficients will be computed from the new piping analysis which considers all LOCA and SRV related dynamic loads. The valves will be qualified to meet these dynamic coefficients or a new piping

support arrangement will be developed to reduce the dynamic coefficients to acceptable levels. In addition, active valves will undergo a review to assure that the stress allowables for operability are also met.

V. T-QUENCHER ASSESSMENT

The impact of the loading combinations associated with the T-Quencher have been assessed. Equipment that needed retesting under rams head loads needs retesting under T-quencher loads. Equipment that was tested and met the requirements of rams head loading would in most cases meet the requirements of T-quencher loads with minor justification. Some equipment qualified by analysis may need additional calculations. No major hardware modifications or retesting of the equipment is anticipated.

TABLE 4.4-1

LOAD COMBINATIONS FOR EQUIPMENT AND PIPING

<u>Load Case</u>	<u>P</u>	<u>W</u>	<u>SRV</u> <u>ALL</u>	<u>SRV</u> <u>ADS</u>	<u>OBE</u>	<u>SSE</u>	<u>SBA</u> <sup>(4)</sup>	<u>IBA</u> <sup>(4)</sup>	<u>DBA</u> <sup>(5)</sup>	<u>Acceptance Criteria</u>
1	X	X	X							Upset
2	X	X	X		X					Upset
3	X	X	X			X				Emergency <sup>(2)</sup>
4	X	X		X	X		X			Emergency <sup>(2) (3)</sup>
5	X	X		X	X			X		Emergency <sup>(2) (3)</sup>
6	X	X		X		X	X <sup>(1)</sup>	X <sup>(1)</sup>		Emergency <sup>(2)</sup>
7	X	X				X			X	Emergency <sup>(2)</sup>

P - Pressure  
W - Weight  
SRV - Safety Relief Valve  
ADS - Automatic Depressurization System  
OBE - Operating Basis Earthquake  
SSE - Safe Shutdown Earthquake  
SBA - Small Break Accident  
IBA - Intermediate Break Accident  
DBA - Design Basis Accident

1. IBA or SBA, Whichever Governs
2. Faulted for Non-Essential Subsystems
3. Active Equipment Evaluated to Upset
4. Chugging
5. Condensation Oscillation or Annulus Pressurization

4.4-7

LSCS-MARK II DAR

Rev. 7 1/80

TABLE 4.4-2

LOAD COMBINATIONS AND ALLOWABLE STRESS LIMITS FOR BOP EQUIPMENTA. Nonfluid System Equipment

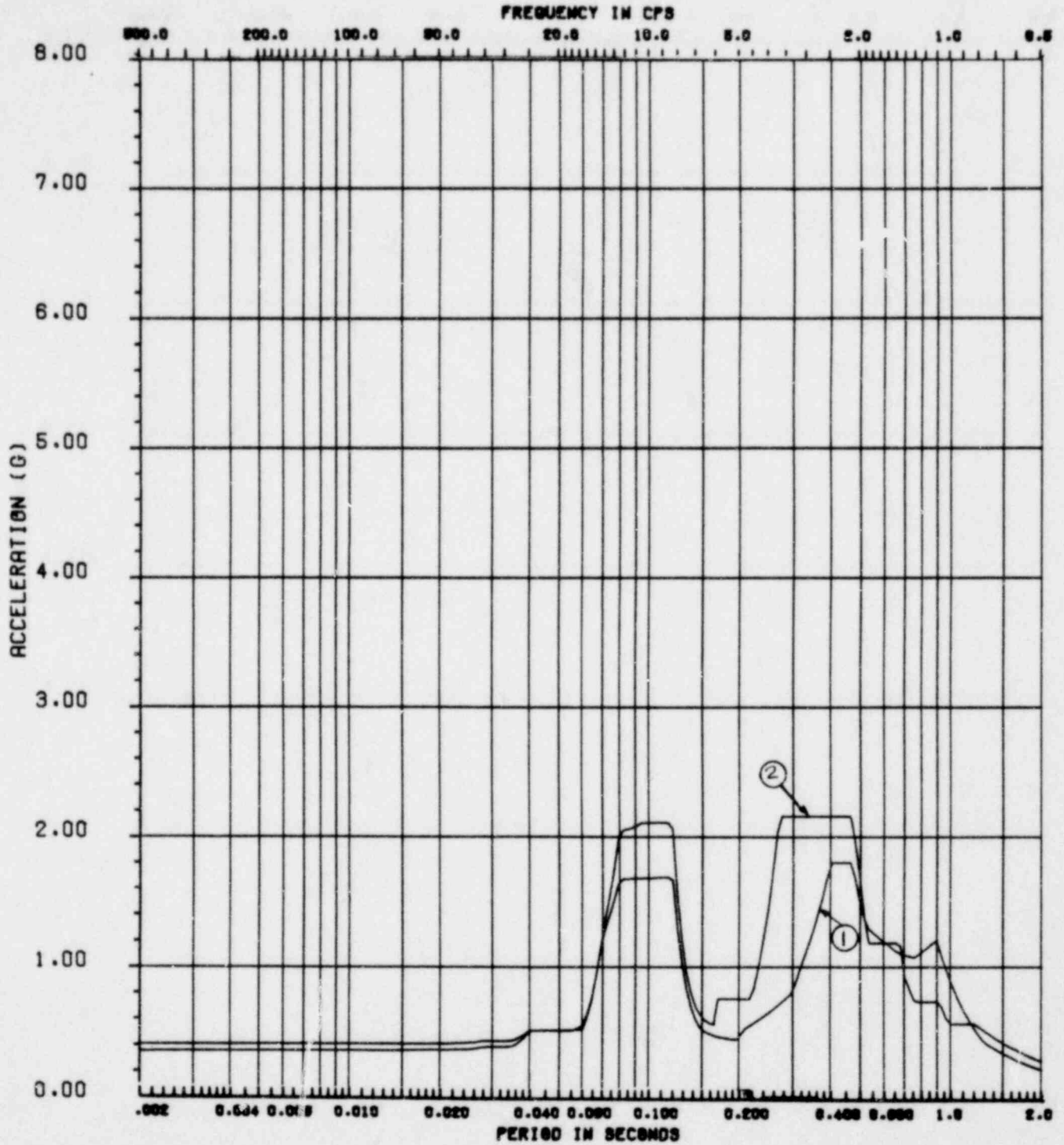
<u>PLANT CONDITION</u>	<u>ACTIVE (ELASTIC DEFLECTION)</u>	<u>NONACTIVE (AND ACTIVE EXACT DEFLECTION)</u>
<u>Upset</u>		
(Normal Operating Loads + SRV <sub>ALL</sub> + OBE Seismic)	$\sigma_m \leq 0.6 S_y$ (D.M.) $\leq 0.3 S_u$ (B.M.)	$\sigma_m \leq 0.6 S_y$ (D.M.) $\leq 0.4 S_u$ (B.M.)
	$\sigma_t \leq 0.7 S_y$ (D.M.) $\leq 0.4 S_u$ (B.M.)	$\sigma_t \leq 0.9 S_y$ (D.M.) $\leq 0.6 S_u$ (B.M.)
<u>Emergency</u>		
(Normal Operating Loads + SRV <sub>ALL</sub> + SSE Seismic)	} $\sigma_m \leq 0.7 S_y$ (D.M.) $\leq 0.4 S_u$ (B.M.)	} $\sigma_m \leq 0.9 S_y$ (D.M.) $\leq 0.6 S_u$ (B.M.)
(Normal Operating Loads + SSE Seismic + CO <sub>2-7</sub> )		
	} $\sigma_t \leq 0.95 S_y$ (D.M.) $\leq 0.6 S_u$ (B.M.)	} $\sigma_t \leq 1.5 S_y$ (D.M.) $\leq 0.9 S_u$ (B.M.)

B. Active Fluid System Equipment

<u>PLANT CONDITION</u>	<u>ASME CLASS 1</u>	<u>ASME CLASS 2 &amp; 3</u>
<u>Upset</u>		
(SRV <sub>ALL</sub> + OBE + Normal Operating Loads)	Per ASME Sec. III Same as Nonactive	Per ASME Sec. III Same as Nonactive
<u>Emergency</u>		
(SRV <sub>ALL</sub> + SSE + Normal Operating Loads)	} $\sigma_m \leq 1.00 S_m$ $\sigma_t \leq 1.5 S_m$	} $\sigma_m \leq 1.00 S_h$ $\sigma_t \leq 1.65 S_h$
(CO <sub>2-7</sub> + SSE + Normal Operating Loads)		

Where:

$\sigma_m$	= Membrane stress	$S_u$	= Ultimate stress at corresponding temperature
$\sigma_t$	= Membrane + bending stress	D.M.	= Ductile material
$S_h, S_m$	= As defined by Section III	B.M.	= Brittle material
$S_y$	= Yield stress at corresponding temperature		

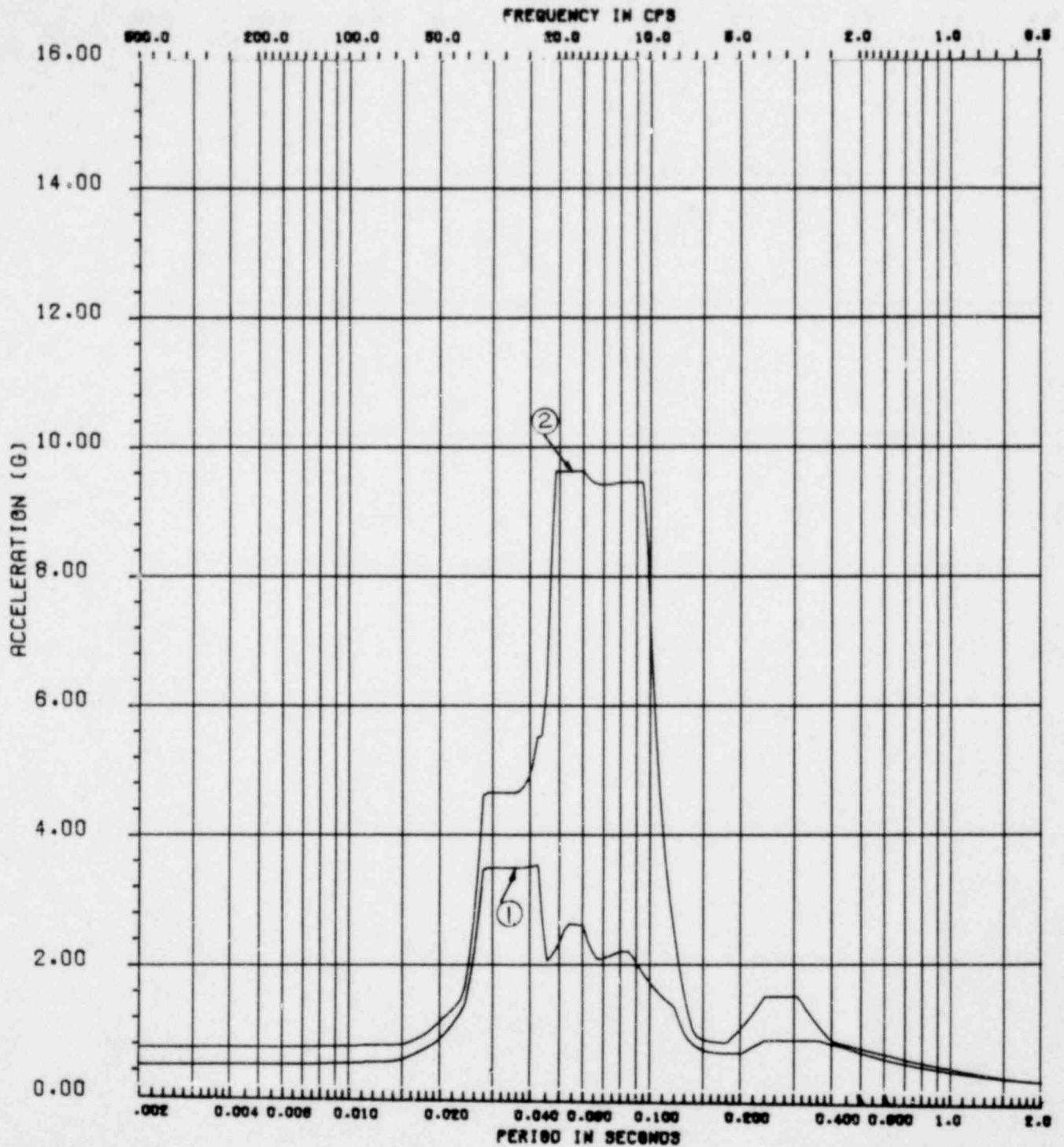


SET-1 REACTOR SLAB EL. 694'-6" N-S  
 COMB. 1. =  $[SSE^2 + CHUG^2 + (SRV_{ADS})^2]^{\frac{1}{2}}$   
 \*COMB. 2. =  $[(SSE)^2 + (SRVRH)^2]^{\frac{1}{2}}$   
 \*DESIGN BASIS

**LA SALLE COUNTY STATION**  
 MARK II DESIGN ASSESSMENT REPORT

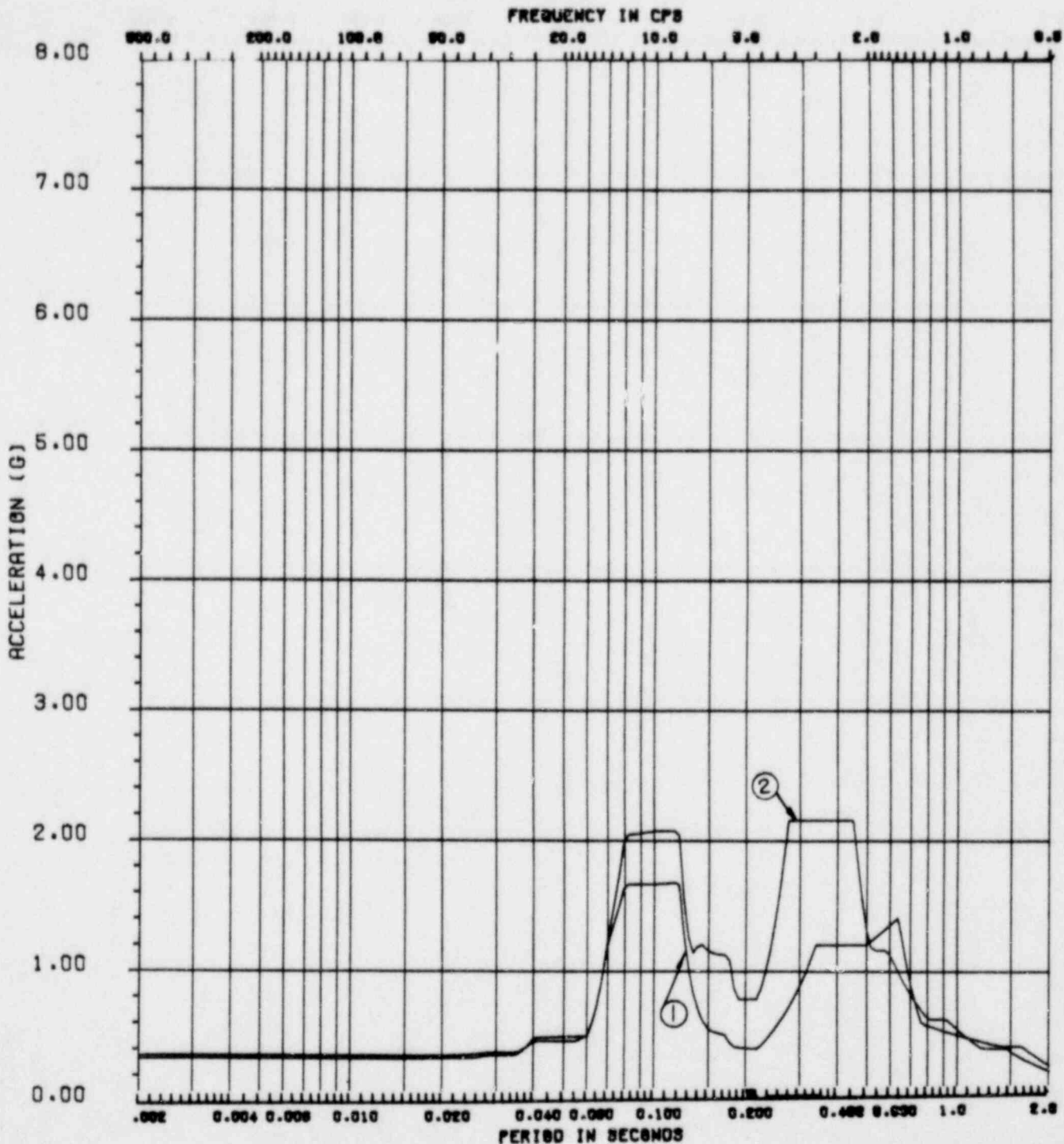
---

FIGURE 4.4-1  
 RESPONSE SPECTRA COMPARISON DESIGN  
 BASIS VS. CHUGGING  
 (SHEET 1 of 18)



SET-1 REACTOR SLAB EL. 694'-6" VERT  
 COMB. 1. =  $[SSE^2 + CHUG^2 + (SRV_{ADS})^2]^{1/2}$   
 \*COMB. 2. =  $[(SSE)^2 + (SRVRH)^2]^{1/2}$   
 \*DESIGN BASIS

<p><b>LA SALLE COUNTY STATION</b>                  MARK II DESIGN ASSESSMENT REPORT</p>
<p>FIGURE 4.4-1                  RESPONSE SPECTRA COMPARISON DESIGN                  BASIS VS. CHUGGING                  (SHEET 2 of 18)</p>

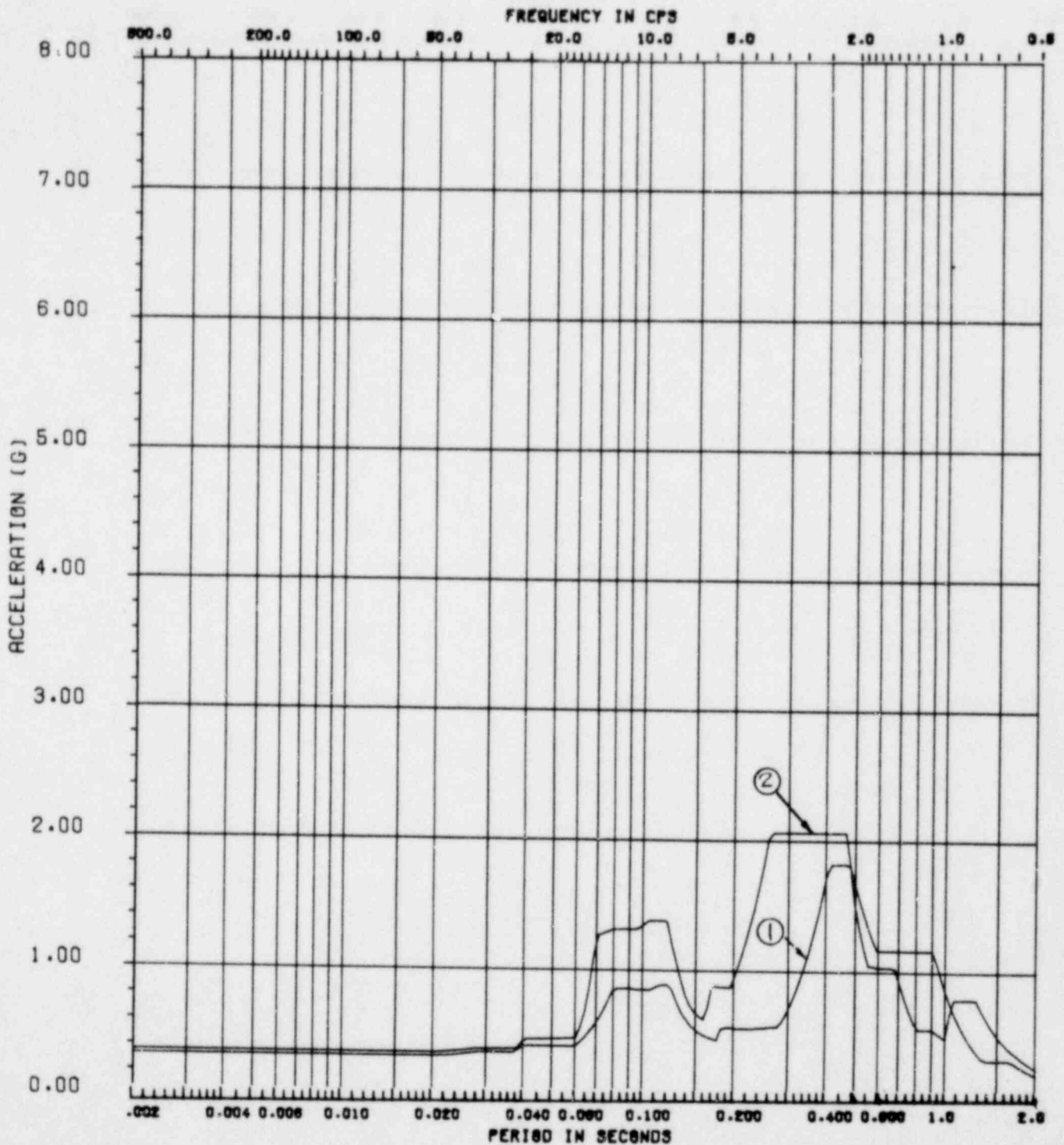


SET-1 REACTOR SLAB EL. 694'-6" E-W  
 COMB. 1. =  $[SSE^2 + CHUG^2 + (SRV_{ADS})^2]^{\frac{1}{2}}$   
 \*COMB. 2. =  $[(SSE)^2 + (SRVRH)^2]^{\frac{1}{2}}$   
 \*DESIGN BASIS

**LA SALLE COUNTY STATION**  
 MARK II DESIGN ASSESSMENT REPORT

---

FIGURE 4.4-1  
 RESPONSE SPECTRA COMPARISON DESIGN  
 BASIS VS. CHUGGING  
 (SHEET 3 of 18)

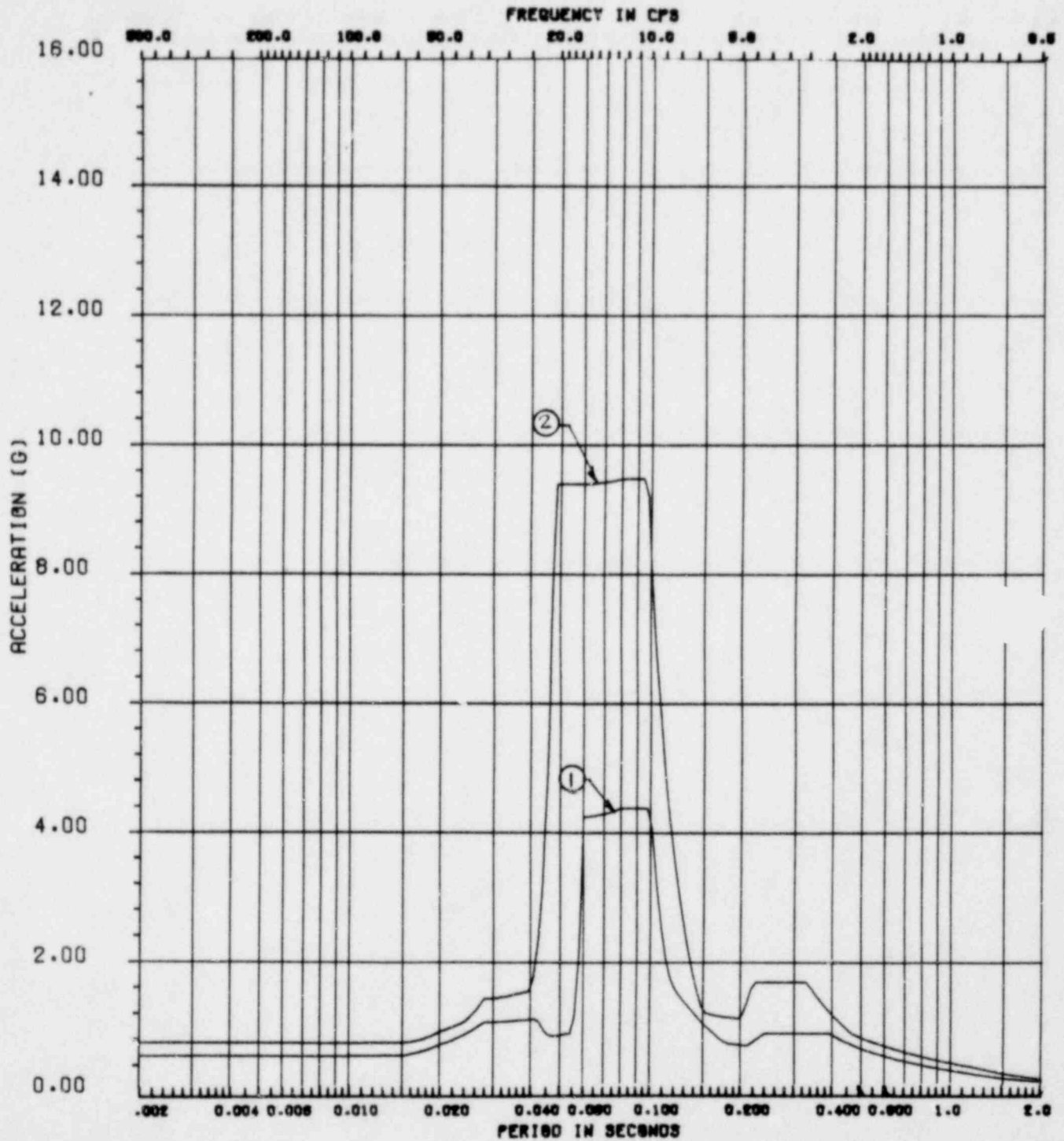


SET-1 REACTOR SLAB EL. 740'-0" N-S  
 COMB. 1. =  $[SSE^2 + CHUG^2 + (SRV_{ADS})^2]^{\frac{1}{2}}$   
 \*COMB. 2. =  $[(SSE)^2 + (SRVRH)^2]^{\frac{1}{2}}$   
 \*DESIGN BASIS

**LA SALLE COUNTY STATION**  
 MARK II DESIGN ASSESSMENT REPORT

---

FIGURE 4.4-1  
 RESPONSE SPECTRA COMPARISON DESIGN  
 BASIS VS. CHUGGING  
 (SHEET 4 of 18)

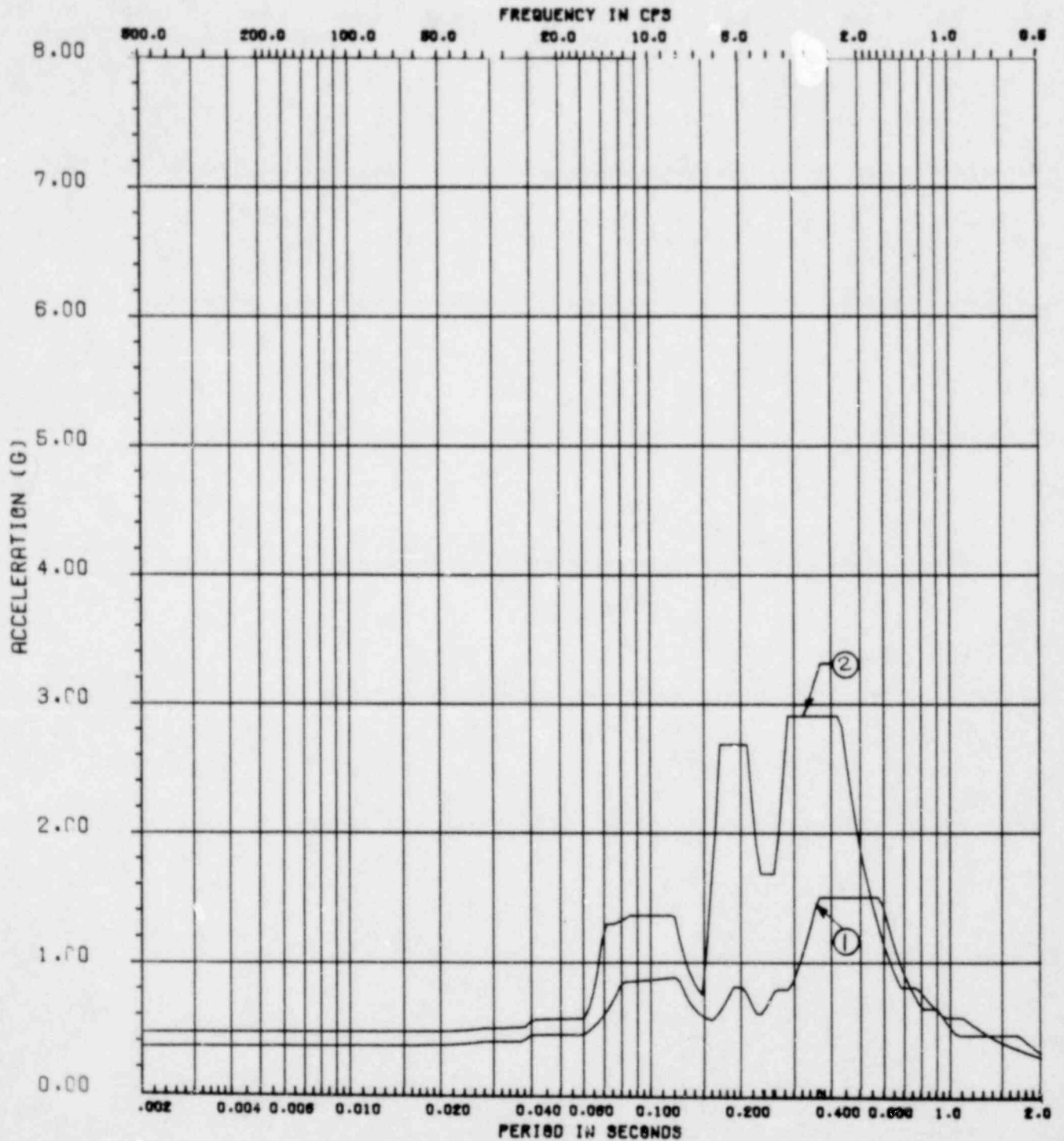


SET-1 REACTOR SLAB EL. 740'-0" VERT  
 COMB. 1. =  $[SSE^2 + CHUG^2 + (SRV_{ADS})^2]^{\frac{1}{2}}$   
 \*COMB. 2. =  $[(SSE)^2 + (SRVRH)^2]^{\frac{1}{2}}$   
 \*DESIGN BASIS

**LA SALLE COUNTY STATION**  
 MARK II DESIGN ASSESSMENT REPORT

---

FIGURE 4.4-1  
 RESPONSE SPECTRA COMPARISON DESIGN  
 BASIS VS. CHUGGING  
 (SHEET 5 of 18)

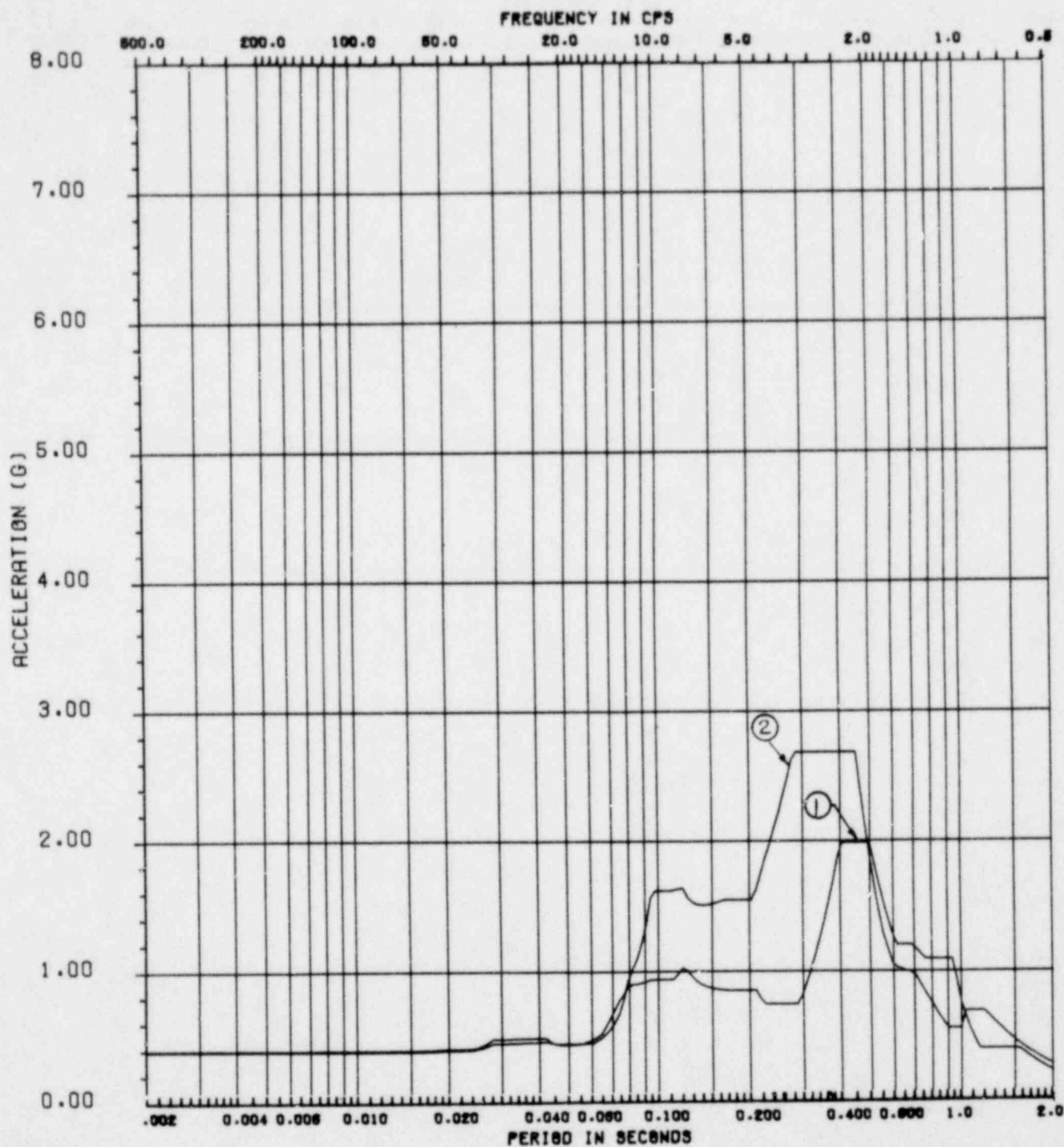


SET-1 REACTOR SLAB EL. 740'-0" E-W  
 COMB. 1. =  $[SSE^2 + CHUG^2 + (SRV_{ADS})^2]^{\frac{1}{2}}$   
 \*COMB. 2. =  $[(SSE)^2 + (SRVRH)^2]^{\frac{1}{2}}$   
 \*DESIGN BASIS

**LA SALLE COUNTY STATION**  
 MARK II DESIGN ASSESSMENT REPORT

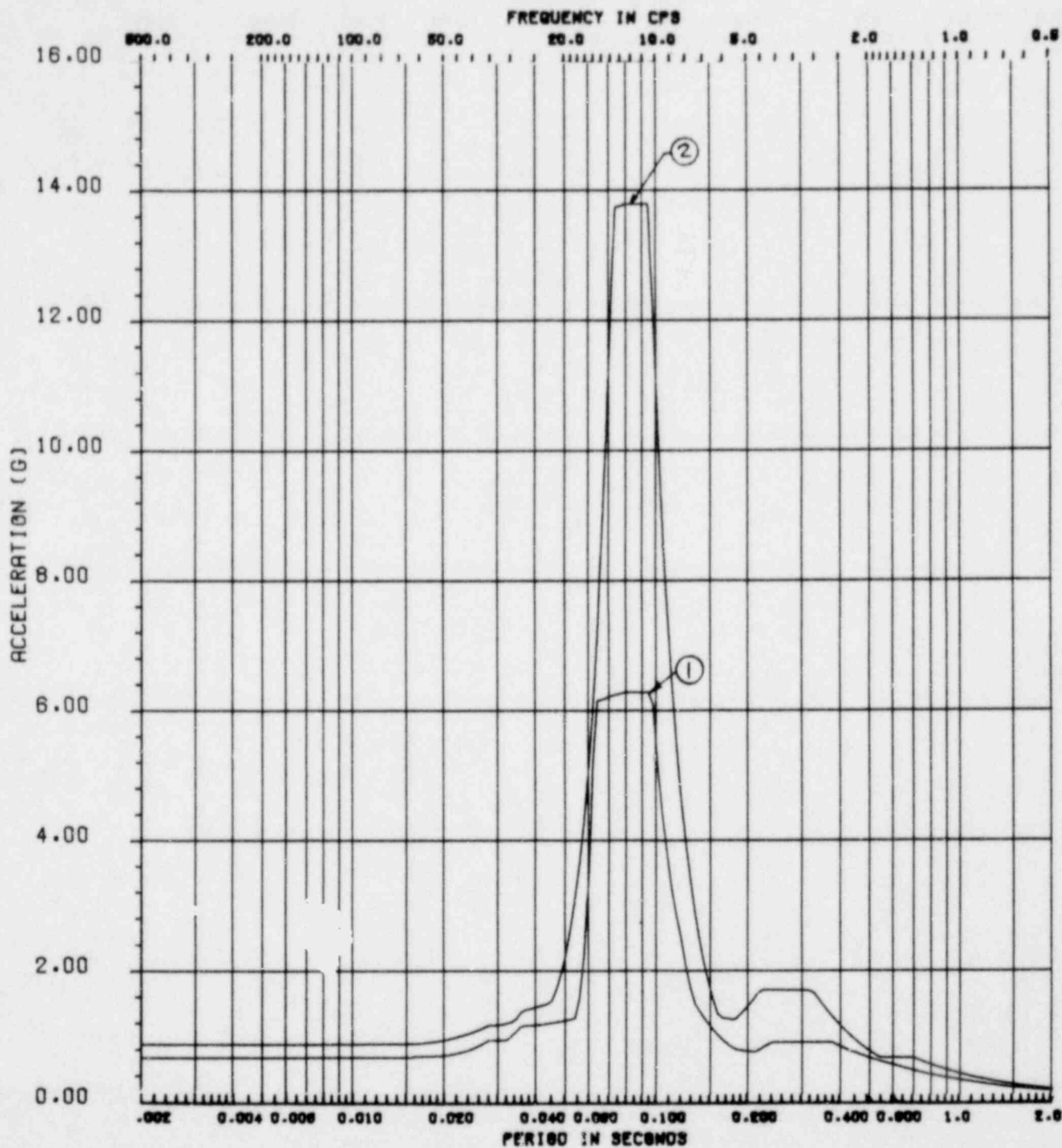
---

FIGURE 4.4-1  
 RESPONSE SPECTRA COMPARISON DESIGN  
 BASIS VS. CHUGGING  
 (SHEET 6 of 18)



SET-1 REACTOR SLAB EL. 843'-6" N-S  
 COMB. 1. =  $[SSE^2 + CHUG^2 + (SRV_{ADS})^2]^{\frac{1}{2}}$   
 \*COMB. 2. =  $[(SSE)^2 + (SRVRH)^2]^{\frac{1}{2}}$   
 \*DESIGN BASIS

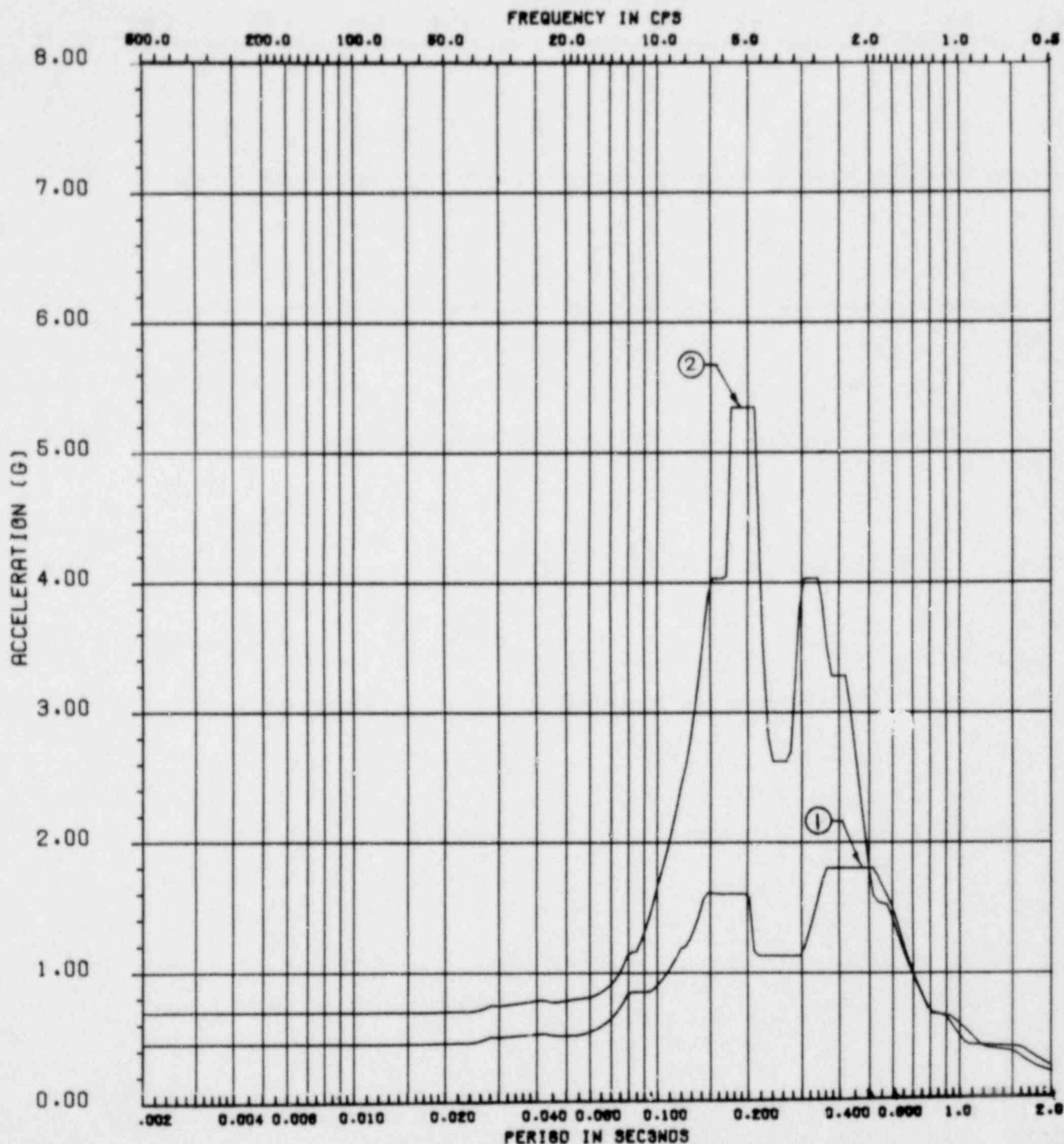
<p><b>LA SALLE COUNTY STATION</b>                  MARK II DESIGN ASSESSMENT REPORT</p>
<p>FIGURE 4.4-1                  RESPONSE SPECTRA COMPARISON DESIGN                  BASIS VS. CHUGGING                  (SHEET 7 of 18)</p>



SET-1 REACTOR SLAB EL. 843'-6" VERT  
 COMB. 1. =  $[\text{SSE}^2 + \text{CHUG}^2 + (\text{SRV}_{\text{ADS}})^2]^{1/2}$   
 \*COMB. 2. =  $[(\text{SSE})^2 + (\text{SRVRH})^2]^{1/2}$   
 \*DESIGN BASIS

**LA SALLE COUNTY STATION**  
 MARK II DESIGN ASSESSMENT REPORT

FIGURE 4.4-1  
 RESPONSE SPECTRA COMPARISON DESIGN  
 BASIS VS. CHUGGING  
 (SHEET 8 of 18)



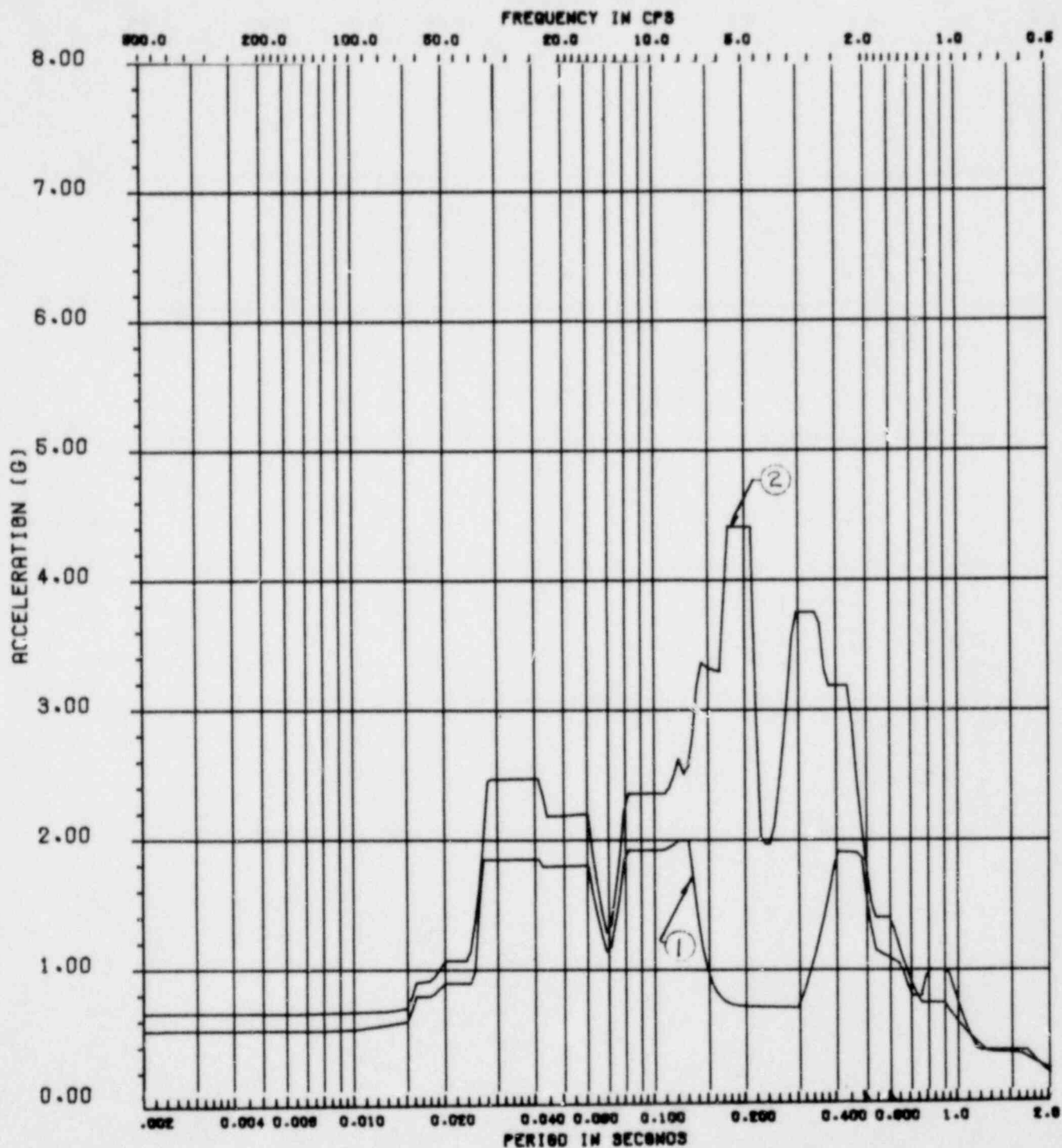
SET-1 REACTOR SLAB EL. 843'-6" E-W

$$\text{COMB. 1.} = [\text{SSE}^2 + \text{CHUG}^2 + (\text{SRV}_{\text{ADS}})^2]^{1/2}$$

$$\text{*COMB. 2.} = [(\text{SSE})^2 + (\text{SRVRH})^2]^{1/2}$$

\*DESIGN BASIS

<p><b>LA SALLE COUNTY STATION</b></p> <p>MARK II DESIGN ASSESSMENT REPORT</p>
<p>FIGURE 4.4-1</p> <p>RESPONSE SPECTRA COMPARISON DESIGN BASIS VS. CHUGGING</p> <p>(SHEET 9 of 18)</p>

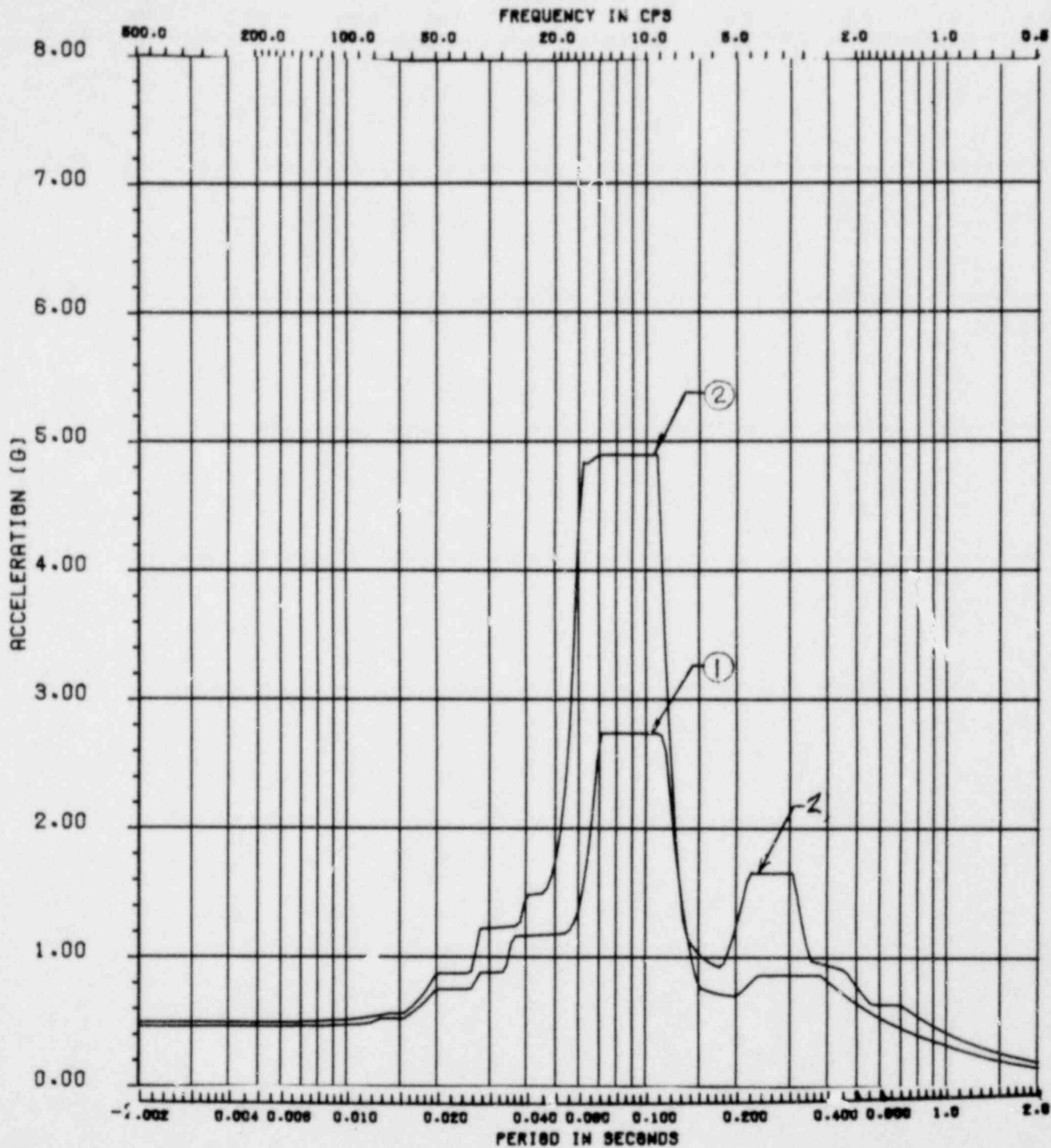


SET-1 CONT. WALL EL. 786'-0" E-W  
 COMB. 1. =  $[SSE^2 + CHUG^2 + (SRV_{ADS})^2]^{\frac{1}{2}}$   
 \*COMB. 2. =  $[(SSE)^2 + (SRVRH)^2]^{\frac{1}{2}}$   
 \*DESIGN BASIS

**LA SALLE COUNTY STATION**  
 MARK II DESIGN ASSESSMENT REPORT

---

FIGURE 4.4-1  
 RESPONSE SPECTRA COMPARISON DESIGN  
 BASIS VS. CHUGGING  
 (SHEET 10 of 18)

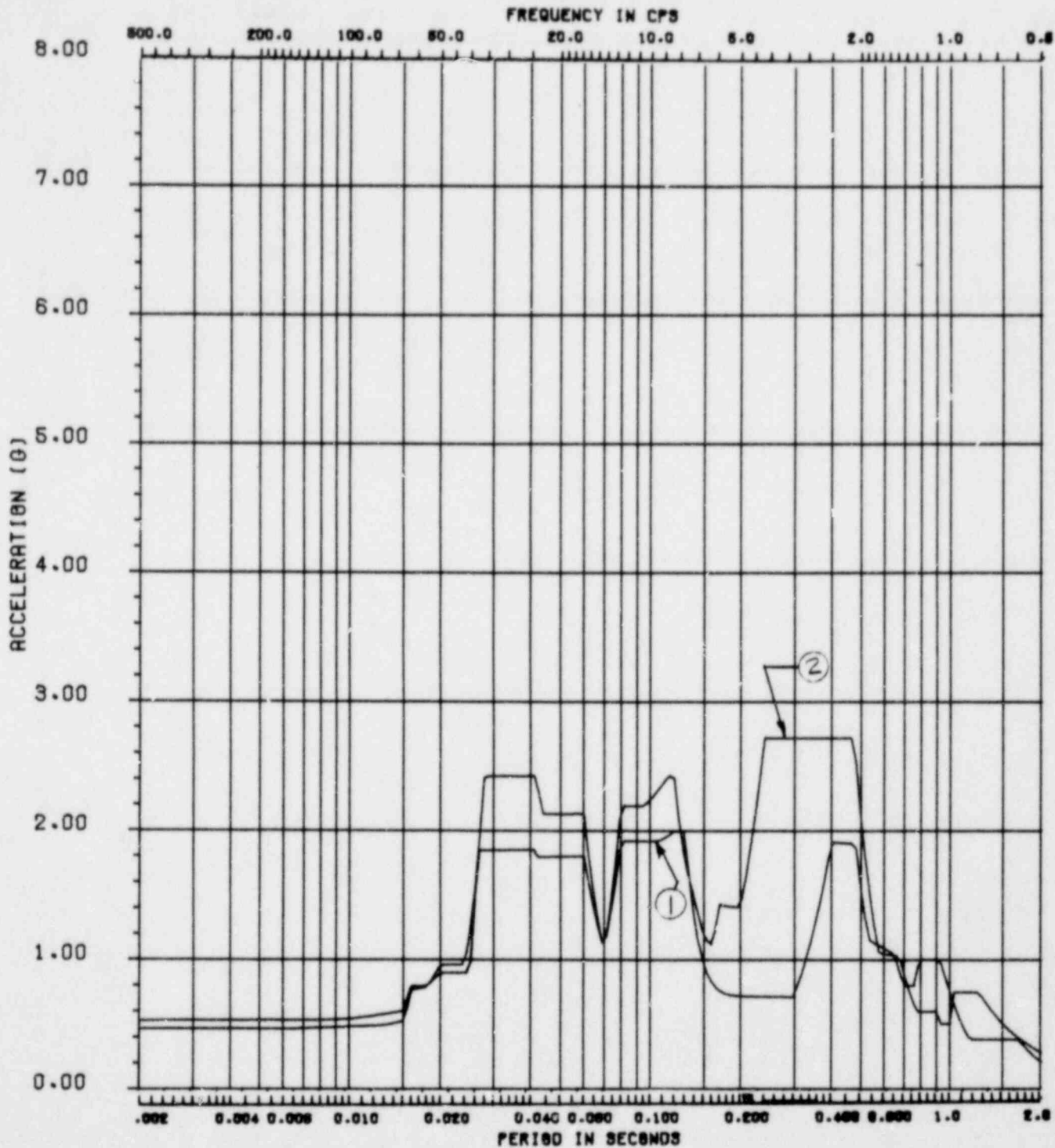


SET-1 CONT. WALL EL. 786'-0" VERT  
 COMB. 1. =  $[SSE^2 + CHUG^2 + (SRV_{ADS})^2]^{\frac{1}{2}}$   
 \*COMB. 2. =  $[(SSE)^2 + (SRVRH)^2]^{\frac{1}{2}}$   
 \*DESIGN BASIS

**LA SALLE COUNTY STATION**  
 MARK II DESIGN ASSESSMENT REPORT

---

FIGURE 4.4-1  
 RESPONSE SPECTRA COMPARISON DESIGN  
 BASIS VS. CHUGGING  
 (SHEET 11 of 18)



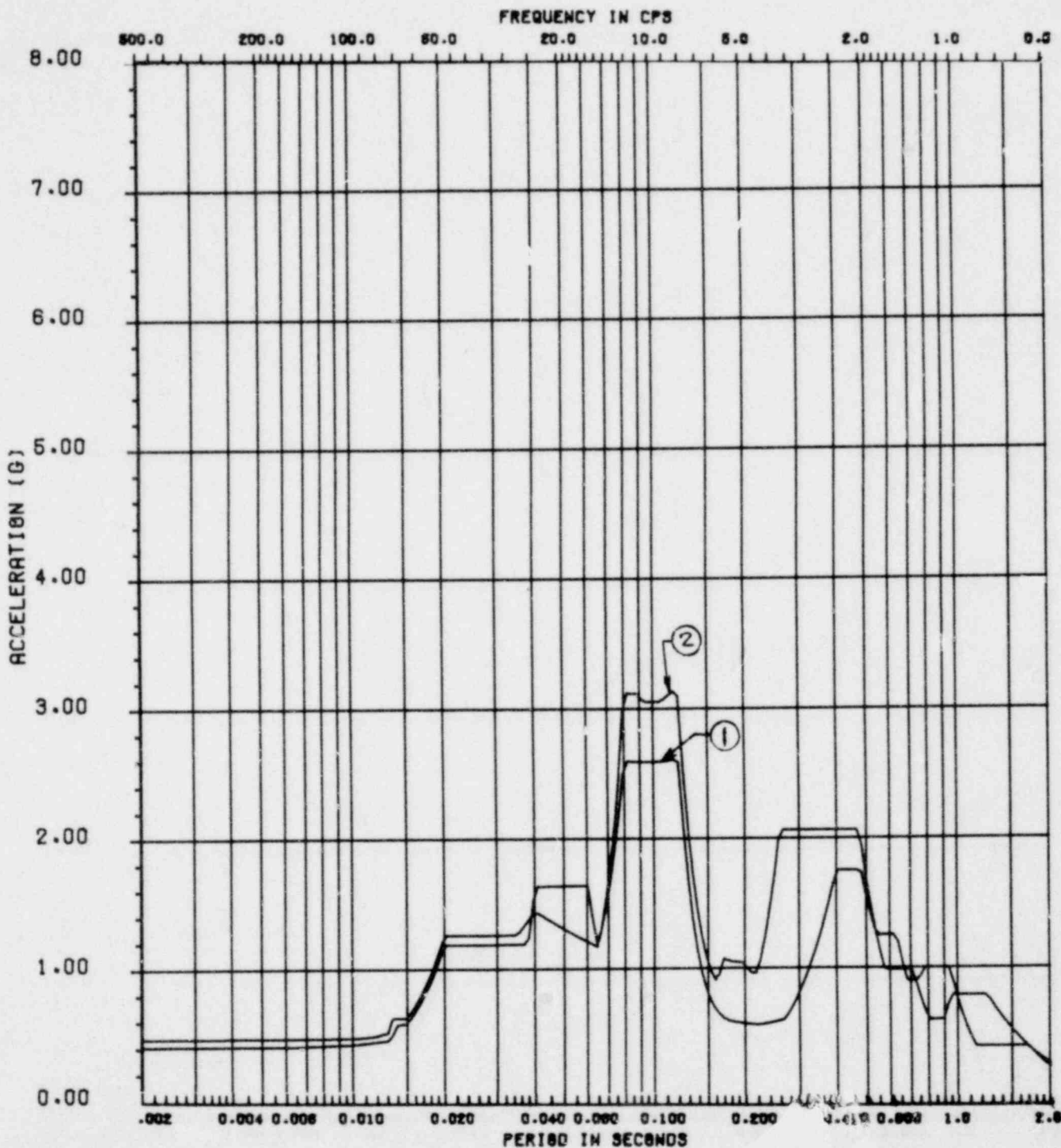
SET-1 CONT. WALL EL. 786'-0" N-S

$$\text{COMB. 1.} = [\text{SSE}^2 + \text{CHUG}^2 + (\text{SRV}_{\text{ADS}})^2]^{\frac{1}{2}}$$

$$\text{*COMB. 2.} = [(\text{SSE})^2 + (\text{SRVRH})^2]^{\frac{1}{2}}$$

\*DESIGN BASIS

<p><b>LA SALLE COUNTY STATION</b></p> <p>MARK II DESIGN ASSESSMENT REPORT</p>
<p>FIGURE 4.4-1</p> <p>RESPONSE SPECTRA COMPARISON DESIGN BASIS VS. CHUGGING</p> <p>(SHEET 12 of 18)</p>



SET-1 DRYWELL FLOOR EL. 736'-0" N-S

$$\text{COMB. 1.} = [\text{SSE}^2 + \text{CHUG}^2 + (\text{SRV}_{\text{ADS}})^2]^{\frac{1}{2}}$$

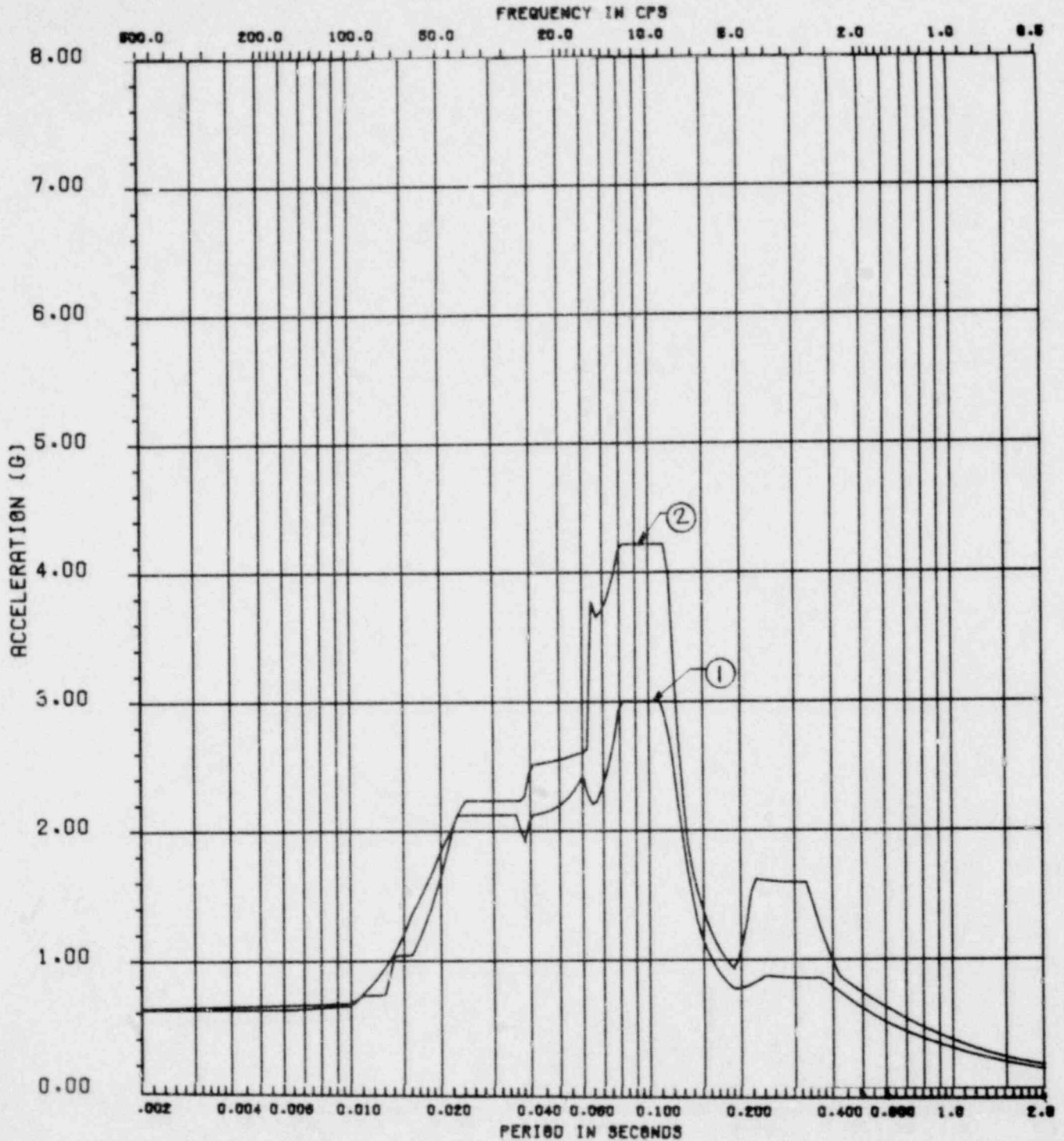
$$\text{*COMB. 2.} = [(\text{SSE})^2 + (\text{SRVRH})^2]^{\frac{1}{2}}$$

\*DESIGN BASIS

**LA SALLE COUNTY STATION**  
**MARK II DESIGN ASSESSMENT REPORT**

---

FIGURE 4.4-1  
 RESPONSE SPECTRA COMPARISON DESIGN  
 BASIS VS. CHUGGING  
 (SHEET 13 of 18)

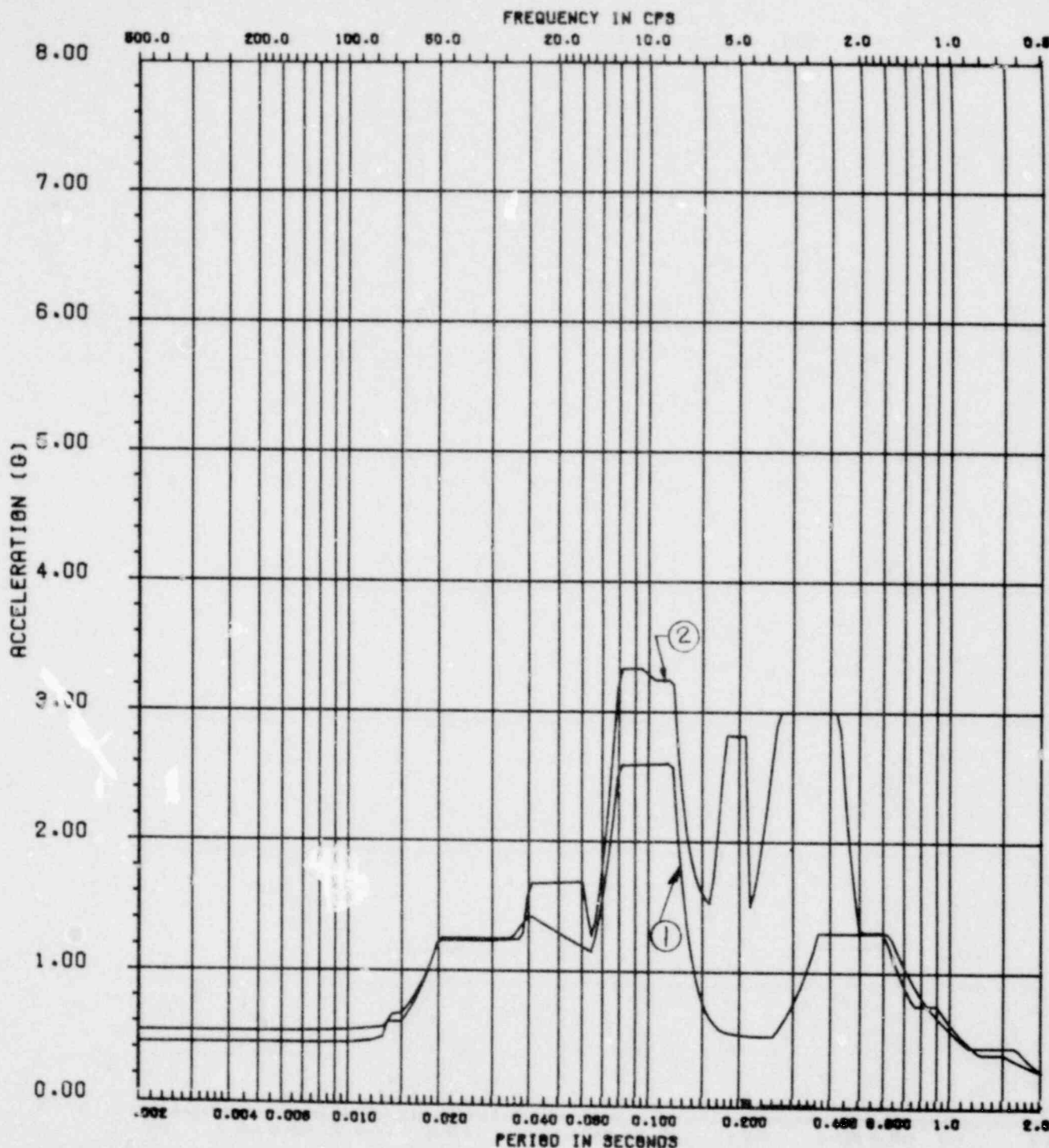


SET-1 DRYWELL FLOOR EL. 736'-0" VERT  
 COMB. 1. =  $[SSE^2 + CHUG^2 + (SRV_{ADS})^2]^{\frac{1}{2}}$   
 \*COMB. 2. =  $[(SSE)^2 + (SRVRH)^2]^{\frac{1}{2}}$   
 \*DESIGN BASIS

**LA SALLE COUNTY STATION**  
 MARK II DESIGN ASSESSMENT REPORT

---

FIGURE 4.4-1  
 RESPONSE SPECTRA COMPARISON DESIGN  
 BASIS VS. CHUGGING  
 (SHEET 14 of 18)

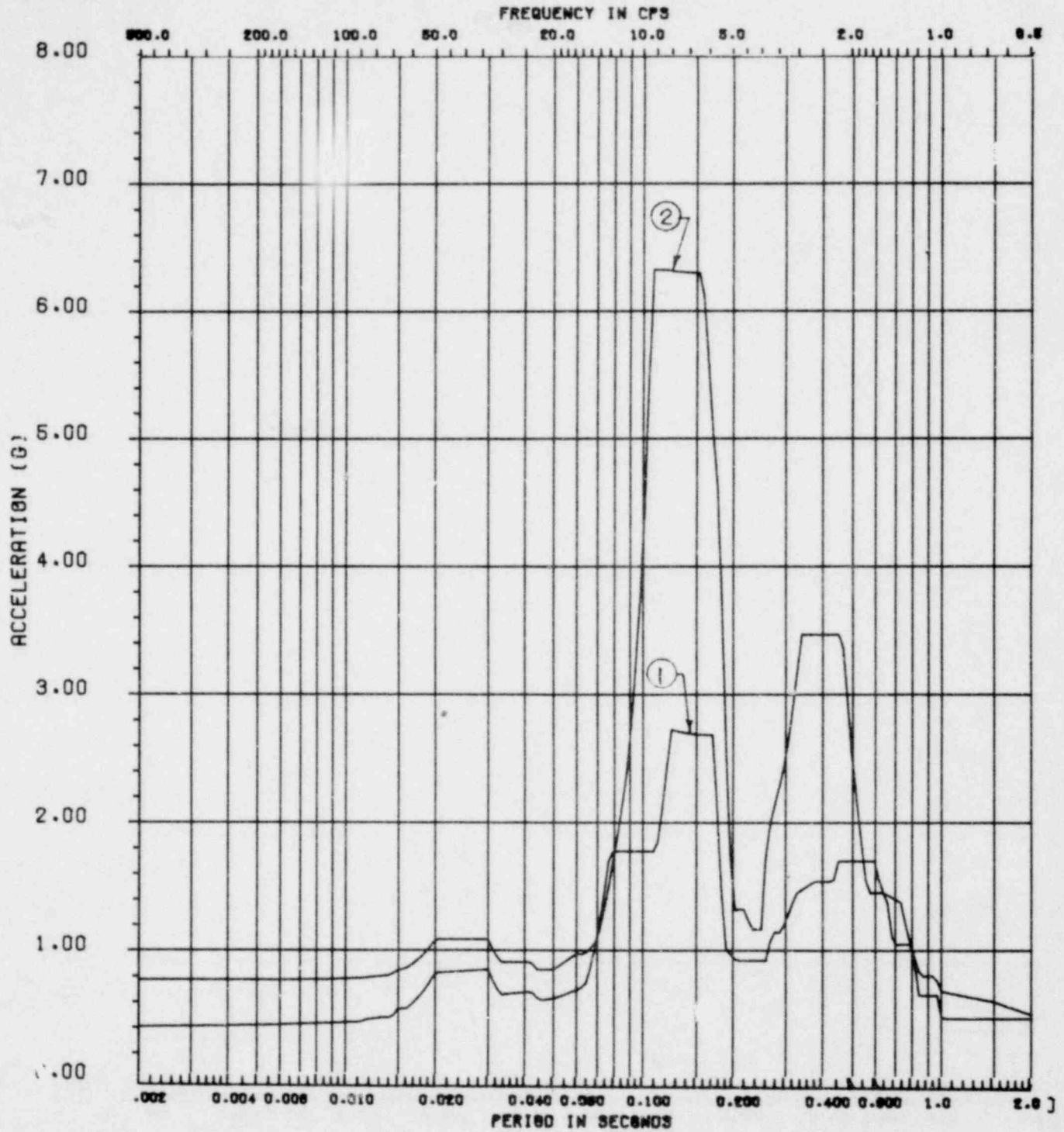


SET-1 DRYWELL FLOOR EL. 736'-0" E-W  
 COMB. 1. =  $[SSE^2 + CHUG^2 + (SRV_{ADS})^2]^{\frac{1}{2}}$   
 \*COMB. 2. =  $[(SSE)^2 + (SRVRH)^2]^{\frac{1}{2}}$   
 \*DESIGN BASIS

**LA SALLE COUNTY STATION**  
 MARK II DESIGN ASSESSMENT REPORT

---

FIGURE 4.4-1  
 RESPONSE SPECTRA COMPARISON DESIGN  
 BASIS VS. CHUGGING  
 (SHEET 15 of 18)

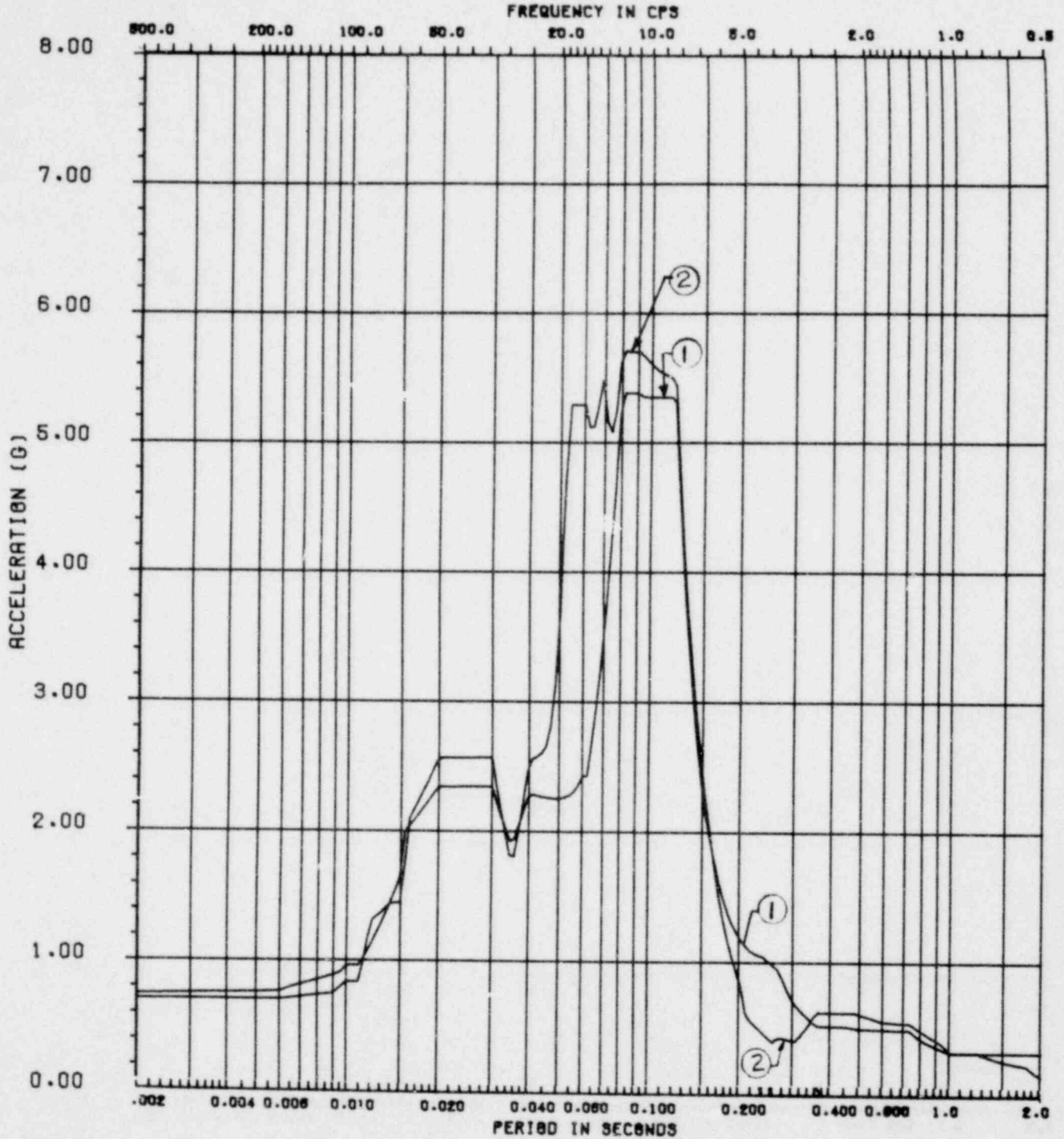


SET-1 RPV EL. 786'-0" N-S  
 COMB. 1. =  $[SSE^2 + CHUG^2 + (SRV_{ADS})^2]^{\frac{1}{2}}$   
 \*COMB. 2. =  $[(SSE)^2 + (SRVRH)^2]^{\frac{1}{2}}$   
 \*DESIGN BASIS

**LA SALLE COUNTY STATION**  
 MARK II DESIGN ASSESSMENT REPORT

---

FIGURE 4.4-1  
 RESPONSE SPECTRA COMPARISON DESIGN  
 BASIS VS. CHUGGING  
 (SHEET 16 of 18)

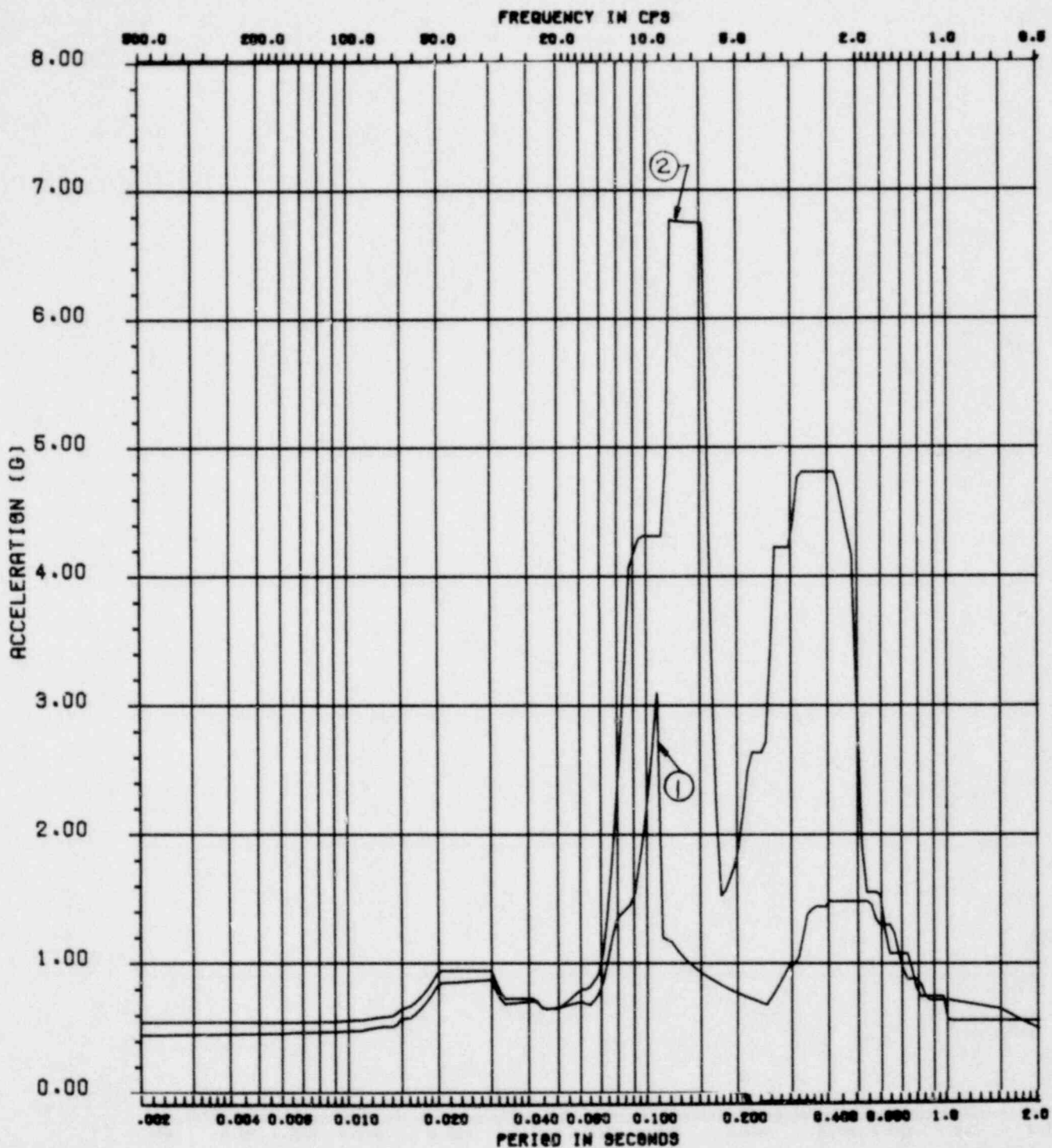


SET-1 RPV EL. 786'-0" VERT  
 COMB. 1. =  $[\text{SSE}^2 + \text{CHUG}^2 + (\text{SRV}_{\text{ADS}})^2]^{\frac{1}{2}}$   
 \*COMB. 2. =  $[(\text{SSE})^2 + (\text{SRVRH})^2]^{\frac{1}{2}}$   
 \*DESIGN BASIS

**LA SALLE COUNTY STATION**  
 MARK II DESIGN ASSESSMENT REPORT

---

FIGURE 4.4-1  
 RESPONSE SPECTRA COMPARISON DESIGN  
 BASIS VS. CHUGGING  
 (SHEET 17 of 18)



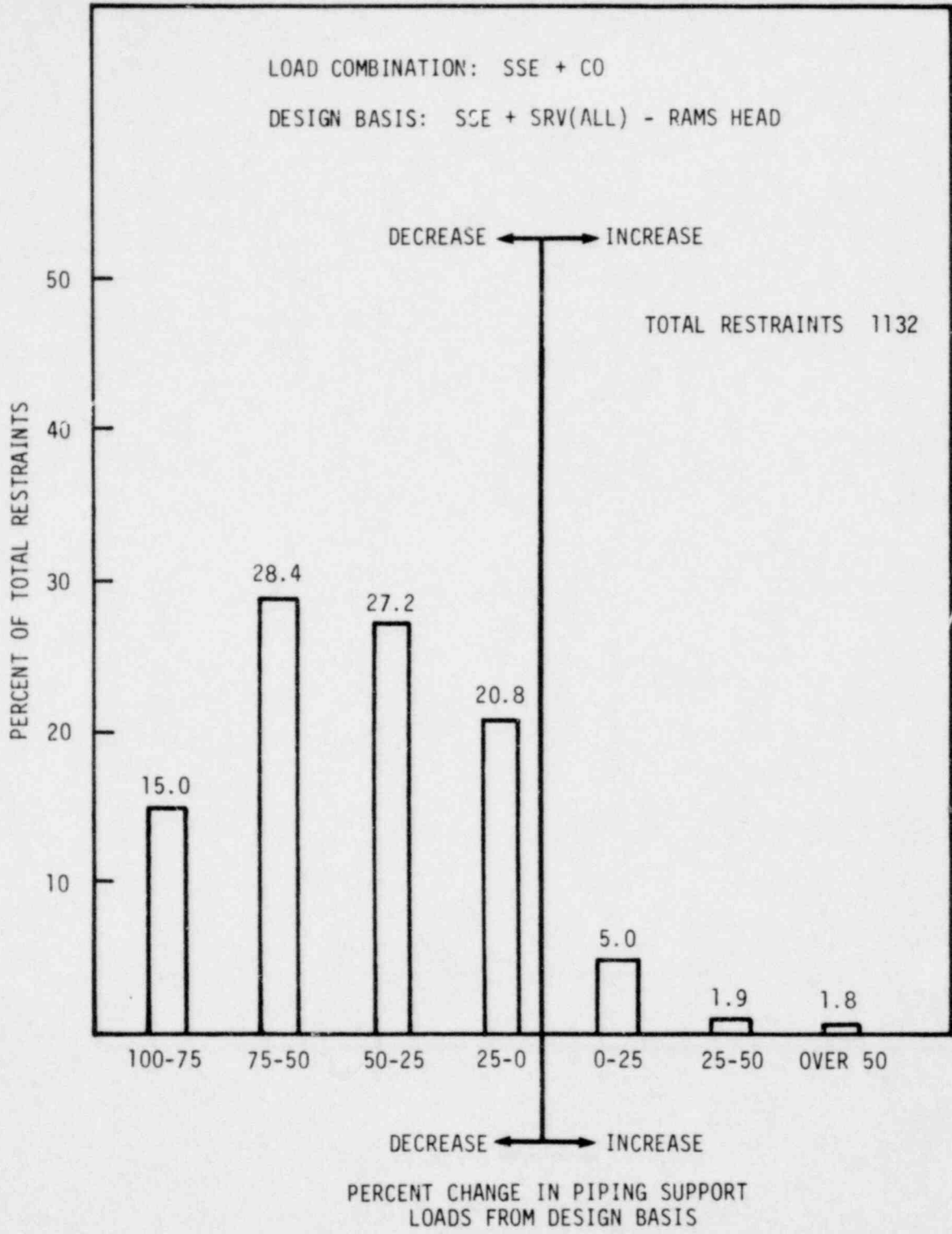
SET-1 RPV EL. 786'-0" E-W

$$\text{COMB. 1.} = [\text{SSF} \cdot \text{CHUG}^2 + (\text{SRV}_{\text{ADS}})^2]^{\frac{1}{2}}$$

$$\text{*COMB. 2.} = [(\text{SSE})^2 + (\text{SRVRH})^2]^{\frac{1}{2}}$$

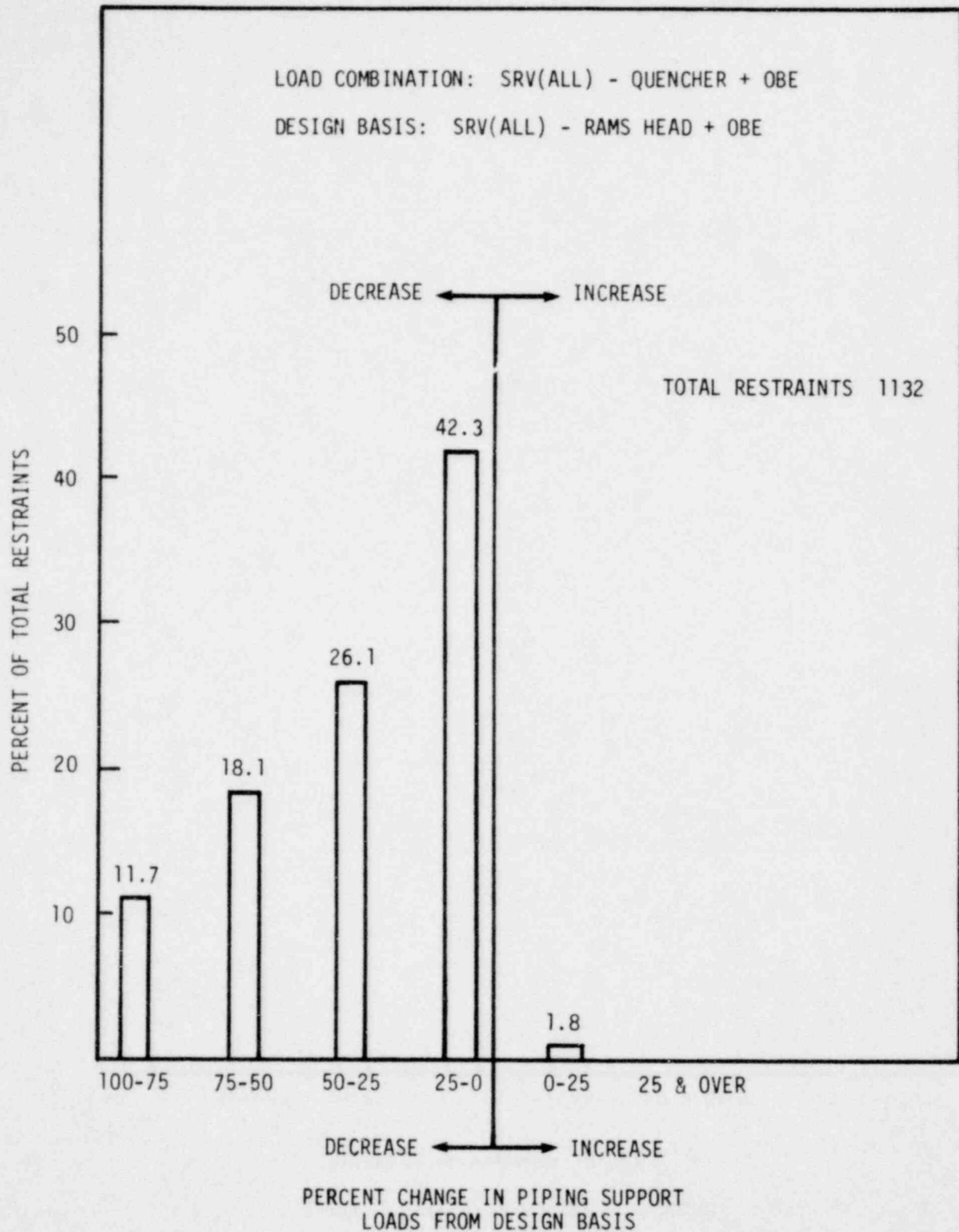
\*DESIGN BASIS

<b>LA SALLE COUNTY STATION</b> <b>MARK II DESIGN ASSESSMENT REPORT</b>
FIGURE 4.4-1 RESPONSE SPECTRA COMPARISON DESIGN BASIS VS. CHUGGING (SHEET 18 of 18)



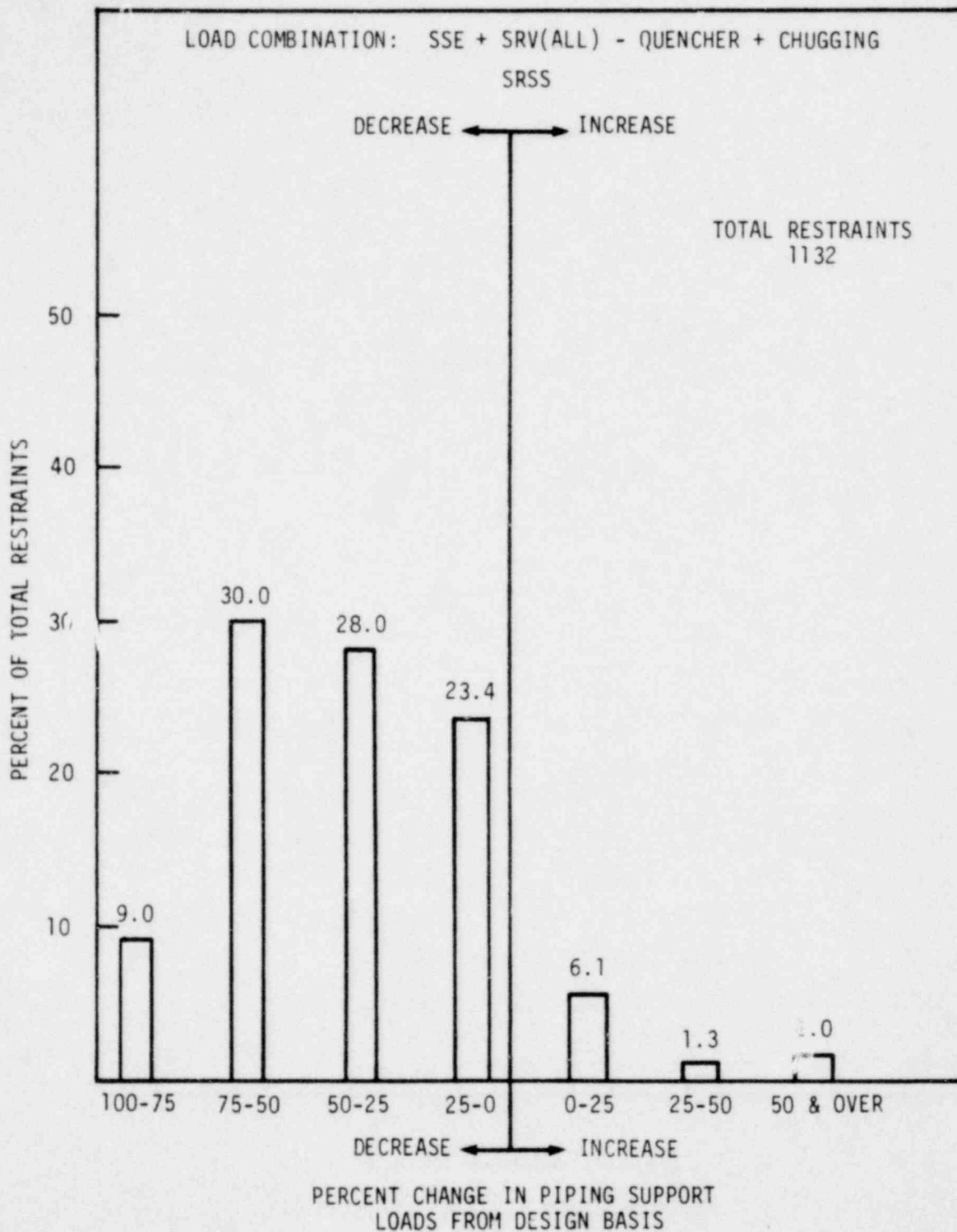
**LA SALLE COUNTY STATION**  
**MARK II DESIGN ASSESSMENT REPORT**

FIGURE 4.4-2  
RESTRAINT LOAD CHANGE DISTRIBUTION  
(SHEET 1 of 3)



**LA SALLE COUNTY STATION**  
MARK II DESIGN ASSESSMENT REPORT

FIGURE 4.4-2  
RESTRAINT LOAD CHANGE DISTRIBUTION  
(SHEET 2 of 3)



LA SALLE COUNTY STATION

MARK II DESIGN ASSESSMENT REPORT

FIGURE 4.4-2

RESTRAINT LOAD CHANGE DISTRIBUTION

(SHEET 3 of 3)

#### 4.5 NSSS PIPING AND EQUIPMENT

##### 4.5.1 Loading Combinations and Acceptance Criteria

The load combinations and acceptance criteria used for the analysis of NSSS piping systems, equipment, reactor pressure supports, and internal component analysis are shown in Table 4.5-1. The information presented in Table 4.5-1 has been discussed with the staff in various Mark II Owner's Group/NRC meetings. Table 4.5-1 is in agreement with a conservative, general interpretation of the NRC technical position, "Stress Limits for ASME Class 1, 2, and 3 Components and Component Supports of Safety-Related Systems and Class CS Core Support Structures Under Specified Service Loading Combinations". Note that the NSSS piping, equipment, and the reactor pressure vessel support and internals are treated in the analysis as "Type 1" components.

In response to questions from the staff, additional technical justification has been provided for the following load combinations in Table 4.5-1 for:

- a.  $N + OBE + SRV$ .
- b.  $N + LOCA (1-7)$ .

These additional justifications are presented in Reference 1.

Peak response due to related dynamic loads postulated to occur in the same time frame but from different events are combined by the square-root-of-the-sum-of-the-squares method (SRSS). A detailed discussion of this load combination technique is presented in Reference 2. In addition, Reference 3 provides an overview summary of the SRSS method with a summary of its historical precedents and additional technical considerations.

The technical justification for the time load combinations/acceptance criteria mentioned above and for the use of the SRSS method is currently under review by the NRC.

#### 4.5.2 References

1. Transmittal letter, MFN19378, L. J. Sobon to NRC (attention J. T. Knight), dated May 5, 1978, "Mark II Containment Program-Responses to NRC Request for additional Information" (Response to additional information, S. A. Varga (NRC) to Niagara Mohawk Power Corp., March 21, 1978, Docket No. 50410).
2. General Electric report NEDO-24310, "Technical Bases for the Use of the Square Root of the Sum of squares (SRSS) Method for Combining Dynamic Loads for Mark II Plant," July 1977.
3. Transmittal letter R. A. Hill to NRC (attention J. P. Knight), dated April 3, 1978, "General Electric-Executive Summary Report and Supplement Technical Bases for the SRSS Method of Combining Dynamic Responses".
4. Transmittal letter, MFN-175-78, E. D. Fuller to NRC (attention J. P. Knight), dated April 24, 1978, "Square Root Sum of the Squares (SRSS) Meeting Viewgraphs" (presented April 6, 1978).

TABLE 4.5-1

LOAD COMBINATIONS AND ACCEPTANCE CRITERIA  
FOR NSSS PIPING AND EQUIPMENT

(Vessel and Internals/Piping and  
Equipment Operating Condition Categories)

<u>LOAD COMBINATION*</u>	<u>OPERATING CONDITION CATEGORIES</u>	
	<u>DESIGN BASIS</u>	<u>EVAL. ONLY</u>
N + SRV (all)	Upset	Upset
N + OBE	Upset	Upset
N + SSE	Faulted	Faulted
N + (OBE + SRV (ALL))	Emergency	Upset
N + (SSE + SRV (ALL))	Faulted	Faulted
N + (SBA + SRV (2))	Emergency	Emergency
N + (IBA + SRV (2))	Faulted	Faulted
N + (SBA + SRV (ADS))	Emergency	Emergency
N + (SBA/IBA + SSE + SRV (ADS))	Faulted	Faulted
***N + (LOCA <sub>(1-6)</sub> + SSE)	Faulted	Faulted
**N + (LOCA <sub>(1-7)</sub> )	Faulted	
***N + (LOCA <sub>7</sub> + SSE)		Faulted

\*See Legend on the following pages for definition of terms and criteria for combining loads.

\*\*From all initial conditions.

\*\*\*From rated power initial conditions.

TABLE 4.5-1 (Cont'd)

LOAD DEFINITION LEGEND

- Normal (N) - Normal and/or abnormal loads depending on acceptance criteria.
- OBE - Operational basis earthquake loads.
- SSE - Loads due to vibratory motion from safe shutdown earthquake loads.
- SPV (2) - Safety/relief valve discharge induced loads from 2 adjacent valves.
- SRV (ALL) - The loads induced by actuation of all safety/relief valves which activate within milliseconds of each other (e.g., turbine trip operational transient).
- SRV (ADS) - The loads induced by the actuation of safety/relief valves associated with automatic depressurization system which actuate within milliseconds of each other during the postulated small or intermediate size pipe rupture.
- LOCA - The loss of coolant accident associated with the postulated pipe rupture of large pipes (e.g., main steam, feedwater, recirculation piping).
- LOCA<sub>1</sub> - Pool swell drag/fallback loads on piping and components located between the main vent discharge outlet and the suppression pool water upper surface.
- LOCA<sub>2</sub> - Pool swell impact loads acting piping and components located above the suppression pool water upper surface.
- LOCA<sub>3</sub> - Oscillating pressure induced loads on submerged piping and components during condensation oscillations, i.e., chugging.
- LOCA<sub>4</sub> - Building motion induced loads from chugging (condensation oscillation).
- LOCA<sub>5</sub> - Building motion induced loads from main vent air clearing.
- LOCA<sub>6</sub> - Vertical and horizontal loads on main vent piping.
- LOCA<sub>7</sub> - Annulus pressurization loads.
- SBA - Small break accident.
- IBA - Intermediate break accident.



## 5.0 REEVALUATION AND DESIGN ASSESSMENTS

### 5.1 CONTAINMENT AND INTERNAL CONCRETE STRUCTURES

The containment and internal concrete structures were reevaluated for the pool dynamic loads to include the fluid structure interaction (FSI) effect and to assess the pool dynamic loads that were not previously defined. The details of the individual analyses and reevaluation are summarized in this section.

#### 5.1.1 Structural Analysis for SRV Loads

The various SRV loads used in the reevaluation are described in Section 3.0.

The containment structure was analyzed for the SRV dynamic loads using the Sargent & Lundy version of the finite element computer program DYNAX described in Appendix A. The reactor building and containment structure have been modeled with axisymmetric finite elements. Figure 5.1-1 shows the refined structural analytical model which includes the primary containment, the basemat, founding soil, idealized reactor building walls and slabs, drywell floor, the reactor pressure vessel (RPV), and the fluid in the pool including FSI effect. Also included in the model are the suppression chamber columns, RPV stabilizer truss, refueling bellows, and the refueling/spent fuel pool slabs and walls. The model uses 362 elements and 399 nodes to represent the structure. Of the 362 elements used, 187 are thin shell elements represent the modified reactor support, 40 solid elements represent the suppression pool water, and 158 solid elements represent the soil. The RPV is represented with 13 shell elements.

The containment building walls and pool slab are included as axisymmetric shells to account for their mass and approximate their stiffening influence.

The soil is modeled with 158 axisymmetric solid finite elements in 14 horizontal layers down to the bedrock level. The dynamic strain dependent stiffness and damping characteristics of the soil were used in the analysis to determine the soil elements material properties.

In order to include the plant unique fluid structure interaction (FSI) effect, the water in the suppression pool is simulated by fluid finite elements described in Reference 1. The water is modeled with 40 solid finite elements in four layers.

The SRV loads were represented by Fourier harmonics to account for the spatial pressure distribution in the circumferential direction. To account for the pressure distribution in the meridional direction, the suppression pool walls were divided into nine zones and to each zone an individual load time-history is specified.

The response of the structure to the pool dynamic loads was determined by direct numerical integration of the governing differential equations. The resulting acceleration time-histories were then used to determine the response spectra at the desired locations using the computer program RSG described in Appendix A. The same procedure was used to analyze the SRV loads from various modes of actuation.

The resulting structural responses to the various SRV loads are combined with the other appropriate loads as per the load combinations shown in Table 4.1-1. The margin factors from these load combinations are presented in Tables 5.1-1 through 5.1-13.

### 5.1.2 Structural Analysis for LOCA Loads

The analysis of the structure for the LOCA loads was performed as a set of analyses covering each LOCA related phenomena separately. The methods used for each analysis are summarized in the following for the LOCA induced loads of chugging, condensation oscillation, pool swell, and vent clearing.

#### 5.1.2.1 Vent Clearing Analysis

The vent clearing load for analysis is described in Section 3.0.

The model used in the analysis of the vent clearing loads is described in Subsection 5.1.1.

The containment structure was analyzed for the effects of the vent clearing load statically using Sargent & Lundy's axisymmetric finite element computer program DYNAX. See Appendix A for a description of the computer program.

The resulting structural response to the vent clearing load are combined with the other appropriate loads as per the load combinations shown in Table 4.1-1. The margin factors from these load combinations are presented in Tables 5.1-1 through 5.1-13.

#### 5.1.2.2 Pool Swell Analysis

The postulated pool swell phenomena induced loads are described in Section 3.0.

The model used in the analysis is described in Subsection 5.1.1.

The containment structure was analyzed for the effects of the pool swell loads statically using Sargent & Lundy's

axisymmetric finite element computer program DYNAX. See Appendix A for a description of the computer program.

Two loading cases were considered; symmetric and asymmetric. The spatial pressure load distributions in the circumferential direction were represented by using Fourier harmonics.

The resulting forces and moments on the structures design sections were obtained directly from the DYNAX computer output.

The resulting structural responses to the pool swell loads are combined with the other appropriate loads as per the load combinations shown in Table 4.1-1. The margin factors from these load combinations are presented in Tables 5.1-1 through 5.1-13.

#### 5.1.2.3 Condensation Oscillation Analysis

The condensation oscillation loads used in the analysis are described in Section 3.0.

The finite element model used in the analysis is described in Subsection 5.1.1.

The method of analysis used for the condensation oscillation loads is similar to the one described in Subsection 5.1.2.4.

The resulting structural responses to the condensation oscillation loads are combined with the other appropriate loads as per the load combinations shown in Table 4.1-1. In these load combinations, it was conservatively assumed that an intermediate pipe break accident (IBA) could result in a high steam mass flux which induces a condensation oscillation (CO) load. Therefore, CO load plus  $SRV_{AD\bar{E}}$  was considered as one of the possible combinations. The margin factors from these combinations are presented in Tables 5.1-1 through 5.1-13.

#### 5.1.2.4 Chugging Analysis

The chugging loads used in the analysis are described in Section 3.0.

The finite element model used in the analysis is described in Subsection 5.1.2.2.

For the chugging loads as defined in Section 3.0, the direct method of dynamic analysis cannot be used because the frequency of these dynamic loads is a variable. Therefore, the dynamic analysis was performed in the frequency domain rather than in the time domain. The method of such an analysis is known as "Fourier Transform Method" or "Frequency Response Method." This method is somewhat analogous to the influence line method used in static analyses.

The external load which is usually expressed in the time domain is also expressed in the frequency domain, using "Fast Fourier Transform" algorithm. Using this algorithm, a given function is transformed from time domain to frequency domain and vice versa.

The analysis was performed in the following steps:

- a. The containment structural model described in Subsection 5.1.2 was analyzed using the Sargent & Lundy version of the finite element program DYNAX which is capable of analyzing axisymmetric shells and solids subjected to arbitrary symmetric and asymmetric static or dynamic loads.

The chugging loads were applied as Fourier sine and/or cosine harmonics for each case. A band-limited white-noise time-history was used for the analysis. The Fourier transform of such a

time-history has a constant magnitude at all values within the frequency range of interest.

- b. The response (force, moment) time-histories obtained from the above white-noise analysis were stored in electronic files.
- c. The transfer functions of the responses were obtained by the computer program FAST described in Appendix A.

The Transfer Function is computed as follows:

$$T_k(\omega) = \frac{R_k(\omega)}{F(\omega)}$$

in which:

$R_k(\omega)$  = structural response of a node/element,

$T_k(\omega)$  = transfer function of the  $k^{\text{th}}$  response, and

$F(\omega)$  = Fourier transform of the external load.

The resulting structural responses to the chugging loads are combined with the other appropriate loads as per the load combinations shown in Table 4.1-1. The margin factors from these load combinations are presented in Tables 5.1-1 through 5.1-13.

#### 5.1.2.5 ECCS Reflood Analysis

The pressure distributions within the containment associated with an assumed ECCS reflooding of the drywell chamber are described in Section 3.0.

The analysis procedure used for this loading is similar to that described in Subsection 5.1.2.2.

The resulting structural responses to this loading are combined with the other appropriate loads as per the load combinations shown in Figure 4.1-1. The margin factors from these load combinations are presented in Tables 5.1-1 through 5.1-13.

#### 5.1.3. Downcomer Effects on the Drywell Floor

The downcomer vents are now subjected to a variety of submerged structure dynamic loads resulting from SRV and LOCA loads.

The loads on the downcomers resulting from submerged hydrodynamic forces are described in Section 3.0.

In addition to the pool dynamic loads on the downcomers, the effects of the structures response to the pool dynamic and seismic loads is also considered in the analysis.

The analytical models used to compute the responses of the downcomers from the various loadings is described in Sub-section 5.3.3.

The structural analysis model of the drywell floor is shown in Figure 5.1-2. The drywell floor was modeled as a thin elastic circular plate with a circular hole in the middle. The slab was assumed to be fully restrained at the pedestal and containment walls and supported at the columns.

An influence coefficient method described in the following was used to compute the forces induced in the drywell floor by the combined loads on the downcomers.

The locations of the downcomers lie along four rings at radii 19 feet 9 inches, 23 feet 3 inches, 32 feet 9 inches, and 36 feet 3 inches.

A concentrated radial or circumferential moment, in the form of Fourier harmonics, is applied at a point on each one of the downcomer rings. The moments induced in the floor in the radial and circumferential directions are obtained from KALSHEL, an S&L computer program (see Appendix A for a description), analysis.

Figure 5.1-3 shows the circumferential distribution of floor moments induced by a concentrated radial moment applied at radius 23 feet 3 inches. For computational convenience, the ordinates are normalized to make the induced radial moment equal to unity. Figure 5.1-4 shows the radial distribution of floor moments induced by the concentrated radial moment applied at radius 23 feet 3 inches. Figures 5.1-5 and 5.1-6 respectively, show the circumferential moment applied at radius 23 feet 3 inches. Similar sets of curves are generated for the other rings of downcomers.

The magnitude of the multiple lateral loads acting on the downcomer tip producing the applied moments on the drywell floor are given in Figure 4-10 of the DFFR Revision 2.

Using the moment coefficients from these curves in the following equations, the radial and circumferential design moments at any design section resulting from the downcomer loads can be calculated.

$$m_{\phi} = \sum_{n=1}^4 \left[ \left( M_{\phi n} \cdot k_{\phi n} \cdot \beta_{\phi \phi n} \cdot \sum_{\theta=0}^{360^{\circ}} \beta_{\phi \phi n \theta} \right) + \left( M_{\theta n} \cdot k_{\theta n} \cdot \beta_{\phi \theta n} \cdot \sum_{\theta=0}^{360^{\circ}} \beta_{\phi \theta n \theta} \right) \right]$$

$$m_{\theta} = \sum_{n=1}^4 \left[ \left( M_{\theta n} \cdot k_{\theta n} \cdot \beta_{\theta \theta n} \cdot \sum_{\theta=0}^{360^{\circ}} \beta_{\theta \theta n \theta} \right) + \left( M_{\phi n} \cdot k_{\phi n} \cdot \beta_{\theta \phi n} \cdot \sum_{\theta=0}^{360^{\circ}} \beta_{\theta \phi n \theta} \right) \right]$$

where:

- $m_{\phi}$  = radial moment induced at a design section;
- $n$  = number of rings of downcomers ( $n = 1, 2, 3, 4$ );
- $M_{\phi n}$  = radial moment applied at a point on the  $n^{\text{th}}$  ring;
- $k_{\phi n}$  =  $m_{\phi n} / M_{\phi n}$ ;
- $m_{\phi n}$  = radial moment induced in the floor at the point where  $M_{\phi n}$  is applied;
- $M_{\theta n}$  = circumferential moment applied at a point on the  $n^{\text{th}}$  ring.
- $m_{\theta n}$  = radial moment induced in the floor at the point where  $M_{\theta n}$  is applied;
- $k_{\theta n}$  =  $m_{\theta n} / M_{\theta n}$ ;
- $\beta_{\phi \phi n}$  = normalized radial moment along the radius through the point where  $M_{\phi n}$  is applied;
- $\beta_{\phi \theta n}$  = normalized radial moment along the radius through the point where  $M_{\theta n}$  is applied;
- $\beta_{\phi \phi n \theta}$  = normalized radial moment along the  $n^{\text{th}}$  ring due to  $M_{\phi n}$ ;
- $\beta_{\phi \theta n \theta}$  = normalized radial moment along the  $n^{\text{th}}$  ring due to  $M_{\theta n}$ ;
- $\beta_{\theta \theta n \theta}$  = normalized circumferential moment along the  $n^{\text{th}}$  ring due to  $M_{\theta n}$ ; and
- $\beta_{\theta \phi n \theta}$  = normalized circumferential moment along the  $n^{\text{th}}$  ring due to  $M_{\phi n}$ .

The absolute values of the moment coefficients are used to account for the random direction of the downcomer lateral loads and to obtain the absolute maximum values of  $m_{\phi}$  and  $m_{\theta}$  for design assessment.

The design forces and moments on the drywell floor were obtained by combining these downcomer induced forces with other loads in the load combinations defined in Table 4.1-1. The conservative ABS method was used for combining the loads, even though the SRSS method is more appropriate. The margin factors from these load combinations are presented in Table 5.1-13.

#### 5.1.4 Design Assessment Margin Factors

##### 5.1.4.1 Critical Design Sections

The primary containment and internal structures have been checked as to the structural capacity to withstand the dynamic loads due to SRV discharges and LOCA in addition to the other appropriate loads described in the FSAR. The methods of analysis used have been described in the preceding subsections and the design load combinations are given in Table 4.1-1. The structural capacity acceptance criteria are the same as in the FSAR for which all design sections have been evaluated using the computer program TEMCO IV (described in Appendix A).

Figures 5.1-7 through 5.1-14 illustrate the reinforcing steel and prestressing tendon layout including all modifications and reinforcing additions discussed in Section 7.0. It should be noted that Figure 5.1-12 shows all of the original and additional reinforcing in the pedestal and the concrete fill discussed in Section 7.0. The details of the concrete filled portion of the pedestal are shown in Figure 5.1-11.

Figures 5.1-15 and 5.1-16 show the design sections used for the structural assessment in the basemat, containment, reactor support, and drywell floor. Figures 5.1-17 and 5.1-18 give typical design section capacity interaction diagrams for the basemat and containment.

#### 5.1.4.2 Design Forces and Margin Factors

The design forces in the critical design sections were obtained by combining with the ABS method the peak effects of all the loads according to the load combinations defined in Table 4.1-1.

The material stresses in the critical design sections were obtained using computer program TEMCO IV described in Appendix A.

Margin factors, defined as the ratio between the allowable stress and the actual stress in the section, were computed for each design section. If any of the loads (such as temperature) other than dead load reduced the design forces, it was decided from load combination to obtain the most conservative margin factor.

Margin factors for the basemat, containment wall, reactor support and drywell floor are reported in the following tables:

- a. basemat - Tables 5.1-1 through 5.1-4,
- b. containment wall - Tables 5.1-5 through 5.1-8,
- c. reactor support, Tables 5.1-9 through 5.1-12, and
- d. drywell floor, Table 5.1-13.

Even though a few of the margins reported in the tables are close to 1.0, it must be emphasized that conservative loads, analysis procedures, and material strengths were used in the assessment in order to expeditiously verify the adequacy of the structure for the pool dynamic loads. Therefore, the margins reported are the most conservative. The actual margins will be higher than reported.

### 5.1.5 References

1. A. J. Kalinowski, "Transmission of Shock Waves into Submerged Fluid Filled Vessels," ASME Conference on FSI Phenomena in Pressure Vessel and Piping Systems, TVP-TB-026, 1977.
2. K. T. Patton, "Tables of Hydrodynamic Mass Factors for Translational Motion," ASME Paper No. 65-WA/UNT-2, 1965.

TABLE 5.1-1

MARGIN TABLE FOR BASE MAT FOR ALL VALVES DISCHARGE  
(With Plant Unique FSI)

LOAD COMBINATION EQUATION*	STRESS COMPONENT	REINFORCING STEEL		CONCRETE		SHEAR	
		MARGIN** FACTOR	CRITICAL*** SECTION	MARGIN FACTOR	CRITICAL SECTION	MARGIN FACTOR	CRITICAL SECTION
1		2.03	2	4.72	2	1.05	2
2		2.27	2	5.23	2	1.30	2
3		1.33	2	3.01	2	1.01	2
4		NA	NA	NA	NA	NA	NA
4a		NA	NA	NA	NA	NA	NA
5		NA	NA	NA	NA	NA	NA
5a		NA	NA	NA	NA	NA	NA
6		1.30	2	2.91	2	1.04	2
7		NA	NA	NA	NA	NA	NA
7a		NA	NA	NA	NA	NA	NA

NOTES:

- \*Refer to Table 4.1-1
- \*\*Margin Factor = Allowable Stress/Actual Stress
- \*\*\*Refer to Figures 5.1-15 and 5.1-16.
- NA = Not Applicable

5.1-13

LSCS-MARK II DAR

Rev. 7 1/80

TABLE 5.1-2

MARGIN TABLE FOR BASE MAT FOR 2 VALVES DISCHARGE

(With Plant Unique FSI)

LOAD COMBINATION EQUATION*	STRESS COMPONENT	REINFORCING STEEL		CONCRETE		SHEAR	
		MARGIN** FACTOR	CRITICAL*** SECTION	MARGIN FACTOR	CRITICAL SECTION	MARGIN FACTOR	CRITICAL SECTION
1		2.61	2	6.07	2	1.35	2
2		2.92	2	6.73	2	1.68	2
3		1.71	2	3.87	2	1.27	2
4		2.07	2	5.05	2	2.16	2
4a		NA	NA	NA	NA	NA	NA
5		1.58	2	3.59	2	1.64	2
5a		NA	NA	NA	NA	NA	NA
6		1.67	2	3.75	2	1.32	2
7		1.39	2	3.28	2	1.50	2
7a		NA	NA	NA	NA	NA	NA

NOTES:

\*Refer to Table 4.1-1

\*\*Margin Factor = Allowable Stress/Actual Stress

\*\*\*Refer to Figures 5.1-15 and 5.1-16.

NA = Not Applicable

5.1-14

LSCS-MARK II DAR

Rev. 7 1/80

TABLE 5.1-3

MARGIN TABLE FOR BASE MAT FOR ADS VALVES DISCHARGE

(With Plant Unique FSI)

LOAD COMBINATION EQUATION*	STRESS COMPONENT	REINFORCING STEEL		CONCRETE		SHEAR	
		MARGIN** FACTOR	CRITICAL*** SECTION	MARGIN FACTOR	CRITICAL SECTION	MARGIN FACTOR	CRITICAL SECTION
1		NA	NA	NA	NA	NA	NA
2		NA	NA	NA	NA	NA	NA
3		NA	NA	NA	NA	NA	NA
4		1.39	2	3.24	2	1.68	2
4a		NA	NA	NA	NA	NA	NA
5		1.06	2	2.40	2	1.27	2
5a		NA	NA	NA	NA	NA	NA
6		NA	NA	NA	NA	NA	NA
7		1.00	2	2.32	2	1.16	2
7a		NA	NA	NA	NA	NA	NA

NOTES:

\*Refer to Table 4.1-1

\*\*Margin Factor = Allowable Stress/Actual Stress

\*\*\*Refer to Figures 5.1-15 and 5.1-16.

NA = Not Applicable

5.1-15

LSCS-MARK II DAR

Rev. 7 1/80

TABLE 5.1-4

MARGIN TABLE FOR BASE MAT FOR LOCA PLUS SINGLE SRV

(With Plant Unique FSI)

LOAD COMBINATION EQUATION*	STRESS COMPONENT	REINFORCING STEEL		CONCRETE		SHEAR	
		MARGIN** FACTOR	CRITICAL*** SECTION	MARGIN FACTOR	CRITICAL SECTION	MARGIN FACTOR	CRITICAL SECTION
1		NA	NA	NA	NA	NA	NA
2		NA	NA	NA	NA	NA	NA
3		NA	NA	NA	NA	NA	NA
4		NA	NA	NA	NA	NA	NA
4a		1.51	2	2.76	2	1.79	2
5		NA	NA	NA	NA	NA	NA
5a		1.12	2	2.22	2	1.30	2
6		NA	NA	NA	NA	NA	NA
7		NA	NA	NA	NA	NA	NA
7a		1.04	2	2.11	2	1.19	2

NOTES: \*Refer to Table 4.1-1  
 \*\*Margin Factor = Allowable Stress/Actual Stress  
 \*\*\*Refer to Figures 5.1-15 and 5.1-16.  
 NA = Not Applicable

5.1-16

LSCS-MARK II DAR

Rev. 7 1/80

TABLE 5.1-5

MARGIN TABLE FOR CONTAINMENT FOR ALL VALVES DISCHARGE

(with Plant Unique FSI)

LOAD COMBINATION EQUATION*	STRESS COMPONENT	REINFORCING STEEL		CONCRETE		SHEAR	
		MARGIN** FACTOR	CRITICAL*** SECTION	MARGIN FACTOR	CRITICAL SECTION	MARGIN FACTOR	CRITICAL SECTION
1		4.33	1	2.17	1	1.23	13
2		4.16	1	2.02	1	1.26	13
3		2.44	14	1.82	1	1.26	13
4		NA	NA	NA	NA	NA	NA
4a		NA	NA	NA	NA	NA	NA
5		NA	NA	NA	NA	NA	NA
5a		NA	NA	NA	NA	NA	NA
6		2.16	14	1.83	1	1.27	13
7		NA	NA	NA	NA	NA	NA
7a		NA	NA	NA	NA	NA	NA

NOTES:

\*Refer to Table 4.1-1

\*\*Margin Factor = Allowable Stress/Actual Stress

\*\*\*Refer to Figures 5.1-15 and 5.1-16.

NA = Not Applicable

TABLE 5.1-6

MARGIN TABLE FOR CONTAINMENT FOR 2 VALVES DISCHARGE

(With Plant Unique FSI)

LOAD COMBINATION EQUATION*	STRESS COMPONENT	REINFORCING STEEL		CONCRETE		SHEAR	
		MARGIN** FACTOR	CRITICAL*** SECTION	MARGIN FACTOR	CRITICAL SECTION	MARGIN FACTOR	CRITICAL SECTION
1		6.22	1	3.12	1	1.23	13
2		5.97	1	2.90	1	1.26	13
3		3.50	14	2.61	1	1.26	13
4		2.69	14	3.42	1	1.28	13
4a		NA	NA	NA	NA	NA	NA
5		1.75	14	3.04	1	1.28	13
5a		NA	NA	NA	NA	NA	NA
6		3.10	14	2.63	1	1.27	13
7		1.52	14	2.97	1	1.28	13
7a		NA	NA	NA	NA	NA	NA

NOTES:

\*Refer to Table 4.1-1

\*\*Margin Factor = Allowable Stress/Actual Stress

\*\*\*Refer to Figures 5.1-15 and 5.1-16.

NA = Not Applicable

TABLE 5.1-7

MARGIN TABLE FOR CONTAINMENT FOR ADS VALVES DISCHARGE

(With Plant Unique FSI)

LOAD COMBINATION EQUATION*	STRESS COMPONENT	REINFORCING STEEL		CONCRETE		SHEAR	
		MARGIN** FACTOR	CRITICAL*** SECTION	MARGIN FACTOR	CRITICAL SECTION	MARGIN FACTOR	CRITICAL SECTION
1		NA	NA	NA	NA	NA	NA
2		NA	NA	NA	NA	NA	NA
3		NA	NA	NA	NA	NA	NA
4		1.87	14	2.38	1	1.28	13
4a		NA	NA	NA	NA	NA	NA
5		1.22	14	2.12	1	1.28	13
5a		NA	NA	NA	NA	NA	NA
6		NA	NA	NA	NA	NA	NA
7		1.06	14	2.07	1	1.28	13
7a		NA	NA	NA	NA	NA	NA

NOTES:

\*Refer to Table 4.1-1

\*\*Margin Factor = Allowable Stress/Actual Stress

\*\*\*Refer to Figures 5.1-15 and 5.1-16

NA = Not Applicable

TABLE 5.1-8

MARGIN TABLE FOR CONTAINMENT FOR LOCA PLUS SINGLE SRV

(With Plant Unique FSI)

LOAD COMBINATION EQUATION*	STRESS COMPONENT	REINFORCING STEEL		CONCRETE		SHEAR	
		MARGIN** FACTOR	CRITICAL*** SECTION	MARGIN FACTOR	CRITICAL SECTION	MARGIN FACTOR	CRITICAL SECTION
1		NA	NA	NA	NA	NA	NA
2		NA	NA	NA	NA	NA	NA
3		NA	NA	NA	NA	NA	NA
4		NA	NA	NA	NA	NA	NA
4a		1.57	14	2.59	1	1.52	8
5		NA	NA	NA	NA	NA	NA
5a		1.08	14	2.66	1	1.50	8
6		NA	NA	NA	NA	NA	NA
7		NA	NA	NA	NA	NA	NA
7a		1.00	14	2.6	1	1.54	8

NOTES:

- \*Refer to Table 4.1-1
- \*\*Margin Factor = Allowable Stress/Actual Stress
- \*\*\*Refer to Figures 5.1-15 and 5.1-16
- NA = Not Applicable

5.1-20

LSCS-MARK II DAR

Rev. 7 1/80

TABLE 5.1-9

MARGIN TABLE FOR REACTOR SUPPORT FOR ALL VALVES DISCHARGE

(with plant unique FSI)

LOAD COMBINATION EQUATION*	STRESS COMPONENT	REINFORCING TENSION		CONCRETE COMPRESSION		SHEAR	
		MARGIN** FACTOR	CRITICAL*** SECTION	MARGIN FACTOR	CRITICAL SECTION	MARGIN FACTOR	CRITICAL SECTION
1		3.7	1	8.31	1	8.9	16
2		2.23	17	4.95	18	2.95	20
3		1.45	18	4.16	18	3.77	20
4		NA	NA	NA	NA	NA	NA
4a		NA	NA	NA	NA	NA	NA
5		NA	NA	NA	NA	NA	NA
5a		NA	NA	NA	NA	NA	NA
6		1.47	20	4.21	18	3.8	20
7		NA	NA	NA	NA	NA	NA
7a		NA	NA	NA	NA	NA	NA

## NOTES:

- \*Refer to Table 4.1-1  
 \*\*Margin Factor = Allowable Stress/Actual Stress  
 \*\*\*Refer to Figures 5.1-15 and 5.1-16  
 NA = Not Applicable

5.1-21

LSCS-MARK II DAR

Rev. 7 1/80

TABLE 5.1-10

MARGIN TABLE FOR REACTOR SUPPORT FOR 2 VALVES DISCHARGE

(with plant unique FSI)

LOAD COMBINATION EQUATION*	STRESS COMPONENT	REINFORCING TENSION		CONCRETE COMPRESSION		SHEAR	
		MARGIN** FACTOR	CRITICAL*** SECTION	MARGIN FACTOR	CRITICAL SECTION	MARGIN FACTOR	CRITICAL SECTION
1		11.10	11	9.78	6	11.9	19
2		2.3	17	5.47	18	1.99	10
3		1.55	20	5.70	17	1.50	16
4		1.82	20	5.08	18	3.07	20
4a		NA	NA	NA	NA	NA	NA
5		1.66	20	5.47	6	3.09	20
5a		NA	NA	NA	NA	NA	NA
6		1.44	1	5.67	17	3.20	20
7		1.21	20	3.80	18	3.29	20
7a		NA	NA	NA	NA	NA	NA

NOTES:

\*Refer to Table 4.1-1

\*\*Margin Factor = Allowable Stress/Actual Stress

\*\*\*Refer to Figures 5.1-15 and 5.1-16

NA = Not Applicable

5.1-22

LSCS-MARK II DAR

Rev. 7 1/80

TABLE 5.1-11

MARGIN TABLE FOR REACTOR SUPPORT FOR ADS VALVES DISCHARGE

(with plant unique FSI)

LOAD COMBINATION EQUATION*	STRESS COMPONENT	REINFORCING TENSION		CONCRETE COMPRESSION		SHEAR	
		MARGIN** FACTOR	CRITICAL*** SECTION	MARGIN FACTOR	CRITICAL SECTION	MARGIN FACTOR	CRITICAL SECTION
1		NA	NA	NA	NA	NA	NA
2		NA	NA	NA	NA	NA	NA
3		NA	NA	NA	NA	NA	NA
4		1.67	15	4.10	18	3.21	18
4a		NA	NA	NA	NA	NA	NA
5		1.33	15	4.15	18	3.52	20
5a		NA	NA	NA	NA	NA	NA
6		NA	NA	NA	NA	NA	NA
7		1.13	18	3.54	18	3.41	20
7a		NA	NA	NA	NA	NA	NA

NOTES:

- \*Refer to Table 4.1-1
- \*\*Margin Factor = Allowable Stress/Actual Stress
- \*\*\*Refer to Figures 5.1-15 and 5.1-16
- NA = Not Applicable

5.1-23

LSCS-MARK II DAR

Rev. 7 1/80

TABLE 5.1-12

MARGIN TABLE FOR REACTOR SUPPORT FOR LOCA PLUS SINGLE SRV

(with plant unique FSI)

LOAD COMBINATION EQUATION*	STRESS COMPONENT	REINFORCING TENSION		CONCRETE COMPRESSION		SHEAR	
		MARGIN** FACTOR	CRITICAL*** SECTION	MARGIN FACTOR	CRITICAL SECTION	MARGIN FACTOR	CRITICAL SECTION
1		NA	NA	NA	NA	NA	NA
2		NA	NA	NA	NA	NA	NA
3		NA	NA	NA	NA	NA	NA
4		NA	NA	NA	NA	NA	NA
4a		1.02	15	4.11	18	2.51	15
5		NA	NA	NA	NA	NA	NA
5a		1.07	15	4.16	18	2.84	15
6		NA	NA	NA	NA	NA	NA
7		NA	NA	NA	NA	NA	NA
7a		1.00	15	3.48	18	3.12	15

5.1-24

LSCS-MARK II DAR

Rev. 7 1/80

NOTES: \*Refer to Table 4.1-1  
 \*\*Margin Factor = Allowable Stress/Actual Stress  
 \*\*\*Refer to Figures 5.1-15 and 5.1-16  
 NA = Not Applicable

TABLE 5.1-13

MARGIN TABLE FOR DRYWELL FLOOR AND SRV AND LOCA LOADS

(with plant unique FSI)

LOAD COMBINATION EQUATION*	STRESS COMPONENT	REINFORCING TENSION		CONCRETE COMPRESSION		SHEAR	
		MARGIN** FACTOR	CRITICAL*** SECTION	MARGIN FACTOR	CRITICAL SECTION	MARGIN FACTOR	CRITICAL SECTION
1		5.6	3	11.2	3	4.1	1
2		5.4	4	4.5	4	2.7	1
3		2.08	6	2.50	4	2.02	1
4		1.23	8	2.21	8	1.44	1
4a		1.04	8	2.05	8	1.17	8
5		1.38	8	2.45	8	1.82	8
5a		1.16	8	2.27	8	1.30	1
6		2.06	6	2.42	4	1.87	1
7		1.33	8	2.31	8	1.44	1
7a		1.10	8	2.10	8	1.15	1

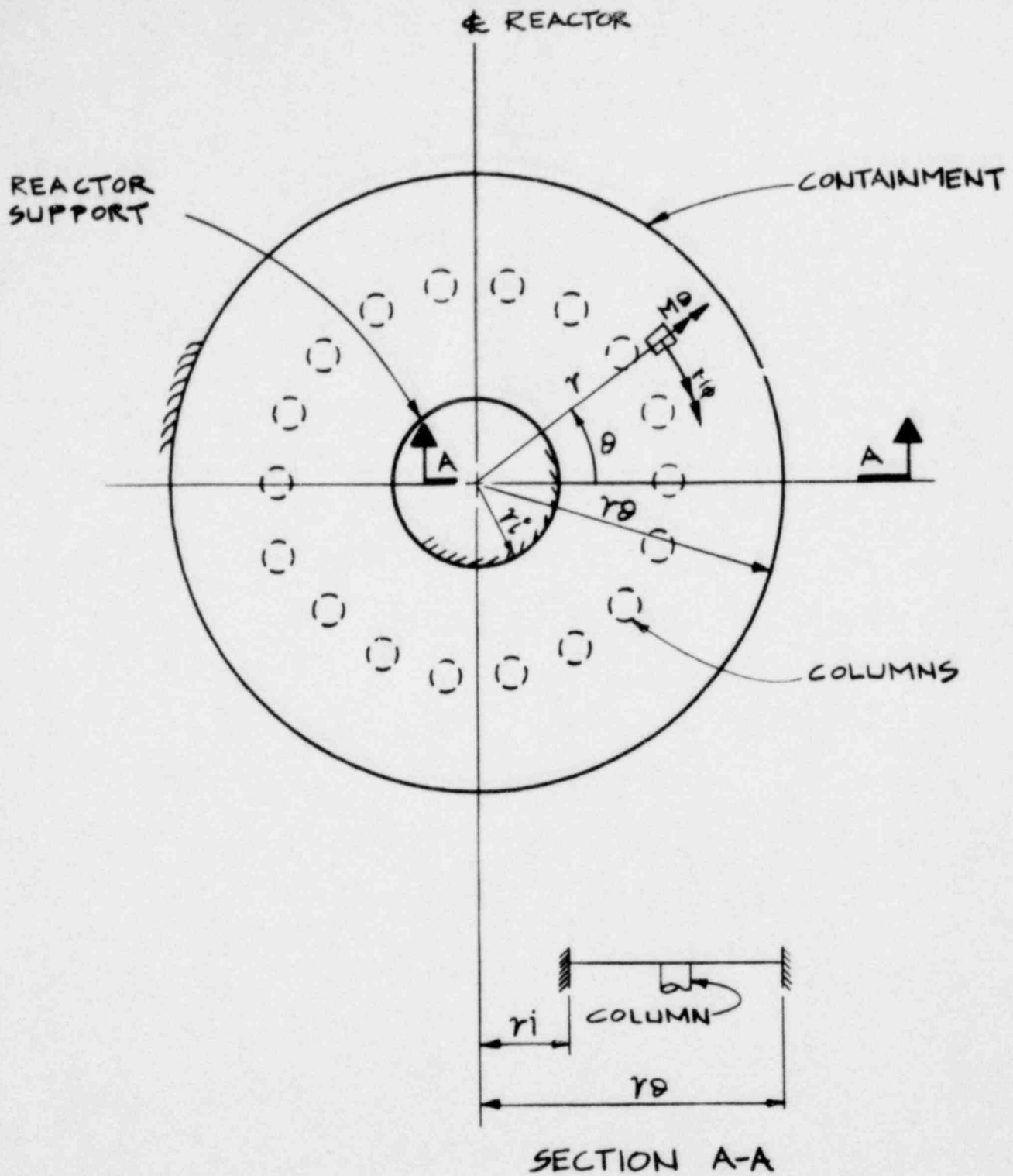
5.1-25

LSCS-MARK II DAR

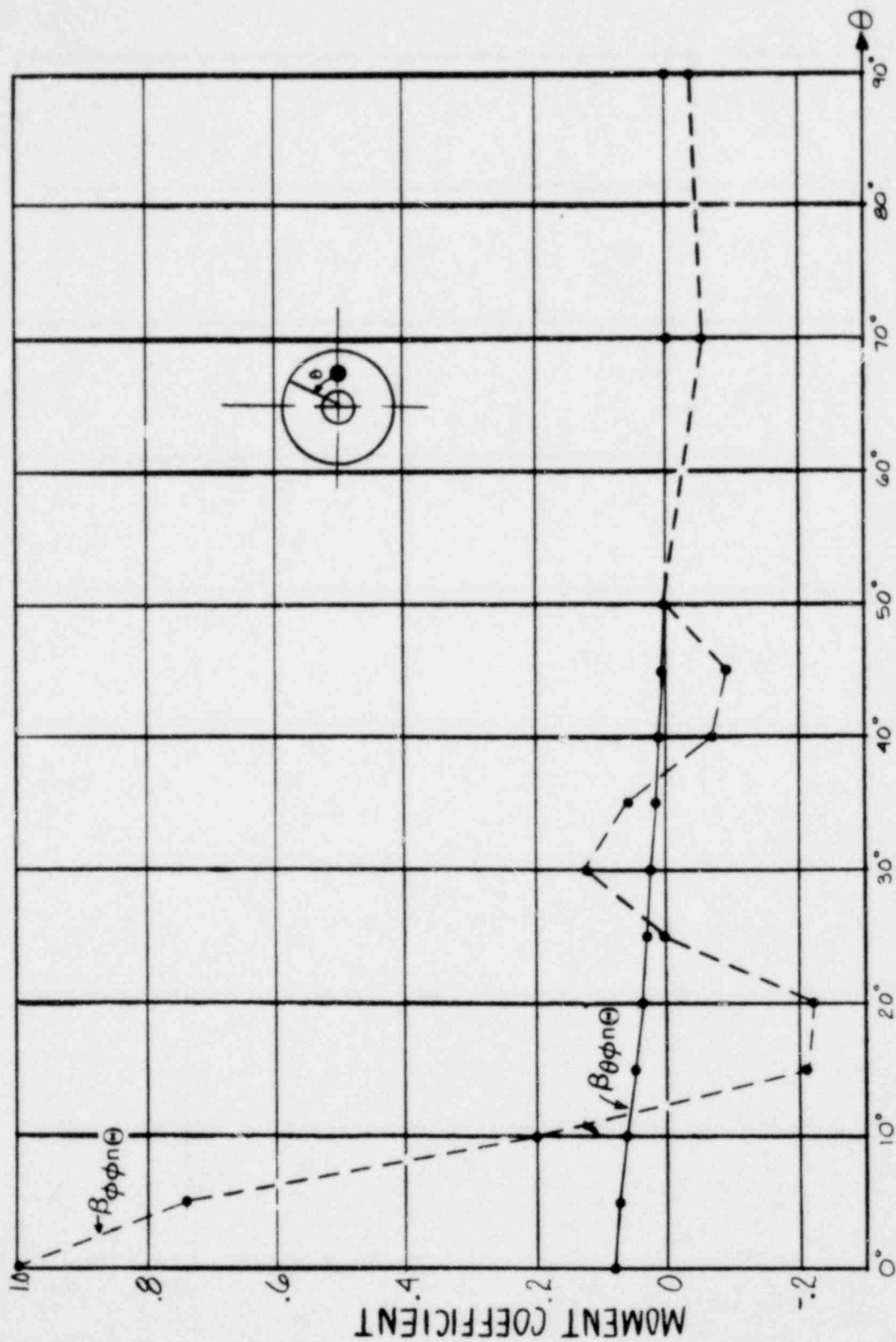
Rev. 7 1/80

NOTES: \*Refer to Table 4.1-1  
 \*\*Margin Factor = Allowable Stress/Actual Stress  
 \*\*\*Refer to Figures 5.1-15 and 5.1-16

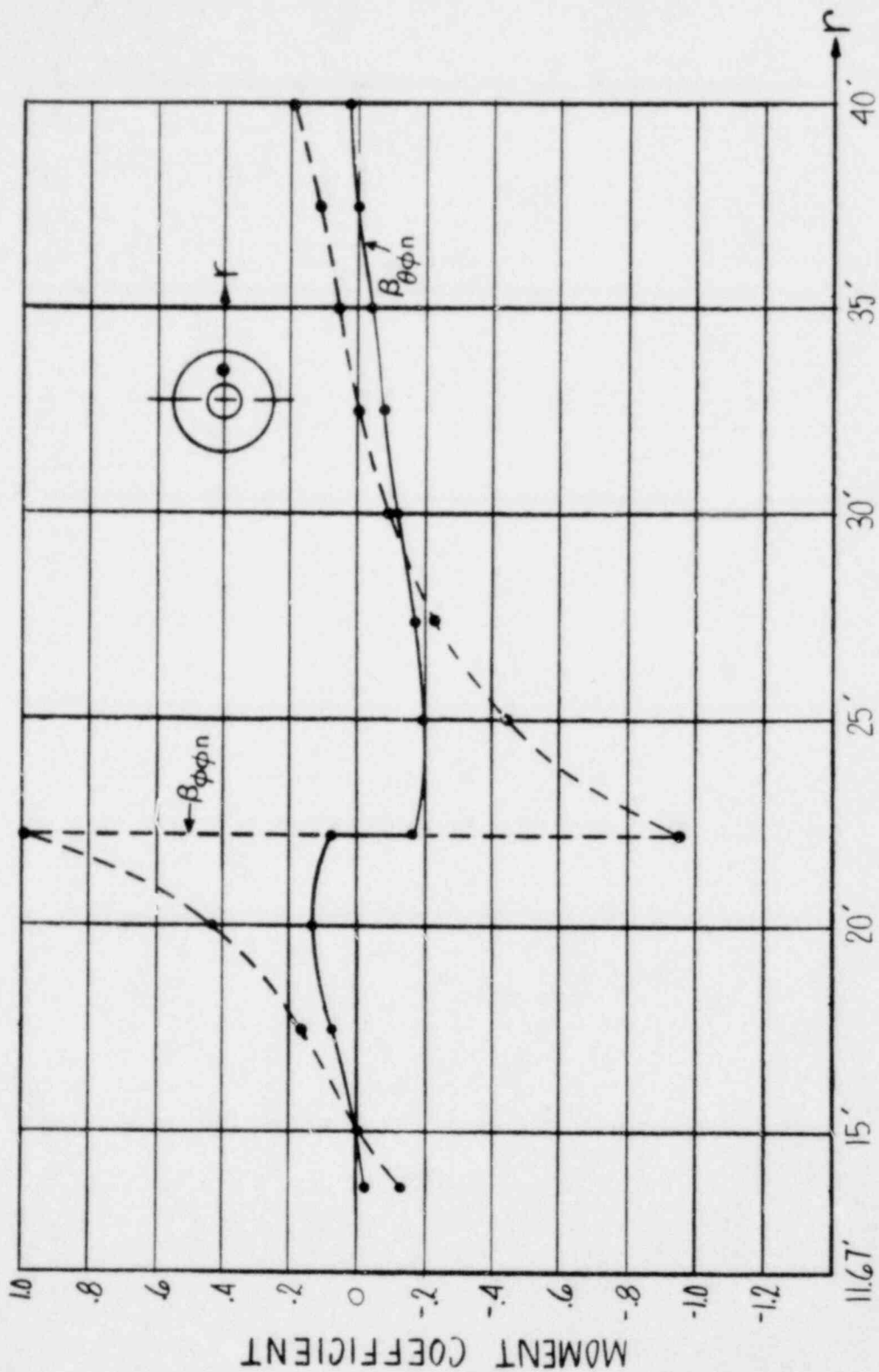




LA SALLE COUNTY STATION MARK II DESIGN ASSESSMENT REPORT
FIGURE 5.1-2 DRYWELL FLOOR ANALYTICAL MODEL



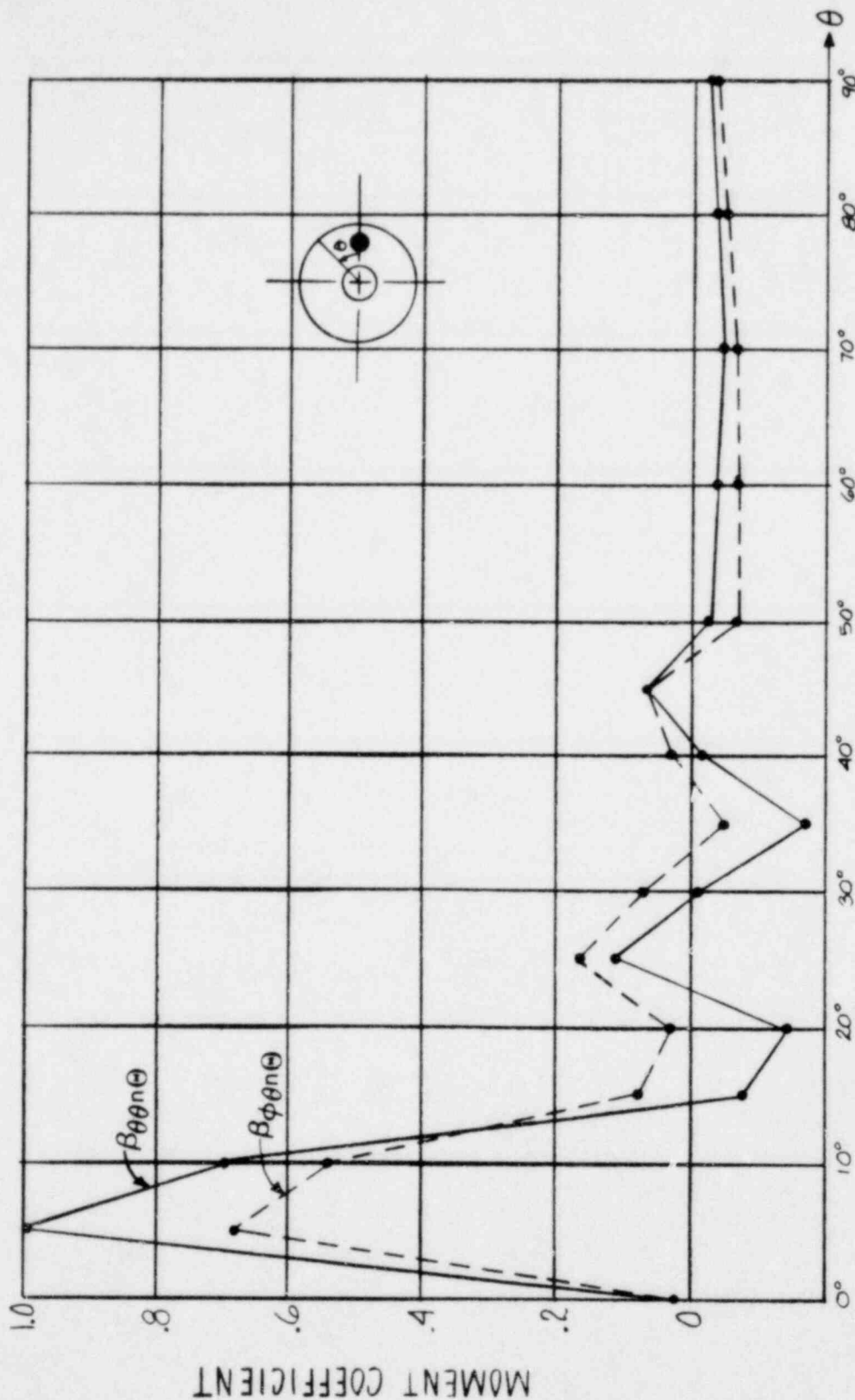
**LA SALLE COUNTY STATION**  
 MARK II DESIGN ASSESSMENT REPORT  
 FIGURE 5.1-3  
 CIRCUMFERENTIAL VARIATION OF MOMENT  
 IN DRYWELL FLOOR DUE TO CONCENTRATED  
 RADIAL MOMENT APPLIED AT  
 RADIUS 23'-3"



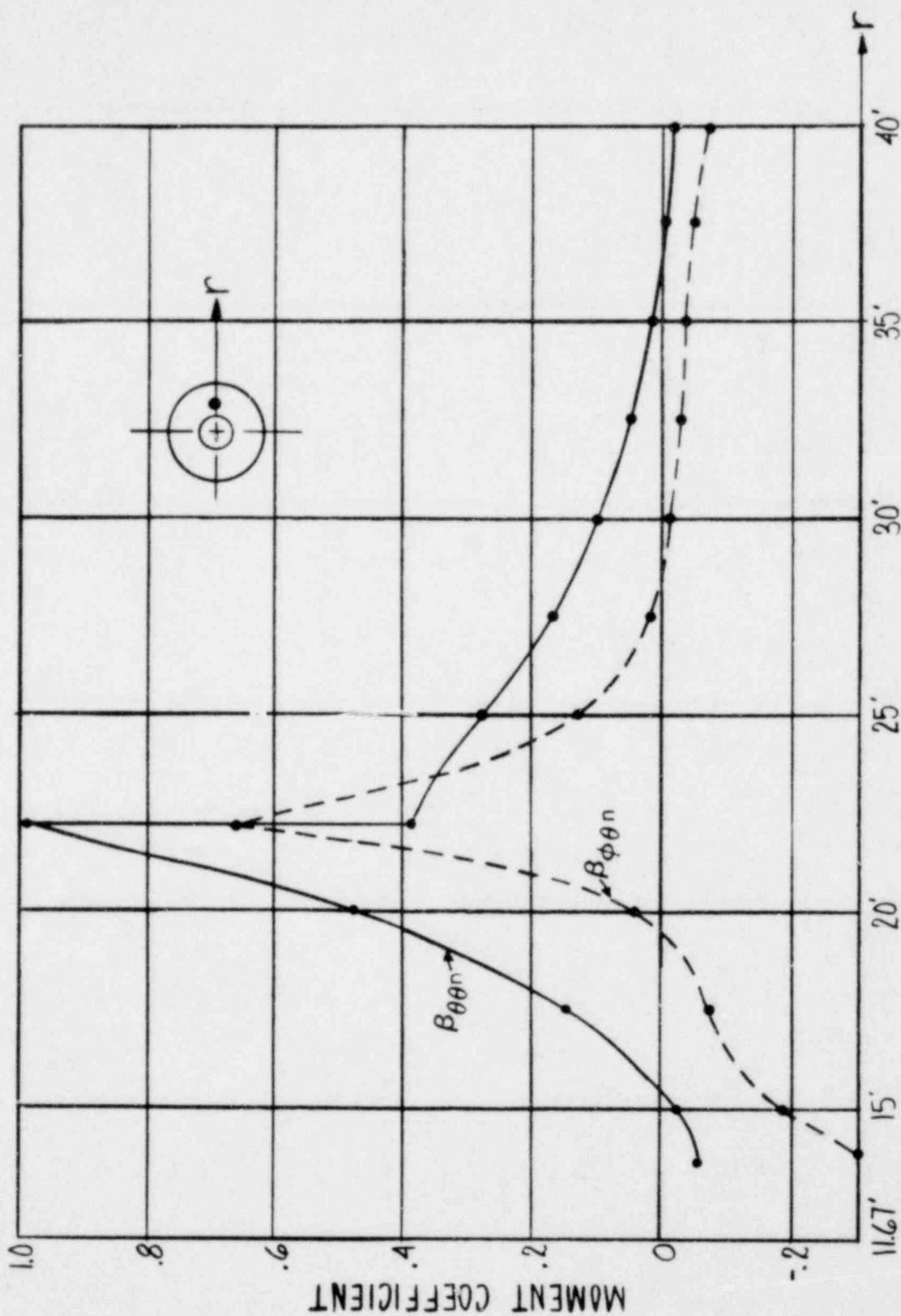
**LA SALLE COUNTY STATION**  
 MARK II DESIGN ASSESSMENT REPORT

FIGURE 5.1-4

RADIAL VARIATION OF MOMENT IN DRYWELL FLOOR DUE TO CONCENTRATED RADIAL MOMENT APPLIED AT RADIUS 23'-3"



**LA SALLE COUNTY STATION**  
 MARK II DESIGN ASSESSMENT REPORT  
 FIGURE 5.1-5  
 CIRCUMFERENTIAL VARIATION OF MOMENT IN  
 DRYWELL FLOOR DUE TO CONCENTRATED  
 CIRCUMFERENTIAL MOMENT APPLIED AT  
 RADIUS 23'-3"

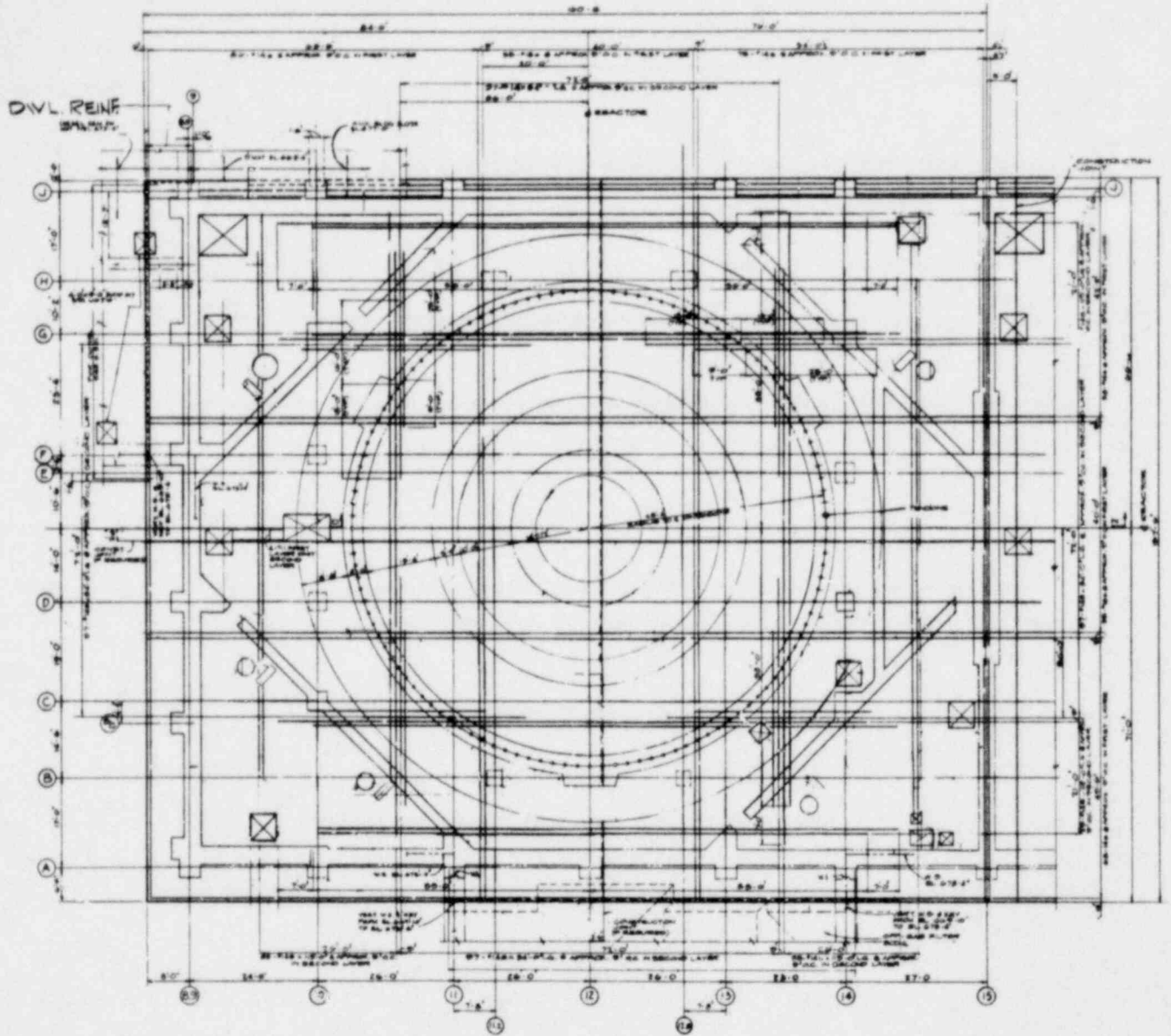


LA SALLE COUNTY STATION  
 MARK II DESIGN ASSESSMENT REPORT

FIGURE 5.1-6

RADIAL VARIATION OF MOMENT IN DRYWELL FLOOR DUE TO CONCENTRATED CIRCUMFERENTIAL MOMENT APPLIED AT RADIUS 23'-3"

# POOR ORIGINAL

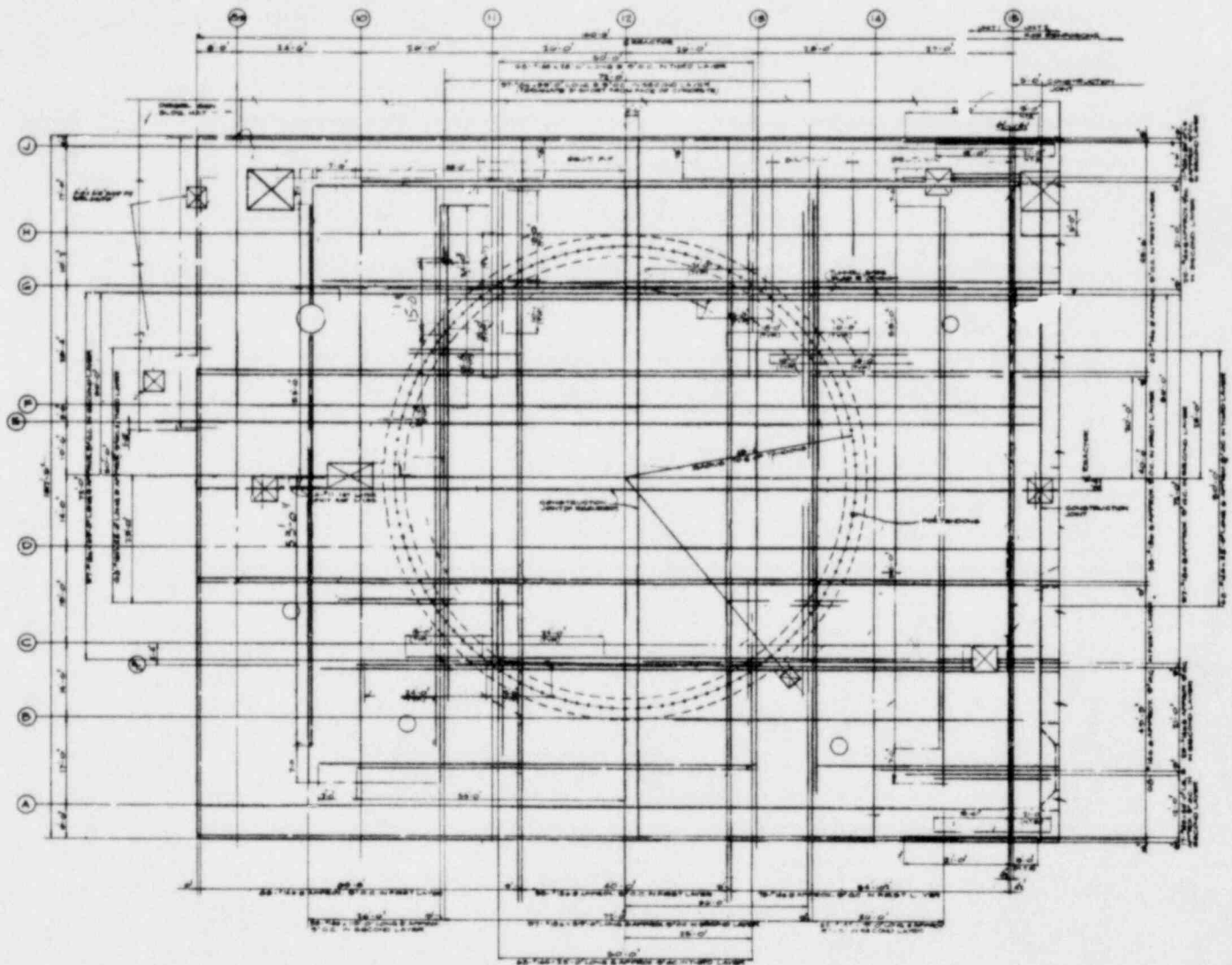


LA SALLE COUNTY STATION  
MARK II DESIGN ASSESSMENT REPORT

FIGURE 5.1-7

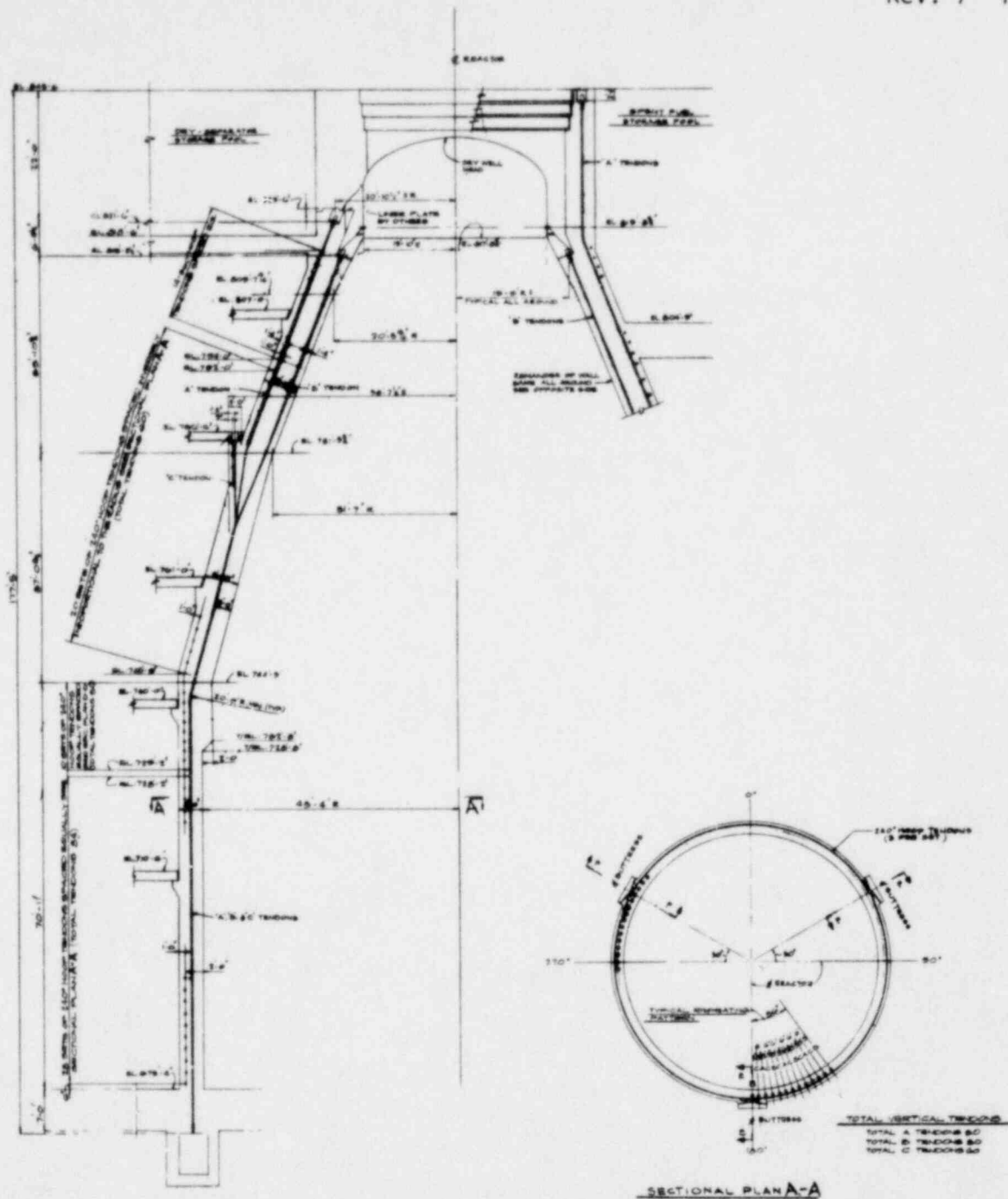
BASE MAT PLAN - TOP REINFORCING LAYOUT

POOR ORIGINAL



LA SALLE COUNTY STATION  
MARK II DESIGN ASSESSMENT REPORT

FIGURE 5.1-8  
BASE MAT PLAN - BOTTOM  
REINFORCING LAYOUT

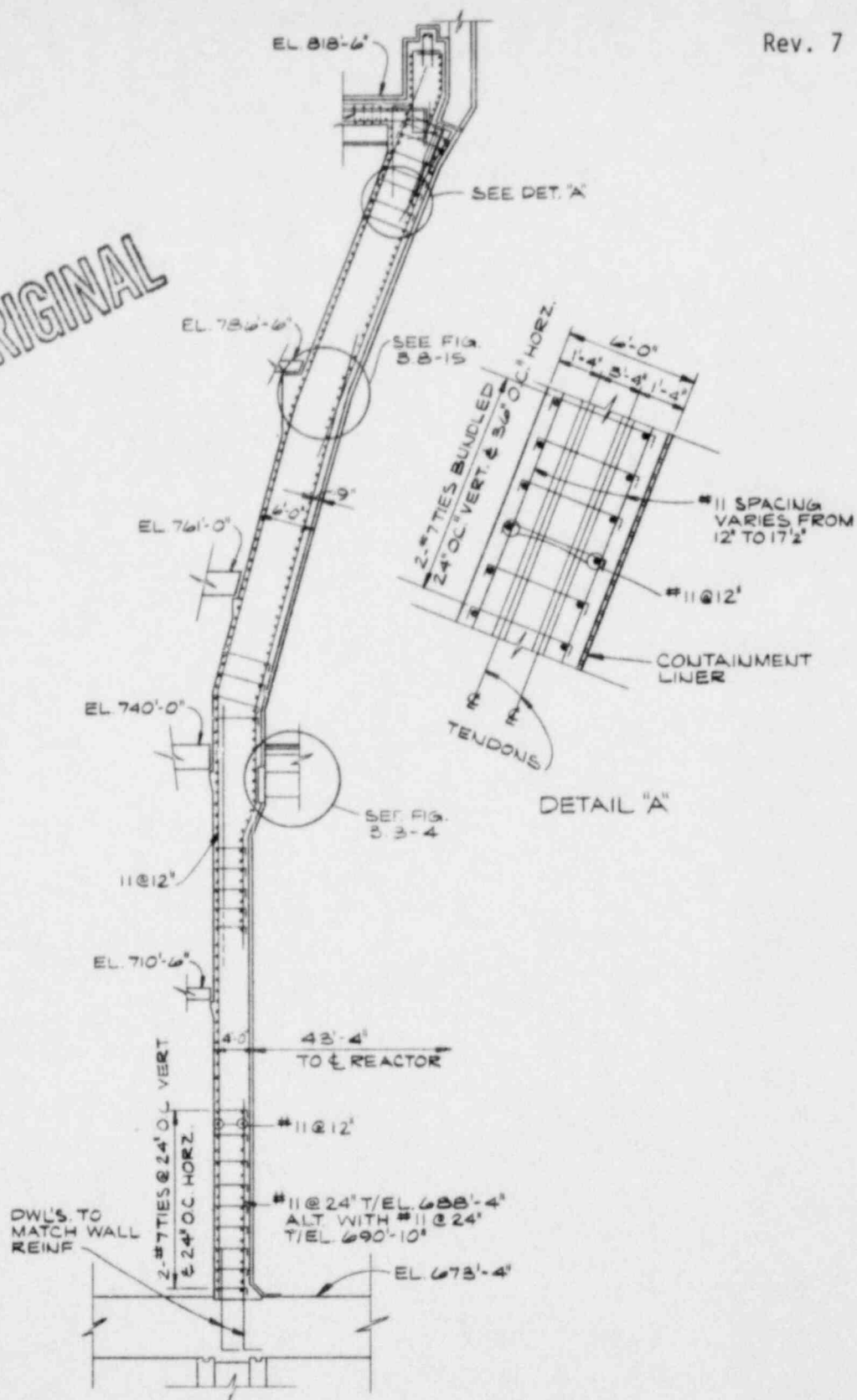


POOR ORIGINAL

LA SALLE COUNTY STATION  
MARK II DESIGN ASSESSMENT REPORT

FIGURE 5.1-9  
CONTAINMENT WALL POST-TENSIONING  
TENDON LAYOUT

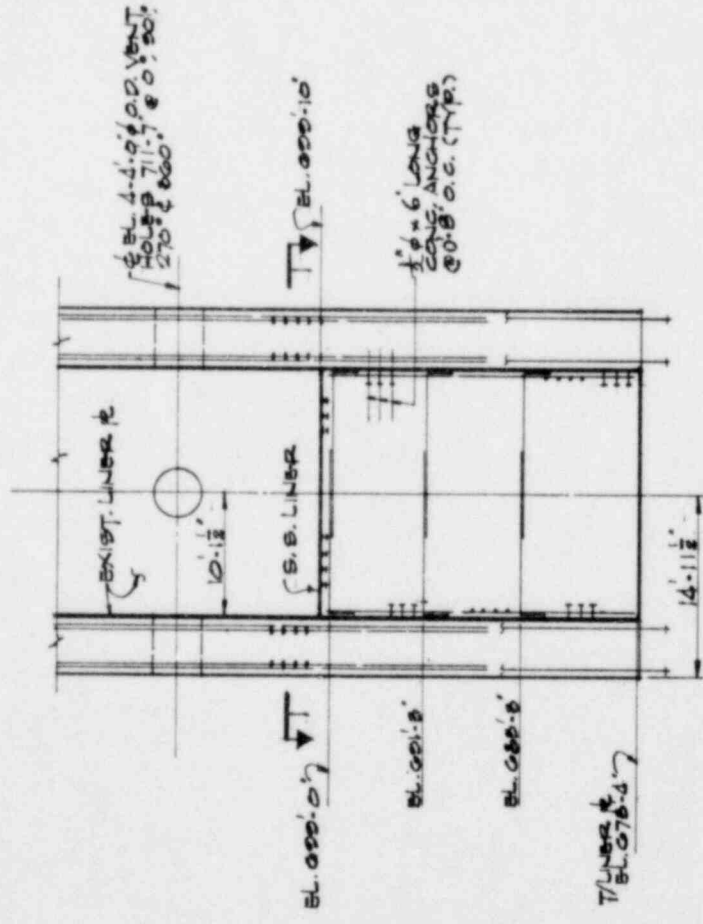
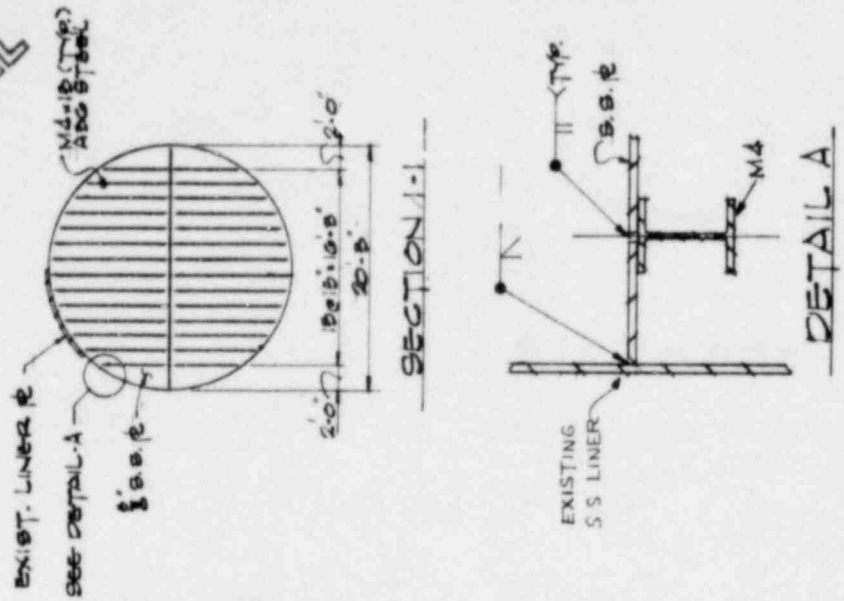
POOR ORIGINAL



LA SALLE COUNTY STATION  
 MARK II DESIGN ASSESSMENT REPORT

FIGURE 5.1-10  
 CONTAINMENT WALL -  
 REINFORCING LAYOUT

POOR ORIGINAL



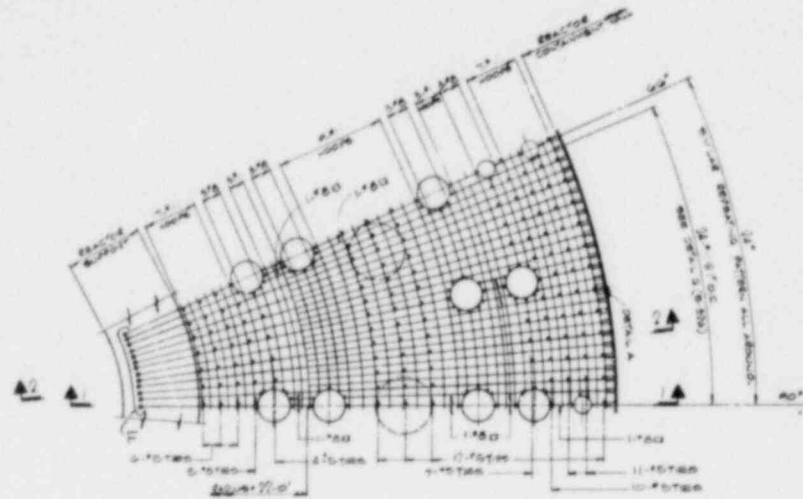
LA SALLE COUNTY STATION  
 MARK II DESIGN ASSESSMENT REPORT

FIGURE 5.1-11

REACTOR SUPPORT - CONCRETE PLUG

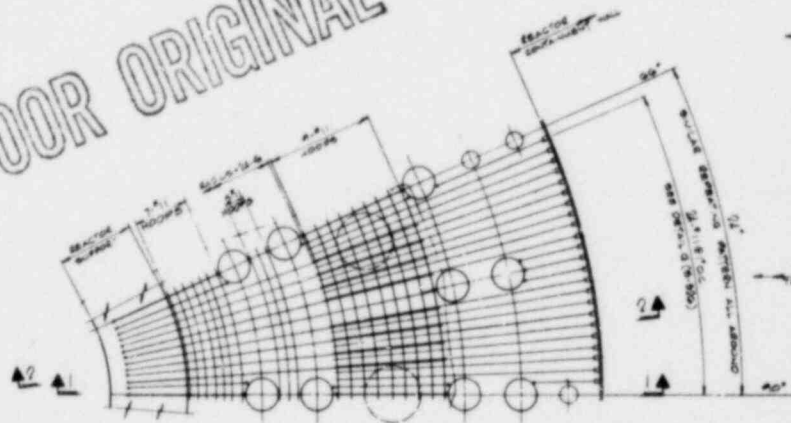


152-6

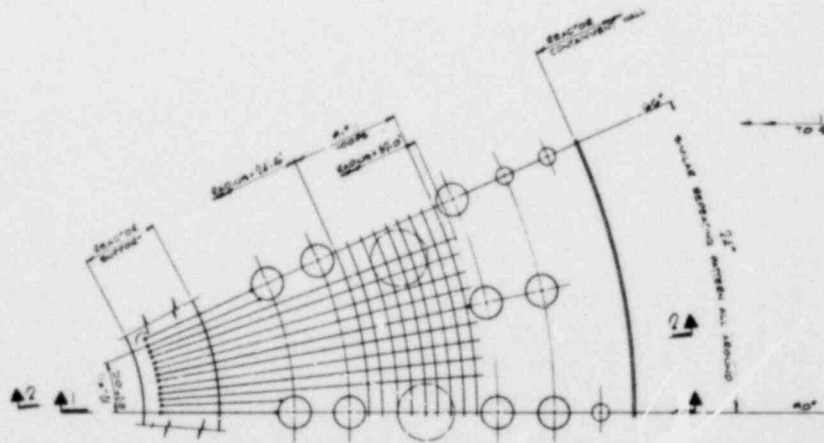


TOP & BOTTOM REINFORCING PLAN (1st LAYER)  
SCALE 1/4"=1'-0"

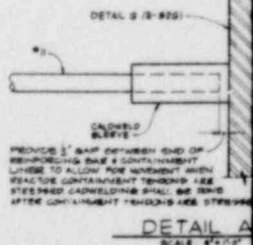
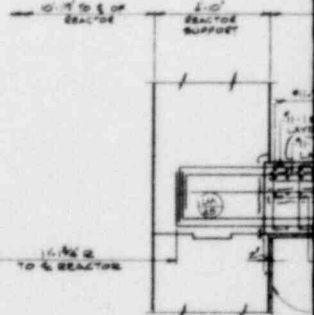
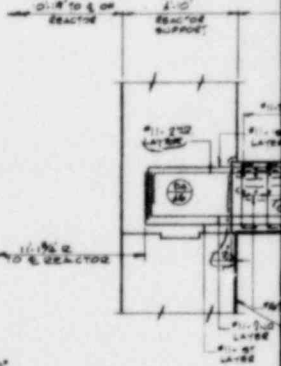
POOR ORIGINAL



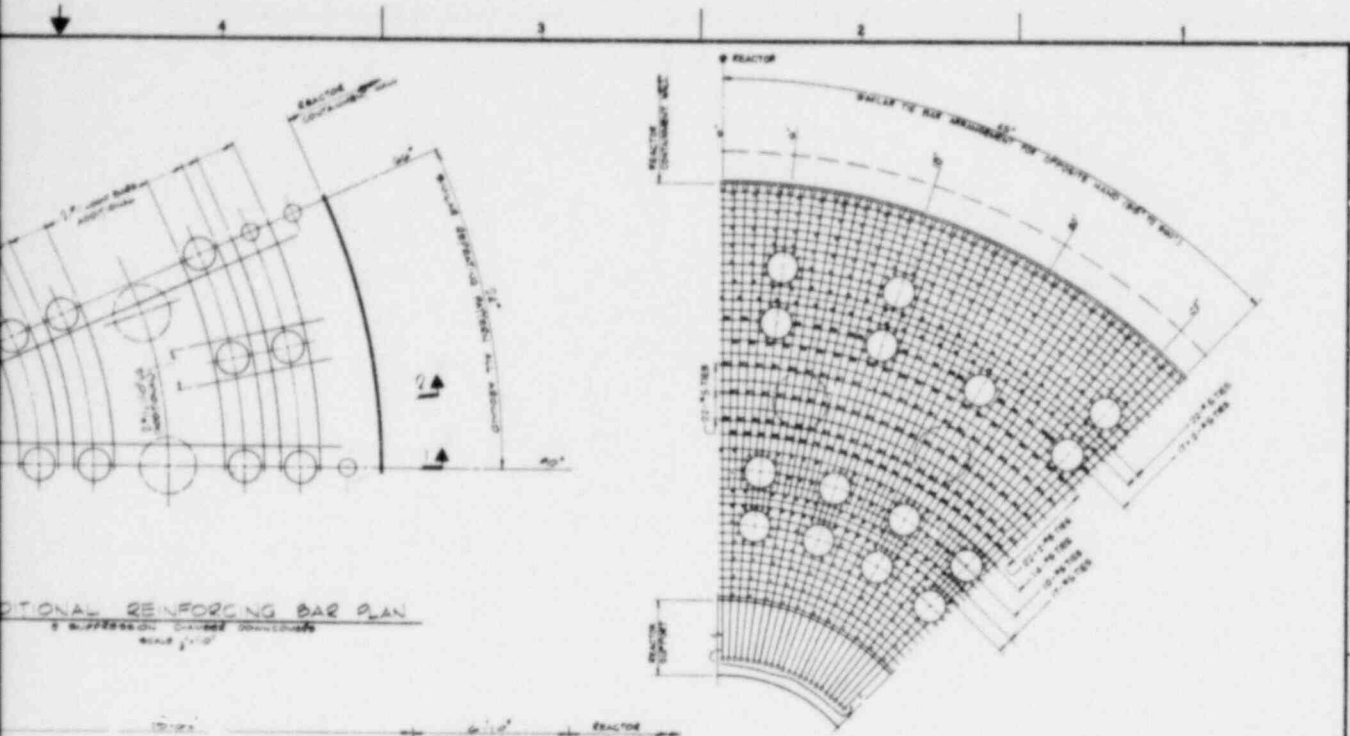
TOP REINFORCING PLAN (2nd LAYER)  
SCALE 1/4"=1'-0"



BOTTOM REINFORCING PLAN (2nd LAYER)  
SCALE 1/4"=1'-0"

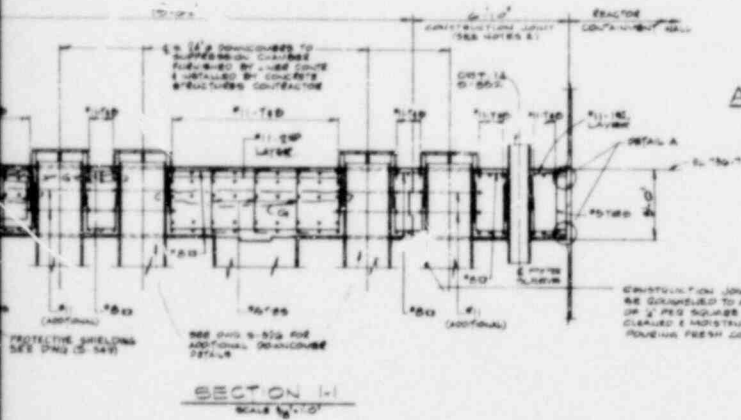


DETAIL B (2nd LAYER)  
SCALE 3/4"=1'-0"



ADDITIONAL REINFORCING BAR PLAN  
SCALE: 1/4"=1'-0"

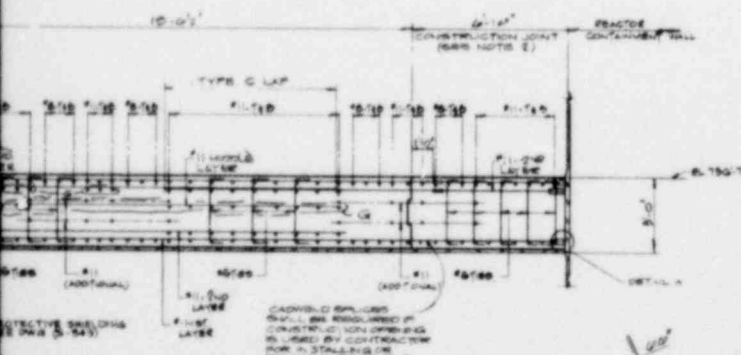
ADDITIONAL TIE BAR REINFORCING PLAN  
SCALE: 1/4"=1'-0"



SECTION 1-1  
SCALE: 1/4"=1'-0"

CONSTRUCTION JOINT SHALL BE DISKED TO AN AMPLITUDE OF 1/2" PER SQUARE YARD AND CLEANED & PROTECTED BEFORE POURING FRESH CONCRETE.

- NOTES**
1. FOR GENERAL NOTES SEE DWG. 5-501
  2. THIS AREA SHALL BE REINFORCED AFTER CONTAINMENT BENCHES ARE INSTALLED
  3. THIS DWG. SHALL BE REVIEWED WITH DWGS. 5-502 & 5-503 FOR DIMENSIONS & DETAILS
  4. CAPPED SLEEVES AND ENDS OF REINFORCING BARS SHALL BE KEPT ADEQUATELY PROTECTED BY LAPPING OR WRAPPING UNTIL CAPPING IS DONE



SECTION 2-2  
SCALE: 1/4"=1'-0"

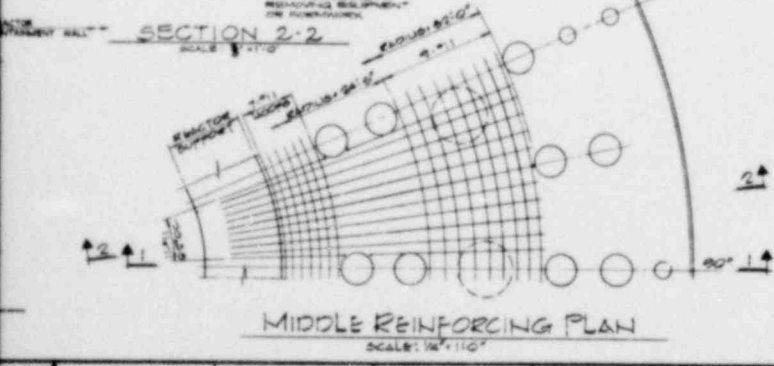
POOR ORIGINAL

**LA SALLE COUNTY STATION**  
MARK II DESIGN ASSESSMENT REPORT

---

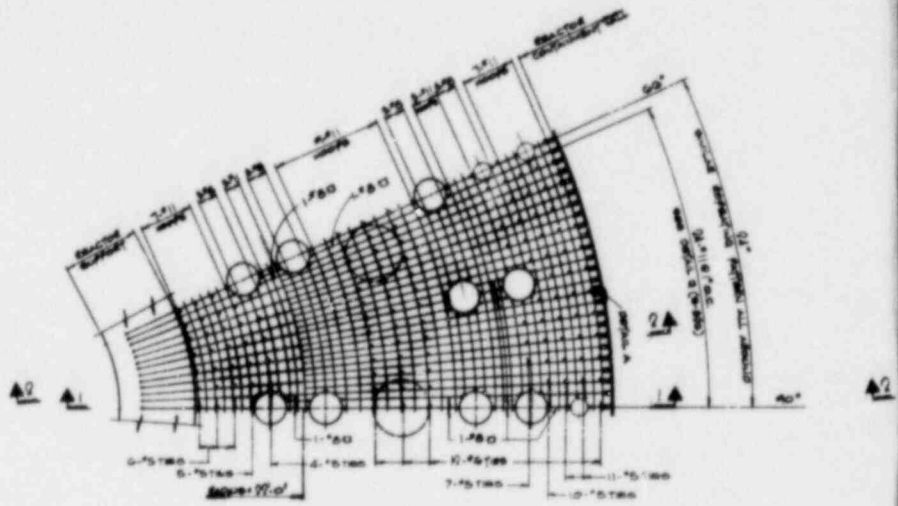
FIGURE 5.1-13

UNIT 1 - DRYWELL FLOOR -  
REINFORCING LAYOUT

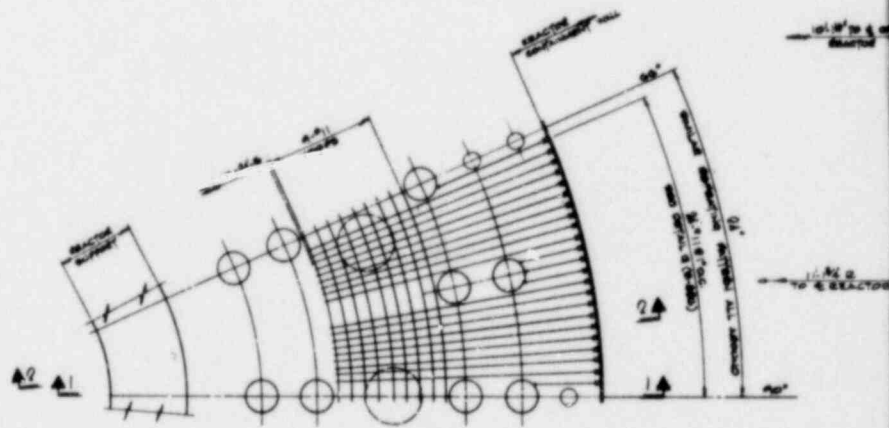


MIDDLE REINFORCING PLAN  
SCALE: 1/4"=1'-0"

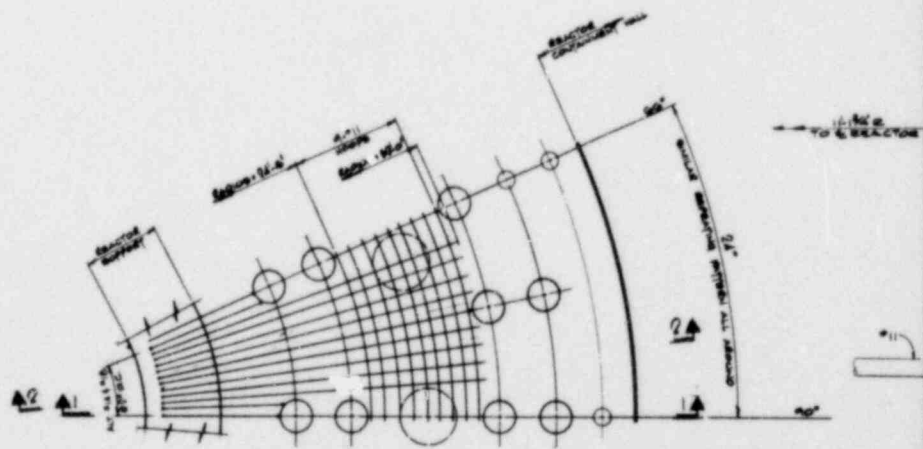
158-S



TOP & BOTTOM REINFORCING PLAN (1ST LAYER)  
SCALE 3/4"=1'-0"

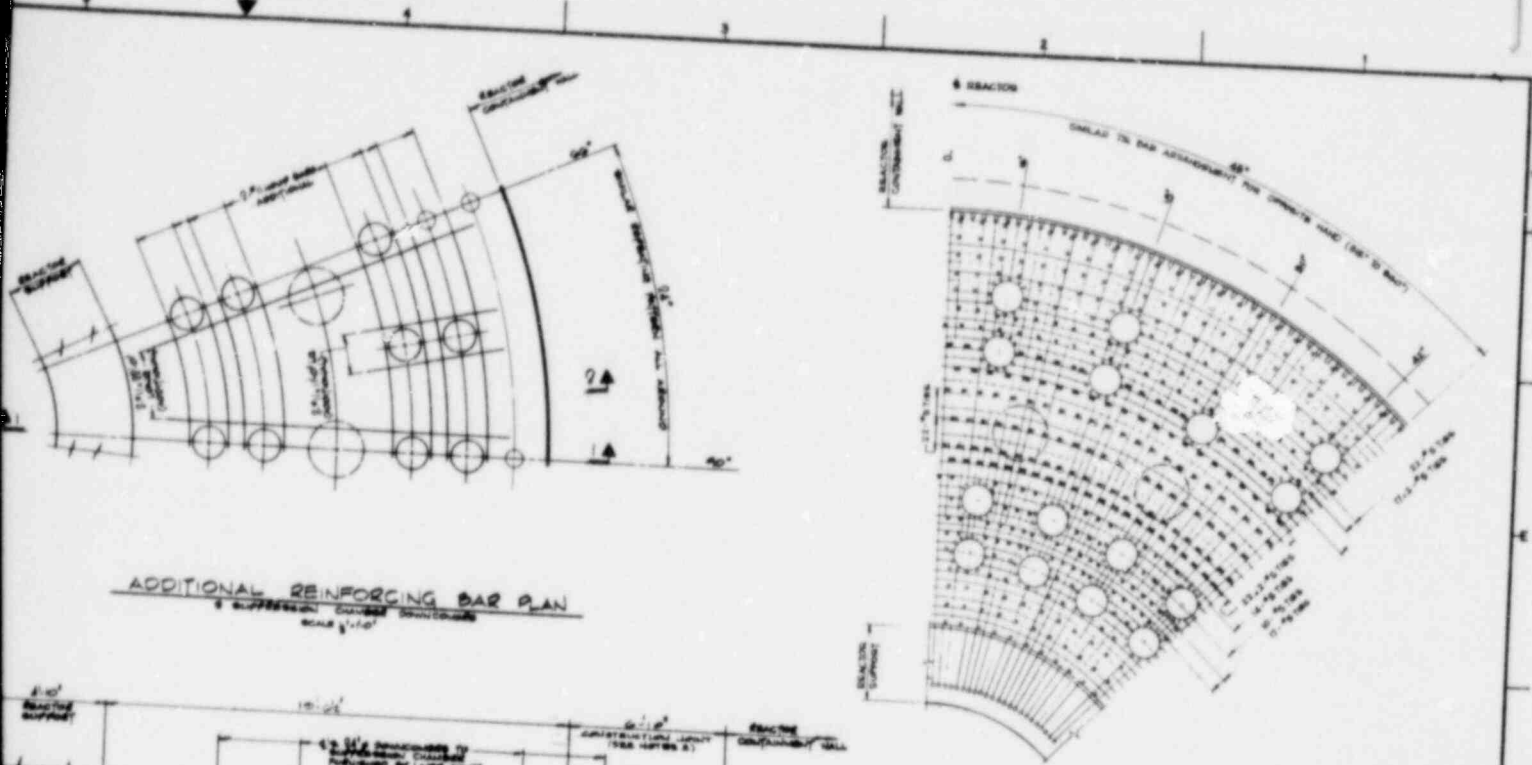


TOP REINFORCING PLAN (2ND LAYER)  
SCALE 3/4"=1'-0"



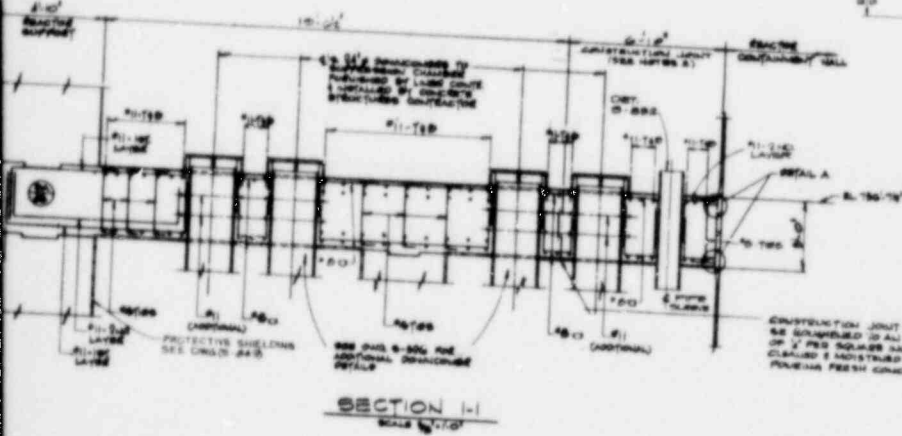
BOTTOM REINFORCING PLAN (2ND LAYER)  
SCALE 3/4"=1'-0"

POOR ORIGINAL

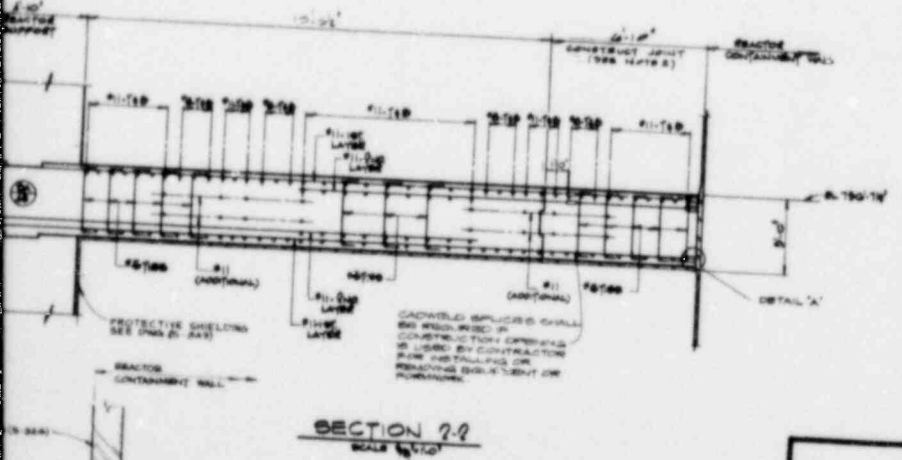


ADDITIONAL REINFORCING BAR PLAN  
SCALE 1/4" = 1'-0"

ADDITIONAL TIE BAR REINFORCING PLAN  
SCALE 3/4" = 1'-0"



SECTION H-I  
SCALE 1/4" = 1'-0"



SECTION 2-2  
SCALE 1/4" = 1'-0"

POOR ORIGINAL

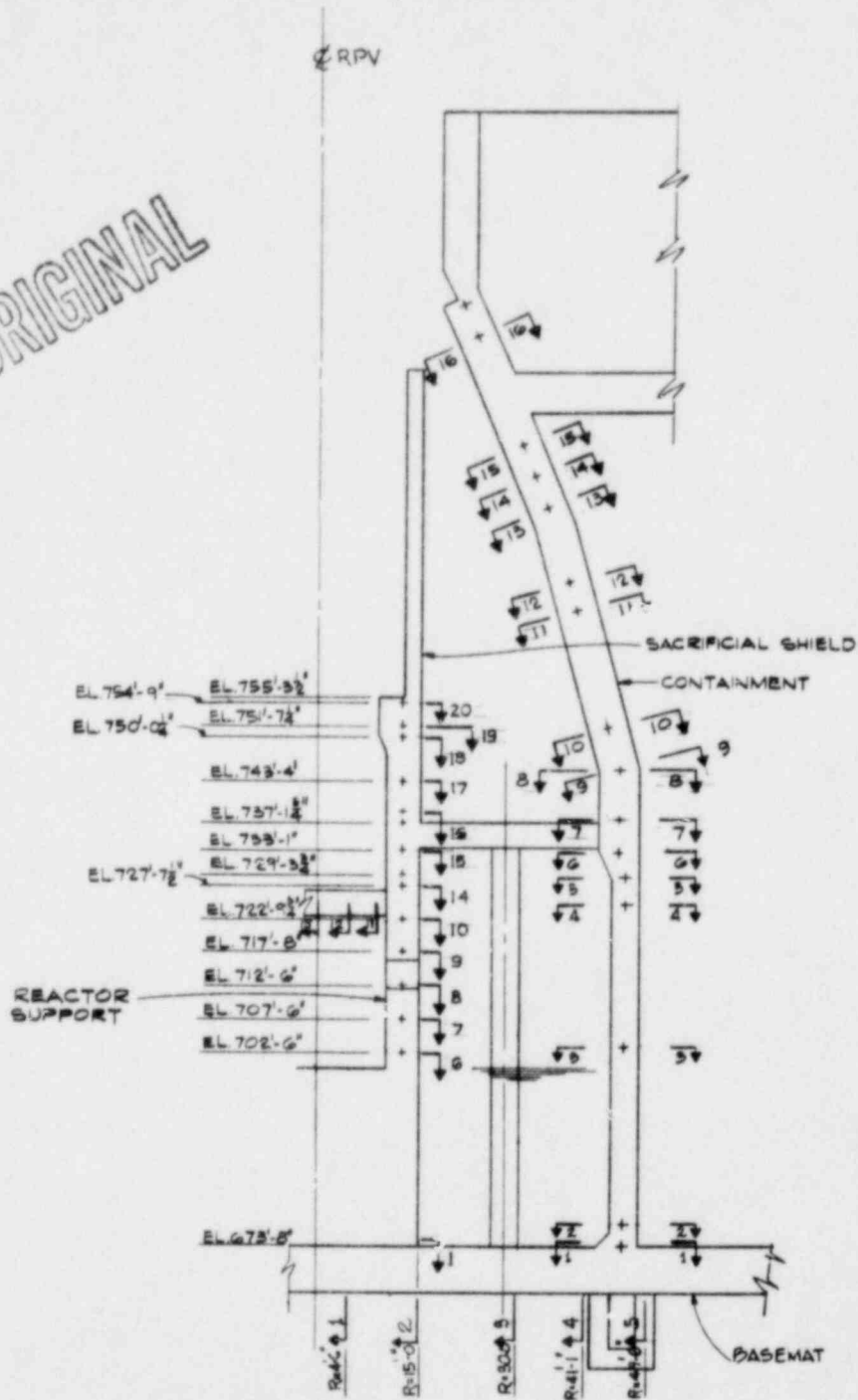
- NOTES
1. FOR GENERAL NOTES SEE THE 5-107
  2. THIS AREA SHALL BE RAISED AFTER CONTAINMENT
  3. THIS ONE SHALL BE COVERED WITH OVER 6" MIN 1500 PSI CONCRETE & DETAILS
  4. CATCHWELD BUCKLE AND ENDS OF REINFORCING SHALL BE KEPT ADEQUATELY PROTECTED BY CARPING OR WRAPPING UNTIL CONCRETE IS DONE

LA SALLE COUNTY STATION  
MARK II DESIGN ASSESSMENT REPORT

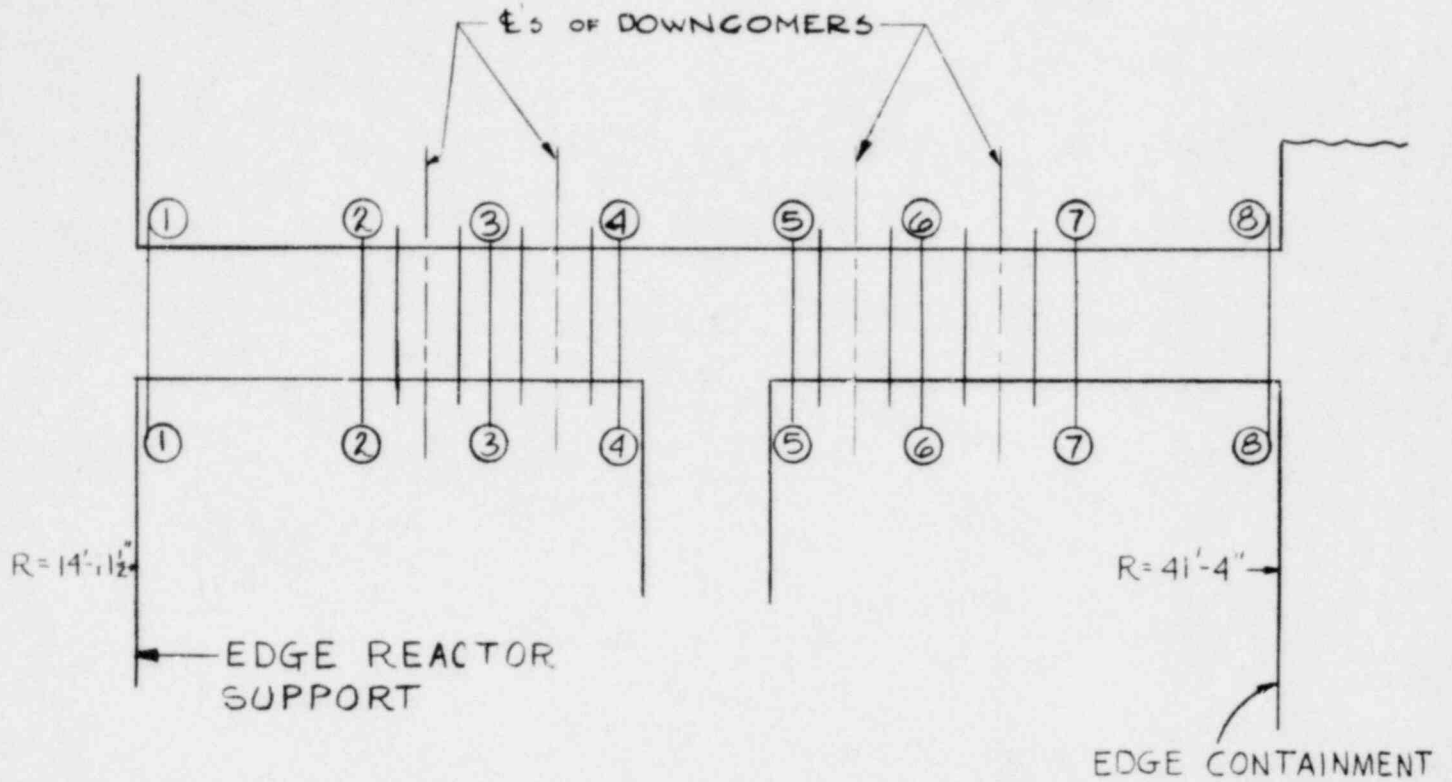
FIGURE 5.1-14  
UNIT 2 - DRYWELL FLOOR -  
REINFORCING LAYOUT

PROVIDE 1" GAP BETWEEN  
SIDE OF REINFORCED BAR  
& CONTAINMENT WALL  
TO ALLOW FOR MOVEMENT  
BETWEEN REINFORCEMENT  
WALLS AND CONCRETE  
CALCULATIONS SHALL BE DONE  
AFTER CONTAINMENT WALLS  
ARE REVEALED.

POOR ORIGINAL



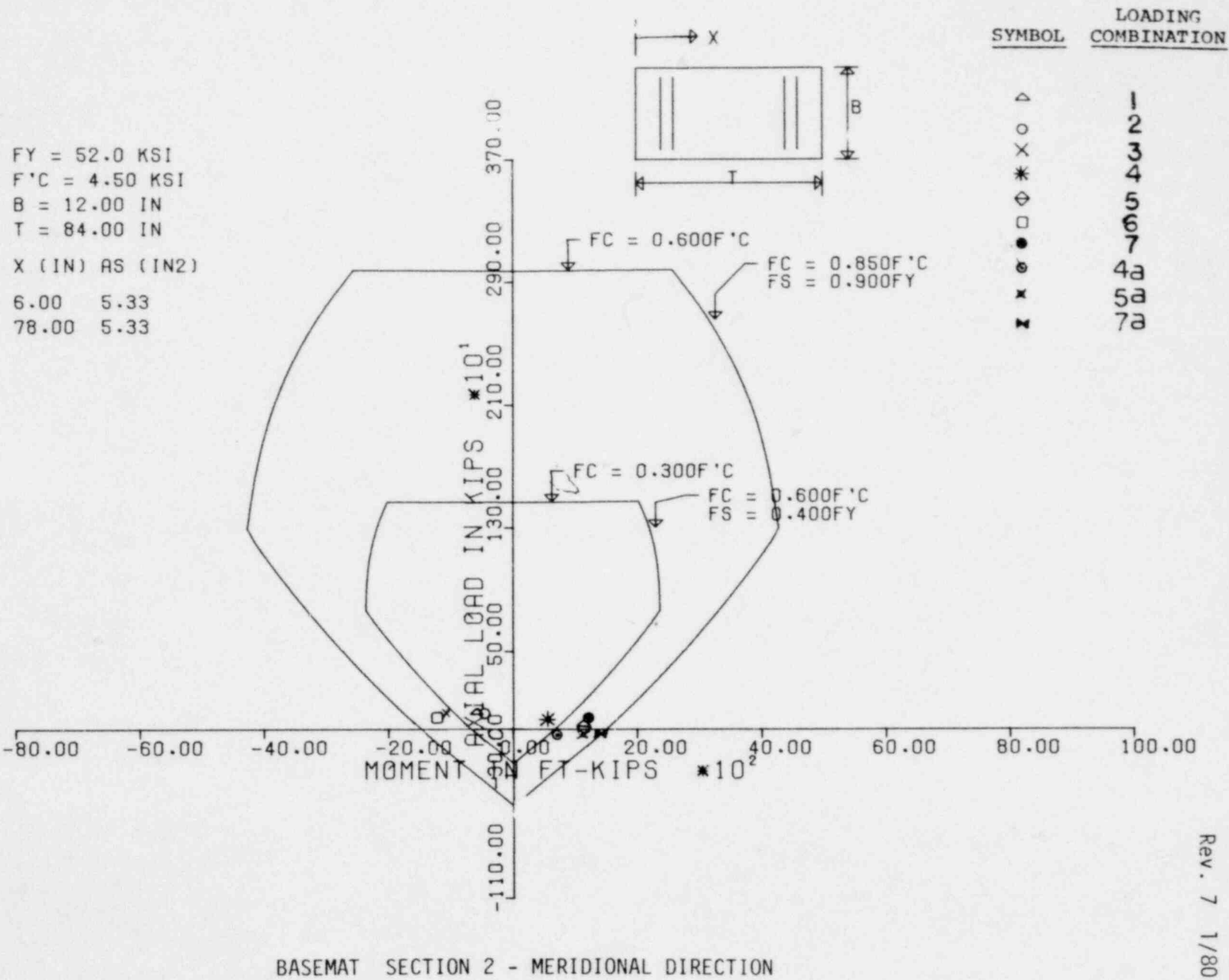
LA SALLE COUNTY STATION  
MARK II DESIGN ASSESSMENT REPORT  
FIGURE 5.1-15  
DESIGN SECTIONS - PRIMARY CONTAINMENT  
AND REACTOR SUPPORT



SECTION NUMBER	1	2	3	4	5	6	7	8
RADIUS (feet)	14.96	20.96	22.96	26.96	30.17	32.17	36.17	41.33

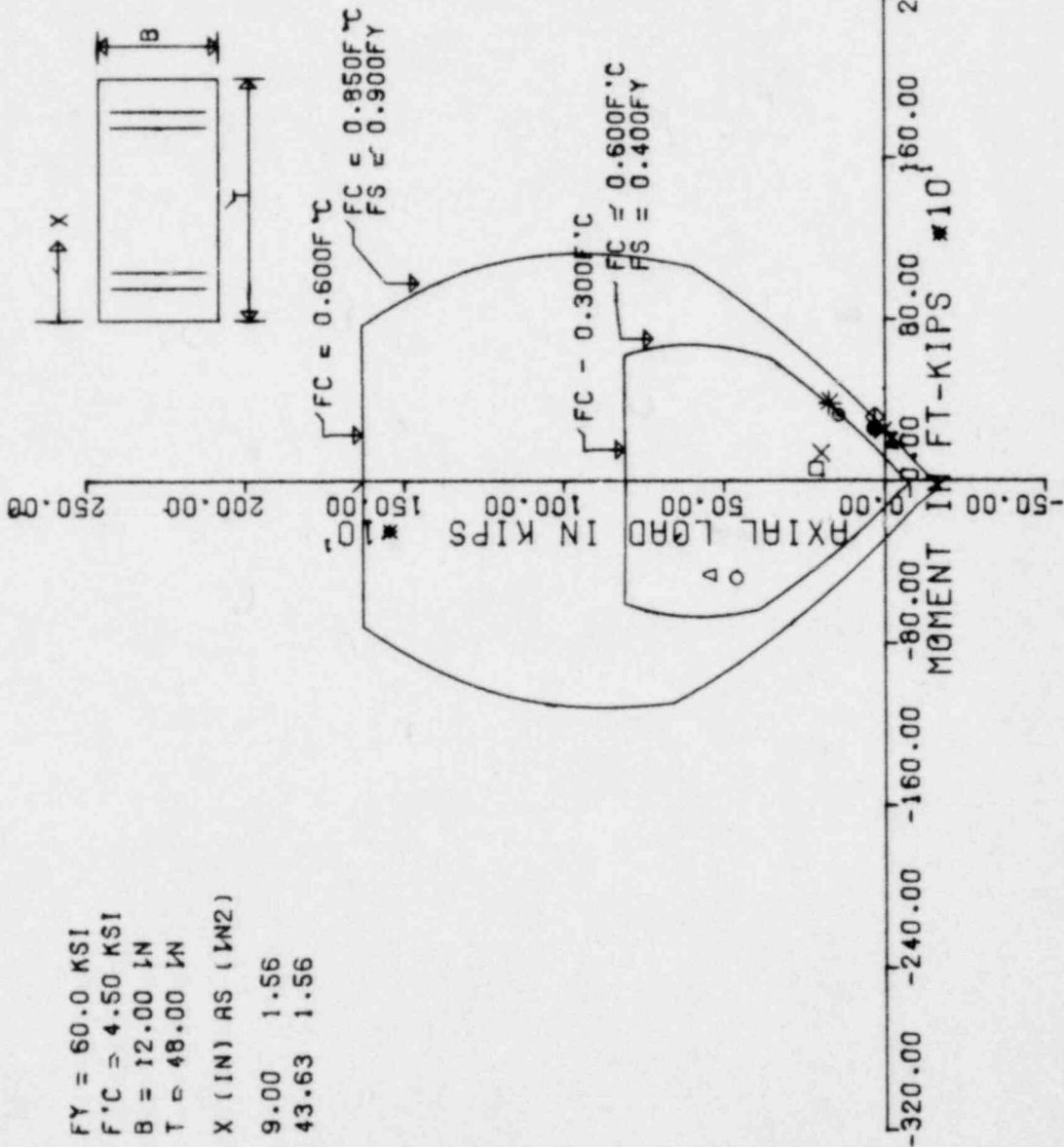
**LA SALLE COUNTY STATION**  
 MARK II DESIGN ASSESSMENT REPORT  
 FIGURE 5.1-16  
 DESIGN SECTIONS - DRYWELL FLOOR

**LA SALLE COUNTY STATION**  
 MARK II DESIGN ASSESSMENT REPORT  
 FIGURE 5.1-17  
 REPRESENTATIVE BASE MAT  
 INTERACTION DIAGRAM



SYMBOL      LOADING COMBINATION

- |   |    |
|---|----|
| △ | 1  |
| ○ | 2  |
| × | 3  |
| * | 4  |
| ⊕ | 5  |
| □ | 6  |
| ● | 7  |
| ⊙ | 4a |
| × | 5a |
| ✱ | 7a |



CONTAINMENT SECTION 1 - MERIDIONAL DIRECTION

LA SALLE COUNTY STATION  
 MARK II DESIGN ASSESSMENT REPORT

FIGURE 5.1-18  
 REPRESENTATIVE CONTAINMENT  
 INTERACTION DIAGRAM

## 5.2 CONTAINMENT WALL AND BASEMAT LINER ANALYSIS

### 5.2.1 Basemat Liner

#### 5.2.1.1 Description of Liner and Liner Stiffeners

The basemat liner plate consists of a 1/4-inch thick plate of Grade SA240 Type 304 stainless steel material. The basemat liner plates are anchored with M4 x 13 structural steel sections at a maximum spacing of 9 feet 3 inches. Refer to Figure 5.2-1 for the basemat liner anchorage details.

The basemat liner has been modified by adding stiffeners to provide additional capacity to resist the hydrodynamic uplift pressures resulting from SRV and LOCA loads. The stiffeners are made of 3/8 inch thick plates, Grade SA204 Type 304 stainless steel, folded into the shape of a channel with a 6-inch web and 3-3/4 inch flanges. Refer to Figure 5.2-2 for the basemat liner stiffener details.

#### 5.2.1.2 Loads for Analysis

The loads acting on the liner plate, described in Section 3.0 of this report, are included. These loads are divided into two main categories: (1) self-limiting loads; and, (2) mechanical loads (each of these is discussed in the following).

##### Self-Limiting Loads

Strains in the liner plate and anchorage system are introduced due to dead loads, post-tensioning, creep, shrinkage, and thermal effects.

## Mechanical Loads

These loads are introduced due to SRV and LOCA discharge within the suppression pool area. Due to the oscillating nature of the loads, the liner plate and anchorage system could experience stress reversals. For analysis it has been assumed that there are 3886 actuations (DFFR) with 10 stress reversals per actuations.

### 5.2.1.3 Load Combinations

The liner and anchorage systems are designed for the load combinations listed in Table 4.1-1 except that all load factors are taken as unity.

### 5.2.1.4 Acceptance Criteria

The strains in the liner plate due to self-limiting loads are limited to the allowable values specified in Table CC-3720 of the ASME Boiler and Pressure Vessel Code, Section III, Division 2, and the displacements of the liner anchorage are limited to the displacement values in Table CC-3730-1 of the ASME Boiler and Pressure Vessel Code, Section III, Division 2.

Primary membrane stresses due to mechanical loads in the liner plate and anchorage system (weld and anchor) is checked according to Subsection NE-3221.1 of the ASME B&PV Code, Section III, Division 1. Primary plus secondary membrane plus bending stress is checked according to Subsection NE-3222.2 of the same code, and fatigue strength evaluation is based on Subsection NE-3222.4 of Section III. Allowable design stress intensity values, design fatigue curves, and material properties are obtained from Subsection NA, Appendix I of the ASME B&PV Code, Section III, Division I.

Subsection NB-3356 of the ASME B&PV Code, Section III, Division I is used to obtain a fatigue strength reduction factor of 4.0 for the fillet weld attachment of the containment wall liner plate and anchorage system.

Capacity of the liner anchor for concrete pull out due to negative SRV loads is limited to the service load allowables in ACI 318-71.

#### 5.2.1.5 Analysis

The liner plate is analyzed for a postulated probable maximum, static equivalent, hydrodynamic net uplift pressure of 8 psi. Consequently, the liner plate has been modified by the addition of stiffeners to provide the required additional capacity. The analysis is divided into two phases: first, assessing the liner plate between the stiffeners to ensure that the plate has the capacity to transfer the loads to the stiffeners; and secondly, analyzing the stiffeners as beams of varying span numbers that are supported at the anchorages.

#### 5.2.2 Containment Wall Liner

##### 5.2.2.1 Description of Liner

The suppression chamber wall liner consists of a  $\frac{1}{4}$ -inch plate of Grade SA240 Type 304 stainless steel material. This liner plate is anchored at a maximum spacing of 1 foot 3 inches with 3 x 2 x  $\frac{1}{4}$  inch angles welded to the plate intermittently with a  $\frac{1}{4}$ -inch fillet weld at 4 inches every 12 inches center-to-center spacing. Refer to Figure 5.2-3 for the containment liner detail.

#### 5.2.2.2 Loads for Analysis

The loads for analysis are described in Subsection 5.2.1.2.

#### 5.2.2.3 Load Combinations

The load combinations are described in Subsection 5.2.1.3.

#### 5.2.2.4 Acceptance Criteria

The acceptance criteria for the containment wall liner is described in Subsection 5.2.1.4.

#### 5.2.2.5 Analysis

To study the response of the liner plate due to the oscillating SRV discharge loads, a dynamic finite element analysis is performed. Since the liner plate experiences bending between anchor supports predominantly in one direction, a two-dimensional representation is used for the dynamic analysis. Several beam elements are used to represent the flexibility of the liner plate between two anchor locations. The ends of the model which represent the anchor supports are assumed to be fixed against both in plane rotation and displacements. In addition, a nonlinear stiffness matrix is used to simulate the stiffness of the concrete to resist compressive loads only, with no resistance towards tensile or negative SRV discharge loads. The time-pressure history of the oscillating air bubble, which has approximately 10 negative pulses per actuation, is used as the input forcing function to the finite element model. The results of the dynamic analysis show that the dynamic load factor is approximately equal to 1.0. The liner plate can, therefore, be analyzed for SRV discharge loads by using a static solution procedure.

TABLE 5.2-1

SUMMARY OF CONTAINMENT WALL LINER PLATE  
STRESSES/STRAINS FOR ALL SRV CASES

I MECHANICAL LOADS  
(Suction Loads)

<u>STRESS CATEGORY</u>	<u>ACTUAL STRESS OR USAGE FACTOR</u>	<u>ALLOWABLE STRESS OR USAGE FACTOR</u>	<u>SAFETY MARGIN</u>
Primary ( $P_b$ ) Bending	8,400 psi	1.5 $S_m = 30$ ksi	3.6
Secondary (Q)	57,600 psi	3.0 $S_m = 60$ ksi	1.04
Peak (F)	0.04	1.0	25.0

II SELF-LIMITING LOADS

<u>STRAIN CATEGORY</u>	<u>ACTUAL STRAIN (in/in)</u>	<u>ALLOWABLE STRAIN (in/in)</u>	<u>SAFETY MARGIN</u>
Self-limiting	.001	.002	2.0

TABLE 5.2-2

SUMMARY OF CONTAINMENT WALL LINER ANCHORAGE  
LOAD/DISPLACEMENT FOR ALL SRV CASES

I MECHANICAL LOADS  
(Suction Loads)

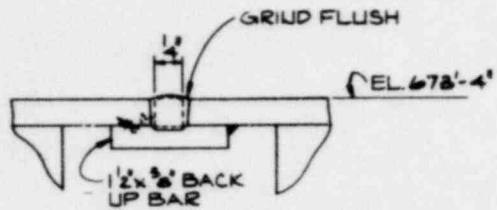
	<u>STRESS CATEGORY</u>	<u>ACTUAL STRESS OR USAGE FACTOR</u>	<u>ALLOWABLE STRESS OR USAGE FACTOR</u>	<u>SAFETY MARGIN</u>
Weld	Primary ( $P_b$ ) Bending	800 psi	$1/2 S_m =$ 10 ksi	12.5
	Peak (F)	0.04	1.0	25.0
Angle	Primary ( $P_b$ ) Bending	300 psi	$S_m = 13.9$ ksi	46.3

II MECHANICAL LOADS  
(Suction Loads)

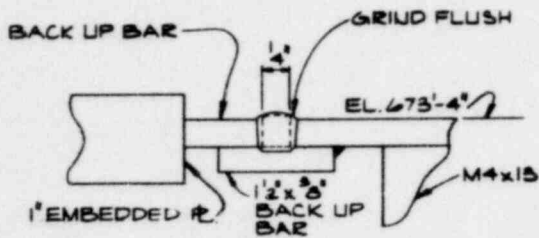
	<u>STRESS CATEGORY</u>	<u>ACTUAL LOAD OR STRESS</u>	<u>ALLOWABLE LOAD OR STRESS</u>	<u>SAFETY MARGIN</u>
Concrete	Diagonal Tension Failure	75.0 lbs/in	860.0 lbs/in	11.4

III SELF-LIMITING LOADS

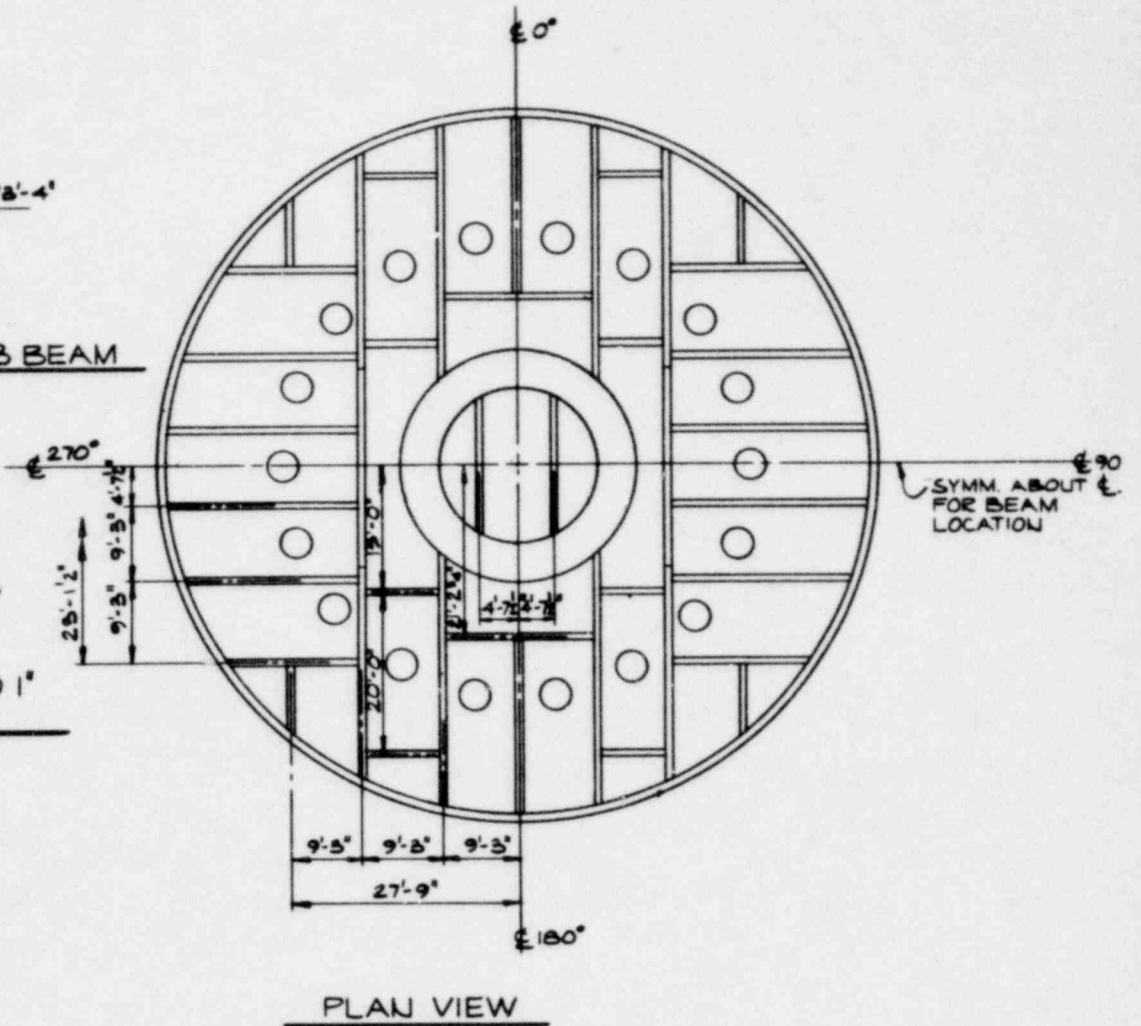
	<u>STRESS CATEGORY</u>	<u>ACTUAL DISPLACEMENT (in)</u>	<u>ALLOWABLE DISPLACEMENT (in)</u>	<u>SAFETY MARGIN</u>
	Anchorage System	.015	.045	3.0



TYPICAL CONNECTION FOR M4x13 BEAM



TYPICAL CONNECTION OF M4x13 TO 1" EMBEDDED PIPE

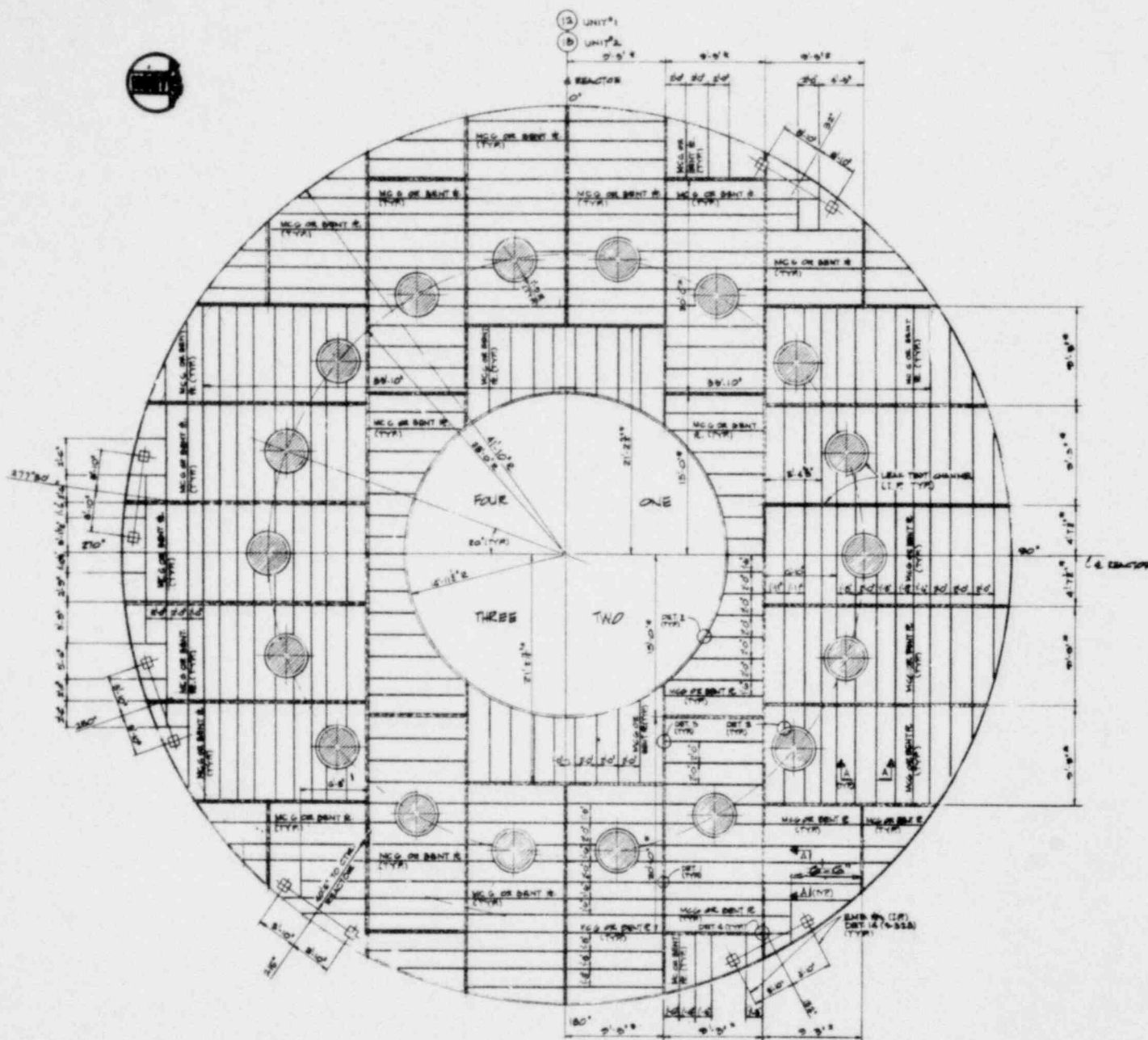


PLAN VIEW

LA SALLE COUNTY STATION  
MARK II DESIGN ASSESSMENT REPORT

FIGURE 5.2-1

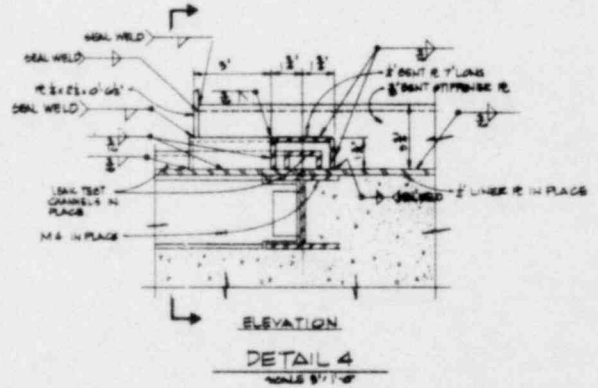
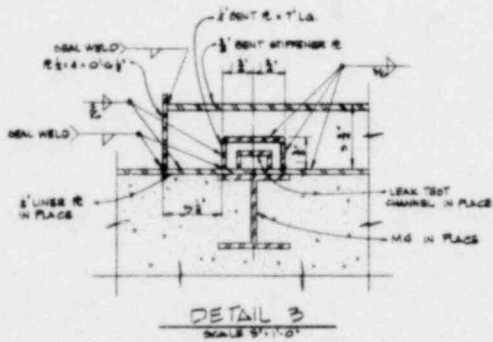
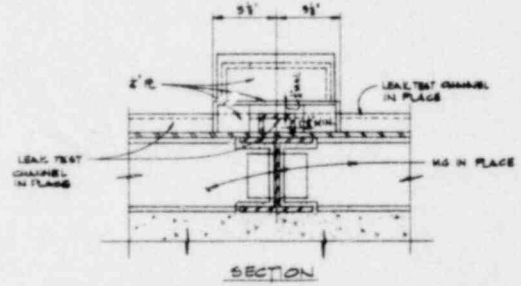
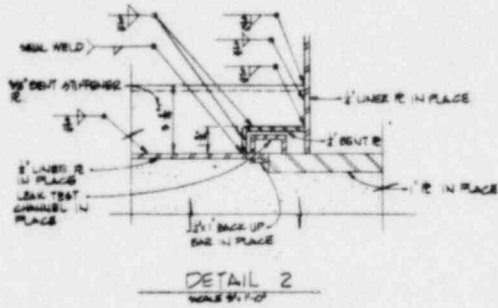
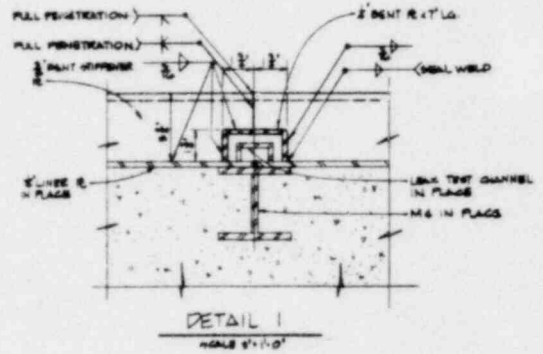
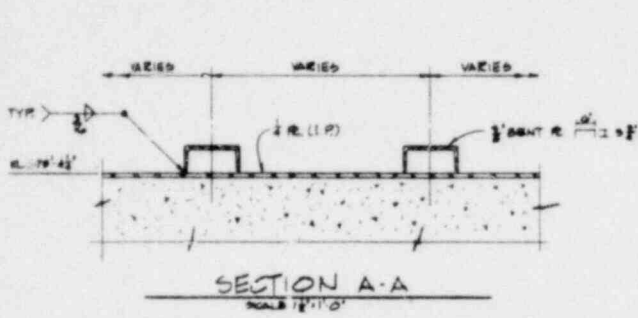
BASE MAT LINER DETAIL



SUPPRESSION POOL FLOOR LINER PLAN EL. 675' 4 1/2"  
(LINER APPROXIMATE TYP ALL 4 QUADRANTS U.N.)

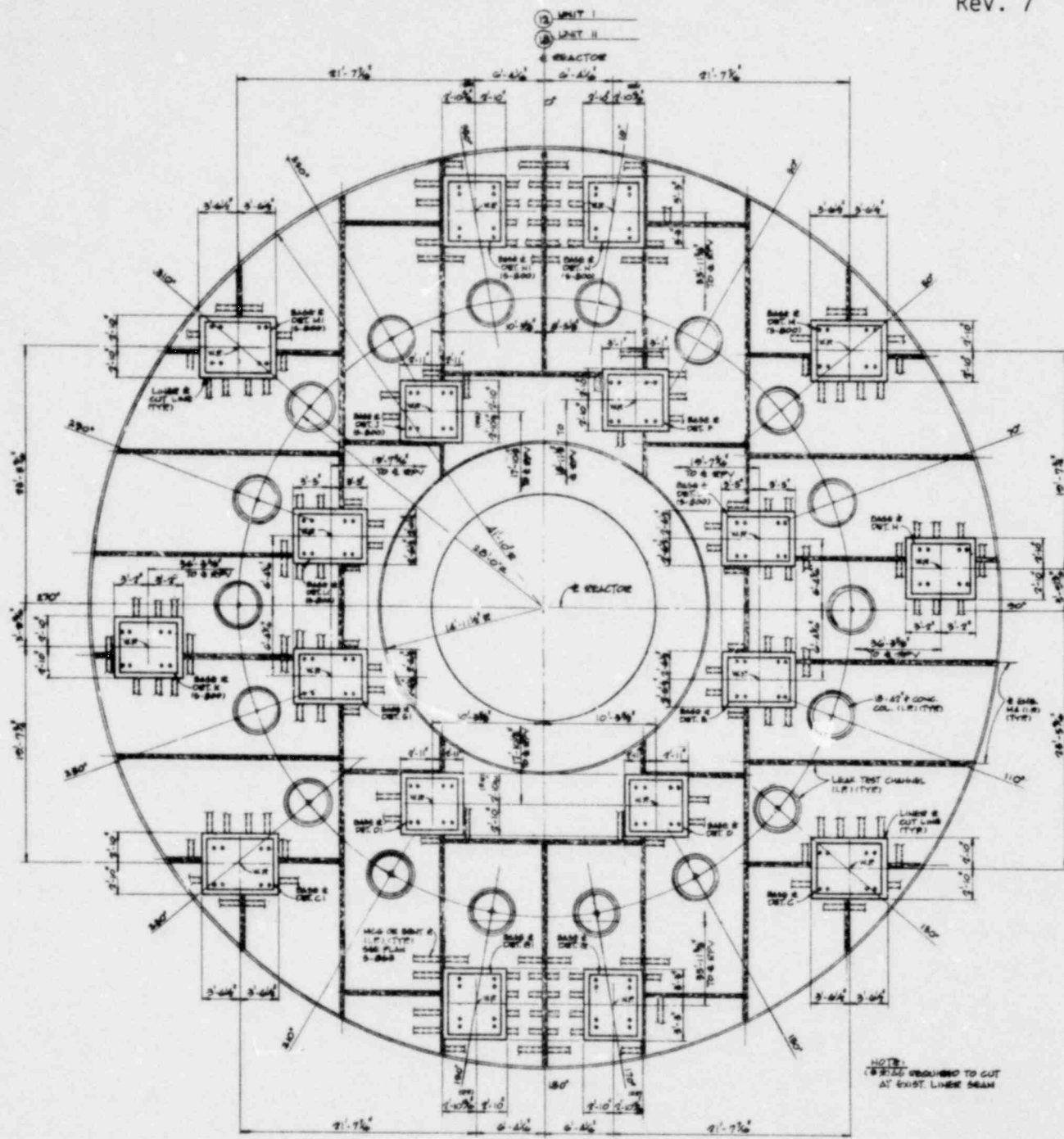
LA SALLE COUNTY STATION  
MARK II DESIGN ASSESSMENT REPORT

FIGURE 5.2-2  
BASE MAT LINER STIFFENER DETAIL  
(SHEET 1 of 4)



LA SALLE COUNTY STATION  
 MARK II DESIGN ASSESSMENT REPORT

FIGURE 5.2-2  
 BASE MAT LINER STIFFENER DETAIL  
 (SHEET 2 of 4)

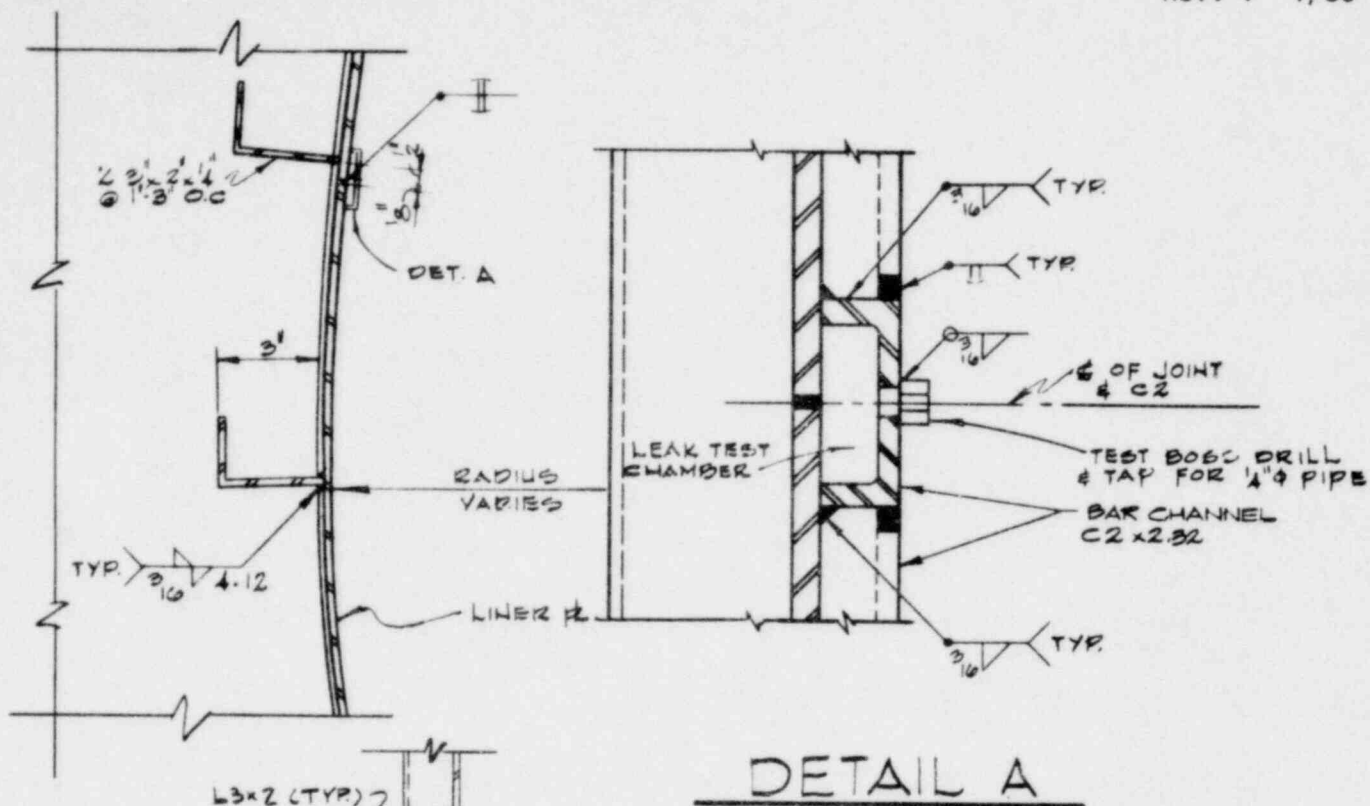


KWU QUENCHER BASE PLATE INSTALLATION PLAN  
TOP OF 1/2\"/>

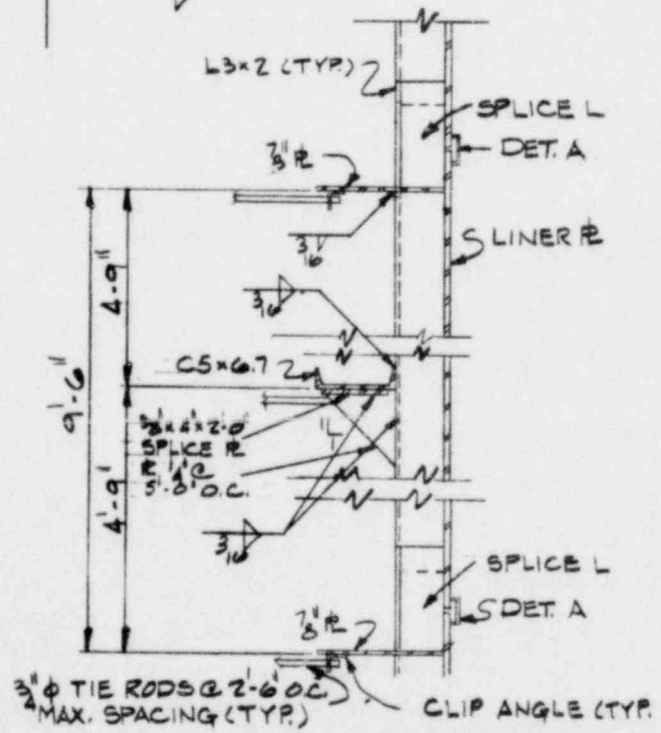
LA SALLE COUNTY STATION  
MARK II DESIGN ASSESSMENT REPORT

FIGURE 5.2-2  
BASE MAT LINER STIFFENER DETAIL  
(SHEET 3 of 4)





DETAIL A



TYP. ARR'T. OF HORIZ. & VERT. STIFF.  
IN THE CYLINDRICAL SECT. OF THE CONTAINMENT

<p>LA SALLE COUNTY STATION MARK II DESIGN ASSESSMENT REPORT</p>
<p>FIGURE 5.2-3 CONTAINMENT WALL LINER DETAIL</p>

### 5.3 OTHER STRUCTURAL COMPONENTS

#### 5.3.1 Concrete Structures

The load combinations including pool dynamic loads considered in the reassessment of concrete structures (other than containment and concrete structures) such as shear walls, slabs, and beams are shown in Table 5.3-1.

For concrete structures, the peak effects resulting from seismic and pool dynamic loads were combined by the conservative ABS method even though the SRSS method is more appropriate since the probability of all peak effects occurring at the same time is very small. The concrete members were found to be structurally adequate to sustain the ABS loads. No field modifications are required for these concrete elements.

##### 5.3.1.1 Acceptance Criteria

The acceptance criteria used in the reassessment of reinforced concrete structures other than containment and internal concrete structures are the same criteria defined in Subsection 3.8.4.5 of the LSCS FSAR and are identified in Table 5.3-1 for each load combination. The stresses and strains are limited to those specified in ACI 318-71. As indicated in Table 5.3-1, ultimate strength design method has been used for all load combinations. No overstress is allowed for seismic loads. As stated in the FSAR, when a LOCA occurs outside the containment, as in load combinations 4, 4a, 5, 7, and 7a, yield line theory is used to design reinforced concrete walls and slabs.

Table 5.3-3 gives a summary of the capability of the "other" concrete and steel structures affected by the additional pool dynamic loads. The table reflects the status of the reassessment to date. (See Appendix D for details of the assessment.)

The percentages given in the table represent the portion of the structural elements which have the reserve strength to sustain the SRSS/ABS loading.

### 5.3.2 Steel Structures

The load combinations including pool dynamic loads considered in the reassessment of steel structures such as framing, containment galleries, embedments, hangers for cable trays, conduits, and ducts are listed in Table 5.3-2.

For cable tray, conduit and HVAC duct hangers, the peak effects resulting from seismic and pool dynamic loads were combined by the SRSS method. Structural steel framings in the drywell and in the reactor building and their corresponding embedments had the peak effects of the seismic and pool dynamic loads combined by the absolute sum method, and the stiffening of structural elements for such a combination is in progress.

#### 5.3.2.1 Acceptance Criteria

For steel structures, stresses, and strains in accordance with the 1969 AISC specifications are used for load combinations 1 through 3 defined in Table 5.3-2. No overstress is allowed for seismic loads. For load combinations involving abnormal or extreme environmental loads as in load combinations 4 through 7a of Table 5.3-2, the steel stresses were conservatively limited to  $0.95 f_y$ . No plastic deformations were allowed.

### 5.3.3 Downcomers and Downcomer Vent Bracing

The downcomer vents are subjected to static and dynamic loads due to normal, upset, emergency, and faulted plant conditions. The downcomer vents are braced at elevation 721'-0", well above the pool swell impact zone to reduce the forces and moments being transmitted through the downcomers to the

drywell floor. Additional bracing is provided at elevation 697'-1" to support the downcomers against bounding submerged structure loads defined in Section 3.0.

#### 5.3.3.1 General Description

General features of the downcomers are as follows:

- a. 98 downcomers per unit,
- b. pipe outside diameter - 24.25 inches,
- c. pipe wall thickness - 00.375 inch,
- d. pipe weight per unit length - 7.883 lb/in., and
- e. pipe material - SA-240 TP 304.

The downcomer vent bracing at elevation 721'-0" is shown in Figure 5.3-1. General features of this bracing are as follows:

- a. The bracing plate girders are composed of 5/8 inch thick webs 2 feet deep, and 3/4 inch thick flanges 14-1/2 inches wide.
- b. Connection of the bracing to the downcomers is accomplished through a stiffened ring welded to the downcomer. The ring assures that transfer of forces between converging bracing members while preserving the integrity of the downcomer vent. The ring is constructed with a 5/8-inch thick web 2 feet deep, and 3/4 inch thick flanges 7 inches wide whose cross-sectional shape is that of a channel.
- c. A-572 Grade 50 steel is used in the bracing system.

The downcomer vent bracing at elevation 697'-1" is shown in Figure 5.3-2. General features of this bracing are as follows:

- a. The bracing members are composed of 8" diameter double extra strong pipes. This shape has been chosen to minimize drag loads on the bracing system.
- b. Two outer rows of the downcomers have been braced together and their bracing system is anchored into the containment wall. Similarly, two inner rows of downcomers are braced together with the bracing system anchored into the reactor support.
- c. To provide anchorage for the bracing system embedment plates with pretensioned bolts have been provided on the containment wall and the pedestal.
- d. The bracings members are rigidly connected to the downcomers through a collar, whereas a pinned connection is provided at the junction of bracing members and the embedment plates on this containment wall and pedestal.
- e. Bracing members are composed of A618 Grade II seamless pipes, whereas embedment plates are of A588 Lukens Fineline material.

#### 5.3.3.2 Loads for Analysis

The loads affecting the downcomers and downcomer bracing are identified in the following. The loads are described in detail in Section 3.0.

##### Load Description

##### a. Dead Weight

This is the static force acting vertically down due to the weight of the downcomer.

b. Pressure Load

The pressure differential between the drywell atmosphere and wetwell atmosphere produces loads on the downcomer walls as it acts as a pressure retaining boundary during a loss-of-coolant accident.

c. Operating Basis Earthquake (OBE)

The downcomer experiences dynamic loads due to its response to the base excitation produced in the drywell floor and bracing anchorage locations on the containment wall and the pedestal.

The OBE also causes water oscillations inside the suppression pool. The drag and inertia forces of these oscillations will produce a dynamic loading on the submerged position of the downcomer.

d. Safe Shutdown Earthquake (SSE)

The SSE causes dynamic loading of the downcomer due to the excitation it produces in the drywell floor and bracing anchorage locations on the containment wall and pedestal.

The SSE accelerations also create water oscillations inside the suppression pool. The drag and inertia forces of these oscillations produce dynamic loading of the downcomer.

e. LOCA Loads

1. At high mass flow rates, viscous and pressure forces will act on the downcomer walls.
2. At low mass flow rates, random movement of the steam/water interface at the vent exit

causes intermittent lateral impingement of the suppression pool water on the vents which results in a random lateral load on the downcomers as discussed in Section 3.3.

3. The downcomer drywell floor anchor points experience acceleration loadings in the vertical and horizontal directions due to LOCA loads on the suppression pool boundary.

f. SRV Discharge Dynamic Loads

The air discharge from the SRV vent line forms high-pressure bubbles which expand and contract periodically until they rise to the pool surface. The downcomers were analyzed for the time varying forces produced by the SRV bubble oscillations on the submerged surface of the downcomers.

The time varying forcing function produced by the SRV bubble oscillations on the submerged surfaces of the wetwell walls create dynamic loading on the downcomers due to the excitation it produces in the drywell floor and bracing anchorage locations on the containment wall and pedestal.

g. Thermal Transient Loads

The temperature variations with respect to time, between the interior and exterior of the downcomer, produce thermal gradient stresses through the downcomer walls.

5.3.3.3 Design Load Combinations

The loads identified in Subsection 5.3.3.1 are combined in Table 4.1-1, when applicable, with the load factors set to unity.

#### 5.3.3.4 Acceptance Criteria

##### Downcomer Vents

The stresses within the downcomer are considered acceptable if they satisfy the ASME Boiler and Pressure Vessel Code, Section III, Subsection NE. As permitted by Subsection NE-1120 for MC components the downcomers were analyzed using Subsection NB-3650 of Section III, however, the lower allowable stresses ( $S_m$ ) from Table I-10.2 for MC components were used when performing the analysis.

The allowable stress,  $S_m$ , for the downcomer material is 21177 psi. This was obtained from the tabulated value in Section III for  $S_m$  at the design temperature of 340° F multiplied by a factor of 1.17. This factor was obtained from the ratio of the minimum yield stress obtained from test results on the downcomer material to the values tabulated in Section III.

##### Stress Intensity Limits

The primary stress intensity includes the primary membrane stresses plus the primary bending stresses depend upon the downcomer loading conditions as follows:

- a. The limit of stresses under upset condition is  $1.5 S_m$ .
- b. The limit of stresses under emergency condition is  $2.25 S_m$ .
- c. The limit of stresses under faulted condition is  $2.25 S_m$ .

### Downcomer Bracing

The allowable stresses for the downcomer bracing are:

- a. The AISC allowables, for load combinations 1, 2, and 3 of Table 4.1-1.
- b. 1.6 times AISC allowables, but no greater than  $0.95 f_y$ , for load combinations 4, 4A, 5, 5A, 6, 7 and 7A (Reference 2).

Welding of the bracing to the downcomer is designed to satisfy the ASME B&PV Code, Section III, Subsection NF (Reference 1).

#### 5.3.3.5 Analysis

The downcomer vents and bracing have been analyzed for the loads described in Subsection 5.3.3.2 with PIPSYS computer program. See Appendix A for a description of PIPSYS.

The structural components of the bracing system and the downcomers are modeled as beam elements. The intersection of the downcomer vents and the drywell floor are modeled as rigidly fixed. The lower tip of the downcomers are modeled as free. The intersections of the bracing system and the containment wall are modeled as pinned, and the intersections of the bracing and the pedestal are modeled as pinned in the vertical direction and fixed in the horizontal direction. These boundary conditions reflect the structural connections provided between the bracing and the containment wall and between the bracing and the pedestal. The detailed models used for the analyses are shown in Figures 5.3-3 and 5.3-4.

The inertia effect of the water surrounding the submerged portion of the downcomer (12 feet) was approximated by the addition of a water mass (Reference 2) equivalent to a column

of water 12 feet long and 24.25 inches in diameter (the outside diameter of the downcomer) to this portion in the model. The mass of water inside the submerged portion of the downcomer is also considered in the model, and is used for all dynamic loads input through the drywell floor (building response loads). The effects of fluid damping were conservatively neglected. For the dynamically defined submerged structure loads, the inside water mass is either considered or neglected in order that the bounding maximum responses can be obtained.

The analyses were performed for each load independently using the structural model described above. Then the maximum responses from each load were combined with the ABS method for bracing and SRSS method for downcomers, using the appropriate load combinations described in Subsection 5.3.3.3.

#### 5.3.4 References

1. ASME Boiler and Pressure Vessel Code, Section III, Subsection NF, 1977 edition, including the Winter 1977 Addenda.
2. Sir Horce Lamb, "Hydrodynamics," Sixth Edition, Dover Press, New York, 1945.

TABLE U.3-1

LOCA AND  
SRV DESIGN LOAD COMBINATIONS  
REINFORCED CONCRETE STRUCTURES OTHER THAN CONTAINMENT

<u>EQN</u>	<u>LOAD COND</u>	<u>D</u>	<u>L*</u>	<u>F</u>	<u>P<sub>O</sub></u>	<u>T<sub>O</sub></u>	<u>R<sub>O</sub></u>	<u>E<sub>O</sub></u>	<u>E<sub>SS</sub></u>	<u>P<sub>B</sub></u>	<u>P<sub>A</sub></u>	<u>T<sub>A</sub></u>	<u>R<sub>A</sub></u>	<u>R<sub>R</sub></u>	<u>SRV**</u>	<u>ADS</u>	<u>ALL</u>	<u>ASYM-MET-RICAL</u>	<u>SINGLE</u>	<u>DESIGN STRENGTH</u>
1	Normal w/o Temp	1.4	1.7	1.0	1.0	-	-	-	-	-	-	-	-	-	1.5	0	X	X		ACI 318-71
2	Normal w/Temp	1.0	1.3	1.0	1.0	1.0	1.0	-	-	-	-	-	-	-	1.2	0	X	X		ACI 318-71
3	Normal Sev. Env.	1.0	1.0	1.0	1.0	1.0	1.0	1.25	-	-	-	-	-	-	1.25	0	X	X		ACI 318-71
4	Abnormal	1.0	1.0	1.0	-	-	-	-	-	1.25	-	1.0	1.0	-	1.25	X	0	X		Yield Limit
4a		1.0	1.0	1.0	-	-	-	-	-	-	1.25	1.0	1.0	-	1.0	0	0	0	X	
5	Abnormal Sev. Env.	1.0	1.0	1.0	-	-	-	1.1	-	1.1	-	1.0	1.0	-	1.1	X	0	X		Yield Limit
5a		1.0	1.0	1.0	-	-	-	1.1	-	-	1.1	1.0	1.0	-	1.0	0	0	0	X	
6	Normal Ext. Env.	1.0	1.0	1.0	1.0	1.0	1.0	-	1.0	-	-	-	-	-	1.0	0	X	X		ACI 318-71
7	Abnormal Ext. Env.	1.0	1.0	1.0	-	-	-	-	1.0	1.0	-	1.0	1.0	1.0	1.0	X	0	X		Yield Limit
7a		1.0	1.0	1.0	-	-	-	-	1.0	-	1.0	1.0	1.0	1.0	1.0	0	0	0	X	

LOAD DESCRIPTION

- |  |   |
|--|---|
| D = Dead Loads   | E <sub>SS</sub> = Safe Shutdown Earthquake                  |
| L = Live Loads   | P <sub>B</sub> = SBA and IBA Pressure Load                  |
| F = Prestressing Loads                                       | T <sub>A</sub> = Pipe Break Temperature Load                |
| P <sub>O</sub> = Normal Operating Pressure Differential Load | R <sub>A</sub> = Pipe Break Temperature Reactions Loads     |
| T <sub>O</sub> = Operating Temperature Loads                 | P <sub>A</sub> = DBA LOCA Pressure Loads                    |
| R <sub>O</sub> = Operating Pipe Reactions                    | R <sub>R</sub> = Reactions and Jet Forces Due to Pipe Break |
| P <sub>V</sub> = Operating Pressure Loads                    | * = Varies in Magnitude and Intensity                       |
| SRV = Safety/Relief Valve Loads                              | ** = Only One SRV Load should be Combined at One Time       |
| E <sub>O</sub> = Operating Basis Earthquake                  |   |

TABLE 5.3-2

LOCA AND  
SRV DESIGN LOAD COMBINATIONS  
STRUCTURAL STEEL ELASTIC DESIGN

EQN	LOAD COND	D	L*	F	P <sub>O</sub>	T <sub>O</sub>	R <sub>O</sub>	E <sub>O</sub>	E <sub>SS</sub>	P <sub>B</sub>	P <sub>A</sub>	T <sub>A</sub>	R <sub>A</sub>	R <sub>R</sub>	SRV**	ADS	ALL	ASYM-MET-RICAL	SINGLE	DESIGN STRESS
1	Normal w/o Temp	1.0	1.0	1.0	1.0	-	-	-	-	-	-	-	-	-	1.0	0	X	X		AISC Allowable
2	Normal w/Temp	1.0	1.0	1.0	1.0	1.0	1.0	-	-	-	-	-	-	-	1.0	0	X	X		AISC Allowable
3	Normal Sev. Env.	1.0	1.0	-	1.0	1.0	1.0	1.0	-	-	-	-	-	-	1.0	0	X	X		AISC Allowable
4	Abnormal	1.0	1.0	1.0	-	-	-	-	-	1.0	-	1.0	1.0	-	1.0	X	0	X		1.0 AISC Allowable
4a		1.0	1.0	1.0	-	-	-	-	-	-	1.0	1.0	1.0	-	1.0	0	0	0	X	≤ .95 Fy
5	Abnormal Sev. Env.	1.0	1.0	-	-	-	-	1.0	-	1.0	-	1.0	1.0	-	1.0	X	0	X		1.6 AISC Allowable
5a		1.0	1.0	-	-	-	-	1.0	-	-	1.0	1.0	1.0	-	1.0	0	0	0	X	≤ .95 Fy
6	Normal Ext. Env.	1.0	1.0	-	1.0	1.0	1.0	-	1.0	-	-	-	-	-	1.0	0	X	X		1.6 AISC Allowable
7	Abnormal Ext. Env.	1.0	1.0	-	-	-	-	-	1.0	1.0	-	1.0	1.0	1.0	1.0	X	0	X		1.6 AISC Allowable
7a		1.0	1.0	-	-	-	-	-	1.0	-	1.0	1.0	1.0	1.0	1.0	0	0	0	X	≤ .95 Fy

LOAD DESCRIPTION

- |   |   |
|---|---|
| D = Dead Loads  | E <sub>SS</sub> = Safe Shutdown Earthquake                  |
| L = Live Loads  | P <sub>B</sub> = SBA and IBA Pressure Load                  |
| S = Stability Loads                                   | T <sub>A</sub> = Pipe Break Temperature Load                |
| P <sub>O</sub> = Operating Pressure Differential Load | R <sub>A</sub> = Pipe Break Temperature Reactions Loads     |
| R <sub>O</sub> = Operating Pipe Reactions             | P <sub>A</sub> = DBA LOCA Pressure Loads                    |
| P <sub>V</sub> = Operating Pressure Loads             | R <sub>R</sub> = Reactions and Jet Forces Due to Pipe Break |
| SRV = Safety/Relief Valve Loads                       | ** = Only One SRV Should be Combined at One Time            |
| E <sub>O</sub> = Operating Basis Earthquake           |   |
| * = Varies in Magnitude and Intensity                 |   |

NOTE: In loading Combinations 2 and 3, the design stress is 1.5 AISC Allowable when T<sub>O</sub> is considered.

TABLE 5.3-3

CAPABILITY OF CONCRETE (OTHER THAN CONTAINMENT) AND STEEL STRUCTURES

<u>STRUCTURAL ELEMENT</u>	<u>CAPABILITY FOR</u>	
	<u>SRSS*</u>	<u>ABSOLUTE SUM</u>
Gallery Steel Beams	100%	100%
Gallery Steel Pedestals	100%	100%
Embed. Pl's	100%	100%
Cable Tray Hangers	100%	50%
Conduit Hangers	100%	100%
HVAC Hangers	100%	100%
Concrete Slabs and Beams	100%	100%
Shear Walls	100%	100%

\*The structural elements have been shown to be 100% capable of taking seismic and pool hydrodynamic loads if combined by the SRSS method. This percentage, however, does not reflect the effects of annulus pressurization on the hangers attached to the containment galleries. A majority of these hangers have been found to be overstressed for SRSS combination of annulus pressurization inertia loads with SSE and are being stiffened for the combination. When these hangers are stiffened, they will be designed for all the loads and load combinations given in Table 5.3-2.

Rev. 7/1/80  
DRYWELL FLOOR  
EL. 736'-7 1/2"

BRACING  
EL. 721'-0"

TOTAL SWELL  
EL. 717'-10"

1.5H = 18'-0"

INITIAL  
POOL  
EL. 699'-10"

H = 12'-0"

VENT EXIT  
EL. 687'-10"

CONTAINMENT

BASE MAT  
EL. 673'-4"

PEDESTAL

DOWNCOMER  
VENTS

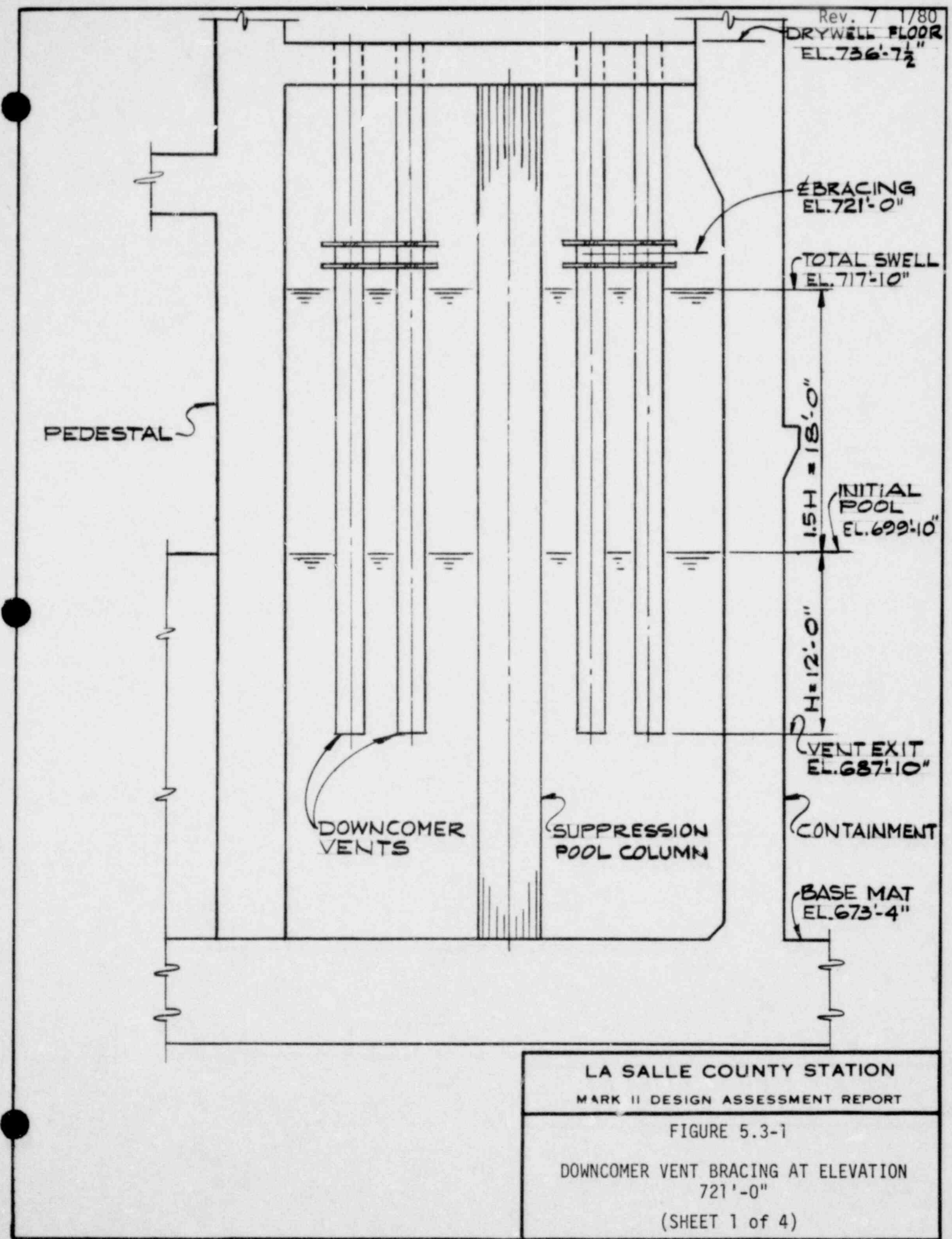
SUPPRESSION  
POOL COLUMN

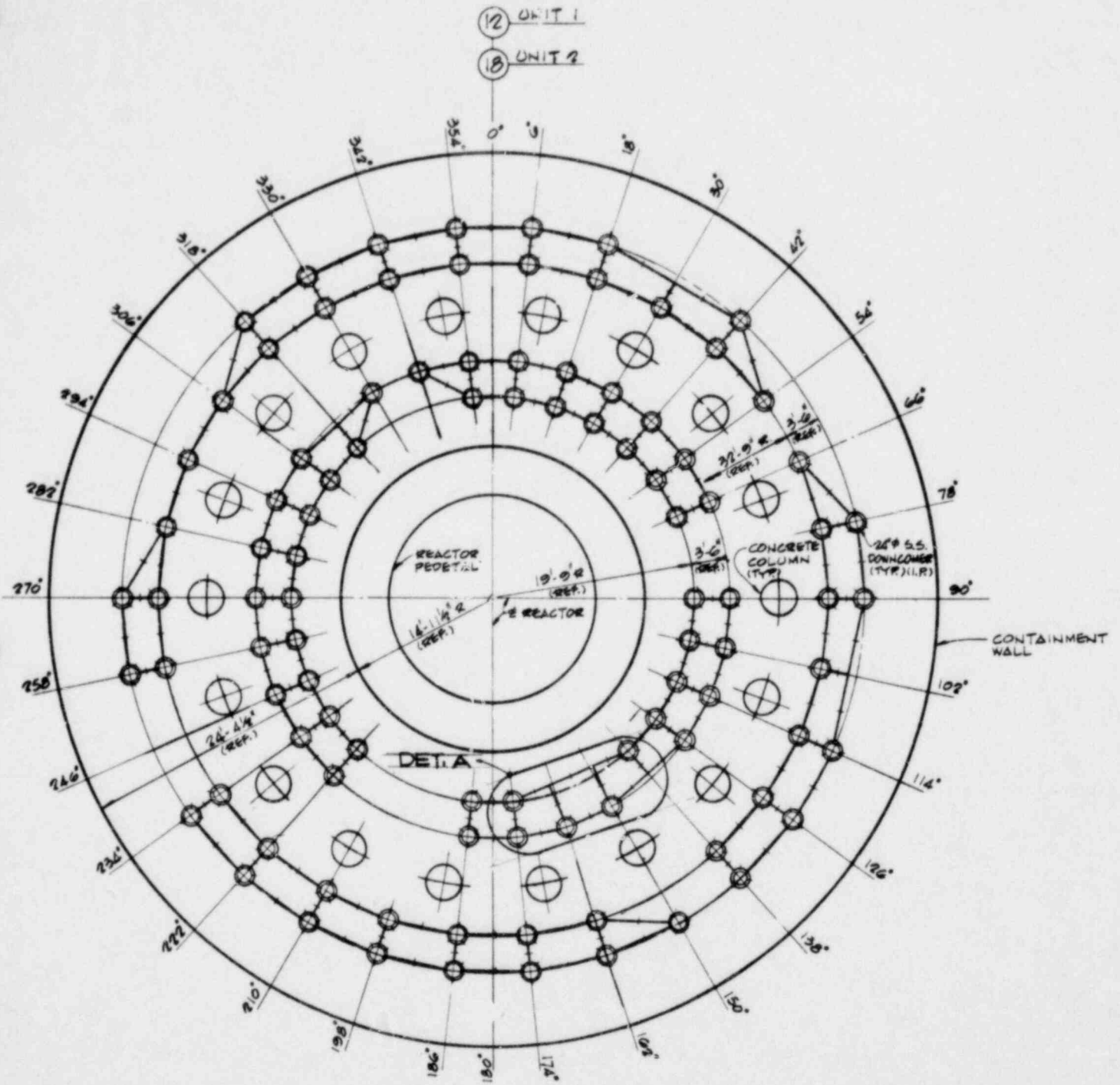
LA SALLE COUNTY STATION  
MARK II DESIGN ASSESSMENT REPORT

FIGURE 5.3-1

DOWNCOMER VENT BRACING AT ELEVATION  
721'-0"

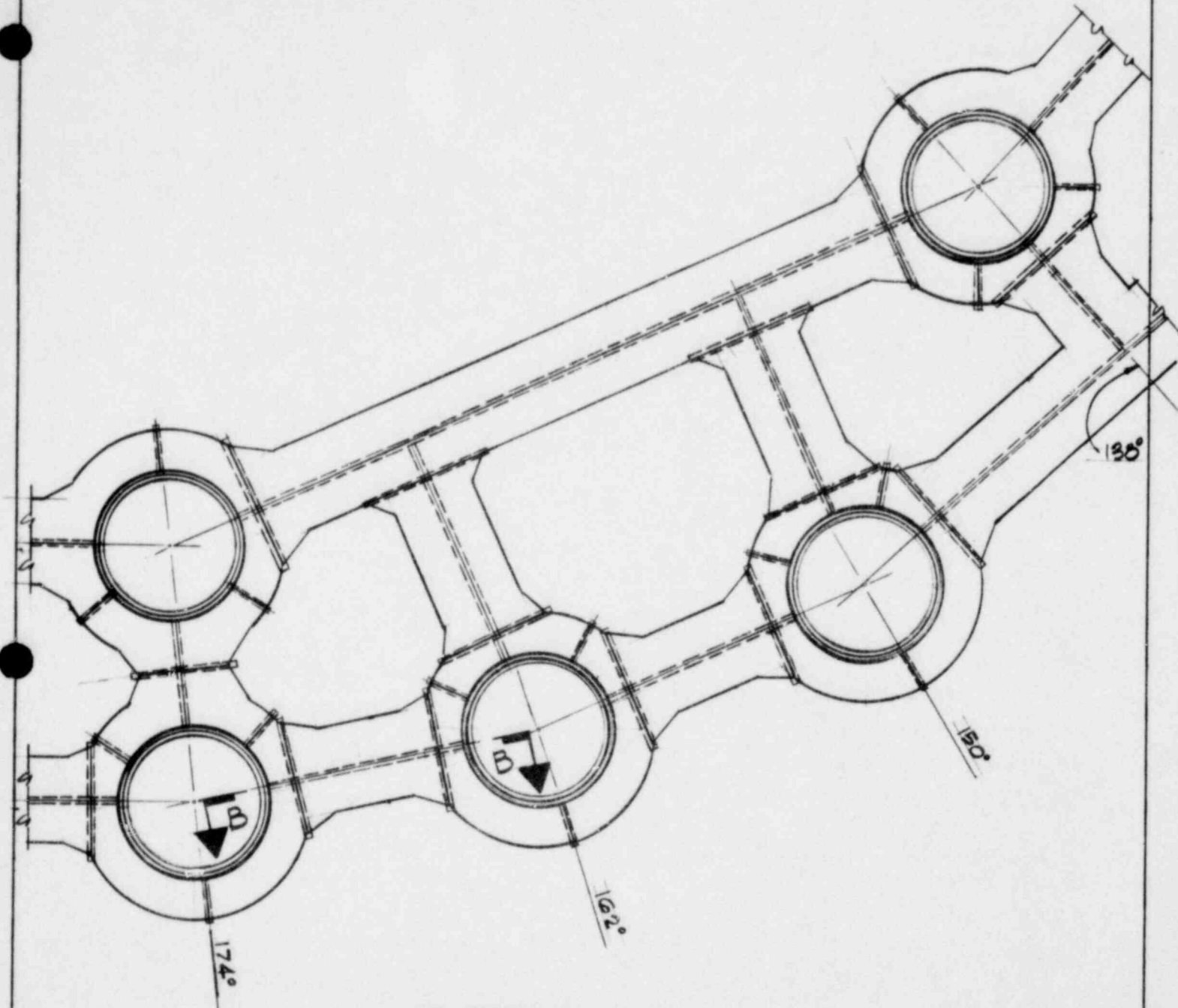
(SHEET 1 of 4)





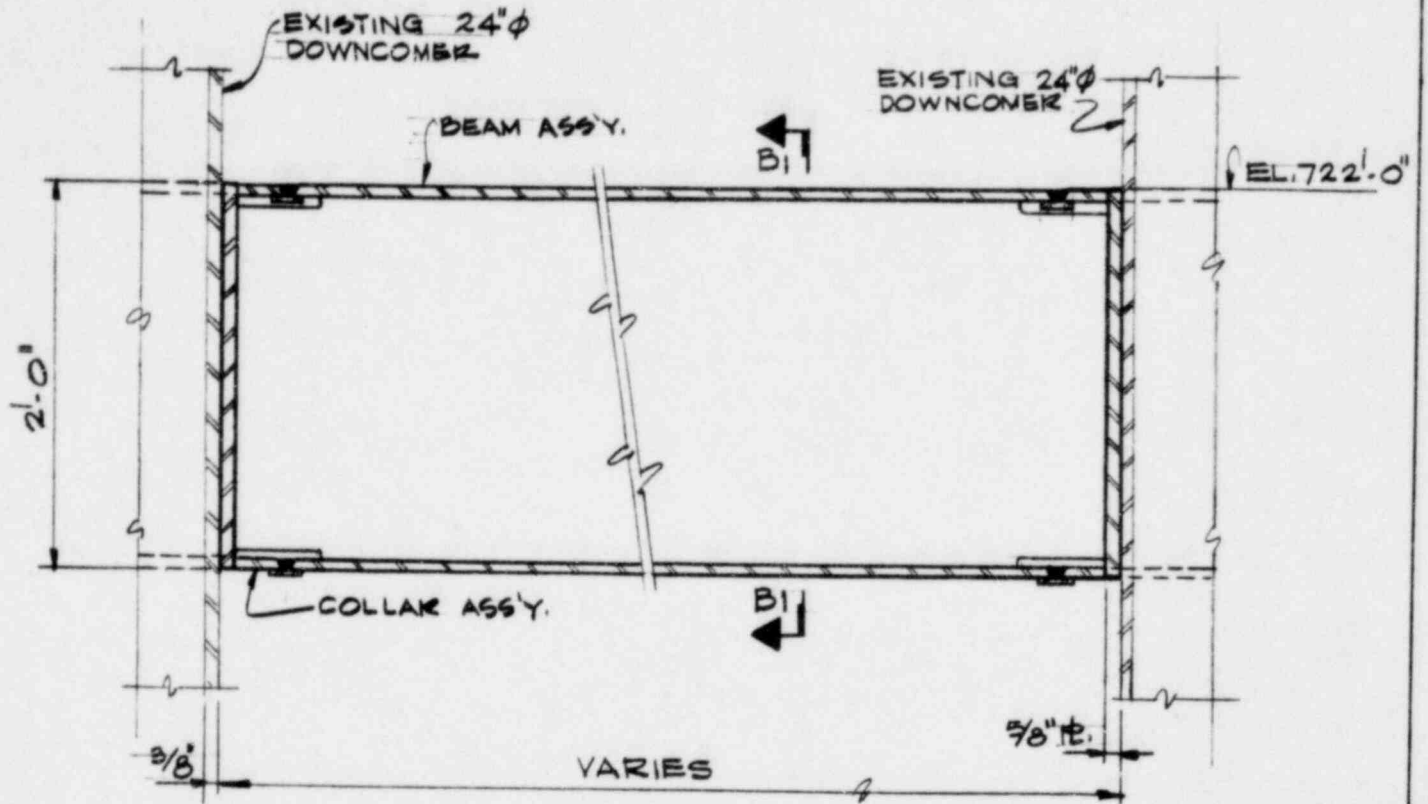
PLAN

<p>LA SALLE COUNTY STATION MARK II DESIGN ASSESSMENT REPORT</p>
<p>FIGURE 5.3-1 DOWNCOMER VENT BRACING AT ELEVATION 721'-0" (SHEET 2 of 4)</p>

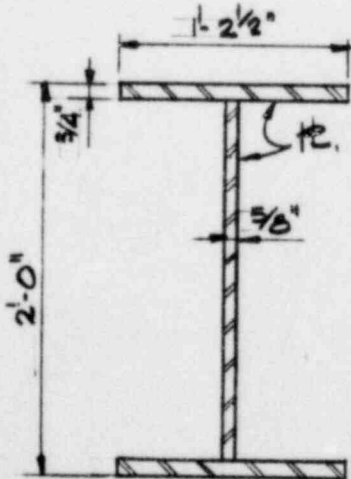


DETAIL A

<p>LA SALLE COUNTY STATION MARK II DESIGN ASSESSMENT REPORT</p>
<p>FIGURE 5.3-1 DOWNCOMER VENT BRACING AT ELEVATION 721'-0" (SHEET 3 of 4)</p>



SECTION B-B

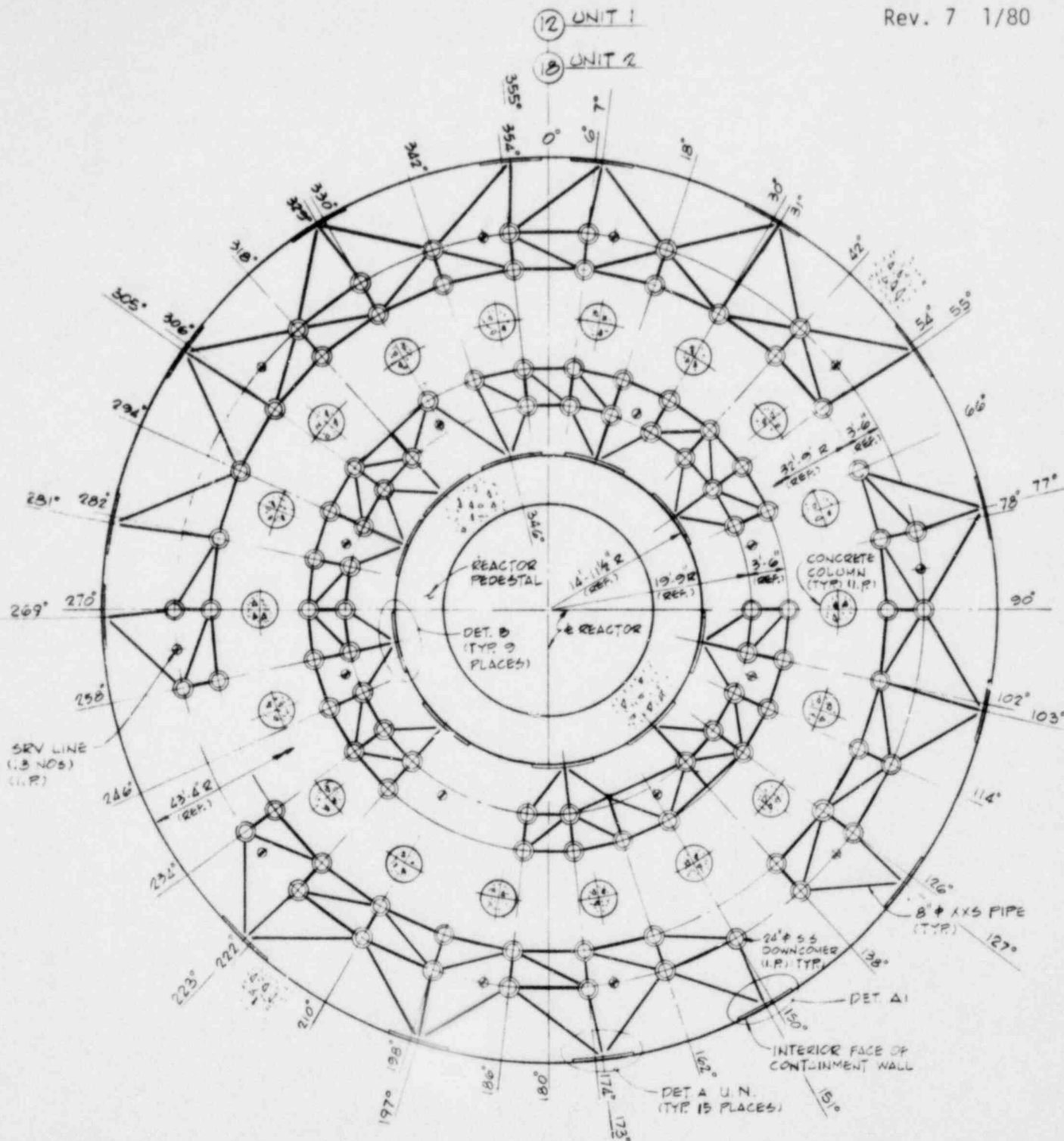


SECTION B1-B1

LA SALLE COUNTY STATION  
MARK II DESIGN ASSESSMENT REPORT

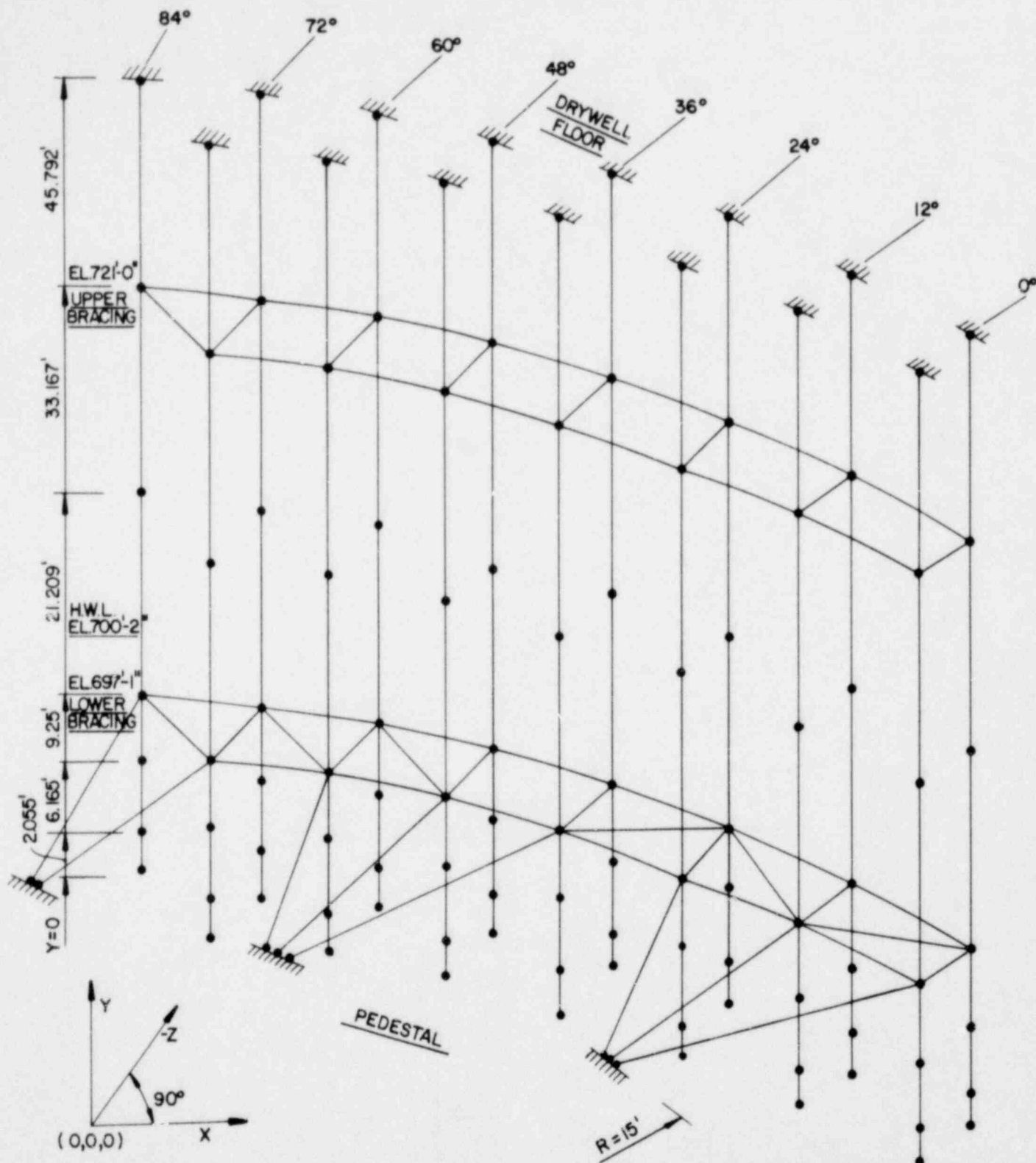
FIGURE 5.3-1  
DOWNCOMER VENT BRACING AT ELEVATION  
721'-0"

(SHEET 4 of 4)



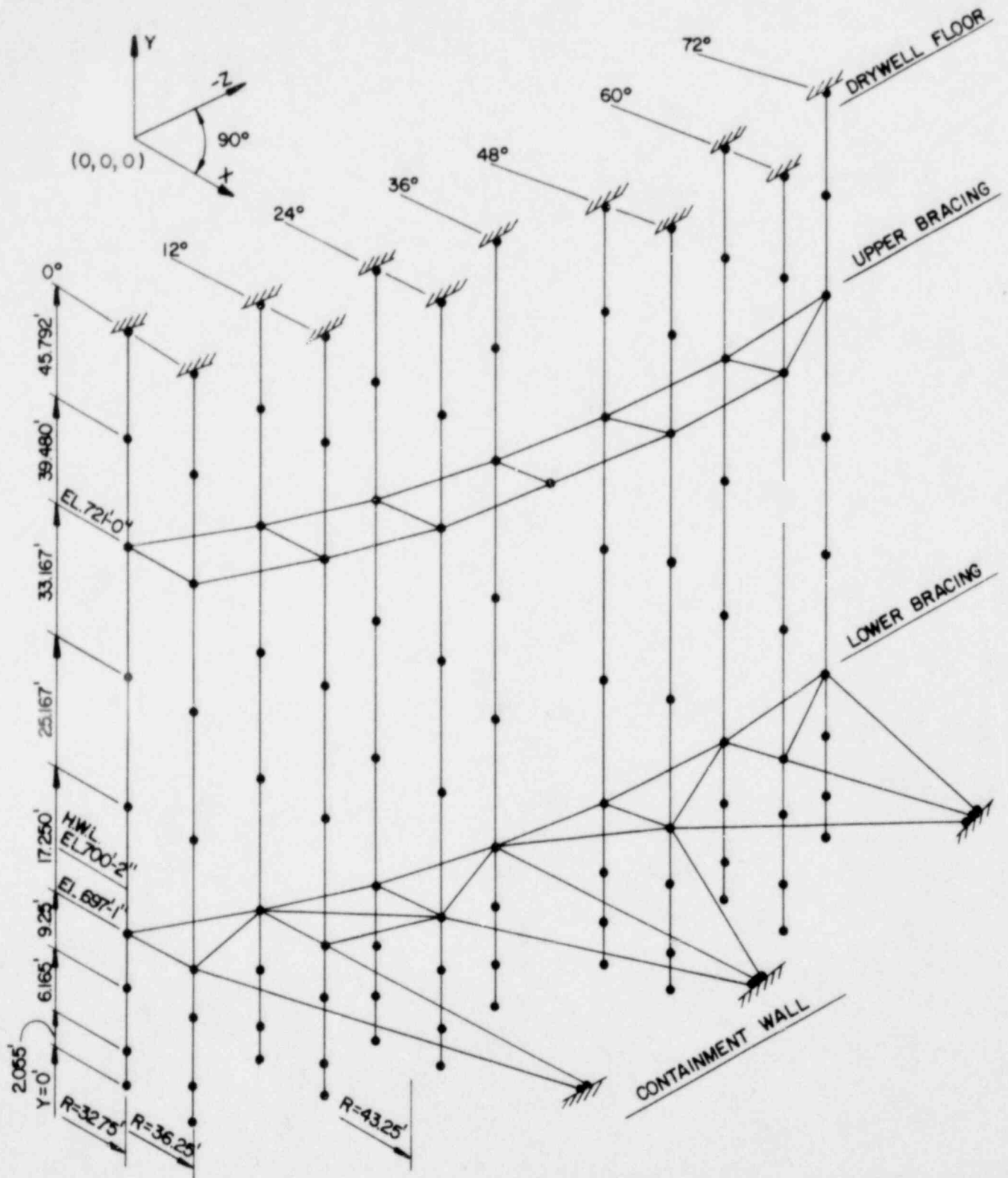
PLAN  
SCALE: 1/8" = 1'-0"

<p>LA SALLE COUNTY STATION MARK II DESIGN ASSESSMENT REPORT</p>
<p>FIGURE 5.3-2 DOWNCOMER VENT BRACING AT ELEVATION 697'-0"</p>



LA SALLE COUNTY STATION  
MARK II DESIGN ASSESSMENT REPORT

FIGURE 5.3-3  
PARTIAL DOWNCOMER BRACING MODEL  
INNER RINGS 1 AND 2



LA SALLE COUNTY STATION  
MARK II DESIGN ASSESSMENT REPORT

FIGURE 5.3-4  
PARTIAL DOWNCOMER BRACING MODEL  
OUTER RINGS 3 AND 4

#### 5.4 BOP PIPING ANALYSIS

Piping was analyzed to the bounding load combinations using the rams head load definition as described in Section 4.4. Results of these analyses are shown in Tables 3.9-34 through 3.9-36 of the LSCS FSAR.

## 5.5 EQUIPMENT (BOP)

### 5.5.1 Reevaluation and Design Assessment Methods

#### 5.5.1.1 Analysis

##### 5.5.1.1.1 Static Analysis

Static analysis was used to seismically qualify rigid equipment (i.e., equipment with fundamental natural frequency  $FNF \geq 33$  Hz). These types of equipment were assessed and reevaluated using the following method.

The peak acceleration value in the frequency range of 33 to 100 Hz from the new loading combination response spectrum curve (RSC) mentioned in Subsection 4.4.3 were determined. Then they were compared to the acceleration value (ZPA) used in the original equipment seismic qualification analysis.

If the new acceleration value is less than or equal to the original ZPA, the equipment is qualified for the new loading combinations and no additional analysis is needed.

If the new acceleration values exceed the original ZPA, the analysis is repeated using the new acceleration values.

##### 5.5.1.1.2 Dynamic Analysis

Dynamic analysis methods were used for flexible equipment (i.e., equipment with fundamental natural frequency  $< 33$  Hz).

These types of equipment were assessed and reevaluated using the following method.

The response spectrum curves (RSC) for the new loading combinations were compared to the original RSC used in the dynamic analysis of the equipment.

If the new RSC is less than or equal to the original RSC, the equipment is qualified and no additional analysis is needed.

If the new RSC is higher than the original RSC, a new dynamic analysis is performed using the new RSC.

#### 5.5.1.1.2.1 Acceptance Criteria

See Table 4.4-2.

#### 5.5.1.2 Testing

##### 5.5.2.1 Single Frequency Testing

The new acceleration values for the new loading combinations are determined (see Subsection 5.5.1.1.1) and compared to the original acceleration values used in the seismic test. If the new acceleration value is less than or equal to the original acceleration value, the equipment is qualified, otherwise, retesting of the equipment is required.

##### 5.5.1.2.2 Random Frequency Testing

The new RSC for the new loading combinations is compared to the test response spectrum (TRS) used in the original seismic test.

If the new RSC is less than or equal to the original TRS, the equipment is qualified, otherwise, retesting is required.

##### 5.5.1.2.3 Acceptance Criteria

Equipment should perform its intended safety function during and after the test using the new acceleration values or RSC.



## 6.0 SUPPRESSION POOL WATER TEMPERATURE MONITORING SYSTEM

### 6.1 SYSTEM DESIGN

#### 6.1.1. Safety Design Basis

The safety design basis for setting the temperature limits for the suppression pool temperature monitoring system are based on providing the operator with adequate time to take the necessary action required to assure that the suppression pool temperature will always remain below the 200° F temperature limit established by the NRC in NUREG-0487. The system design also provides the operator with necessary information regarding localized heatup of the pool water while the reactor vessel is being depressurized. If relief valves are selected for actuation, they may be chosen to assure mixing and uniformity of heat energy injection to the pool.

#### 6.1.2 General System Description

The suppression pool temperature monitoring system monitors the pool temperature in order to prevent the local pool water temperature from exceeding 200° F during SRV discharge and provides the operator with the information necessary to prevent excessive pool temperatures during a transient or accident. Temperatures in the pool are recorded and alarmed in the main control room. The instrumentation arrangement in the suppression pool consists of two bulk and 14 local temperature sensors mounted on the pool and pedestal wall and located within a 13-foot line of sight of each quencher centerline.

The two bulk temperature sensors are dual-element chromel constantan thermocouples located at elevation 683 feet 0 inch, and at azimuths 17° and 197°, respectively. These sensors provide signals which are used to indicate to the operator the bulk temperature of the suppression pool.

The local temperature sensors consist of 14 dual-element, 100  $\Omega$ , platinum RTD's located 1 foot below the low water level, at elevation 698 feet 10 inches. Ten of the sensors are located on the outer suppression pool wall at azimuths 0°, 30°, 67°, 113°, 150°, 180°, 210°, 247°, 293°, and 330°. The other four are located on the pedestal at azimuths 0°, 90°, 180°, and 270°.

The sensors are powered from ESS-1 and ESS-2 divisions and local discharge areas are monitored by two sensors, one from each division. This represents a conservative measurement of local pool water heatup. All instrumentation will be qualified Seismic Category I. The time constant of the thermocouple installation will be no greater than 15 seconds. The time from output of sensor to initiation of function will be no greater than 0.5 second. The difference between measurement reading and actual temperature will be within  $\pm 2^\circ$  F. The sampling technique for monitoring the pool temperature is to continuously record the measurements made by each of the 14 RTD's. The discharge locations and spacing are such that the number of sensors and their arrangement provides conservative monitoring of localized suppression pool water heatup in addition to bulk pool temperature.

The quenching of the steam at the quencher discharge forms jets that heat the water and generate convection currents in the suppression pool. These currents eventually rise and displace cooler water near the pool surface.

During an extended blowdown, a large temperature gradient is expected initially near the quencher. After a short time the pool gradients will stabilize with a bulk to local temperature difference of about 10° F. (Bulk and local temperature are defined in NUREG-0487.) The adequacy of the temperature monitoring system will be confirmed by the in-plant SRV testing.

### 6.1.3 Normal Plant Operation

The temperature monitoring system is utilized during normal plant operation to ensure that the pool temperature will remain low enough to condense all quantities of steam that may be released in any anticipated transient or postulated accident. When rams head devices were specified for design, there was an NRC concern that high pool temperature might result in high pool dynamic loads during SRV discharge because of unstable steam condensation. Installation of T-quenchers has eliminated this concern. The local pool temperature (temperature measured on the containment wall at the elevation of the T-quencher) limit is specified to be 200° F in accordance with the NRC Lead Plant Acceptance Criteria (NUREG-0487). During normal plant operation, the system is in continuous operation recording the suppression pool water temperature in the main control room. An alarm is actuated in the control room if the pool temperature limit is reached.

### 6.1.4 Abnormal Plant Operation

BWR plants take advantage of the large thermal capacity of the suppression pool during plant transients which require relief valve actuation. The discharge of each relief valve is piped to the suppression pool, where the steam is condensed. This results in an increase in pool water temperature but with a negligible increase in containment pressure. However, certain events have the potential for substantial energy addition to the suppression pool and could result in a high local pool temperature if timely corrective action is not taken. When rams head discharge devices are used, test results and operating experience indicate that high magnitude oscillatory loads may occur when a high steam mass flux is injected into a pool with local temperature above 170° F. Although analysis demonstrates that the pool temperature will remain below 150° F when the steam mass flux is high enough to cause these loads,

T-quenchers have been installed instead of the rams heads to provide additional margin to the pool temperature limits.

Most of the transients that result in energy discharge to the suppression pool are of short duration and have little effect on the suppression pool temperature. However, three events have the potential for substantially high energy release to the pool that could result in undesirably high pool temperatures if timely corrective action is not taken. These events are: (1) events that result in the isolation of the plant from the main condenser; (2) stuck-open relief valve; and (3) automatic Depressurization system (ADS) operation. A brief description of each of these events follows:

a. Primary System Isolation

When the primary system is isolated from the main condenser, the reactor is scrammed automatically and the stored energy in the vessel internals, the fuel relaxation energy, and the decay heat are rejected to the suppression pool. The amount of heat rejected to the pool depends on reactor size, power level, and primary system heat-removal capability. This includes condensing type heat exchangers which remove steam directly from the RPV.

b. Stuck-Open Relief Valve

The steam flow rate through a safety/relief valve (SRV), is proportional to reactor pressure. One method of terminating energy input to the pool is to scram the reactor and depressurize the RPV

in the event the relief valve cannot be closed. During the energy dump, the pool temperature will increase at a rate determined by the RPV pressure, the flow capacity of the SRV, the primary system heat-removal system capability, and the suppression pool water heat-removal capability.

c. Automatic Depressurization System (ADS)

Activation of ADS results in rapid depressurization of the RPV by the opening of a designated number of safety/relief valves. During this transient, the bulk suppression pool temperature rises. In a typical case, the RPV is depressurized below 150 psia in about 10 minutes.

There are seven plant depressurization transients that were considered as limiting events (with rams heads) for energy released to the suppression pool. These events are numbered 1 through 7 for ease of reference and are described in the following paragraphs:

Event 1 is a stuck-open relief valve with the reactor at full power. The reactor is scrammed and depressurization begun via the stuck-open valve. The initial pool temperature is the maximum pool temperature allowed for continuous operation. This is the only event that is not truly limiting, since all RHR heat exchanger equipment is considered operational.

Event 2 is identical to Event 1, except that one RHR heat exchanger is considered unavailable. The remaining heat exchanger equipment is placed in the suppression pool cooling mode.

## 6.2 SUPPRESSION POOL TEMPERATURE RESPONSE

### 6.2.1 Introduction

The La Salle County Station (LSCS) (Units 1 and 2) take advantage of the large thermal capacitance of the suppression pool during plant transients requiring safety/relief valve (SRV) actuation. The discharged steam is piped from the reactor pressure vessel (RPV) to the suppression pool where it condenses, resulting in a temperature increase of the pool water, but a negligible increase in the containment pressure. Most transients that result in relief valve actuations are of very short duration and have a small effect on the suppression pool temperature. However, certain postulated events with conservative assumptions present the potential for substantial energy additions to the suppression pool that could result in high pool temperature.

Commonwealth Edison was asked to demonstrate for several postulated transients at both LSCS units that the steam discharge from the rams heads into the suppression pool will take place so that the condensation stability limits will not be exceeded. Stable condensation is expected for rams heads if the suppression pool bulk temperature does not exceed 150° F when the rams head mass flux is greater than 40 lbm/sec-ft<sup>2</sup>. The condensation phenomenon is determined by the local temperature in the vicinity of the discharge device, whereas the calculations assume a bulk temperature. The bases for the 10° F temperature difference between bulk and local temperature and the condensation phenomenon are given in document NEDE-21078.

The results of the pool temperature transient analysis show that the rams head design is adequate for LSCS. However, to provide additional margin and to conform with NUREG-0487, T-quenchers have been installed. The quencher local pool

temperature limit of 200° F will result in increased design margin. Reanalysis is being performed for T-quencher discharge cases. The results of the rams head calculations are presented in the following subsections to demonstrate the adequacy of the LSCS design for the more limiting discharge device.

Both LOCA and non-LOCA events were investigated. The LOCA event consists of an intermediate break accident with ADS (0.1 ft<sup>2</sup> liquid break), and the non-LOCA events consist of:

- a. Stuck-Open Relief Valve
  1. From power operation.
  2. From hot standby.
  
- b. SRV Discharge Events During RPV Isolation
  1. Isolation and reactor depressurization (depressurization starts when suppression pool temperature reaches 120° F).
  2. Isolation and reactor depressurization (depressurization starts at 10 minutes after scram).

It should be noted that this analysis assumed the use of a rams head device on the SRV discharge lines in the suppression pool. The results reported herein are conservative for the use of a quencher device on these SRV discharge lines because the quencher device increases the bulk temperature limit to 200° F as specified in NUREG-0487 and at the same time provides decreased containment loads due to SRV discharge.

#### 6.2.2 Temperature Response Analysis

This analysis was performed for the rams head SRV discharge

device. Therefore pool temperatures were not calculated for SRV discharge mass flux below 40 lbm/sec-ft<sup>2</sup>. These analyses will be extended for the T-quencher temperature limit and submitted in the first quarter of 1980.

#### 6.2.2.1 Model Description

##### Non-LOCA Events

To solve the transient response of the reactor vessel and suppression pool temperature due to the postulated events, a coupled reactor vessel and suppression pool thermodynamic model was used. The model is based on the principles of conservation of mass and energy and accounts for any possible flow to and from the reactor vessel and the suppression pool.

The model incorporates a control volume approach for the reactor pressure vessel and suppression pool. It is capable of tracking a collapsed reactor vessel water level and having a rate of change of temperature or pressure imposed on it. The various modes of operation of the residual heat removal (RHR) system can be simulated, as well as the relief valves, HPCS, RCIC, and feedwater functions. The model also simulates system setpoints (automatic and manual) and operator actions and accepts as input the specific plant geometry and equipment capability.

##### Intermediate Break Accident Model

In the intermediate break accident analysis, the mass and energy conservation laws are applied to a control volume which includes all of the reactor vessel contents and its walls. This control volume is subjected to the boundary conditions of decay heat input. The break and the safety/relief valve flow rates and the associated fluid enthalpies are derived from the state of fluid in the control volume

undergoing the transient and the specified flow areas and locations.

The time-dependent break and safety/relief valve mass and energy flows are then input to another control volume containing the suppression pool. The pool temperature transient is obtained using the energy and mass balance equations on the suppression pool. As an added conservatism, the RHR system is not assumed to be in the pool cooling mode in the time period of this analysis.

#### 6.2.2.2 General Assumptions and Initial Conditions

The following common assumptions were used throughout the analysis of the LSCS suppression pool temperature response:

- a. Decay heat per ANS 5-20/10.
- b. Full crudded RHR heat exchangers.
- c. RCIC and HPCS water source is the condensate storage tanks.
- d. Wetwell air temperature equal to the suppression pool water temperature.
- e. Turbine-driven feedwater pumps operated at full rated flow until main steamline isolation valve (MSIV) closure. The coastdown of the turbine-driven pumps was included and motor-driven feedwater pump was available.
- f. Condensate storage tank temperature was 80° F.
- g. In calculating the overall heat transfer coefficient of the vessel wall and internal structures, it is

assumed that the heat transfer is dominated by conduction. The heat transfer area of the reactor internals is obtained by assuming that they have the same metal thickness as that of the vessel, which is assumed to be 0.333 foot uniformly.

- f. The control volume of the reactor includes the reactor vessel, the recirculation lines, the feedwater lines from the vessel to the nearest feedwater heaters and the steamlines from the vessel to the inboard main isolation valves (MSIV).
- i. The initial water level in the reactor vessel is calculated based on the assumption that the voids in the two-phase region collapse. Therefore, the ECCS ON/OFF volumes are based on the total liquid volume of the reactor vessel, the feedwater lines and the recirculation lines combined.
- j. The specific heat of the reactor vessel and the internal is assumed to be 0.123 Btu/lbm/° F. The metal density is assumed to be 490 lbm/ft<sup>3</sup>.
- k. A stuck-open relief valve can be detected and the corresponding rams head within the suppression chamber identified.
- l. Additional safety/relief valves are manually opened as necessary to depressurize the reactor.
- m. Minimum technical specification suppression pool water level.
- n. Maximum suppression pool initial temperature.
- o. 122.5% rated ASME safety/relief valve flow rate.

### 6.2.2.3 Description of Non-LOCA Events

This subsection describes the safety/relief valve discharges for non-LOCA events, (Subsection 6.2.2.4 describes the LOCA event). A complete description of the sequence of events for all of the cases, i.e., Events a, b, c, d, and e, is given in Tables 6.2-1 through 6.2-5.

#### 6.2.2.3.1 Stuck-Open Relief Valve (SORV) Conditions

The first group of SRV discharge events considered herein are stuck-open relief valve (SORV) conditions caused by a spurious valve opening and a mechanical failure of a valve to close. Two events were considered in this classification, as follows.

##### Event a: SORV From Power Operation

In this event, conservative plant data and initial conditions were used. Operator action time to scram the reactor has been assumed to be 10 minutes. Other operator actions (e.g., opening additional SRV's) and their times, and the sequence of events is as follows.

The reactor is initially operating at the power level corresponding to 105% rated steam flow and the suppression pool temperature is at 100° F. An SRV is postulated to stick fully open at this point in time (time zero of the transient analyzed). The plant operator is alerted that an SRV has opened and tries to close it. Finding that the SRV cannot be closed (confirmed by other plant parameter indications), the operator initiates a reactor scram at pool temperature of 110° F. The reactor water level reaches level 2, causing the main steam isolation valves (MSIV) to close. At 10.5 seconds after scram, the MSIV's are assumed to be fully closed. During this time period (i.e., from time 0 to 10 minutes + 10.5 seconds),

full feedwater flow is assumed into the reactor vessel. At the time the MSIV's are fully closed, the feedwater turbine-driven pump is assumed to coast down and drop to zero flow, and the motor-driven pump starts at 10% of rated feedwater flow.

The pool temperature rises due to the steam discharge from the SORV into the suppression pool. At 15 minutes after the occurrence of the SORV, the plant operator initiates pool cooling utilizing the RHR heat exchangers in the pool cooling mode and is required to open two additional SRV's to depressurize the reactor vessel rapidly enough that when the bulk pool temperature reaches 150° F, the ram head mass flux at the discharge point is below 40 lbm/sec-ft<sup>2</sup>.

#### Event b: SORV From Hot Standby

In this event, the initial pool temperature is 100° F, and the reactor power level is initially at 105% of rated steam flow at the time of reactor scram. At 10.5 seconds after scram, the main steamline isolation valves are closed and the reactor is held in an extended hot shutdown condition. During the first 30 minutes after scram, the reactor pressure is maintained at SRV setpoint pressure (1090) by operating the SRV's intermittently. At 30 minutes after scram, one SRV is postulated to stick open and 10 minutes later the operator can manually open additional SRV's. At 60 minutes after scram, two RHR heat exchangers are activated in the pool cooling mode. During the entire event, automatic operation of the HPCS and RCIC systems and SRV flow of 122.5% of ASME rated flow is assumed.

#### 6.2.2.3.2 SRV Discharge During RPV Isolation Conditions

The second category of SRV discharge events considered is for the conditions which exist where the vessel is isolated

from the main turbine and condenser (e.g., MSIV closure, loss of condenser vacuum). Under such conditions, the operator has the option of either placing the reactor in the hot shutdown condition or manually depressurizing the vessel using SRV's at a specified cooldown rate.

Event c: Isolation and Reactor Depressurization

The reactor is isolated and scrammed when the initial pool temperature is 100° F and the reactor power level is 105% of rated steam flow. Reactor pressure is maintained at SRV setpoint pressure by operating the SRV's intermittently until the suppression pool bulk temperature equals 120° F (25 minutes after scram). Ten minutes later the operator initiates reactor cooldown by manually opening SRV's. At 30 minutes after the pool temperature reaches 120° F (55 minutes after scram), one RHR heat exchanger is activated in pool cooling mode. Automatic operation of the RCIC and HPCS system is available, and SRV flow of 122.5% of ASME rated flow is assumed.

Event d: Isolation and Reactor Depressurization

In this event, the reactor is isolated and scrammed when the initial pool temperature is 100° F and reactor power level is 105% of the rated steam flow. Reactor pressure is maintained at SRV setpoint pressure by operating the SRV's intermittently. Ten minutes after scram the operator initiates reactor cooldown manually by opening SRV's. At 15 minutes after scram, one RHR heat exchanger is activated in the pool cooling mode. Automatic operation of the HPCS and RCIC systems is available and SRV flow of 122.5% of ASME rated flow is assumed.

#### 6.2.2.4 Description of LOCA Event

##### Event e: Intermediate Break Accident with ADS

This event assumes that a  $0.1\text{-ft}^2$  break occurs on the recirculation line. HPCS is also assumed to be unavailable for the makeup of the vessel liquid inventory depleted due to the break flow. The ADS system is activated when the water level in the reactor vessel drops to level 1. The other necessary signal for ADS activation, high drywell pressure, will have occurred soon after the break. The opening of the ADS valves produces a rapid vessel depressurization.

In this event, the reactor is assumed to be scrammed at a high drywell pressure (2 psig) which occurs at  $t = 10$  seconds after the line break. The vessel pressure after the line break remains constant at the SRV setpoint pressure (1090.7 psia) until the ADS is activated on the low water level signal at  $t = 215$  sec. The depressurization of the vessel through SRV flow causes a rapid increase in the suppression pool temperature. The pool temperature reaches  $126^\circ\text{ F}$  when the vessel pressure drops to 253 psia. The reactor vessel pressure subsequently remains below 253 psia. ( $P_{\text{vessel}} = 253$  corresponds to  $G = 40\text{ lbm/ft}^2\text{ sec}$ . at the rams head discharge.)

#### 6.2.3 Results/Conclusions

The results obtained from the LSCS suppression pool temperature analyses are depicted in Figures 6.2-1 through 6.2-8. Summary results are presented in Table 6.2-6. Conservative assumptions were used for all transient events presented in this report. For example, 122.5% of ASME rated steam flow for SRV discharge, maximum initial pool temperature, minimum initial pool mass, continued addition of feedwater energy into the reactor vessel, and the initial reactor power corresponding to 105%

of rated steam flow (105% rated steam flow is equivalent to 103% of rated thermal power) are conservative parameters that will affect the pool temperature.

For the case of a stuck-open relief valve from power (Figure 6.2-1), calculated suppression pool temperature slightly exceeds the defined condensation instability limit for the rams head discharge device. Considering the conservative assumptions utilized in this analysis, it is expected that stable condensation would, nevertheless, be maintained for this event, if it occurred. For the case of a stuck-open relief valve from hot standby (Figure 6.2-3), the suppression pool temperature and rams head mass flux are maintained well below the condensation instability limit for the entire transient period. The stuck-open relief valve tends to increase the pool temperature rapidly, but two additional manually opened valves result in the rams head mass flux falling below the critical value of 40 lbm/sec-ft<sup>2</sup> prior to the pool temperature reaching 150° F.

The case of reactor depressurization following isolation is given in Figures 6.2-4 and 6.2-5. Figure 6.2-5 is similar to event (b) for the first 30 minutes. When reactor cooldown is initiated, it is done at a controlled depressurization rate as opposed to the uncontrolled rate of event (b). Thus, depressurization is accomplished at a slower rate, and pool temperature increases accordingly before reaching the critical mass flux. For this event, condensation stability is still maintained at the discharge device, with a temperature of 149° F at the critical mass flux.

In addition to event (c), calculations were performed for an isolation depressurization case assuming the operator begins depressurization at 10 minutes after the isolation scram occurs. This is event (d). It is expected that this is a more realistic case than event (c), since the operator

would not attempt to achieve an isolated hot standby condition (which leads to 120° F in the pool in this case) knowing that only one RHR heat exchanger is available. Manual depressurization would be undertaken as soon as possible. Figures 6.2-6 and 6.2-7 show that the pool temperature response is less severe and the condensation stability limit is still maintained with a temperature of 148° F at the critical mass flux.

The case of an intermediate break accident with ADS (Figure 6.2-8) yields the lowest suppression pool temperature for the events examined. As can be seen from Figure 6.2-8 the suppression pool temperature is 126° F at rams head mass flux of 40 lbm/ft<sup>2</sup>-sec.

In conclusion, stable condensation with the rams head discharge device can be maintained for all events considered in this report, given appropriate operator actions.

TABLE 6.2-1

STUCK-OPEN RELIEF VALVE FROM POWER OPERATION - EVENT AInitial Conditions

1. Operation at 105% rated steam flow
2. Design maximum service water temperature
3. Suppression pool temperature at normal tech. spec. limit 100° F
4. Other common initial conditions

EVENT SEQUENCE

<u>Time (Min)</u>	<u>Event Description</u>
0.0	SRV fails open Pool temperature alarm at operating tech. spec. limit
10.0	Reactor scram (and isolation at 10.5 seconds later)
15.0	Single RHR loop lined up for pool cooling
15.0	Two additional SRV's manually actuated

Assumptions

1. Common assumptions
2. Normal automatic operation of RCIC, HPCS
3. Single RHR loop available for pool cooling
4. Maximum operating condensate water temperature
5. 122.5% ASME rated SRV flow rate

Results

Suppression pool bulk<sub>2</sub> temperature = 152° F at rams head  
mass flux = 40 lbm/ft<sup>2</sup>-sec

TABLE 6.2-2

STUCK-OPEN RELIEF VALVE FROM HOT STANDBY - EVENT BInitial Conditions

1. Operation at 105% rated steam flow
2. Design maximum service water temperature
3. Suppression pool temperature at normal tech. spec. limit
4. Other common initial conditions

EVENT SEQUENCE

<u>Time (Min)</u>	<u>Event Description</u>
0.0	Reactor isolation and scram
0 < t < 30.0	Reactor pressure maintained using SRV
30.0	Single SRV sticks open
40.0	Two additional SRV's opened (by operator)
60.0	Two RHR loops lined up for pool cooling

Assumptions

1. Common assumptions
2. Normal automatic operation of RCIC, HPCS
3. Two RHR loops available
4. Maximum operating condensate storage water temperature
5. 122.5% rated ASME SRV flow rate

Results

Suppression pool bulk<sub>2</sub> temperature = 139° F at rams head  
 mass flux = 40 lbm/ft<sup>2</sup>-sec

TABLE 6.2-3

ISOLATION AND REACTOR DEPRESSURIZATION - EVENT CInitial Conditions

1. Operation at 105% rated steam flow
2. Design maximum service water temperature
3. Suppression pool temperature at normal tech. spec. limit 100° F
4. Other common initial conditions

EVENT SEQUENCE

<u>Time (Min)</u>	<u>Event Description</u>
0.0	Reactor isolation and scram
0 < t < 25.0	Reactor pressure maintained using SRV
25.0	Pool temperature at $T_{\max} = 120^{\circ} \text{ F}$
35.0	Initiate reactor cooldown using SRV's
35.0	Single RHR loop lined up for pool cooling

Assumptions

1. Common assumptions
2. Normal automatic operation of RCIC, HPCS
3. Single RHR loop available for pool cooling
4. Maximum operating condensate storage water temperature
5. 122.5% ASME rated SRV flow rate

Results

Suppression pool bulk<sub>2</sub> temperature = 149° F at rams head  
 mass flux = 40 lbm/ft<sup>2</sup>-sec

TABLE 6.2-4

ISOLATION AND REACTOR DEPRESSURIZATION - EVENT DInitial Conditions

1. Operation at 105% rated steam flow
2. Design maximum service water temperature
3. Suppression pool temperature at normal tech. spec. limit 100° F
4. Other common initial conditions

EVENT SEQUENCE

<u>Time (Min)</u>	<u>Event Description</u>
0.0	Reactor isolation and scram
0 < t < 10.0	Reactor pressure maintained using SRV
10.0	Initiate reactor cooldown using SRV's
15.0	Single RHR loop lined up for pool cooling

Assumptions

1. Common assumptions
2. Normal automatic operation of RCIC, HPCS
3. Single RHR loop available for pool cooling
4. Maximum operating condensate storage water temperature
5. 122.5% ASME rated SRV flow rate

Results

Suppression pool bulk<sub>2</sub> temperature = 148° F at rams head  
 mass flux = 40 lbm/ft<sup>2</sup>-sec

TABLE 6.2-5

INTERMEDIATE BREAK ACCIDENT (LIQUID) WITH ADS - EVENT EInitial Conditions

1. Operation at 105% rated steam flow
2. Design maximum service water temperature
3. Suppression pool temperature at normal tech. spec. limit 100° F
4. Other common initial conditions

EVENT SEQUENCE

<u>Time (Min)</u>	<u>Event Description</u>
0	Break Occurs Pool bulk temperature = 100° F
10.0	Reactor scram on high Drywell pressure (2 psig)
10.5	MSIV fully closed
215.0	ADS activated following reactor low water level (level 1)

Assumptions

1. Common assumptions
2. Normal automatic operation of RCIC, HPCS
3. Single RHR loop available for pool cooling
4. Maximum operating condensate storage water temperature
5. 122.5% ASME rated SRV flow rate

Results

Suppression pool bulk<sub>2</sub> temperature = 126° F at rams head  
mass flux = 40 lbm/ft<sup>2</sup>-sec

TABLE 6.2-6

SUMMARY OF RESULTSSUPPRESSION POOL TEMPERATURE RESPONSE ANALYSIS

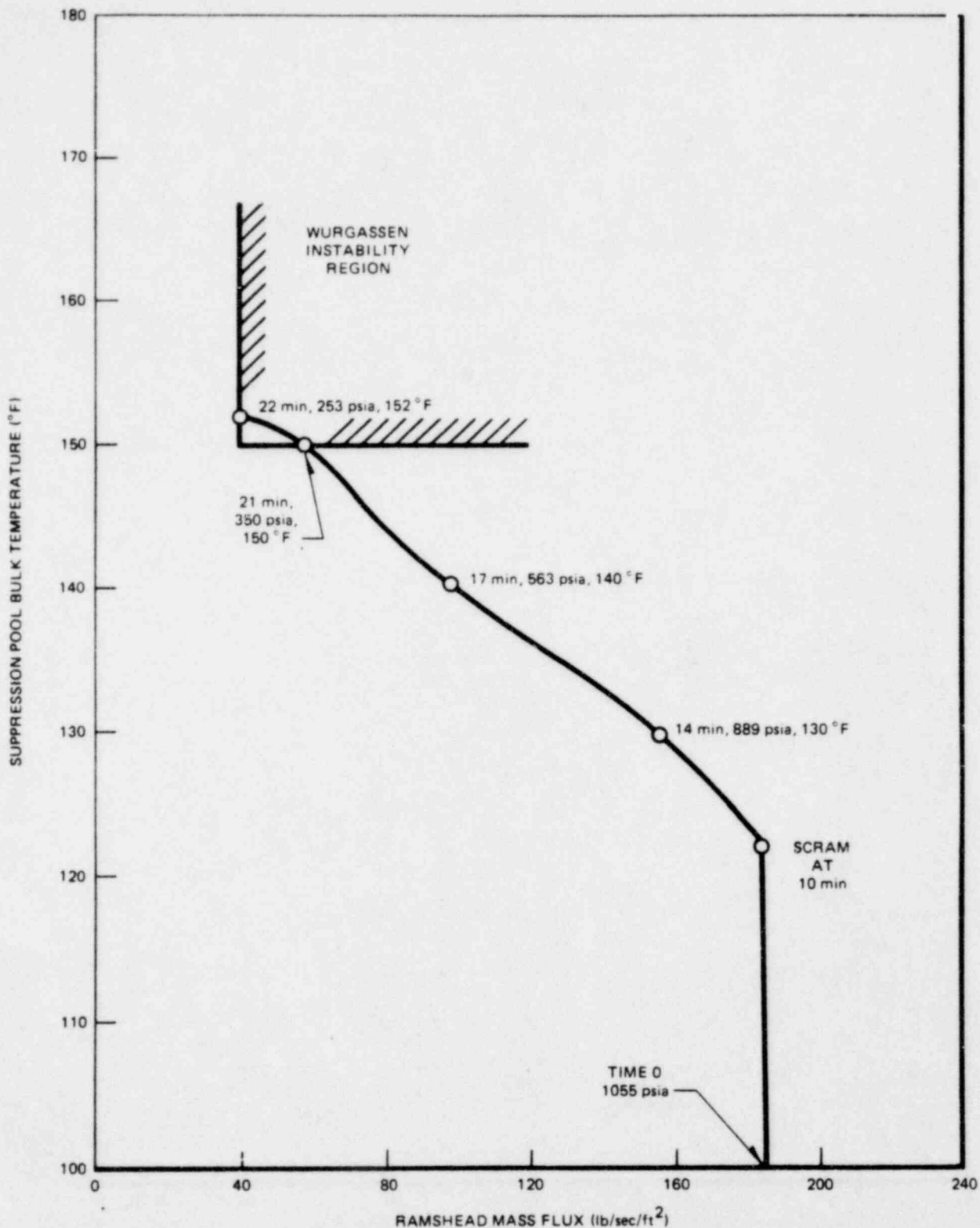
EVENT NO.	REACTOR POWER*	INIT POOL TEMP. (°F)	SERV WATER TEMP. (°F)	OPERATOR ACTIONS			RESULTS					COMMENTS
				SCRAM TIME	MSIV CLOSURE TIME	ADD VALVE	HPCS AND RCIC	RHR HX POOL COOLING	NO. SRV OPENED MANUALLY	G** AT T=150° F	T (°F) AT G=40	
a	105%	100	100	10 min.	10 min. + 10.5 sec	15 min.	Auto	1 Hx 15 min.	2	58	152	SORV From Power Operation
b	105%	100	100	10 min.	10.5 sec	40 min.	Auto	2 Hx 60 min.	2	27	139	SORV From Hot Standby
c	105%	100	100	0 min.	0 min.	35 min.	Auto	1 Hx 55 min.	4	38	149	Depressurization From 120° F
d	105%	100	100	0 min.	0 min.	10 min.	Auto	1 Hx 15 min.	2	38	148	Depressurization at 10 min.
e	105%	100	100	No. Operator Actions			HPCS Inop., RCIC Not Considered	N/A	None	N/A	126	Liquid IBA on Recirc. line. Six ADS valves are used.

\*Reactor power corresponding to 105% rated flow rate (~103% rated power)

\*\*G = mass flux (lbm/ft<sup>2</sup>-sec)

LSCS-MARK II DAR

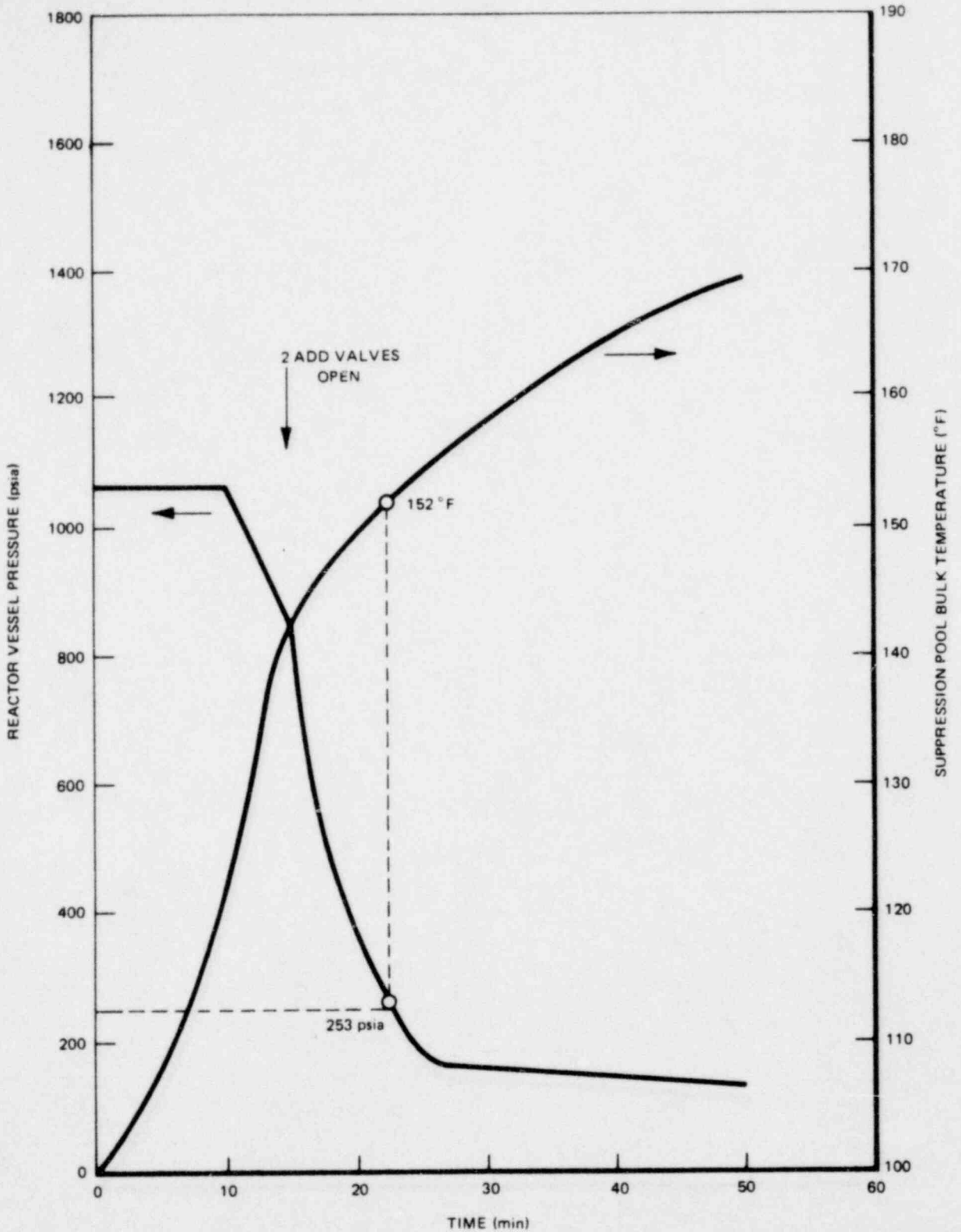
Rev. 7 1/80



**LA SALLE COUNTY STATION**  
**MARK II DESIGN ASSESSMENT REPORT**

---

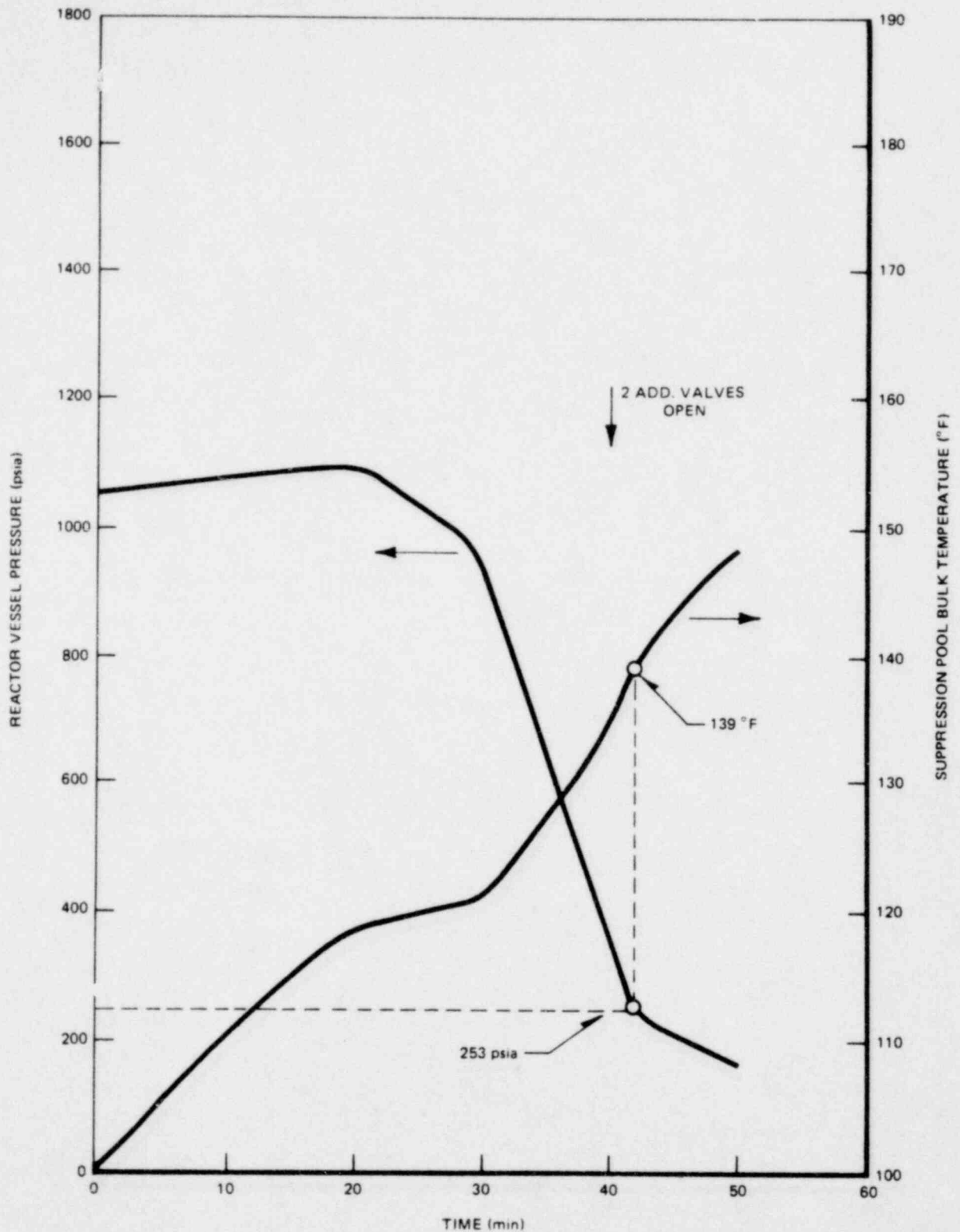
FIGURE 6.2-1  
 POOL TEMPERATURE VS. MASS FLUX -  
 EVENT A: SORV FROM POWER OPERATION



LA SALLE COUNTY STATION  
MARK II DESIGN ASSESSMENT REPORT

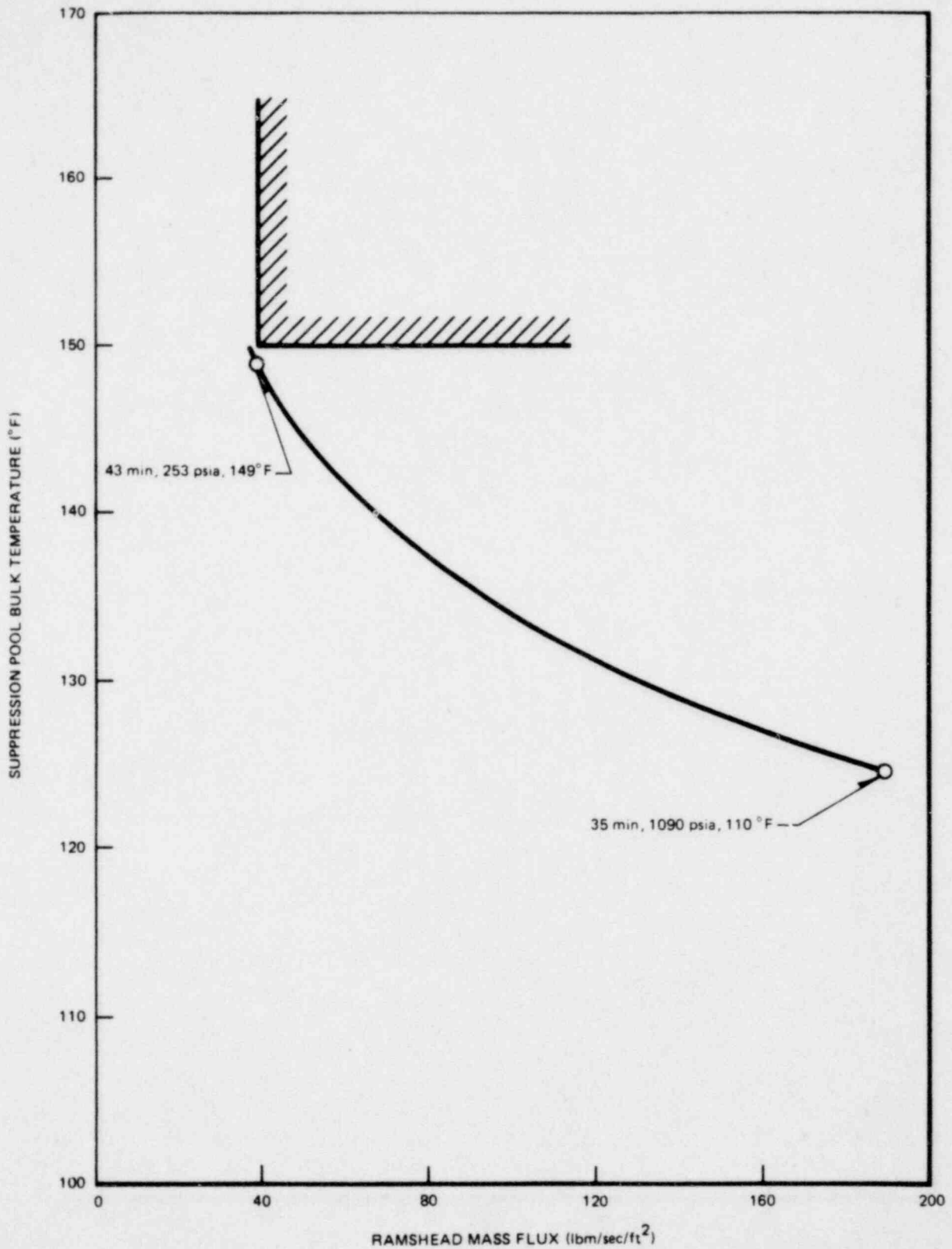
FIGURE G.2-2

POOL TEMPERATURE RESPONSE - EVENT A:  
SORV FROM POWER OPERATION



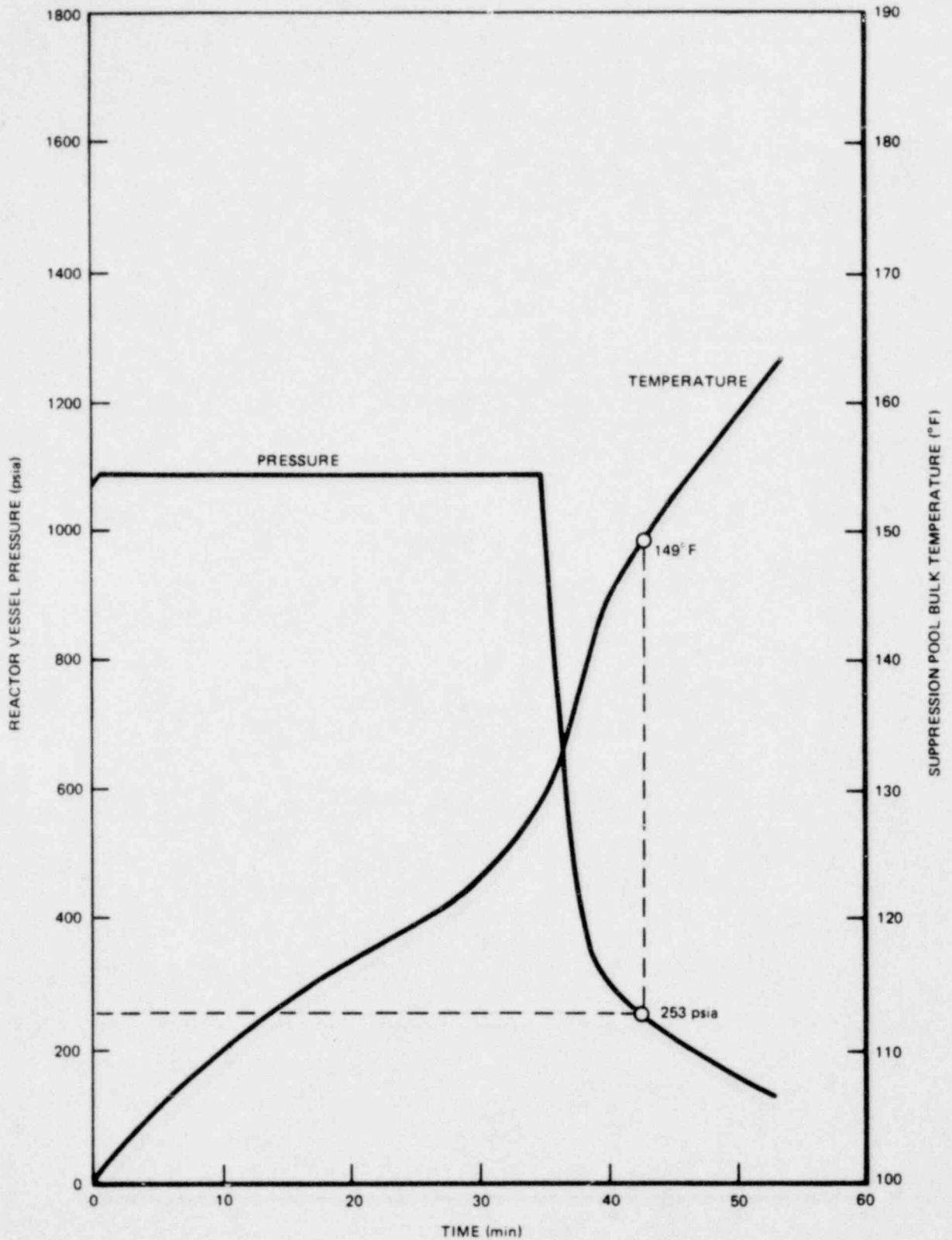
LA SALLE COUNTY STATION  
MARK II DESIGN ASSESSMENT REPORT

FIGURE 6.2-3  
POOL TEMPERATURE RESPONSE - EVENT B:  
SORV FROM HOT STANDBY



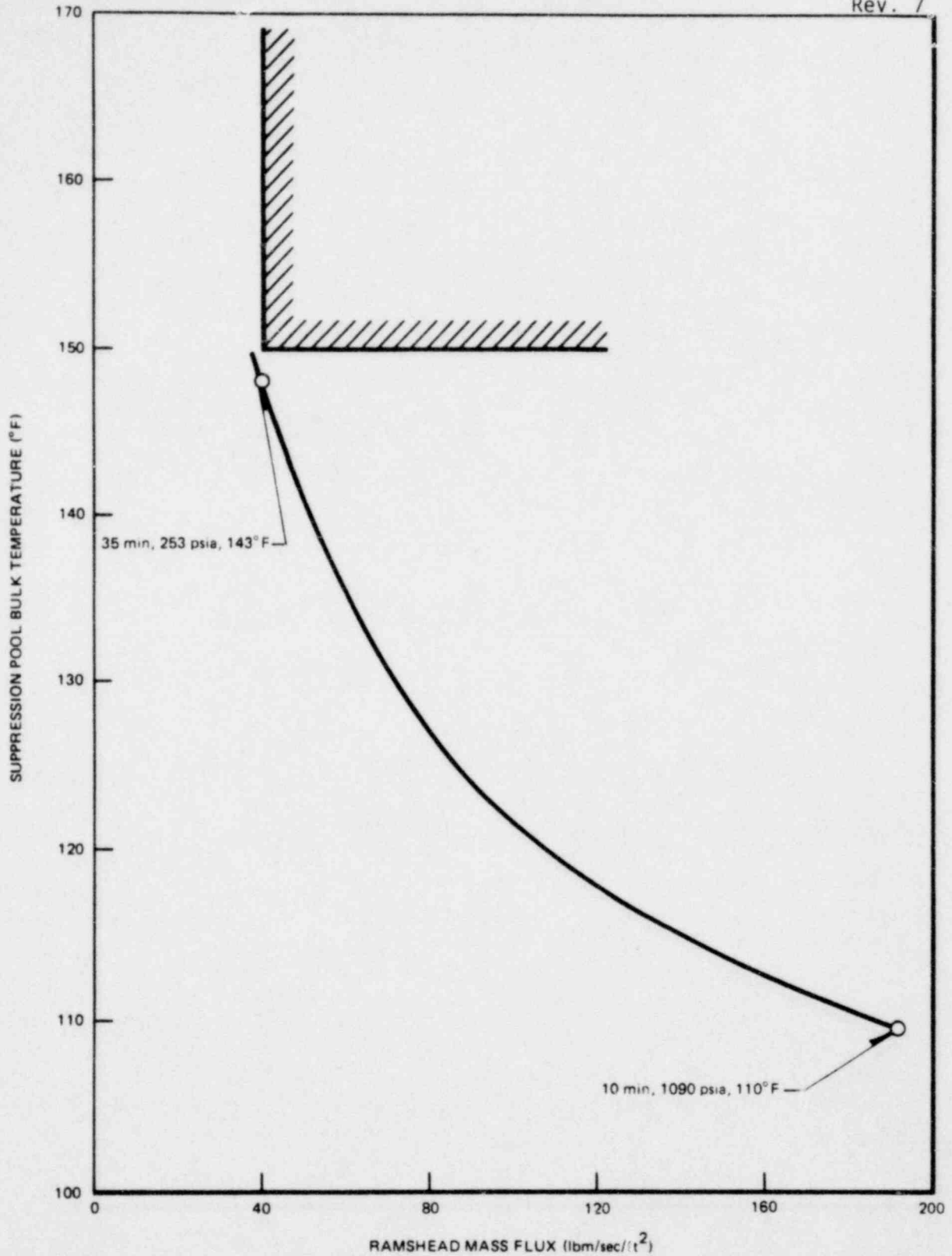
**LA SALLE COUNTY STATION**  
**MARK II DESIGN ASSESSMENT REPORT**

FIGURE 6.2-4  
POOL TEMPERATURE VS. MASS FLUX -  
EVENT C: ISOLATION AND  
REACTOR DEPRESSURIZATION



LA SALLE COUNTY STATION  
MARK II DESIGN ASSESSMENT REPORT

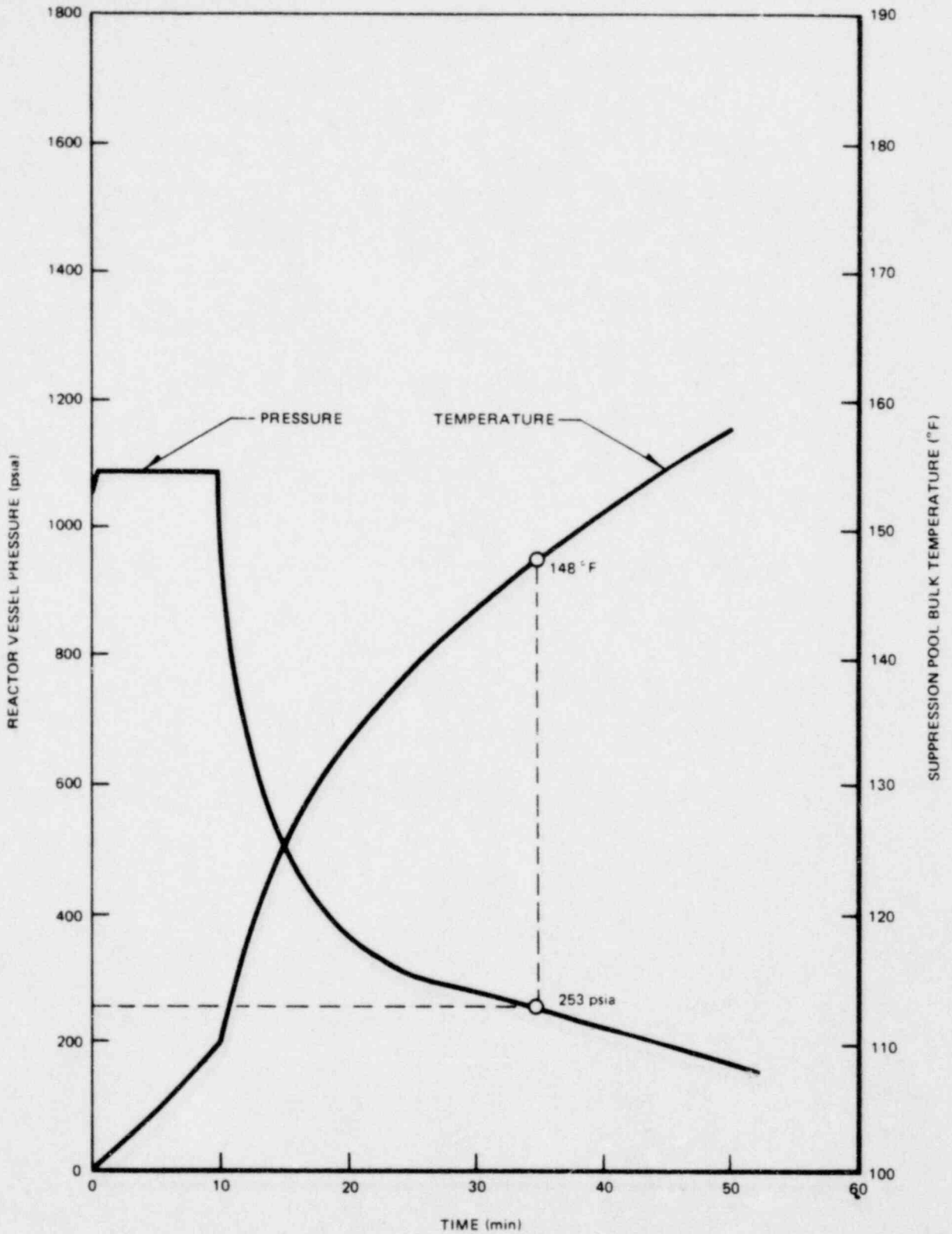
FIGURE 6.2-5  
POOL TEMPERATURE RESPONSE - EVENT C:  
ISOLATION AND REACTOR DEPRESSURIZATION



**LA SALLE COUNTY STATION**  
**MARK II DESIGN ASSESSMENT REPORT**

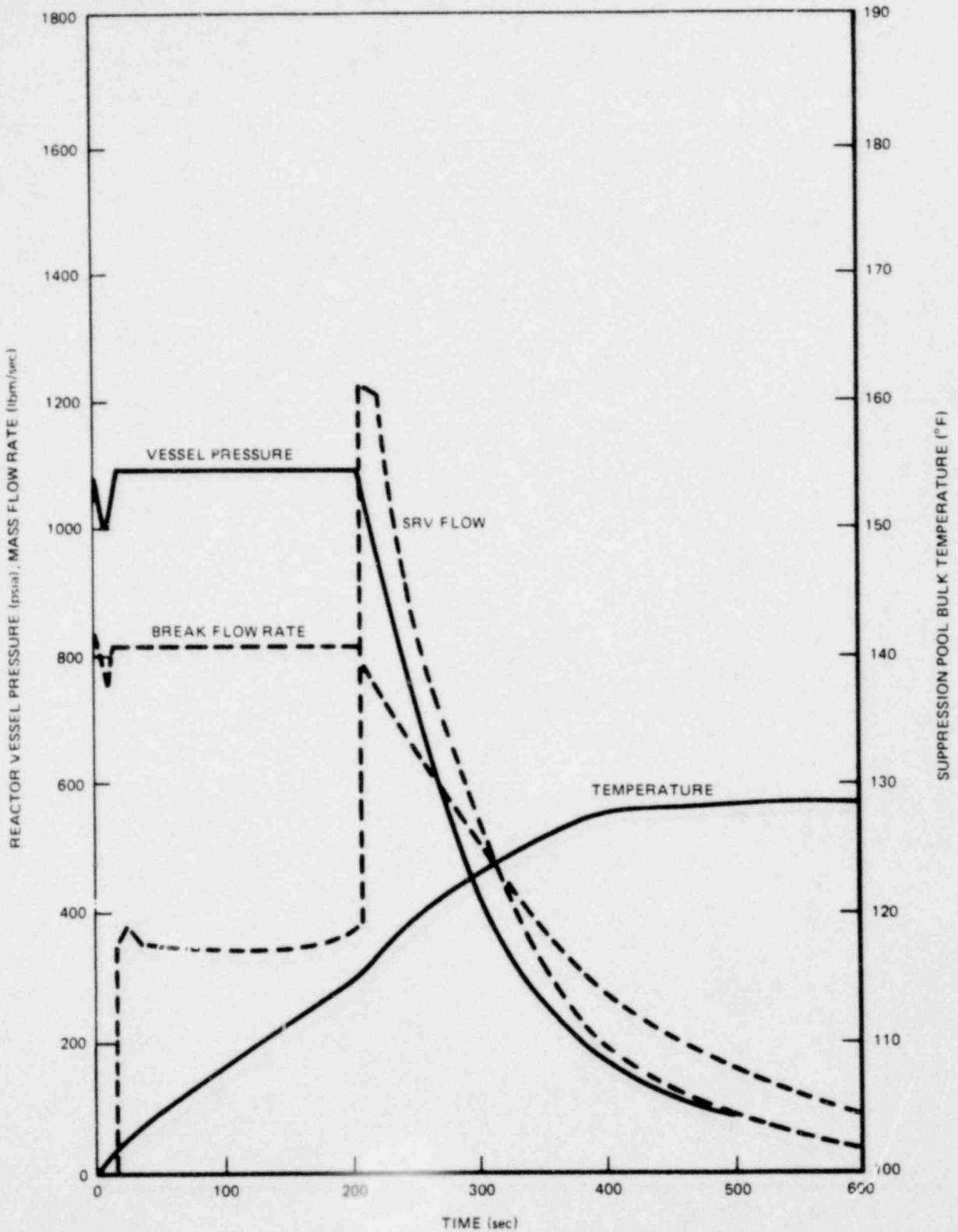
FIGURE 6.2-6

POOL TEMPERATURE VS. MASS FLUX -  
EVENT D: ISOLATION AND  
REACTOR DEPRESSURIZATION



**LA SALLE COUNTY STATION**  
**MARK II DESIGN ASSESSMENT REPORT**

FIGURE 6.2-7  
POOL TEMPERATURE RESPONSE - EVENT D:  
1. ISOLATION AND REACTOR DEPRESSURIZATION



**LA SALLE COUNTY STATION**  
 MARK II DESIGN ASSESSMENT REPORT  
 FIGURE 6.2-8  
 POOL TEMPERATURE RESPONSE - EVENT E:  
 INTERMEDIATE BREAK ACCIDENT WITH  
 ADS (0.1 ft<sup>2</sup> LIQUID BREAK)



## 7.0 PLANT MODIFICATIONS AND RESULTANT IMPROVEMENT

### 7.1 STRUCTURAL MODIFICATIONS

In general, the impact of the addition of the pool dynamic loads was minimal on a majority of the structures. The primary reasons are:

- a. Except in local areas, the design of the containment structure is generally governed by local combinations involving safe shutdown earthquake and design-basis accident.
- b. The original design of reinforced concrete beams, slabs, and shear walls was made based on the conservative working strength design method (ACI 318-63).

A summary of the structural modifications necessitated by the addition of pool dynamic loads is given below:

- a. Shear reinforcements have been added in the containment wall at the intersection of containment and reactor building basemat. (For details, see Figure 5.1-10.)
- b. The inner core of the reactor support pedestal has been filled with concrete up to elevation 699 feet 10 inches to reduce the bending stresses resulting from pool dynamic loads. Additional reinforcing bars and concrete studs have been provided to ensure structural integrity. (Refer to Figures 5.1-11 and 5.1-12 for details of the concrete fill.)
- c. Additional reinforcing bars in both the radial and hoop directions have been provided in the

drywell floor to upgrade the capacity of the floor. (For details, refer to Figures 5.1-13 and 5.1-14.)

- d. Additional embedment plates have been provided in the drywell floor, containment wall, and sacrificial shield to support the increased number of snubbers.
- e. The CRD hydraulic system insert and withdrawal lines penetrating the reactor support pedestal were rerouted and enclosed in separate pipe sleeves to eliminate four large openings provided in the original arrangement.
- f. Stiffeners were added to the basemat liner to provide capacity to carry the maximum probable negative pressure resulting from the pool hydrodynamic loads.
- g. The downcomer vents have been upgraded to meet the requirements of ASME B&PV Code Section III, Class MC. Previously, the downcomers did not meet the requirements of Subsection NE of Section III (see Subsection 5.3.3).
- h. The downcomers in the suppression pool have been braced at elevation 721 feet, well above the pool swell impact zone, to reduce the pool dynamic loads transmitted to the drywell floor. Additional bracing for the downcomers is being installed at elevation 697 feet to support the downcomers against bounding submerged structures loads defined in Chapter 3.0. A detailed description of the downcomer bracing is given in Subsection 5.3.3.

- i. The flanges on every downcomer vent along with the tubular flange projections have been removed. This modification leaves the downcomer exterior smooth and eliminates the associated pool dynamic loads on the flanges.
- j. Embedments have been provided on the basemat to support the KWU quenchers.
- k. About 980 cable tray hangers in the reactor building have been upgraded with stiffer members to withstand the pool dynamic loads.
- l. About 45 HVAC duct hangers in the reactor building have been stiffened to carry the pool dynamic loads.
- m. Containment galleries have been upgraded with stiffer members to accommodate ABS combinations of seismic and pool dynamic loads. The resulting modifications consist of changes to the steel beams by the addition of coverplates, or replacing them with stiffer members, changing the end connections, and stiffening of the steel columns for the gallery at elevation 740 feet 0 inch.
- n. Galleries outside the containment in the reactor building were stiffened to carry additional loads due to pool hydrodynamic loads.

## 7.2 BALANCE OF PLANT PIPING AND EQUIPMENT

### Wetwell Piping

Modifications have been made to the wetwell piping systems to increase their capability to sustain the applied loadings. Modifications to the piping include replacing sections of pipe with heavier schedule pipe and rerouting the line when necessary. Modifications to the support systems include the addition of restraints and the upgrading of their load capacity when necessary. ECCS suction strainers have also been reinforced to increase their load carrying capabilities.

### Non-Wetwell Piping

The upgrading of the design basis of the piping to the design load combinations of Table 4.4-2, required modifications to the piping systems. These modifications consisted of replacing restraints with models of higher load rating, relocation of restraints, and addition of restraints. In some cases, sections of piping were replaced with higher schedule piping to meet the acceptance criteria.

### Equipment

Reevaluation has been completed for all equipment except valves. Reevaluation and requalification of the valves can be completed only after the piping analysis is completed. The piping loads (e.g., levels and nozzle loads) at valve location will be checked against the loads used in the valve qualification.

New tests are planned for the following electrical equipment to meet the new loads.

1. 480-V Motor Control Centers.
2. 250-Vac distribution equipment.

New testing was conducted on various HVAC control and instrumentation equipment as a result of the seismic response spectra and the SRV-ALL response spectra. The subject equipment, shown in Table 7.2-1, were retested to a multifrequency, random motion, biaxial excitation. The results show that the test response spectrum for the instruments and controls in the three tabulated categories were satisfied for each of the prescribed required response spectrum.

TABLE 7.2-1

RETESTED HVAC EQUIPMENTRIGIDLY MOUNTED FIELD INSTRUMENTS

<u>DESCRIPTION</u>	<u>MODEL</u>
Chlorine Detector	50-125A
Chlorine Detector	50-125D
Level Switch	36497
Smoke Detector	DIS-3/5A
Control Unit	CTZ-2
Indicating Unit	FIU-6
Zone Unit	ZIU-6
Temperature Switch	303
Diff. Transmitter	252A
Diff. Transmitter	252A $\sqrt{X}$
Temperature Switch	800
D. P. Switch	7PS

TABLE 7.2-1 (Cont'd)

RIGIDLY PANEL MOUNTED INSTRUMENTS

Transfer Switch	SB-1
Control Switch	SBM
Time Delay Relay	7012AD
Solenoid Valve	8320
Temperature Controller	54
Current Relay	48
Current Relay	56
Control Relay	HMA
Control Relay	HFA
Ammonia Detector (Controller Only)	38-H

FLEXIBLY MOUNTED FIELD INSTRUMENTS

RTD	601
Limit Switch	EA700
Damper Motor	AH91
Damper Motor	NH91
Damper Motor	AH95
Damper Motor	NH95
Smoke Detector	CDA-2
Smoke Detector	DIA-11
NH <sub>3</sub> Detector Head	350-H

### 7.3 NSSS PIPING AND EQUIPMENT

Modifications have been incorporated (or planned) for NSSS components/equipment to accommodate the structural system feedback responses from suppression pool hydrodynamic and LOCA loads. The modifications include:

- a. Upgrading the primary system piping, main steam and recirculation, snubber requirements for additional and increased sizes. The number of restraints was increased by approximately 40%.
- b. Installation of holddown clamps for the reactor pressure vessel top guide.

#### 7.4 SRV DISCHARGE QUENCHER

In addition to the structural and mechanical design changes discussed in previous sections, it was concluded that the plant safety margin could be increased further by removing the SRV discharge rams head and installing a quencher. This quencher device provides increased safety margin in two respects: (1) it increases the threshold temperature limit for steam condensation vibration; and, (2) it provides reduced loads on the containment structure as well as those piping systems in the containment and reactor building. Since the plant was assessed to a conservative SRV discharge load based upon a rams head device, installation of quencher devices will provide significant reductions in loads and consequently increases in the plant safety margin.

The rams head SRV discharge device performs well under the conditions expected in Mark II containments. However, tests have indicated that high steam condensation loads may occur if high mass flux is discharged into a high temperature pool. Although analyses show that the pool temperature will not be high enough to cause problems, quencher devices have been installed to preclude any possibility of increased load.

The quencher eliminates the steam condensation loads by breaking the steam discharge into many small jets ensuring that no large steam bubble forms. Air bubble loads are also decreased because of the small size and dispersion of the air bubbles.

Even though all load magnitudes are reduced, some reanalysis was necessary to verify the adequacy of the design. The quencher arrangement in the pool is different from the rams head arrangement in order to minimize loads and promote pool thermal mixing. The frequency range of the quencher air

bubble discharge is also somewhat different from that expected of the rams head.

The impact of these changes have been assessed by applying the T-quencher load definition (Susquehanna DAR, Chapter 4) to LSCS. The boundary loads specified for the T-quencher were used. Submerged structure loads were calculated by using the rams head submerged structure methodology with the T-quencher locations and a frequency range based on the T-quencher boundary load methodology. The source strength (i.e., pressure magnitude) was determined for first and subsequent SRV actuation using the correlations in NEDO-21061 Revision 3 (DFFR).



## 8.0 PLANT SAFETY MARGINS

### 8.1 CONSERVATISM IN PLANT DESIGN

#### 8.1.1 Conservatism in Pool Dynamic Loads

Conservatism in the safety/relief valve pool dynamic loads have been discussed in detail in Subsection 3.2.1.1. The rams head load definition contains conservatism in each step of the calculation.

This procedure has resulted in a design which is very conservative for the loads expected from SRV rams head discharge. To eliminate RC concerns about high pool temperature operation, quencher devices have been installed in the LSCS plant. An additional significant load reduction results from this change.

LOCA loads also have been treated in a very conservative manner. The design-basis accident is postulated as a double ended guillotine break, clearly an unlikely mode of failure for a large pipe. The pool swell transient, as described in Subsection 3.3.1.1.3, is predicted by a conservative model and has incorporated conservative factors as recommended by NUREG-0487. A bounding load approach has been utilized in calculating the steam condensation design loads, ignoring load reductions due to phasing and the low probability of maximum load magnitude.

Submerged structure loads calculated for both SRV and LOCA events have also been done in a conservative manner. In response to the NRC Acceptance Criteria (NUREG-0487) geometric and transient flow effects have been considered (Subsection 3.2.3). Loads were increased when a potential for higher loads was found but no loads were decreased because of these effects.

### 8.1.2 Structural Conservatism

The margin factors obtained in the original assessment are very conservative for the following reasons:

- a. The peak responses of the individual transient loads are combined by the absolute sum method, even though probabilistically all peak effects will not occur at the same time and it would be more realistic to use SRSS of the peaks.
- b. The fact that the instantaneous peak response induced by loads such as earthquake, SRV discharge, LOCA, etc., do not occur simultaneously at all points along the circumference of the structure is conservatively neglected in the design.
- c. In load combinations, the effects of individual loads are magnified by a load factor to account for potential overloads.
- d. Current ASME Code for the design of concrete containment structures (ACI-359) treats thermal stresses as self-limiting secondary stresses and permits yielding of the reinforcing steel when thermal loads occur in a load combination. However, the structural design criteria for the LSCS containment are very conservative and more stringent than the current practice and do not permit yielding of the reinforcing steel even under thermal loads.
- e. Only the specified minimum material strengths were used in the design assessment even though the actual minimum strengths determined by quality

control tests are greater than the specified minimums.

### 8.1.3 Mechanical Conservatism

The current piping design basis contains several conservatisms. The acceptance criteria are more restrictive than those presented in Table 4.4-2 (Table 6-1 of Rev. 2 of the DFFR), thereby providing margins in the piping stress levels if the DFFR criteria are accepted.

The enveloped response spectra method was used for dynamic analyses, a more conservative approach than a time-history analysis. In addition, although the Mark II owners' position for  $\pm 5\%$  peak broadening building response spectra for pool dynamic loads is technically justified, at least  $15\%$  peak broadening was used for the LSCS plant assessment.

The code allowables used were the minimum required; except for the downcomers, no advantage was taken of the option to use test results to provide higher allowables.

Damping values of  $1/2\%$  and  $1\%$  were used for OBE and SSE response spectra analyses on piping under any service limits.

The maximum horizontal response spectra for SRV related and LOCA related load are assumed to act on both N-S and W-E directions simultaneously.

The cut-off frequency generally exceeds the 33 Hz for seismic and 60 Hz for SRV and LOCA related loads.

The modal responses are combined using the square root of the double sum method which is conservative with respect to the SRSS method recommended by ASME Appendix L.

Elastic models were used in the analyses which are more conservative than elastic-plastic models.

The conservatisms summarized above provide a satisfactory basis on which to proceed with the operation of the piping systems in the plant.

Conservatisms in equipment reevaluation is assured by:

- a. Use of lower damping values than what is recommended by Regulatory Guide 1.61 and IEEE 344-1975.
- b. The resultant radial horizontal response spectrum curves were used in both the horizontal directions simultaneously along with the vertical curve.
- c. Used response spectrum curves than time-history analysis.
- d. Pool dynamics response spectra peaks were broadened at least 15%.

#### 8.1.4 Conservatism in NSSS Design

General Electric is conservatively reevaluating the nuclear steam supply system equipment using a bounding loads approach as discussed throughout this report. However, the conservatisms used are summarized in the following discussion.

The conservative dynamic analysis methods being used have been compared to the nuclear industry practiced methods. The methods compared were:

- a. equipment damping values based on seismic,
- b. response spectra peak broadening limits for suppression pool hydrodynamic and annulus pressurization responses,
- c. combining of primary and secondary loads from the same dynamic event, and
- d. combining of closely spaced modes.

Additionally, the conservative approach for using envelop response spectra at all primary piping attachment points were discussed for nonbounding loads. A conservative screening approach was used for analyzing structure mounted/supported mechanical equipment (that is 1.5 times the peak response spectra acceleration without reference to the equipment actual characteristic frequency).

The reactor pressure vessel supports and internal components are being reviewed and reevaluated using the maximum translation forces and moments within the load combination/acceptance criteria levels.

To support the licensing of the lead Mark II plants the alternate "provisional assessment," using more restrictive load combination methods and acceptance criteria, is being conducted in parallel.

## 8.2 PLANT STRUCTURAL MARGINS DURING MAXIMUM TRANSIENT CONDITIONS

The maximum hydrodynamic loads which will occur during plant operating transients are associated with the actuation of all 18 SRV's. This is the maximum hydrodynamic load anticipated during the life of the plant.

Load combination Equation 1 in Table 4.1-1 represents this loading. It should be noted that the following overload factors have been applied to the loads in this load combination equation:

<u>LOAD</u>	<u>OVERLOAD FACTOR</u>
Dead Load	1.4
Live Load	1.7
Prestress	1.0
SRV - ALL	1.5

Conservative margin factors for this load combination were reported in Tables 5.1-1 through 5.1-13. These safety margins are available in addition to the load factors listed above. Also, these margin factors will be much larger if the conservatisms listed in Subsection 6.1.2 were removed.

Margin factors for the containment structure during the maximum transients are presented in Table 8.2-1. Based on these margin factors, it can be concluded that public safety is not risked for normal and abnormal conditions.

TABLE 8.2-1

MARGIN FACTORS FOR CONTAINMENT DURING MAXIMUM TRANSIENT CONDITIONS\* (1.5 TIMES SRV-ALL)

STRUCTURAL STRESS ELEMENT**/COMPONENT	REINFORCING TENSION		CONCRETE COMPRESSION		SHEAR	
	MARGIN*** FACTOR	CRITICAL† SECTION	MARGIN FACTOR	CRITICAL SECTION	MARGIN FACTOR	CRITICAL SECTION
Containment	12.09	1	1.95	1	1.44	13
Basemat	1.56	2	6.08	2	1.33	2
Reactor Support	3.7	1	8.31	1	7.52	16
Drywell Floor	5.6	3	11.2	3	4.1	1

\*Transient as defined in FSAR Chapter 15.0

\*\*Refer to Table 4.1-1

\*\*\*Margin Factor = Allowable Stress/Actual Stress

†Refer to Figure 5.1-2 and 5.1-3

NA = Not Applicable

020 111 1111

9.0 CONCLUSIONS

All suppression pool hydrodynamic forcing functions which are considered in the final assessment of the La Salle County Station are identified in this report. It is our belief that these forcing functions and assessment methods are consistent with the requirements of NUREG-0487 or alternative methods accepted by the NRC staff. The report includes summary descriptions and references appropriate documents for more detailed descriptions of the very conservative forcing functions applied for the final assessment of La Salle County Station. As described in this report, these forcing functions include the Mark II containment "Lead Plant" information and information which has been used in response to comments from the NRC staff and consultants. With the information included in this report or referenced by this report, the NRC will have adequate information to determine that suppression pool hydrodynamic forcing functions have been satisfactorily identified and described for the final assessment of La Salle County Station.

For loss-of-coolant accident (LOCA) loads related to functioning of the main suppression pool vents, the forcing functions are defined with certainty, because the forcing functions are based primarily on the results of full-scale tests which simulate Mark II containment conditions. In our judgment, the description of these LOCA forcing functions in this report are conservative and consistent with our understanding of NUREG-0487.

For loads associated with operation of the safety/relief valves (SRV), the forcing functions used have been those developed for the "rams head" discharge device. On the basis of assessments described in this DAR, it is our judgment that La Salle County Station will satisfactorily carry the loads and load combinations resulting from the rams head

or T-quencher forcing function described in this report.

To bound any uncertainties in the SRV forcing functions and to expedite NRC approval, T-quenchers are being installed prior to startup.

The final assessment of La Salle County Station including suppression pool hydrodynamic loads is described in this report. This assessment was performed using conservative load combinations, acceptance criteria, and methodology. For La Salle County Station, some of these items are being treated in a more conservative manner than established in the Dynamic Forcing Function Report of the Mark II Owners Group. In our judgment, the Owners Group positions are appropriate and technically preferred; however, to expedite NRC approval, a more conservative position consistent with NUREG-0487 will be used for the evaluation of the La Salle County Station. With the information included in this report or referenced by this report, the NRC will have adequate information to determine that suppression pool hydrodynamic forcing functions have been properly included in the final design assessment of La Salle County Station.

APPENDIX ACOMPUTER PROGRAMSA.1 DYNAX

DYNAX (Dynamic Analysis of Axisymmetric Structures) is a finite element program capable of performing both static and dynamic analyses of axisymmetric structures. Its formulation is based on a small displacement theory.

Three types of finite elements are available; quadrilateral, triangular, and shell. The geometry of the structure can be general as long as it is axisymmetric. Both the isotropic and orthotropic elastic material properties can be modeled. Discrete and distributed springs are available for modeling elastic foundations, etc.

For static analysis, input loads can be structure weight, nodal forces, nodal displacements, distributed loads, or temperatures. Loads can be axisymmetric or nonaxisymmetric. For the solids of revolution, the program outputs nodal displacements, and element and nodal point stresses in the global system (radial, circumferential, and axial). In the case of shells of revolution, the output consists of nodal displacements, and element and nodal point shell forces in a shell coordinate system (meridional, circumferential, and normal).

For dynamic analysis, three methods are available; direct integration method, modal superposition method, and response spectrum method. In the case of dynamic analysis by direct integration method or modal superposition method, a forcing function can be input as, (1) nodal force components versus time for any number of nodes, or (2) vertical or horizontal ground acceleration versus time. For nonaxisymmetric loads the equivalent Fourier expansion is used. In the case of dynamic analysis by response spectrum method, spectral velocity versus natural frequency for up to four damping

constants is input. The output of dynamic analysis is in terms of nodal displacements, element stresses and resultant forces and moments at specified time steps. When the modal superposition method is used, and in the case of earthquake response analysis, the requested number of frequencies and mode shapes are computed and printed together with the cumulative response of all the specified modes, as computed by the root sum square (R.S.S.) method and the absolute sum method.

DYNAX was originally developed under the acronym ASHAD by S. Ghosh and E. L. Wilson of the University of California, Berkeley, in 1969. It was acquired by Sargent & Lundy in 1972 and is operating under EXEC 8 and a UNIVAC 1106.

#### A.2 FAST

FAST is used primarily for the dynamic analysis of linear axisymmetric structures using transfer functions (modeled as a multi-degree-of-freedom system). The structural model is given as input either in the form of its eigenvalues, eigenvectors, participation factors and modal damping ratios, or in the form of its responses for a typical dynamic load. This program is used to obtain the time history, transfer function and response spectra for various response components of the model. The results are given in print and plot forms.

FAST was developed at Sargent & Lundy in 1975. It is currently maintained on a UNIVAC 1106 operating under EXEC 8.

#### A.3 KALSHEL

KALSHEL (Kalnins' Shell of Revolution) is a computer program used to analyze thin axisymmetric shells of revolution for arbitrary load conditions. The solution is obtained by transforming the H. Reissner-Neisser equations to eight first-order ordinary differential equations. An Adams method

of numerical integration is used as a basis for the solution of transformed equations. Since the program is based on classical shell theory, it is the same limitations.

The shell wall may vary in thickness along the meridian and consists of up to four layers of different isotropic or orthotropic materials. Branch shells may be connected to the main shell. Surface loads and line loads in the radial, tangential and/or meridional directions and meridional moments as well as temperature distributions, which are assumed to vary linearly across the thickness, may be considered in the analysis. All loads may be asymmetric.

The program output includes shell displacements in the radial, tangential and meridional directions, meridional rotations, meridional moment, hoop moment, meridional force, hoop force, transverse shear force and twist shear force. In addition, outer fiber stresses calculated from the stress resultants may be obtained.

The program was originally developed by A. Kalrins of Lehigh University. It was acquired by Sargent & Lundy in 1969. This version was modified by Sargent & Lundy to sum displacements and stress resultants of the individual Fourier harmonics along meridians at specified angles. The program is currently maintained on the Sargent & Lundy UNIVAC 1106 operating under EXEC 8.

#### A.4 TEMCO

TEMCO (Reinforced Concrete Sections Under Eccentric Loads and Thermal Gradients) analyzes reinforced concrete sections subject to separate or combined action of eccentric loads and thermal gradients. The effect of temperature is induced in the section by reactions created by the curvature restraint.

The analysis may be done assuming either a cracked or an uncracked section. Material properties can be assumed to be either linear or nonlinear. The program is capable of handling rectangular as well as nonrectangular sections.

The program input consists of section dimensions, areas and location of each layer of reinforcing steel, loads, load combinations and material properties.

The curvature and axial strain corresponding to the given eccentric loads (axial load and bending moment) are determined by an iterative procedure. Thermal gradient is applied on the section by inducing reactions created by the curvature restraint, i.e., there is no curvature change due to a thermal gradient on the section. The axial expansion is assumed to be free after thermal gradient is applied. An iterative procedure is employed again for finding the final strain distribution such that equilibrium of internal and external loads is satisfied.

The program output consists of the echo of input, combined loads, final location of neutral axis, final stresses in steel and concrete and final internal forces. Similar intermediate results (before thermal gradient is applied) can be output if desired.

The program has applications to a wide variety of reinforced concrete beams and columns, slabs, and containment structures, subject to various combinations of external loads and thermal gradients.

The program was developed and is maintained by Sargent & Lundy. Since February 1972, the program has been used extensively at Sargent & Lundy on UNIVAC 1106 hardware operating under EXEC 8.

#### A.5 PIPSYS

PIPSYS (Piping Analysis Information System) is the primary program used in the analysis of stresses on piping systems. It is a composite of several lesser programs. It combines thermal, weight, and seismic analysis into one program. It may also be broken down into a static analysis portion, a dynamic analysis portion, and a stress combination portion which is in accordance with ASME Boiler and Pressure Vessel Code, Section III, Articles NB-3000 and NC-3000.

NUPIPE subroutine is the nuclear code part which combines and computes the stresses in piping components according to ASME Boiler and Pressure Vessel Code, Section III, Articles NB-3000 and NC-3000. It was validated by intercomparison with the results of a Teledyne Corporation program for the same sample problem. The final results were essentially identical.

Like NUPIPE, TEE is also an independent program as well as a subroutine of PIPSYS. It also was validated by hand calculation for an identical problem to that processed by the computer.

TEE determines the blowdown force at the discharge pipe due to the sudden opening of a safety/relief valve. It calculates the stress levels at the branch intersection points and valve outlets according to Power Piping Code ANSI B31.10. Finally, it checks the proper discharge pipe sizing at the valve outlet in order to sustain the dynamic force due to the valve blowout.

DYNAPIPE analyzes the dynamic model and upper bound response of a structure (modeled as a space frame) subjected to prescribed dynamic forces at discrete points or subjected to

earthquake type motion prescribed as acceleration response spectra. Elbows and tees are treated as per piping code.

#### A.6 RSG

RSG (Response Spectrum Generator) generates dynamic response spectra (displacement, velocity and acceleration) for single-degree-of-freedom elastic systems with various dampings, subjected to a prescribed time dependent acceleration.

The program may also be used to obtain a response spectrum-consistent time-history in which the response spectrum of the generated time-history closely envelopes the given spectrum. The differential equation of motion is solved using Newmark's  $\beta$ -method of numerical integration.

The program has the capability of plotting the input time-acceleration function and the response spectra output on the tripartite and/or acceleration versus period frequency grids.

Depending on the option, the program output includes the response spectra of a given time-history or the response spectrum-consistent time-history.

RSG was developed by Sargent & Lundy in 1969. Since 1972 the program has been maintained on UNIVAC 1106 hardware operating under EXEC 8.

#### A.7 SRVA

SRVA is a finite difference program for the analysis of transient flow in a relief valve line discharging to the suppression pool through a rams head or quencher. Transient forces and the pressures at the water column and the valve outlet are calculated for relief valve lines with up to 20 straight segments. Frictional effects as well as losses at

at elbows and the rams head outlet are included.

Output force-time data is compatible with PIPSYS, and force-time history is plotted by a plot subroutine.

The discharge pipe is idealized as straight and uniform. An effective friction coefficient increased to account for the effects of elbows is used.

A finite difference method is used to solve the Eulerian formulation of the basic one-dimensional flow equations, with the effects of friction and of heat transfer to the pipe wall included. The submerged end boundary conditions are found by integrating the equation of motion of the water slug step by step in time. After the water column is expelled, choked flow at the outlet is assumed.

B.O RESPONSE TO NRC QUESTIONS

Appendix B provides a list of the NRC questions by date, which were submitted after Revision 0 of the DAR, and an index giving the particular section(s) of the DFFR or DAR report, where the detailed answers have been provided. Some of the answers have been incorporated in both reports, while others only in one of the reports according to their applicability.

In the interest of completeness and continuity, the responses to NRC questions are presented in this appendix as they were originally submitted or last revised. The revision and date at the top of each page indicates when the respective response was submitted/last revised. It should be noted that the DAR/DFFR sections referenced in the responses may have been re-numbered in subsequent revisions and that redesign or more recently submitted responses to NUREG-0487 may have superseded the original responses as presented here.

QUESTION 020.62

"For the suppression pool temperature monitoring system, provide the following additional information:

1. Type, number and location of the temperature instrumentation that will be installed in the pool.
2. Discuss and justify the sampling or averaging technique that will be applied to arrive at a definitive pool temperature."

RESPONSE

See revised Chapter 6.0.

THIS PAGE INTENTIONALLY LEFT BLANK

## C.0 SUBMERGED STRUCTURE METHODOLOGY

### C.1 Introduction

Mark II suppression pools are expected to experience fluid motion as a result of safety/relief valve (SRV) actuation and postulated loss-of-coolant accident (LOCA). The velocity and acceleration fields will cause drag loads on submerged structures in the pool. These loads have been calculated in the past by assuming the existence of a uniform flow field and applying steady-state standard and acceleration drag coefficients. The NRC Lead Plant Acceptance Criteria (NUREG-0487, October 1978) pointed out that this method might not be conservative under certain flow conditions and for certain structure geometries. This appendix explains the methods used by the lead plants to ensure that the design loads are conservative.

Subsection C.2 presents a method of evaluating the correction to both standard and acceleration drag coefficients in unsteady flow and a method to evaluate the transverse (lift) force in this flow. Subsections C.3 and C.4 describe the effect of neighboring structures on the submerged structure drag loads. This method provides modified drag coefficients for the range of geometries existing in Mark II plants.

Subsection C.5 presents the results of sensitivity studies which verify the adequacy of the nodalization used in predicting loads. These studies show that increasing the number of points at which loads are calculated will not make significant changes in the result.

All of the drag coefficients used for submerged structure load calculations for each particular accident condition were determined directly from the data that are presented in the References shown in Section C.7. In addition, all

modifications made to the drag coefficients describing the effects of neighboring structures and unsteady flow were also based on actual data listed in the References in Section C.7. The theory provided in this section is utilized as background information and provides support to the load calculations performed on this plant. The theory presented also addresses the concerns raised in the NRC Lead Plant Acceptance Criteria (NUREG-0487, October 1978).

## C.2 Drag and Lift Coefficients for Unsteady Flow

### C.2.1 General Considerations

Drag and lift loads on submerged structures in the suppression pool due to the LOCA charging air bubble, pool swell, fallback, and the SRV air bubble are considered. In calculating these loads on submerged structures, acceleration and standard drag and lift coefficients are used whenever they are applicable to a specific situation. The effects of unsteady flow on the above mentioned coefficients are treated in this subsection, and interference effects, if present, are addressed in Subsections C.3 and C.4. The steady-state drag coefficients are corrected appropriately to include the effects of unsteady flow.

Because the majority of the available data for unsteady flow have been developed for a cylinder, the discussion provided herein is in terms of a cylinder. The structures in the La Salle suppression pool are all cylindrical. If differently shaped structures were present, a cylinder with an equivalent diameter would be used for calculations. This approach is conservative for drag load calculations, with the possible exception of the prediction of initiation of vortex shedding. Lift forces due to vortex shedding on sharp-edged structures would be calculated conservatively based on available data.

Possible shapes of submerged structures in a Mark II suppression pool include circular cylinders, box beams and I-beams. Equivalent diameters can easily be determined for these structures.

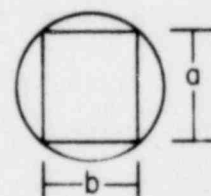
First, to determine the unsteady effects on a submerged structure, a circular cylinder with an equivalent diameter

is considered. Then, from the appropriate literature, the drag coefficients due to unsteady flow for cylinders are determined, and a drag coefficient multiplier is calculated as the ratio of the unsteady drag coefficients to the steady-state drag coefficients. Finally, these multipliers are applied to the steady-state drag coefficients of the particular submerged structure of interest. However, in computing the loads, the actual dimensions of the structure are utilized in order to properly determine the loads.

To determine the equivalent diameter, the length of the particular structure is conserved and an equivalent diameter is then determined by circumscribing a circle about any structure (Reference 1, pg. 4-14). For a cylinder, the equivalent diameter is equal to the diameter of the cylinder.

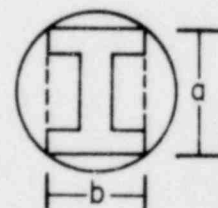
If a box beam is considered, its equivalent diameter is:

$$D_{EQ} = \sqrt{a^2 + b^2}$$



For an I-beam, the equivalent diameter is:

$$D_{EQ} = \sqrt{a^2 + b^2}$$



The nondimensional numbers on which drag coefficients depend are based on the equivalent diameter. They are:

$$a. \text{ Reynolds number} - Re = \frac{U_m D_{EQ}}{\nu}$$

b. Period parameter -  $K = \frac{U_m T}{D_{EQ}}$

c. Strouhal number -  $S = \frac{f D_{EQ}}{U_m}$

where:

$U_m$  = maximum velocity at the location of the loaded structure during the transient,

$D_{EQ}$  = equivalent diameter,

$T$  = period of flow oscillation,

$f$  = vortex shedding frequency, and

$\nu$  = kinematic viscosity.

In order to properly determine the effect of unsteady flow, a drag coefficient multiplier is defined as the ratio of the unsteady to steady-state drag coefficients:

$$f_d = \frac{C_{D1}}{C_D}$$

$$f_m = \frac{C_{M1}}{C_M}$$

where:

$C_D$  = steady-state standard drag coefficient,

$C_{D1}$  = unsteady standard drag coefficient,

$C_M$  = steady-state acceleration drag coefficient,

$C_{M1}$  = unsteady acceleration drag coefficient,

$f_d$  = standard drag coefficient multiplier, and

$f_m$  = acceleration drag coefficient multiplier.

These factors are based on drag coefficients for circular cylinders. Once they are determined for cylinders utilizing the appropriate data, the factors are applied to the steady-state drag coefficients for the particular structure of interest. These steady-state drag coefficients are described in Reference 1. The factors are applied in the following manner:

$$C_{D3} = f_d C_{D2}$$

$$C_{M3} = f_m C_{M2}$$

where:

$C_{D2}$  = steady-state standard drag coefficient for the particular submerged structure,

$C_{D3}$  = corrected unsteady standard drag coefficient,

$C_{M2}$  = steady-state acceleration drag coefficient for the particular submerged structure, and

$C_{M3}$  = corrected unsteady acceleration drag coefficient.

The lift coefficients are determined utilizing the actual lift data for the specific structure analyzed for the applicable transient conditions.

However, if submerged structures of unique shapes are encountered in the suppression pool, they need to be considered on a plant-unique basis.

Finally, when all the coefficients are determined, the standard and acceleration drag forces are calculated based on the corrected drag coefficients and the actual structure dimensions. The sum of these forces is the in-line force.

The transverse force consists only of lift. The following equations present the contributions of the standard and acceleration drag forces to the in-line force:

$$F_S = \frac{C_{D3} A \rho U(t) |U(t)|}{2 g_C}$$

$$F_A = \frac{C_{M3} V_S \rho \dot{U}(t)}{g_C}$$

$$F_{IN-LINE} = F_S + F_A$$

where:

$F_S$  = standard drag force,

$F_A$  = acceleration drag force,

$F_{IN-LINE}$  = total in-line force,

$C_{D3}$  = corrected unsteady standard drag coefficient,

$C_{M3}$  = corrected unsteady acceleration drag coefficient,

$A$  = projected area of submerged structure,

$V_S$  = volume of submerged structure,

$\rho$  = fluid density,

$U(t)$  = velocity in the in-line direction, and

$\dot{U}(t)$  = acceleration in the in-line direction.

The determination of the lift force is considered separately in each of the following sections.

### C.2.2 LOCA Charging Air Bubble

The LOCA charging air bubble is considered to be a non-oscillatory accelerating flow. It is readily observed from the velocity and acceleration time histories of the transient (Figures C-1 and C-2) that the transient exhibited an increasing velocity and high positive values of acceleration. In addition, the fluid flow never reverses and the acceleration is nearly constant. This is true for all locations in the suppression pool. Comparing typical velocity time histories (Figure C-1) to acceleration time histories (Figure C-2), one can observe that the acceleration is the major contributor to the drag load, since the velocity is small. The velocity and acceleration time histories were generated utilizing the LOCA charging air bubble model described in Reference 1.

The geometric configuration that was utilized to determine the LOCA charging air bubble transient on a submerged structure is shown in Figures C-3 and C-4. A 36° segment of a typical Mark II suppression pool was utilized which contained 10 downcomers. The LOCA charging air bubbles were used at these downcomer locations to determine the velocity and acceleration time histories on a vertical submerged structure in the pool.

For this transient, Reference 2 is utilized in determining the standard and acceleration drag coefficients, which are conservatively taken as 1.2 and 2.0, respectively.

Due to the low velocities and small duration of this transient, lift due to vortex shedding is not present. In Reference 2, the author indicates that for unsteady flow, no lift force due to vortex shedding is present for small-period parameters. In addition, the author states that for a fluid starting from rest, a certain finite time is required for separation to occur if vortex shedding is to be present.

With the information in Reference 2, it was determined that the time required for separation to occur was longer than the duration of the LOCA charging air bubble transient (see the following discussion). Therefore, lift due to unsteady flow effects is not considered for this transient.

#### Lift Due to Vortex Shedding

According to Reference 2, the separation necessary for vortex shedding to be present does not occur until a fluid has moved a distance:

$$S = 0.293D$$

where:

S = traveled distance, and

D = cylinder diameter.

The authors also state in Reference 2 that:

$$S = \frac{1}{2} Vt$$

where:

V = velocity, and

t = time for separation to occur.

Assuming a representative case for LOCA charging air bubble velocity in a Mark II suppression pool, the maximum pipe diameter required for separation to occur can be determined. A linear velocity increase from 0.0 to 3.0 ft/sec was assumed to closely resemble the actual transient velocity with a transient duration of 60 msec. Integrating the velocity, a traveled distance S of 0.09 foot was determined. Utilizing the above mentioned equations, the traveled distance

translates to a maximum pipe diameter of 3-1/2 inches. In other words, for a pipe with a diameter of 3-1/2 inches that experienced a velocity transient increasing linearly from 0.0 to 3.0 ft/sec, separation would occur at 60 msec. This is the time when the LOCA charging air bubble transient has ended.

Following this procedure for other piping within the suppression pool experiencing the LOCA charging air bubble transient, it can be concluded that lift due to vortex shedding is not present and does not need to be considered for Mark II pool geometries.

### C.2.3 Pool Swell

Pool swell is regarded as being an oscillatory flow, with the pool swell duration considered to be the half period of the flow field. This flow is exhibited by experimental data, namely, the EPRI and 4T tests. For Reynolds numbers in the subcritical region, the drag coefficients are determined from Reference 3. These drag coefficients are dependent only on the period parameter. However, if the Reynolds number is in the supercritical region ( $>4 \times 10^5$ ), the steady-state standard drag coefficient reduces from 1.2 to 0.71 (Reference 4). To determine the unsteady standard and acceleration drag coefficients for flow at the supercritical Reynolds numbers, Reference 5 is utilized which correlates the Reynolds number, period parameter, and the pipe roughness to both the standard and acceleration drag coefficients. The correlations for smooth pipes are used since these correlations best represent the structures within the Mark II suppression pool.

In addition, lift due to vortex shedding is considered. Reference 6 provides the necessary information to determine lift loads. As before, the lift coefficient is based on the period parameter and the Reynolds number where both are

evaluated at the maximum velocity observed in the transient. Moreover, the vortex shedding frequency must also be defined. Reference 5 provides a correlation of  $f_r$ , the relative frequency, to the period parameter and the Reynolds number evaluated at the maximum velocity.

$$f_r = \frac{f_v}{f_w}$$

where:

$f_r$  = relative frequency,

$f_v$  = vortex shedding frequency, and

$f_w$  = oscillating fluid frequency.

However, if the relative frequency falls out of the range shown in Figure 21 of Reference 5, Reference 6 indicates that a Strouhal number of 0.3 should be utilized at high Reynolds numbers.

When determining the lift force due to vortex shedding, the maximum amplitude is based on the maximum velocity the structure sees (Reference 6):

$$F_L = C_L \frac{A \rho U_m^2 \sin 2 \pi f_v t}{2g_c}$$

where:

$F_L$  = lift force (transverse to flow direction),

$C_L$  = lift coefficient,

$A$  = projected area of structure,

$\rho$  = fluid density,

$U_m$  = maximum in-line velocity the structure observes,

$f_v$  = vortex shedding frequency, and

$t$  = time.

The vortex shedding frequency is specified from the correlation mentioned previously. With the maximum amplitude and frequency, the lift force is defined. The lift force varies with time and is sinusoidal in nature for viscous lift.

In this case, the acceleration drag force considers the effect of gravity and is determined in the following manner:

$$F_A = \frac{V_S \rho C_{M3} \dot{U}(t)}{g_C}$$

where:

$F_A$  = acceleration drag force,

$V_S$  = volume of submerged structure,

$C_{M3}$  = corrected unsteady acceleration drag coefficient,

$\dot{U}(t)$  = acceleration in the in-line direction,

$g_C$  = gravitational acceleration, and

$\rho$  = fluid density.

#### C.2.4 Fallback

Fallback is considered to be a constantly accelerating flow. It is assumed that fallback behaves as a falling water slug. For this case, the standard and acceleration drag coefficients are determined from Reference 2. As with pool swell,

the lift coefficients due to vortex shedding are also determined. The lift coefficient is given by Reference 7 as  $C_L = 1.0$  for Kármán vortices. In order to determine the vortex shedding frequency, Reference 7 indicates that a Strouhal number of 0.22 should be utilized. This is also substantiated by Reference 8. The force is then determined as:

$$F_L = \frac{C_L A \rho U_m^2 \sin 2 \pi f_v t}{2g_c}$$

where:

$F_L$  = lift force,

$C_L$  = lift coefficient,

$A$  = project area,

$\rho$  = fluid density,

$U_m$  = maximum in-line velocity the structure observes,

$f_v$  = vortex shedding frequency, and

$t$  = time.

In this case, the acceleration drag force is determined in the following manner:

$$F_A = \frac{C_H g V_S \rho}{g_c}$$

where:

$F_A$  = acceleration drag force,

$C_H$  = hydrodynamic mass coefficient ( $C_H = C_M - 1$ ),

$V_S$  = volume of submerged structure,

$g$  = gravitational acceleration, and

$\rho$  = fluid density.

#### C.2.5 SRV Air Bubbles

SRV air bubbles are considered to be of oscillatory nature. Reference 3 is utilized to determine the unsteady standard and acceleration drag coefficients. These drag coefficients are based on the period parameter evaluated at the maximum velocity. However, if the unsteady drag coefficients are less than the steady-state drag coefficients, then the steady-state drag coefficients are utilized for load determination. If any lift is present, Reference 3 is used, which also bases the lift coefficients on the period parameter. This reference mentions that no lift is present for period parameters less than 5. The drag loads are determined as described in Subsection C.2.1.

### C.3 Interference Effects on Acceleration Drag

When submerged structures are closely located in a flow field, they can interfere with one another, affecting the acceleration drag. The proximity effect can be accounted for by either 1) utilizing actual data that is presented in References 12, 14, and 15, 2) performing a detailed analysis, or 3) applying a conservative factor of 4 on the acceleration drag. For the La Salle plant, actual data that are presented in References 12, 14, and 15 were utilized to determine the interference effects on acceleration drag.

A detailed method is presented for determining interference effects of nearby cylinders and/or a boundary on the acceleration drag for circular cylinders and is based on References 9 through 14.

According to the method, the interference effect between any two stationary cylinders can be completely determined by six force coefficients which are functions solely of the radius ratio and the relative spacing. For the case of more than two cylinders, the total proximity effect on a given cylinder may be approximately obtained simply by superimposing each interference effect between cylinder pairs.

#### C.3.1 Method of Analysis

The following assumptions are considered in the method:

- a. Two-dimensional potential flow without separations and wakes is considered.
- b. The velocity and acceleration in the flow field are the same as those seen locally by the submerged structure (cylinder).
- c. The containment and pedestal walls are considered as plane boundaries.

## d. Coordinate system

+x : radially outward from reactor pressure vessel centerline.

+y : vertically upward.

+z : by right-hand rule parallel to the plane boundary.

Origin: at the center of cylinder in question.

C.3.2 Two Stationary Cylinders (Real Cylinders)

If the p-th cylinder is isolated in a free stream, the hydrodynamic (acceleration drag) force per unit length of the cylinder is:

$$F_{po} = 2\rho\pi A_p^2 \dot{U}_{\infty n}$$

where:

$F_{po}$  = acceleration drag force per unit length,

$\rho$  = fluid density,

$A_p$  = radius of p-th cylinder, and

$\dot{U}_{\infty n}$  = acceleration normal (in-line) to p-th cylinder.

When the n-th cylinder is in the vicinity of the p-th cylinder, as shown in Figure 1, the change in the force of the p-th cylinder,  $\Delta F_{pn}$ , is:

$$\begin{aligned} \Delta F_{pn} = & \rho\pi A_p^2 |\dot{U}_{\infty n}| \left\{ (C_1 - 1) \exp(i\alpha_1) - C_2 \exp[i(2\beta_{pn} - \alpha_1)] \right\} \\ & + \rho A_p |\dot{U}_{\infty n}|^2 \left\{ (C_3 + C_4) \exp(i\beta_{pn}) - C_5 \exp[i(3\beta_{pn} - 2\alpha_2)] \right. \\ & \left. - C_6 \exp[i(2\alpha_2 - \beta_{pn})] \right\} \end{aligned}$$

where:

$U_{\infty n}$  = velocity normal (in-line) to the p-th cylinder,

$\alpha_1 = \text{Arg} (\dot{U}_{\infty n})$ , angle of acceleration with respect to z-axis,

$\alpha_2 = \text{Arg} (U_{\infty n})$ , angle of velocity with respect to z-axis, and

$\beta_{pn}$  = angle between the line through centers of cylinders and the z-axis.

$$C_1 = 1 + 2 \sum_{j=1}^{\infty} b_{1,2j+1}$$

$$C_2 = 2 \left( \frac{A_n}{A_p} \right)^2 \sum_{j=1}^{\infty} b_{1,2j+1}$$

$$C_3 = 4\pi \sum_{k=1}^{\infty} \sum_{j=1}^{\infty} \frac{b_{1,2k-1} b_{2,2j}}{\left( \frac{L_{pn}}{A_p} - q_{1,2k-1} - \frac{A_n}{A_p} q_{2,2j} \right)^3}$$

$$C_4 = 4\pi \left( \frac{A_n}{A_p} \right)^4 \sum_{k=1}^{\infty} \sum_{j=1}^{\infty} \frac{b_{1,2k-1} b_{2,2j-1}}{\left( \frac{L_{pn}}{A_p} - q_{1,2k} - \frac{A_n}{A_p} q_{2,2j-1} \right)^3}$$

$$C_5 = 4\pi \left( \frac{A_n}{A_p} \right)^2 \sum_{k=1}^{\infty} \sum_{j=1}^{\infty} \frac{b_{1,2k-1} b_{2,2j-1}}{\left( \frac{L_{pn}}{A_p} - q_{1,2k-1} - \frac{A_n}{A_p} q_{2,2j-1} \right)^3}$$

$$C_6 = 4\pi \left( \frac{A_n}{A_p} \right)^2 \sum_{j=1}^{\infty} \sum_{k=1}^{\infty} \frac{b_{1,2k} b_{2,2j}}{\left( \frac{L_{pn}}{A_p} - q_{1,2k} - \frac{A_n}{A_p} q_{2,2j} \right)^3}$$

where:

$$b_{1,1} = 1$$

$$b_{2,1} = 1$$

$$b_{1,m} = b_{2,m-1} q_{1,m}^2 \quad \text{for } m \geq 2$$

$$b_{2,m} = b_{1,m-1} q_{2,m}^2 \quad \text{for } m \geq 2$$

in which:

$$q_{1,1} = 0,$$

$$q_{2,1} = 0,$$

$$q_{1,j} = \frac{A_p}{L_{pn} - A_n q_{2,j-1}} \quad \text{for } j \geq 2,$$

$$q_{2,j} = \frac{A_n}{L_{pn} - A_p q_{1,j-1}} \quad \text{for } j \geq 2,$$

$A_n$  = radius of the n-th cylinder, and

$L_{pn}$  = distance between the centers of cylinders.

### C.3.3 Stationary Cylinders Near a Plane Boundary (Real and Imaginary Cylinders)

A single stationary cylinder in a uniform stream,  $U_{\infty n}$ , is hydrodynamically equivalent to a cylinder moving at a speed  $-U_{\infty n}$  in a still fluid, except that the former cylinder experiences an extra force,  $\rho \pi A_p^2 \dot{U}_{\infty n}$ , from the pressure field that has been created to provide the fluid acceleration,  $\dot{U}_{\infty n}$ . This is also true for any number of cylinders if the cylinders move together.

When a cylinder is moving in an arbitrary direction (on a line or on a curve) with respect to the plane boundary, it can be considered as two equal cylinders moving symmetrically with respect to the plane boundary, since the plane acts as a perfect reflector (mirror) of the hydrodynamic pressure. A similar argument can be applied to multiple cylinders.

Based on the above discussion, the plane boundary can be removed and replaced by an imaginary cylinder of the same size as the original (real) cylinder and located at twice the distance between the real cylinder and the plane boundary away from the original cylinder. Similarly, multiple imaginary cylinders can be obtained by reflecting those multiple real cylinders near the plane boundary.

Now if the n-th imaginary cylinder is in the proximity of the p-th cylinder, the change in the hydrodynamic force of the p-th cylinder,  $\Delta F_{pn}$ , can be derived from Reference 9 and is:

$$\Delta F_{pn} = \rho \pi A_p^2 |\dot{U}_{\infty n}| \left\{ (C_1 - 1) \exp(i\alpha_1) - C_2 \exp[i(\alpha_1 + 2\beta_{pn})] \right\} \\ + \rho A_p |\dot{U}_{\infty n}|^2 \left\{ (C_3 + C_4) \exp(i\beta_{pn}) - C_5 \exp(i3\beta_{pn}) - C_6 \exp(-i\beta_{pn}) \right\}$$

where:

$C_1$  through  $C_6$  are the same as described earlier.

#### C.3.4 Total Acceleration Drag Force

Summing up each effect from all the surrounding N real and imaginary cylinders, the force on the p-th cylinder is approximately given as:

$$F_p = F_{p0} + \sum_{\substack{n=1 \\ n \neq p}}^N \Delta F_{pn} = 2\rho\pi A_p^2 \dot{U}_{\infty n} + \sum_{\substack{n=1 \\ n \neq p}}^N \Delta F_{pn}$$

or:

$$F_p = C_m \rho \pi A_p^2 |\dot{U}_{\infty n}| + C_v \rho A_p |U_{\infty n}|^2$$

where:

$C_m$  = acceleration drag coefficient, and

$C_v$  = convective force coefficient.

### C.3.5 Practical Application

When the increase in force on the p-th cylinder arising from interference effects is calculated, only those real and imaginary cylinders which have a significant contribution should be considered. Significant contributions to the summation equations presented in Subsection C.3.4 arise only from those cylinder pairs within a gap distance of  $3D$ , where  $D$  is the larger diameter of the pair being considered.

If the flow is omnidirectional during a specific transient, a magnification factor  $K_M$  may be obtained from the maximum  $|C_m|$  that is determined in the range of  $0^\circ \leq \alpha_1 \leq 180^\circ$ . This is performed to account for the interference effect on the acceleration drag. Similarly, to account for the lift force, the maximum  $|C_v|$  can be determined by varying  $\alpha_2$  in the range of  $0^\circ \leq \alpha_2 \leq 180^\circ$ . Then the maximum lift coefficient is combined with the standard drag coefficient,  $C_D$ , by the square root of the sum of the squares to include the lift force due to the proximity effect.

The acceleration and drag forces are determined as follows:

$$|F_{Ap}| = \frac{2K_M \rho \pi A_p^2 |\dot{U}_{\infty n}|}{g_c}$$

$$|F_{sp}| = \sqrt{C_D^2 + |C_L|^2} \frac{\rho A_p |U_{\infty n}| U_{\infty n}}{2g_c}$$

where:

$F_{Ap}$  = acceleration drag per unit length on p-th cylinder,

$K_M = |C_m|/2$  magnification factor and  $|C_m|$  is the maximum acceleration drag coefficient,

$\rho$  = fluid density,

$A_p$  = radius of p-th cylinder,

$\dot{U}_{\infty n}$  = acceleration in the normal (in-line) direction to the cylinder,

$U_{\infty n}$  = velocity in the normal (in-line) direction to the cylinder,

$C_D$  = standard drag coefficient,

$|C_L|$  = maximum lift coefficient, and

$F_{sp}$  = standard drag per unit length on p-th cylinder.

The directions of the acceleration and standard drags are the same as those without the interference effect.

However, if the flow field is well defined and the direction of flow known, then the actual acceleration drag and lift coefficients are utilized. In this case, the lift force is applied in the transverse direction. The equations used are then:

$$F_{Ap} = \frac{2 C_m \rho \pi A_p^2 \dot{U}_{\infty n}}{g_c}$$

$$F_{Lp} = \frac{C_L \rho A_p |U_{\infty n}| U_{\infty n}}{2g_c}$$

where:

$C_m$  = acceleration drag coefficient determined through the analysis,

$C_L$  = lift coefficient determined through the analysis, and

$F_{Lp}$  = lift force in the transverse direction.

#### C.3.6 Model/Data Comparisons

The method has been tested numerically as well as experimentally and the results (Figure C-5) indicate excellent agreement with both known numerical values (References 9, 10, 12) and experimental data (References 11, 13).

#### C.4 Interference Effects on Standard Drag

When submerged structures are located closely together in a flow field, they can interfere with one another causing an effect on the standard drag, actual data presented in the references can be utilized, a detailed analysis can be used or a factor of four can be applied to the standard drag force. For the La Salle plant, actual data that are presented in Reference 17 were utilized to determine the interference effects on standard drag.

This section deals with the detailed analysis to determine the interference effects on standard drag.

Three technical papers (References 16 through 18) have described this phenomenon and presented experimental data on interference effects. Most of the data presented in references are applicable to interference between two cylinders. Reference 17 has presented some data for three cylinders whose axes are coplanar. Cylinder spacing, Reynolds number, and the angle between flow direction and the plane containing cylinder axes were varied in the above investigations. In many instances the data obtained from the above references can be applied directly to Mark II suppression pool conditions.

A procedure has been developed to utilize the above data for interference between more than two cylinders. The results have been compared with measured data of three cylinders and are found to be conservative.

##### C.4.1 Interference Between Two Cylinders of Equal Diameter

As indicated by the data given in References 16, 17, and 18, the interference between two parallel cylinders alters the flow direction drag and also induces a lift force normal to flow direction. For two cylinders of equal diameter, the interference effect on drag forces is small, and

in most cases negative (i.e., the drag is reduced due to interference). The lift force, however, is not always insignificant.

The following bounding values for interference between two cylinders of equal diameter can be utilized without any further detailed analysis. A bounding value of  $C_D$  for Reynolds number greater than 8,000 and  $S/d$  ratio greater than 0.2 is 1.4, and the bounding value for  $C_L$  is 1.0.

#### C.4.2 Interference Between More Than Two Cylinders of Equal Diameter

To evaluate the drag coefficient of a cylinder which is interfered by more than one cylinder, the maximum of  $C_{Do}$ ;  $C_{Di}$ ; and  $D_{Di,j}$  should be used.

$$C_{Di} - C_{Do} = \sum_{\substack{j=1 \\ j \neq i}}^n (C_{Di,j} - C_{Do})$$

where:

$C_{Di}$  = standard drag coefficient for the  $i$ -th cylinder,

$C_{Do}$  = standard drag coefficient for a single cylinder without any interference, and

$C_{Di,j}$  = drag coefficient of  $i$ -th cylinder when it is interfered by Cylinder  $j$  alone.

Figure C-6 illustrates an arrangement of cylinders. The standard drag coefficient of Cylinder 1 would be:

$$C_{D1} = C_{Do} + (C_{D1,2} - C_{Do}) + (C_{D1,3} - C_{Do}) + (C_{D1,4} - C_{Do})$$

From this, the maximum value of  $C_{D1}$ ;  $C_{D0}$ ;  $C_{D1,2}$ ;  $C_{D1,3}$ ; and  $C_{D1,4}$  would be used for the standard drag coefficient.

To evaluate the lift coefficient, the maximum of  $C_{Li}$  and  $C_{Li,j}$  should be used:

$$C_{Li} = \sum_{\substack{j=1 \\ j \neq i}}^n C_{Li,j}$$

where:

$C_{Li}$  = lift coefficient of i-th cylinder, and

$C_{Li,j}$  = lift coefficient of i-th cylinder when it is interfered by Cylinder j alone.

From Figure C-6, the lift coefficient would be determined in the following manner:

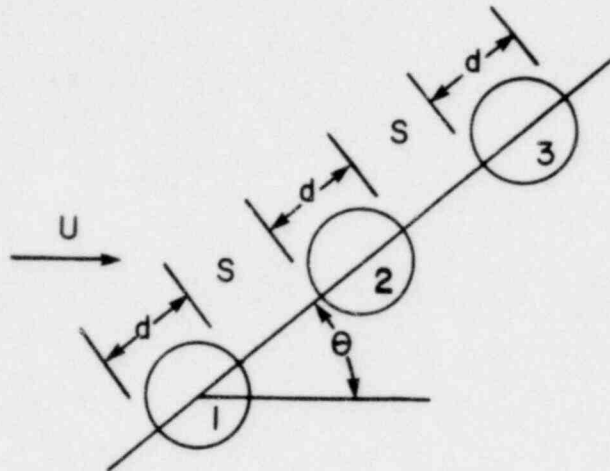
$$C_{Li} = C_{L1,2} + C_{L1,3} + C_{L1,4}$$

The maximum value of  $C_{L1}$ ;  $C_{L1,2}$ ;  $C_{L1,3}$ ; and  $C_{L1,4}$  would be used for the lift coefficient.

The above described method yielding interference on standard drag between more than two cylinders of equal diameter (bounding procedure) is illustrated in the following examples:

Example 1

Consider the three cylinder arrangement shown in the following figure:



Let  $\frac{S}{d} = 1$ ,  $\theta = 60^\circ$ , and  $Re = 2.78 \times 10^4$ .

For this arrangement.

$C_{D1,2}$  = Drag coefficient of Cylinder 1 when interfered by Cylinder 2 only.

$$= 1.01; \left(\frac{S}{d} = 1\right)$$

$$C_{D1,3} = 1.02; \left(\frac{S}{d} = 3\right)$$

$$C_{D0} = 1.16 \text{ [Reference 4, pg. 341]}$$

$$C_{Di} - C_{D0} = (C_{D1,2} - C_{D0}) + (C_{D1,3} - C_{D1})$$

$$C_{Di} = 1.01 + 1.02 - 1.16$$

$$= 0.37$$

$\therefore$  Maximum of  $C_{Di}$ ;  $C_{D1,2}$ ;  $C_{D1,3}$ ;  $C_{D0}$  is 1.16

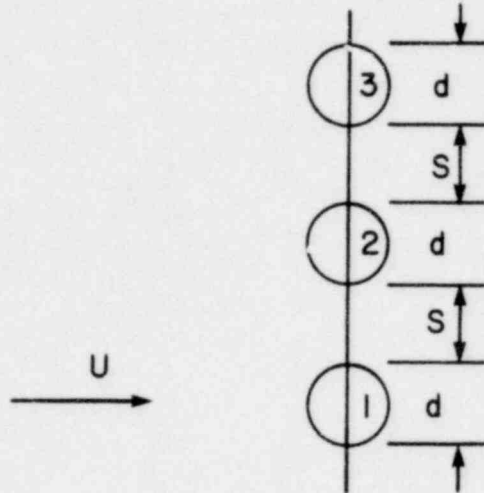
$\therefore$  Use  $C_D = 1.16$

From measurements (Reference 17):

$C_D = 0.97$ , which is less than the calculated drag coefficient.

Example 2

Consider the three cylinder side-by-side arrangement.  
 ( $Re = 2.78 * 10^4$ ,  $\frac{S}{d} = 1$ )



$$C_{D1,2} = 1.03 \left( \frac{S}{d} = 1 \right)$$

$$C_{D1,3} = 1.05 \left( \frac{S}{d} = 3 \right)$$

$$C_{D0} = 1.16$$

$$\therefore C_{D1} - 1.16 = 1.03 - 1.16 + 1.05 - 1.16$$

$$\text{or } C_{D1} = 0.92$$

Maximum of  $C_{D0}$ ;  $C_{D1}$ ;  $C_{D1,2}$ ;  $C_{D1,3}$  is 1.16

$$\text{Use } C_D = 1.16$$

The measured value is 0.98, which is less than the calculated value.

### C.4.3 Drag on Small Cylinder Upstream of Large Cylinder

Figure C-7 presents the flow around cylinders of unequal diameters.

The coordinates of point A (center of smaller cylinder) are  $(-a, b)$ . Let  $R$  and  $R_1$  be the radii of larger and smaller cylinders. The velocity potential of flow around the larger cylinder in the absence of smaller cylinder is

$$\phi = Ux \left( 1 + \frac{R^2}{x^2 + y^2} \right)$$

where:

$\phi$  = velocity potential,

$U$  = free stream velocity, and

$R$  = radius of large cylinder.

If  $u$  and  $v$  are the  $x$  and  $y$  components of velocity at point "A" (smaller cylinder absent) then,

$$u = U \left[ 1 + R^2 \left\{ \frac{b^2 - a^2}{(a^2 + b^2)^2} \right\} \right]$$

and

$$v = \frac{2ab R^2 U}{(a^2 + b^2)^2}$$

where:

$u$  = the velocity parallel to the free stream velocity at the centerline of the smaller cylinder, and

$v$  = the velocity perpendicular to the free stream velocity at the centerline of the smaller cylinder.

In order to use the above velocity correction, it is more convenient to increase the standard drag coefficient and use the corrected standard drag coefficient with the free stream velocity. The standard drag force on the smaller cylinder with interference present is:

$$F_1 = \frac{C_D \rho A (u^2 + v^2)}{2g_c}$$

where:

$F_1$  = standard drag force with interference,

$C_D$  = standard drag coefficient,

$\rho$  = fluid density,

$A$  = projected area of smaller cylinder.

The direction of flow is:

$$\beta = \tan^{-1} \left( \frac{v}{u} \right)$$

The standard drag force without interference is:

$$F = \frac{C_D \rho A U^2}{2g_c}$$

where:

$F$  = standard drag force without interference, and

$U$  = free stream velocity.

The ratio of the two standard drag forces yields the following expression for the correction of the standard drag coefficients:

$$\frac{C_D \text{ (interference)}}{C_D \text{ (without interference)}} = m^2 + n^2$$

where:

$$m = \left[ 1 + R^2 \frac{b^2 - a^2}{(a^2 + b^2)^2} \right], \text{ and}$$

$$n = \frac{2ab R^2}{(a^2 + b^2)^2}.$$

If the determined ratio of the standard drag coefficients is less than 1, then a ratio of 1 is used. However, if the determined ratio is greater than 1, then the determined ratio is utilized.

The standard drag force on the smaller cylinder is then determined by:

$$F_1 = \frac{C_D \rho A U |U|}{2g_c}$$

where:

$F_1$  = standard drag force on smaller cylinder,

$C_D$  = the corrected standard drag coefficient for interference, and

$U$  = free stream velocity in the in-line direction.

The lift force on the smaller cylinder is determined in the same manner as was the standard drag force:

$$\frac{C_L \text{ (interference)}}{C_L \text{ (without interference)}} = m^2 + n^2$$

where m and n are the same as previously described. Once again, if the determined ratio is less than 1, then the ratio of 1 is utilized. However, if the determined ratio is greater than 1, then the determined ratio is used. The lift force is then determined by:

$$F_L = \frac{C_L \rho A U |U|}{2g_c}$$

where:

$F_L$  = lift force, and

$C_L$  = corrected lift coefficient for interference.

The lift force is applied in the transverse direction to the resultant flow.

#### C.4.4 Standard Drag on Smaller Cylinder Downstream of Large Cylinder

If the smaller cylinder is located downstream of the larger cylinder, then the lift and standard drag coefficients are evaluated corresponding to S/d (where S is the distance between the cylinder surfaces and d the diameter of the cylinders) ratios for both cylinders, assuming equal diameters. The coefficients are first determined by assuming both cylinders equal to the diameter of the small cylinder, and then assuming both cylinders equal to the diameter of the large cylinder. When determining the coefficients, the centerline

distance between the two submerged structures is maintained at the actual distance.

Afterwards, the larger coefficients are used for determining submerged structure loads. In addition, if the lift and standard drag coefficients are less than the coefficients without interference, then the coefficients without interference are utilized.

#### C.4.5 Standard Drag on the Large Cylinder

The method described in Subsection C.4.4 is used to determine the standard drag and lift on the large cylinder.

#### C.4.6 Structures of Non-Circular Cross-Section

The methodology of determining an equivalent diameter described in Section 6.4.2 is used to determine the coefficients due to interference effects.

#### C.4.7 Interference Between Non-Parallel Cylinders

To estimate the interference effects between non-parallel structures, the lift and standard drag coefficients are determined by assuming that the structures are parallel. The distance utilized between them would be the minimum distance between the two structures. In the same manner, the larger coefficients of either with or without interference effects are chosen for submerged structure load determination.

### C.5 The Uniform Velocity and Acceleration Evaluated at the Geometric Center of a Structure

In evaluating drag forces, the velocities and accelerations at the geometric center are utilized. These velocities and accelerations are used since the standard and acceleration drag coefficients are defined at the geometric center of a structure. However, if a flow field is not axially uniform along a particular submerged structure, the structure is segmented into smaller sections. Then the velocity and acceleration closely resemble uniform conditions over the segment. In addition, the flow is always assumed to be locally uniform as evaluated normal to and on the axis of the structure at the midpoint of each segment. The parameter  $L/D$  (where  $L$  is the segment length and  $D$  the outside diameter of the structure) is utilized to segment a submerged structure in order to provide an adequate representation of the flow field along the structure. This parameter is a structural criterion and is used in the analysis of submerged structures. It was determined that a segmentation that yields approximately a  $1.0 \leq L/D \leq 1.5$  is adequate to properly describe the flow field along a structure. This segmentation range is valid for all structures and can be utilized for all transients in the suppression pool. Furthermore, as the outside diameter of a submerged structure is increased, the segment length should decrease. When the segment length is decreased, a better representation of the flow field is obtained. If the outside diameter is less than 1.0 foot, the segmentation should be equal to an  $L/D$  of 1.5. However, if the outside diameter is equal to or greater than 1.0 foot, a segmentation equal to an  $L/D$  of 1.0 should be used. If the determined number of segments along a structure is a fraction, i.e. not an integer number, then the fraction number of segments should be rounded up to the greater integer number of segments.

In order to determine the adequacy of the segmentation, a computer program was utilized for evaluating the velocities and accelerations along a structure. Two submerged structures were used to assess the adequacy of the segmentation. The first structure was a 1.0-foot-diameter, 6-foot-long horizontal cylindrical structure. A vertical structure 21 feet long and 3.5 feet in diameter was also used. A bubble was utilized to load both submerged structures, and the method of images was used to provide the velocities and accelerations in the suppression pool. The first structure was segmented into four sections, each 1.5 feet long. This provided for an L/D of 1.5. Then the structure was segmented into eight sections, each 0.75 foot long, which provided for an L/D of 0.75. The segmentation of the structure is shown in Figure C-8. The structure was placed horizontally in the suppression pool, with the bubble located 3.5 feet vertically below and 4.13 feet horizontally away from the centerline of the structure. In addition, the bubble was placed 1.4 feet away from an end point of the structure. The location of the submerged structure in the suppression pool is shown in Figure C-9. In order to represent the actual velocities and accelerations along the structure, the structure was segmented into 32 sections. The second structure was also segmented into four and eight sections, each 5.25 feet and 2.625 feet, respectively. This provided for an L/D of 1.5 and 0.75 when the structure was segmented into four and eight sections. Moreover, to provide an L/D of 1.0, the structure was segmented into six sections, each 3.5 feet in length. In the same manner, to represent the actual velocities and accelerations along the structure, the structure was segmented into 32 sections. The structure was placed vertically in the suppression pool, and the bubble was located 4.0 feet horizontally away from the centerline of the structure and 6.0 feet from an end point of the structure. The segmentation schemes

are shown in Figure C-10, and the location of the structure in the suppression pool in Figure C-11.

Figures C-12 and C-13 illustrate the velocities and accelerations along the horizontal submerged structure. Figures C-14 and C-15 show the velocities and accelerations along the vertical structure for the various segmentation schemes described earlier. One can readily observe from these figures that as the segment length was reduced, the velocities and accelerations were more accurately described in the suppression pool. Figures C-12 and C-13 reveal that the velocities and accelerations for the small horizontal structure do not vary greatly when the number of segments is increased from four to eight. However, Figures C-14 and C-15 indicate that for a large structure, the minimum number of segments that can be used to sufficiently describe the velocities and acceleration along the structure is six, which translates to an L/D of 1.0.

In order to properly assess the adequacy of the segmentation, standard and acceleration drag loads were determined for each segmentation scheme. When the standard drag load along the structure for both the four- and eight-segmented structures was determined, only a 0.12% change resulted from reducing the segment size. When the acceleration drag load was determined along the same structure, a change of approximately 0.07% was attained when the number of segments was increased from four to eight. However, when compared to the results of segmenting the structure into 32 sections, the largest change in the acceleration drag load of 0.09% was exhibited when the segmentation was increased from 4 to 32 sections. A change of only 0.02% resulted in the acceleration drag load when the segmentation was increased from 8 to 32. The increase in the standard drag load was 0.15% and 0.03% when the segmentation was increased from 4 to 32, and 8 to 32, respectively.

When the standard drag load was determined for the vertical submerged structure and compared with the actual standard drag load (32 segments), changes of 14.47%, 1.1%, and 0.11% resulted when the segmentation was increased from 4 to 32, 6 to 32, and 8 to 32, respectively. In the same manner, when the acceleration drag load for the same structure was compared with the actual acceleration drag load (32 segments), changes of 3.5%, 0.23%, and 0.03% resulted when the segmentation was increased from 4 to 32, 6 to 32, and 8 to 32, respectively. Comparing the standard drag load of the structure when segmented into 4 sections with the structure segmented into 32 sections yielded results that inaccurately described the flow field in the suppression pool. As previously noted, a change of 14.47% resulted when the four-segmented structure was compared with the actual representation. The four-segmented structure yielded an L/D of 1.5, which is considered to be inappropriate for large cylinders. When utilizing six segments, an L/D of 1.0 was obtained, which showed very good agreement of the standard drag load with the actual load that resulted in a change of only 1.1%. The acceleration drag load did not vary considerably when the segmentation schemes were differed. This shows that a segmentation of a structure yielding a  $1.0 \leq L/D \leq 1.5$  is sufficient to provide an adequate description of both the velocities and accelerations for design purposes.

C.6 La Salle-Specific Parameters

Submerged Structure Spacing

<u>Structures Considered</u>	<u>Minimum Spacing (ft)</u>
Downcomer to Downcomer	3'-6" to 8'-0"
Downcomer to Column	4'-6" to 5'-3"
Downcomer to SRV Line	2'-3" to 4'-6"

Submerged Structure Size

<u>Structure</u>	<u>Diameter</u>
Downcomer	24"
Column	36"
SRV Line	12"

Flow Characteristics

<u>Phenomena</u>	<u>Flow Type</u>	<u>Period Parameter*</u>	<u>Re<sub>max</sub></u>
LOCA Charging	Constant Acceleration	<0.28	~10 <sup>6</sup>
LOCA Pool Swell	Oscillatory Flow**	50-75	10 <sup>5</sup> -10 <sup>6</sup>
LOCA Fallback	Constant Acceleration	***	10 <sup>6</sup>
SRV Discharge	Decaying Oscillation	< 4	10 <sup>6</sup>

\*Period Parameter =  $\frac{U_m t/d}{s/d}$  (Oscillatory Flow)  
 s/d (Constant Acceleration)

\*\*Pool Swell is considered a portion of a single cell of an oscillatory flow.

\*\*\*Varies greatly with structure size and location. Vortex shedding is assumed and lift force calculated.

C-37

LSCS-MARK II DAR

Rev. 7 1/80

### C.7 References

1. "Analytical Model for Estimating Drag Forces on Rigid Submerged Structures Caused by LOCA and Safety Relief Valve Ramshead Air Discharges," NEDO-21471, September 1977.
2. T. Sarpkaya and C. J. Garrison, "Vortex Formation and Resistance in Unsteady Flow," *Journal of Applied Mechanics*, pp. 16-24, March 1963.
3. T. Sarpkaya, "Forces on Cylinders and Spheres in a Sinusoidally Oscillating Fluid," *Transactions of the ASME*, pp. 32-37, March 1975.
4. G. K. Batchelor, An Introduction to Fluid Dynamics, pg. 341, Cambridge, England, 1967.
5. T. Sarpkaya, "In-Line and Transverse Forces on Cylinders in Oscillatory Flow at High Reynolds Number," *Journal of Ship Research*, Vol. 21, No. 4, pp. 200-216, December 1977.
6. T. Sarpkaya, "Vortex Shedding and Resistance in Harmonic Flow About Smooth and Rough Circular Cylinders at High Reynolds Numbers," NPS-59SL76021, February 1976.
7. J. P. Den Hartog, Mechanical Vibrations, Fourth edition, pp. 305-306, McGraw-Hill Book Co., Inc., New York, 1956.
8. J. A. Roberson and C. T. Crowe, Engineering Fluid Mechanics, pp. 338-340, Houghton Mifflin Co., Illinois, 1975.

9. T. Yamamoto, "Hydrodynamic Forces on Multiple Circular Cylinders," Journal of the Hydraulics Division, ASCE, pp. 1193-1210, September 1976.
10. T. Yamamoto and J. H. Nath, "Hydrodynamic Forces on Groups of Cylinders," Paper No. OTC 2499, presented at the Offshore Technology Conference, Houston, Texas, May 3-7, 1976.
11. T. Yamamoto and J. H. Nath, "Forces on Many Cylinders Near a Plane Boundary," Preprint 2633, presented at the ASCE National Water Resources and Ocean Engineering Convention, San Diego, California, April 5-8, 1976.
12. C. Dalton and R. A. Helfinstein, "Potential Flow Past a Group of Circular Cylinders," Journal of Basic Engineering, ASME, pp. 636-642, December 1971.
13. T. Yamamoto, J. H. Nath, and L. S. Slotta, "Wave Forces on Cylinder Nearby a Plane Boundary," ASCE Journal of Waterways, Harbors and Coastal Engineering Division, pp. 345-359, November 1974.
14. T. Sarpkaya, "Forces on Cylinders Near a Plane Boundary in a Sinusoidally Oscillating Fluid," Journal of Fluids Engineering, ASME, pp. 499-505, September 1976.
15. T. Sarpkaya, "In-Line and Transverse Forces on Cylinders Near a Wall in Oscillatory Flow at High Reynolds Numbers," Paper No. OTC 2898, presented at the Offshore Technology Conference, Houston, Texas, May 2-5, 1977.
16. E. I. Hori, "Experiments on Flow Around a Pair of Parallel Circular Cylinders," proceedings of the 9th Japan National Congress for Applied Mechanics, pp. 231-234, 1959.

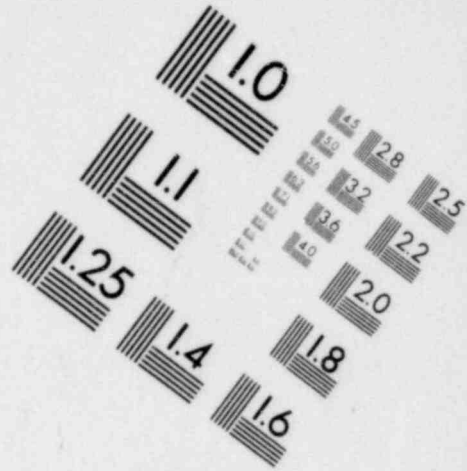
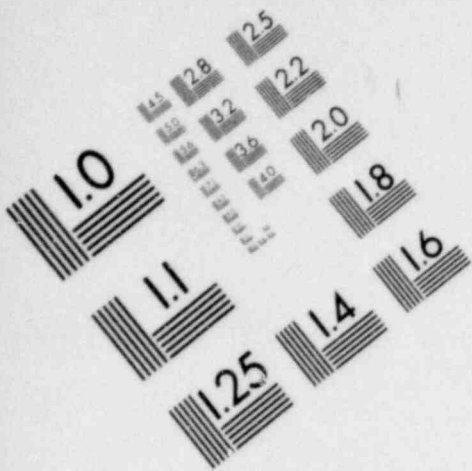
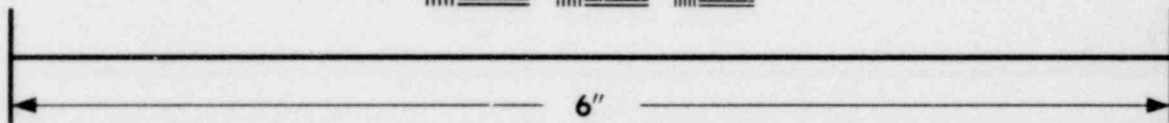
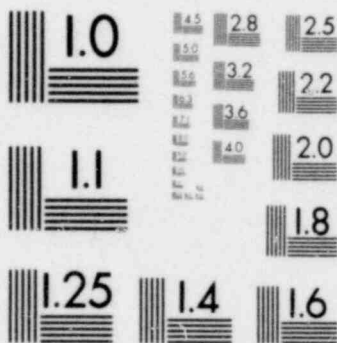
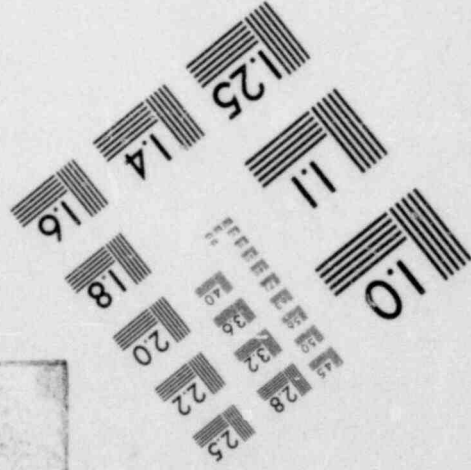
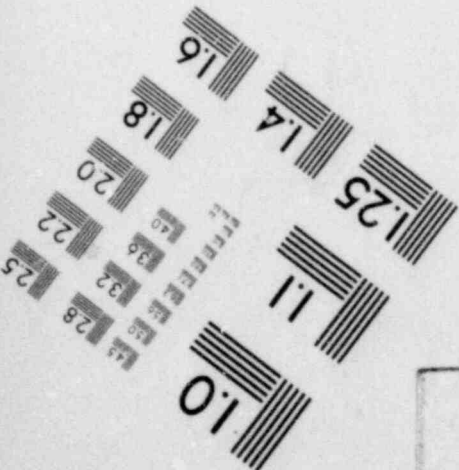


**IMAGE EVALUATION  
TEST TARGET (MT-3)**



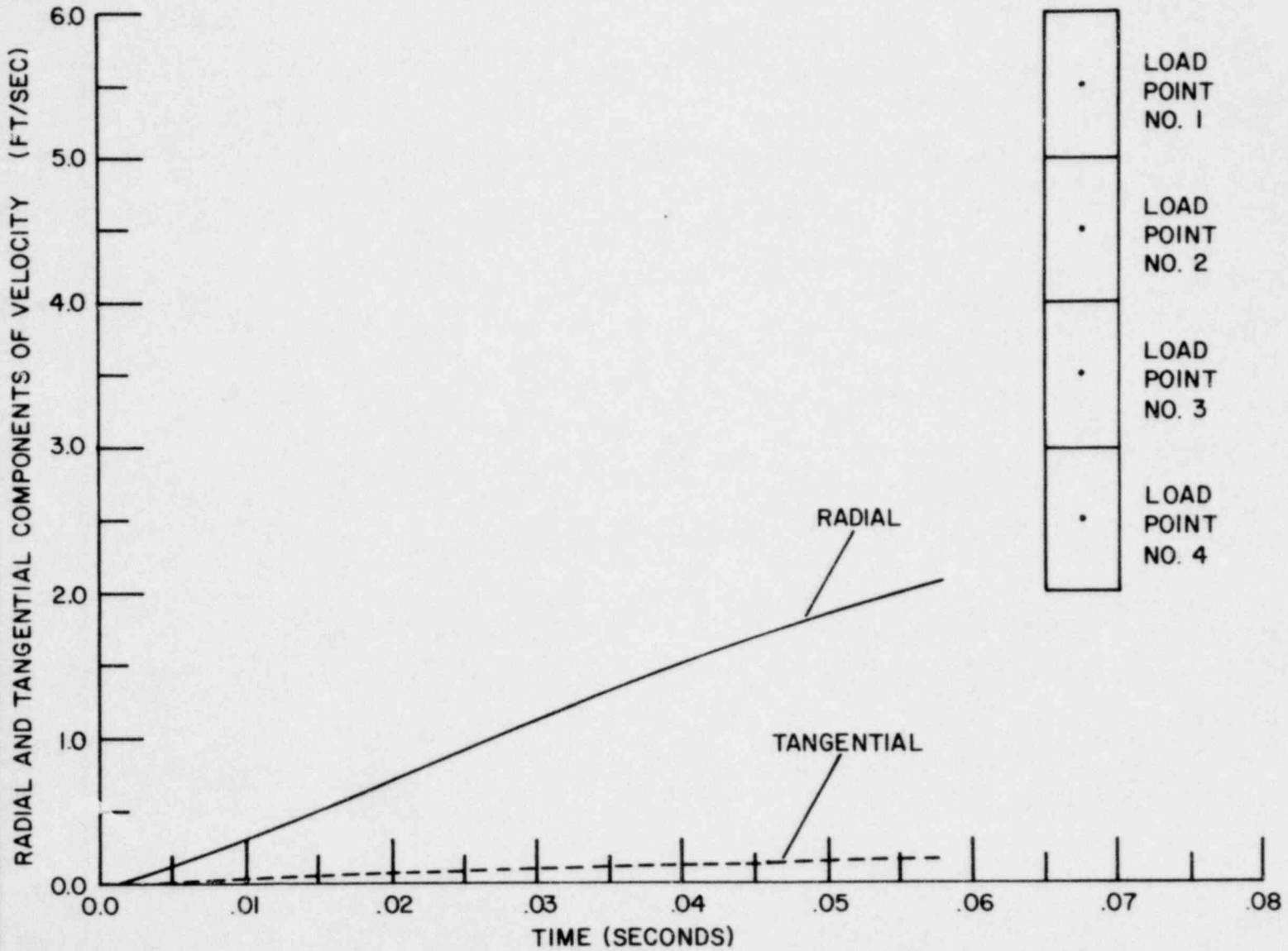
**MICROCOPY RESOLUTION TEST CHART**



17. C. Dalton and J. M. Szabo, "Drag on a Group of Cylinders," Transactions of the ASME, Journal of Pressure Vessel Technology, pp. 152-157, February 1977.
18. M. M. Zdravkovich, "Review of Flow Interference Between Two Circular Cylinders in Various Arrangements," Transactions of the ASME, Journal of Fluids Engineering, pp. 618-633, December 1977.

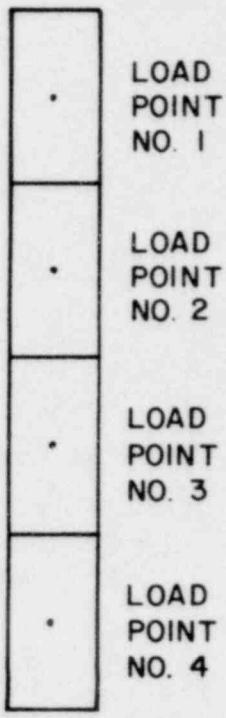
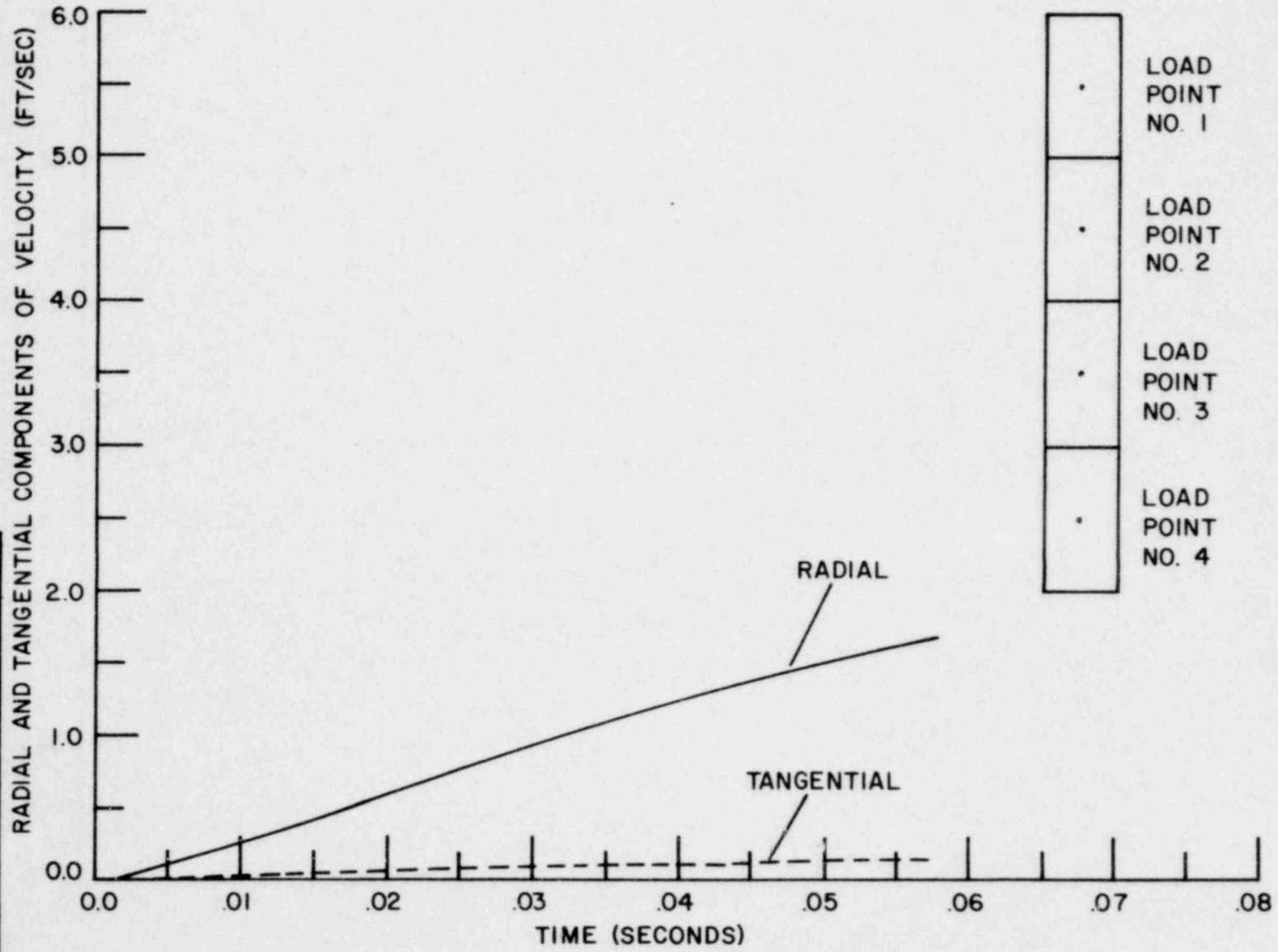
LA SALLE COUNTY STATION  
 MARK II DESIGN ASSESSMENT REPORT  
 FIGURE C-1  
 LOCA AIR CLEARING VELOCITY  
 (SHEET 1 of 4)

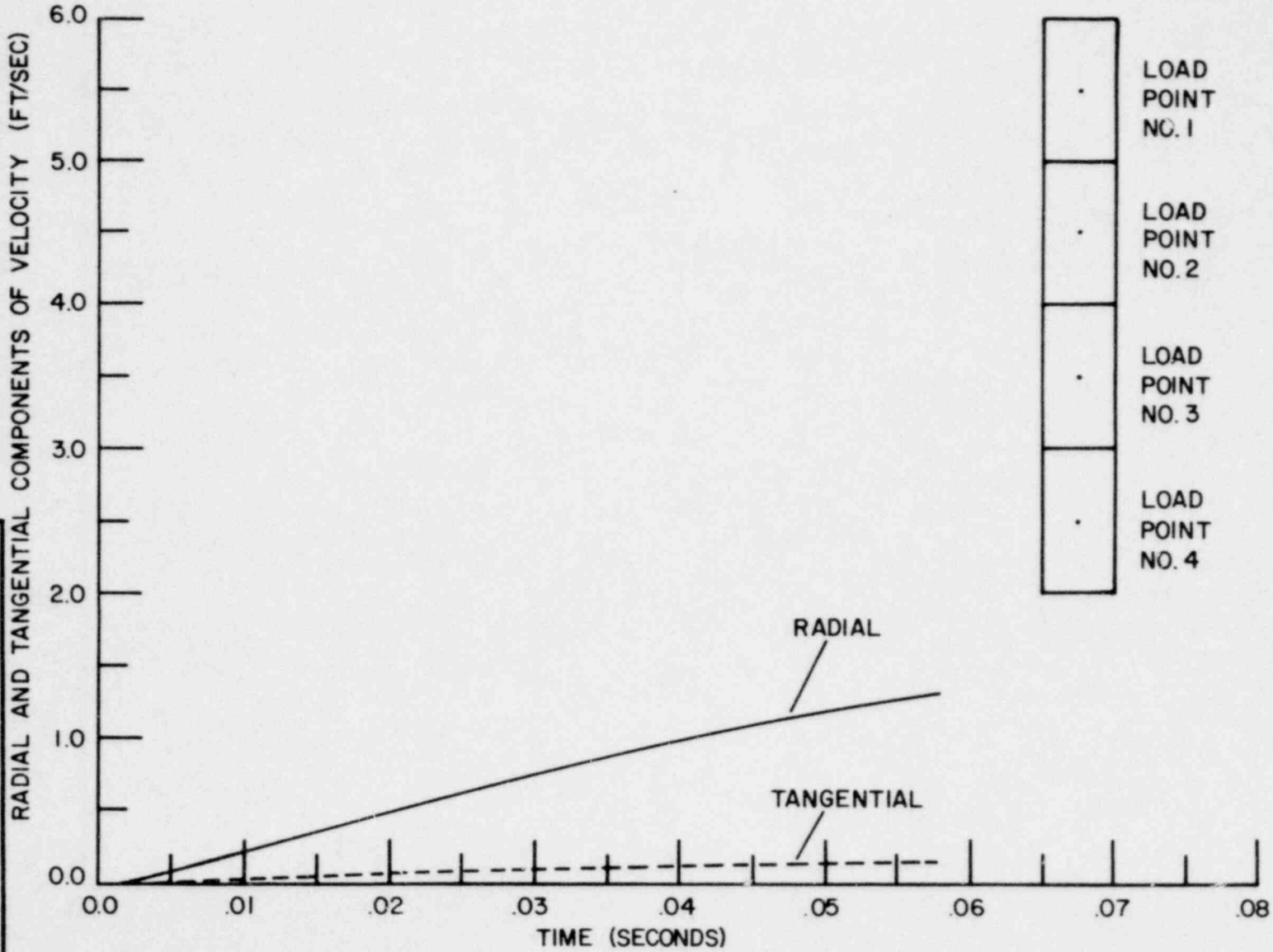
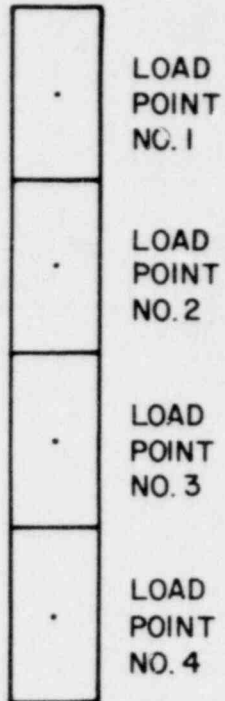
LOAD POINT NO. 1



LA SALLE COUNTY STATION  
 MARK II DESIGN ASSESSMENT REPORT  
 FIGURE C-1  
 LOCA AIR CLEARING VELOCITY  
 (SHEET 2 of 4)

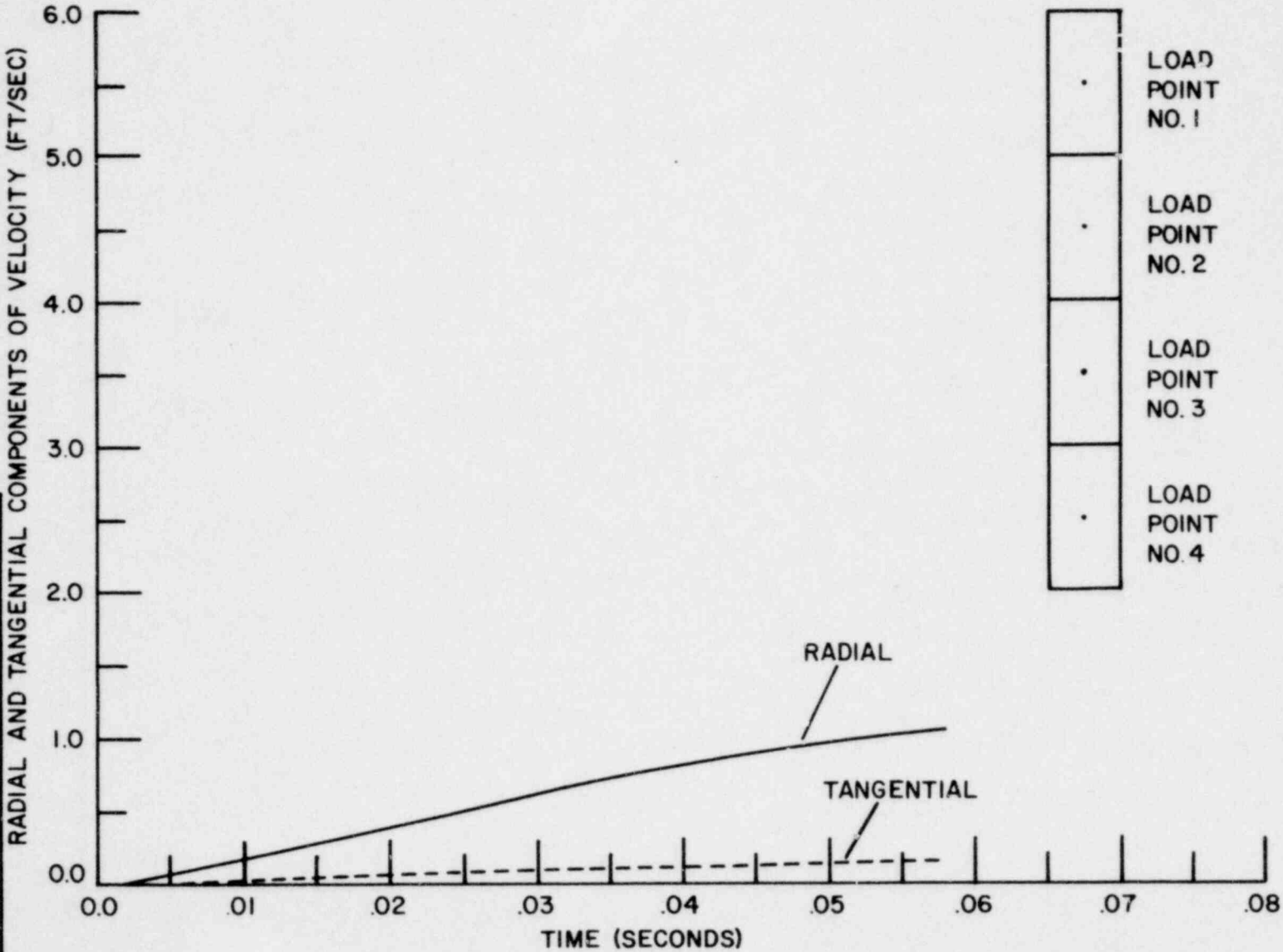
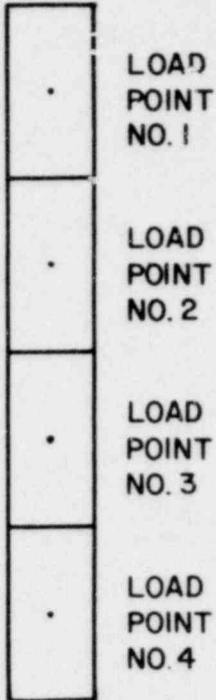
LOAD POINT NO. 2





LOAD POINT NO. 3

LA SALLE COUNTY STATION  
MARK II DESIGN ASSESSMENT REPORT  
FIGURE C-1  
LOCA AIR CLEARING VELOCITY  
(SHEET 3 of 4)

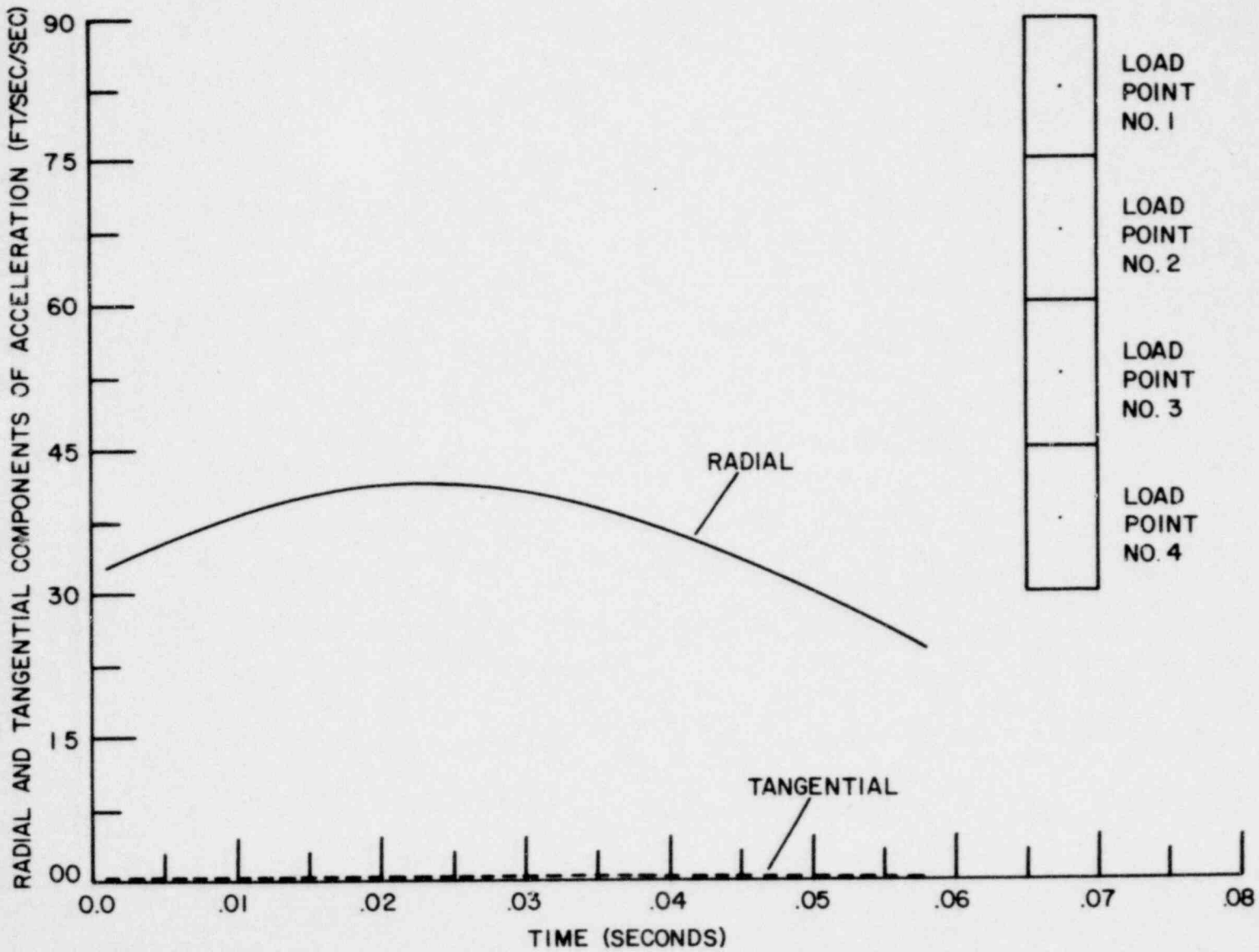


LOAD POINT NO. 4

LA SALLE COUNTY STATION MARK II DESIGN ASSESSMENT REPORT
FIGURE C-1 LOCA AIR CLEARING VELOCITY (SHEET 4 OF 4)

LOAD POINT NO. 1

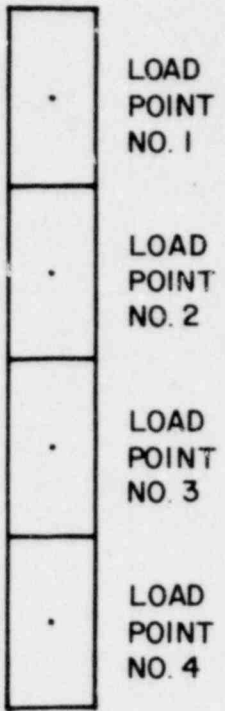
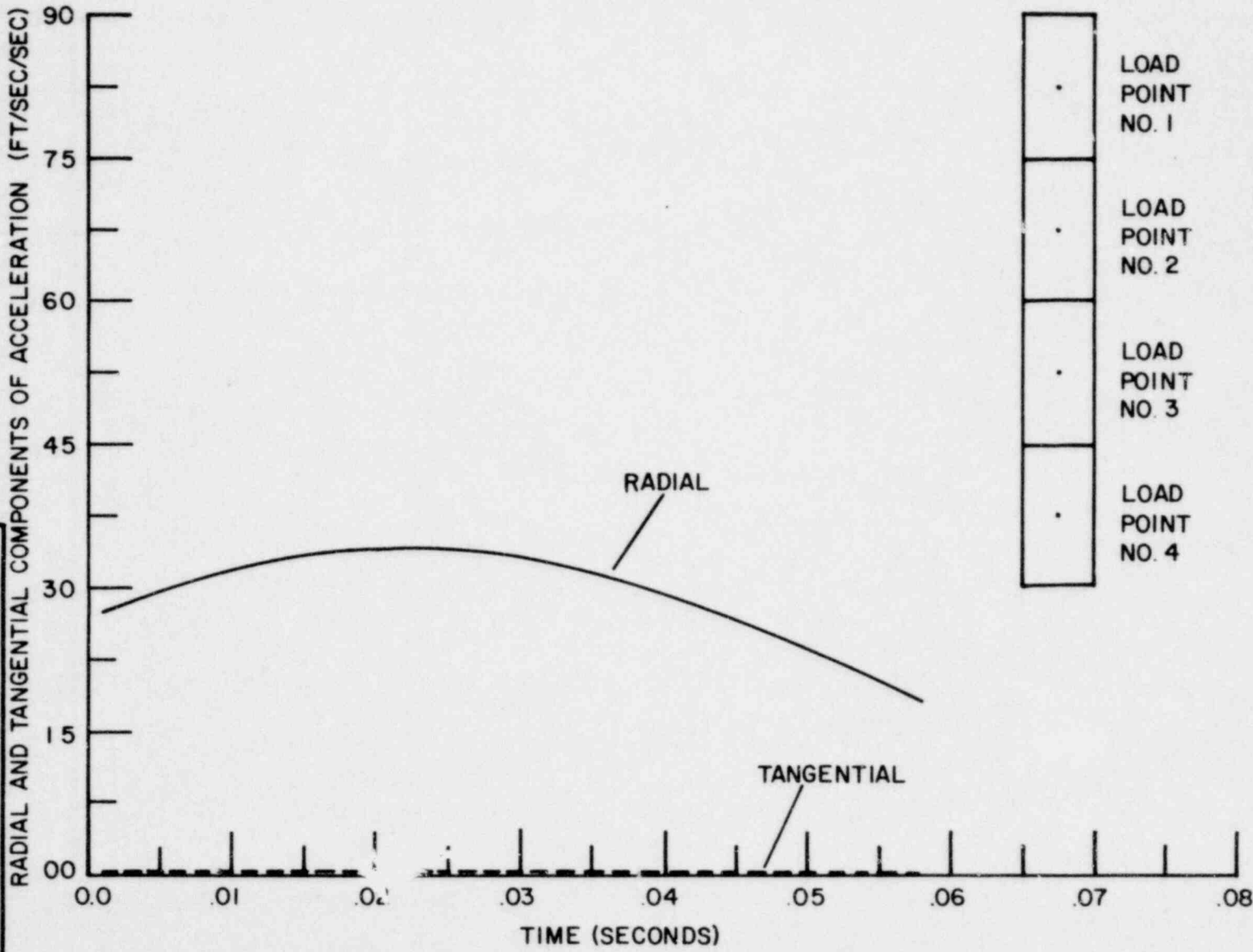
LA SALLE COUNTY STATION  
MARK II DESIGN ASSESSMENT REPC AT  
FIGURE C-2  
LOCA AIR CLEARING ACCELERATION  
(SHEET 1 of 4)



LOAD POINT NO. 1  
LOAD POINT NO. 2  
LOAD POINT NO. 3  
LOAD POINT NO. 4

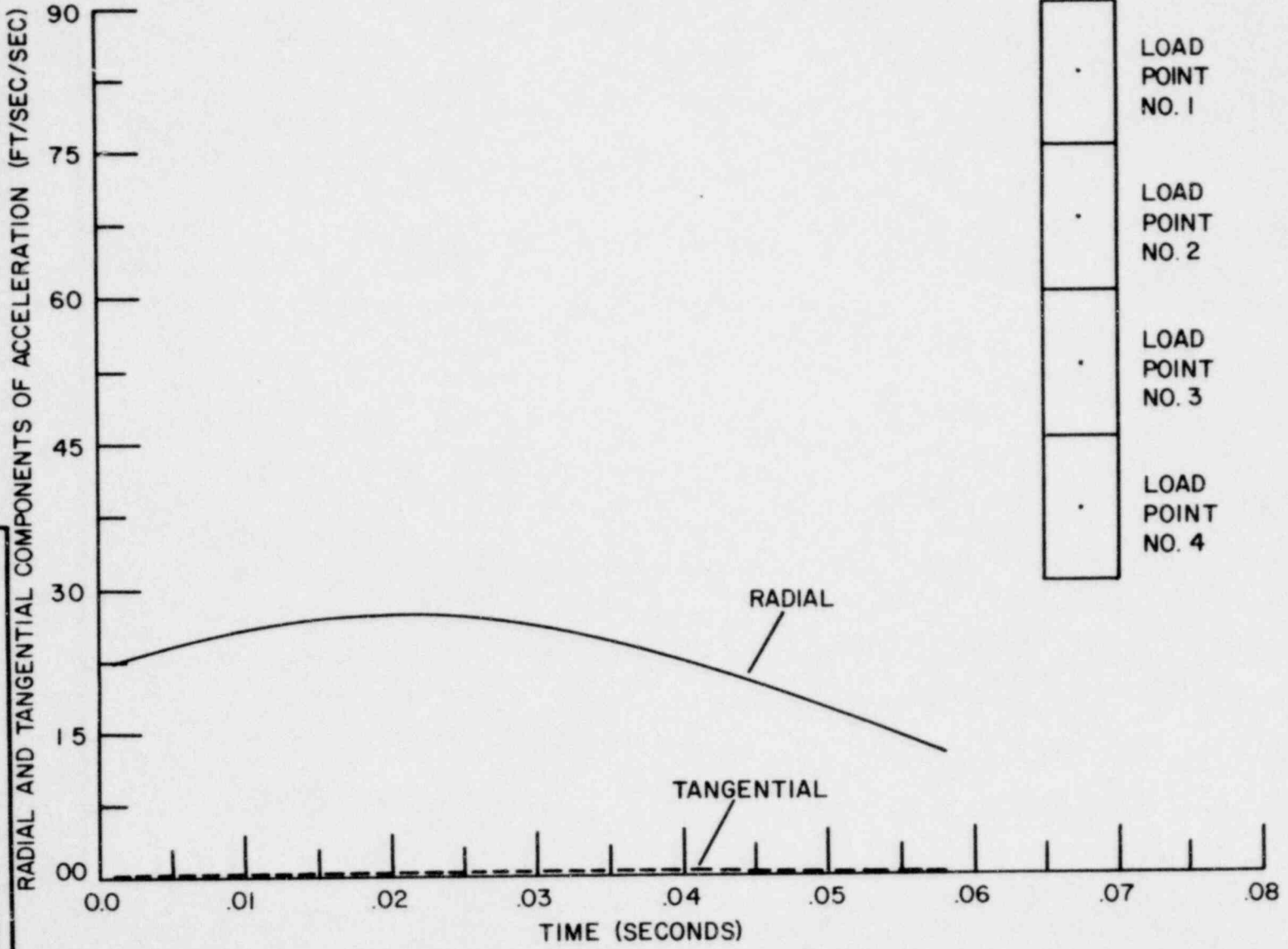
LOAD POINT NO. 2

LA SALLE COUNTY STATION  
MARK II DESIGN ASSESSMENT REPORT  
FIGURE C-2  
LOCA AIR CLEARING ACCELERATION  
(SHEET 2 of 4)



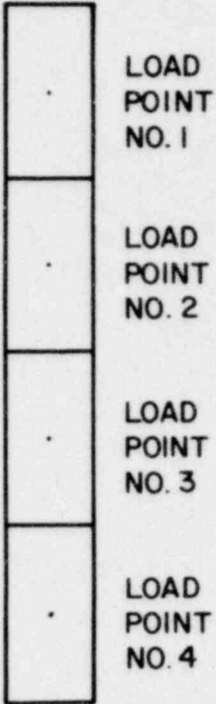
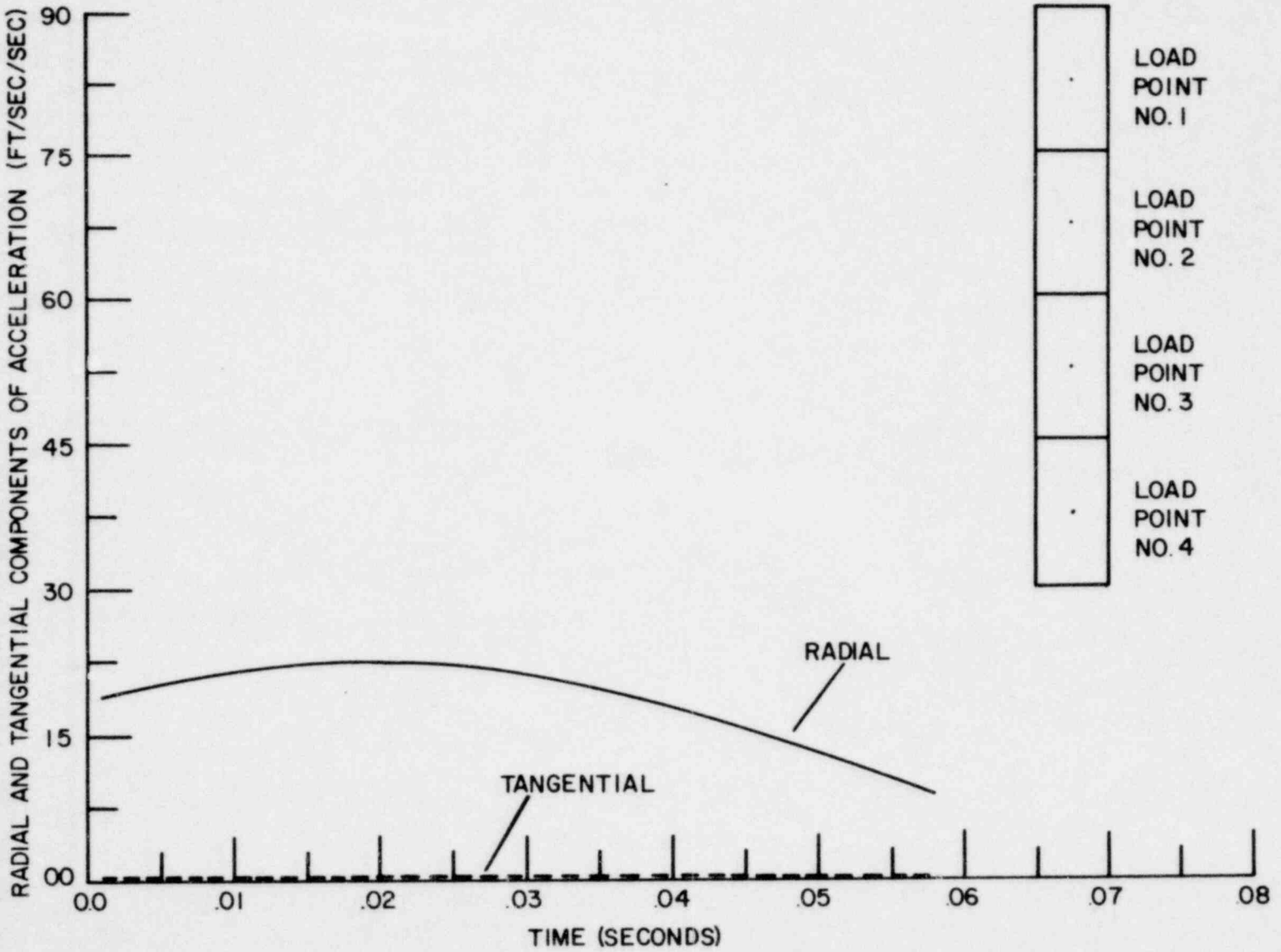
LA SALLE COUNTY STATION  
MARK II DESIGN ASSESSMENT REPORT  
FIGURE C-2  
LOCA AIR CLEARING ACCELERATION  
(SHEET 3 of 4)

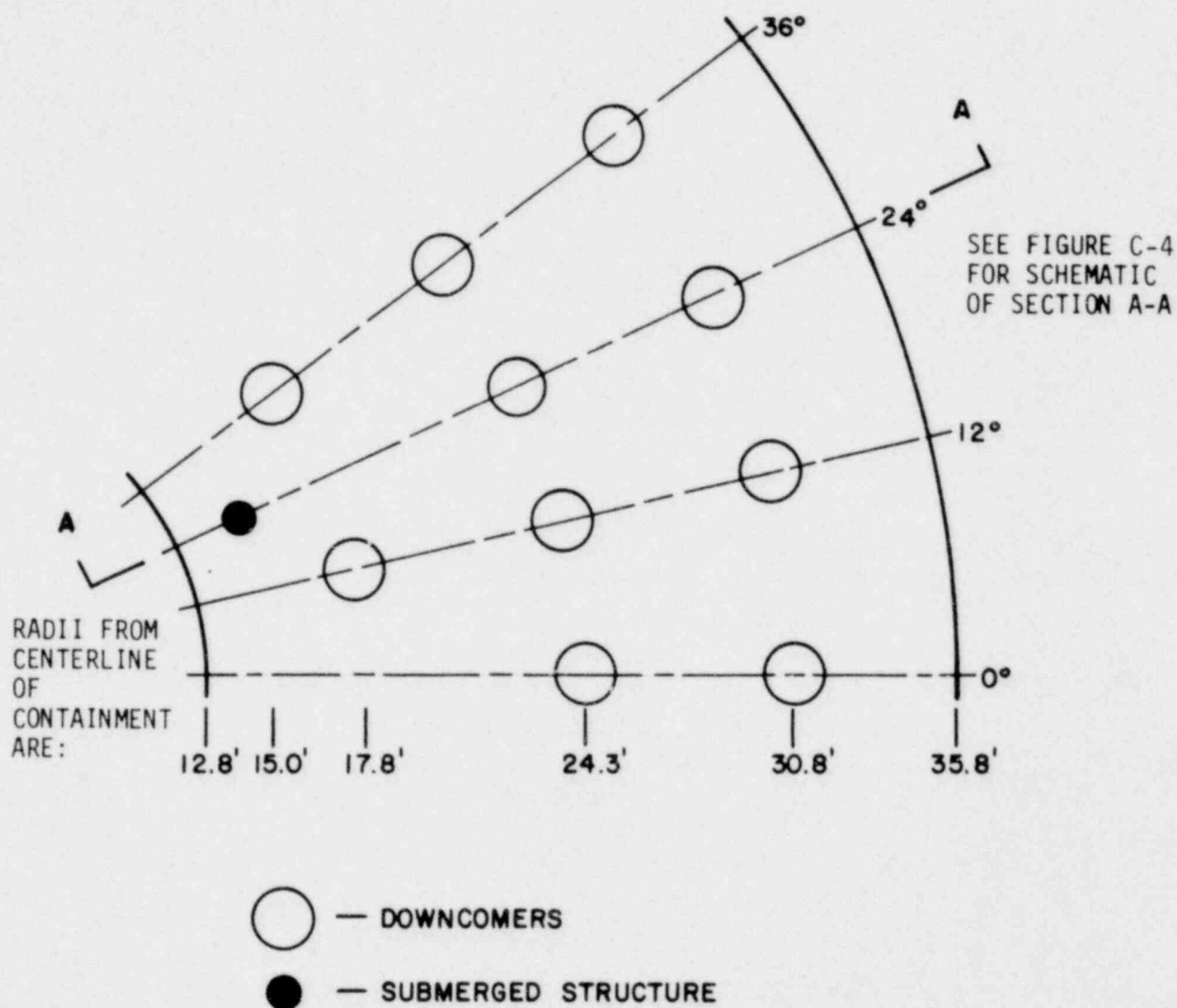
LOAD POINT NO. 3



LOAD POINT NO. 4

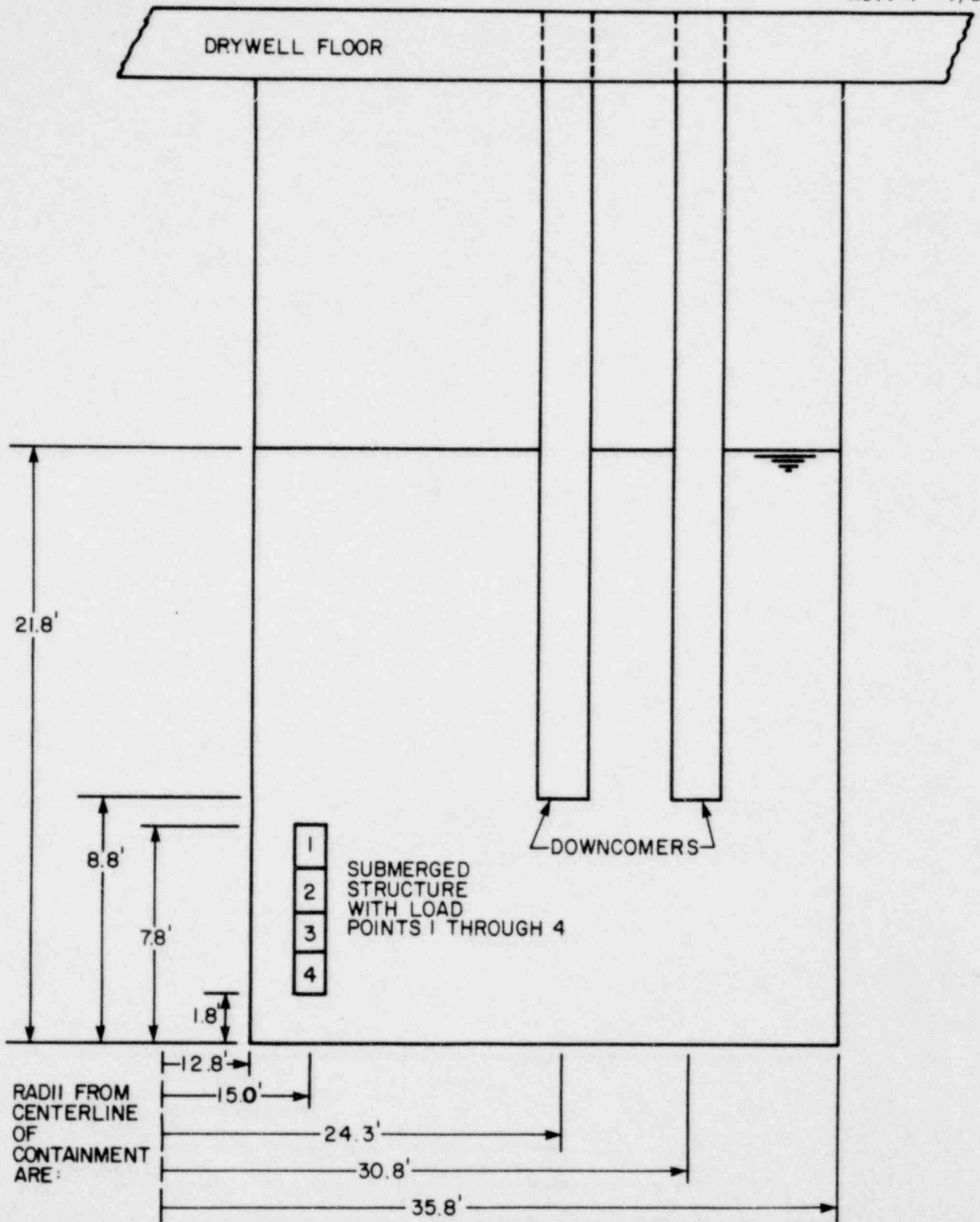
LA SALLE COUNTY STATION  
MARK II DESIGN ASSESSMENT REPORT  
FIGURE C-2  
LOCA AIR CLEARING ACCELERATION  
(SHEET 4 of 4)





LA SALLE COUNTY STATION  
MARK II DESIGN ASSESSMENT REPORT

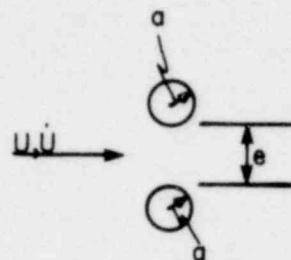
FIGURE C-3  
TOP VIEW OF 36° SECTOR OF A TYPICAL  
MARK II SUPPRESSION POOL



LA SALLE COUNTY STATION  
MARK II DESIGN ASSESSMENT REPORT

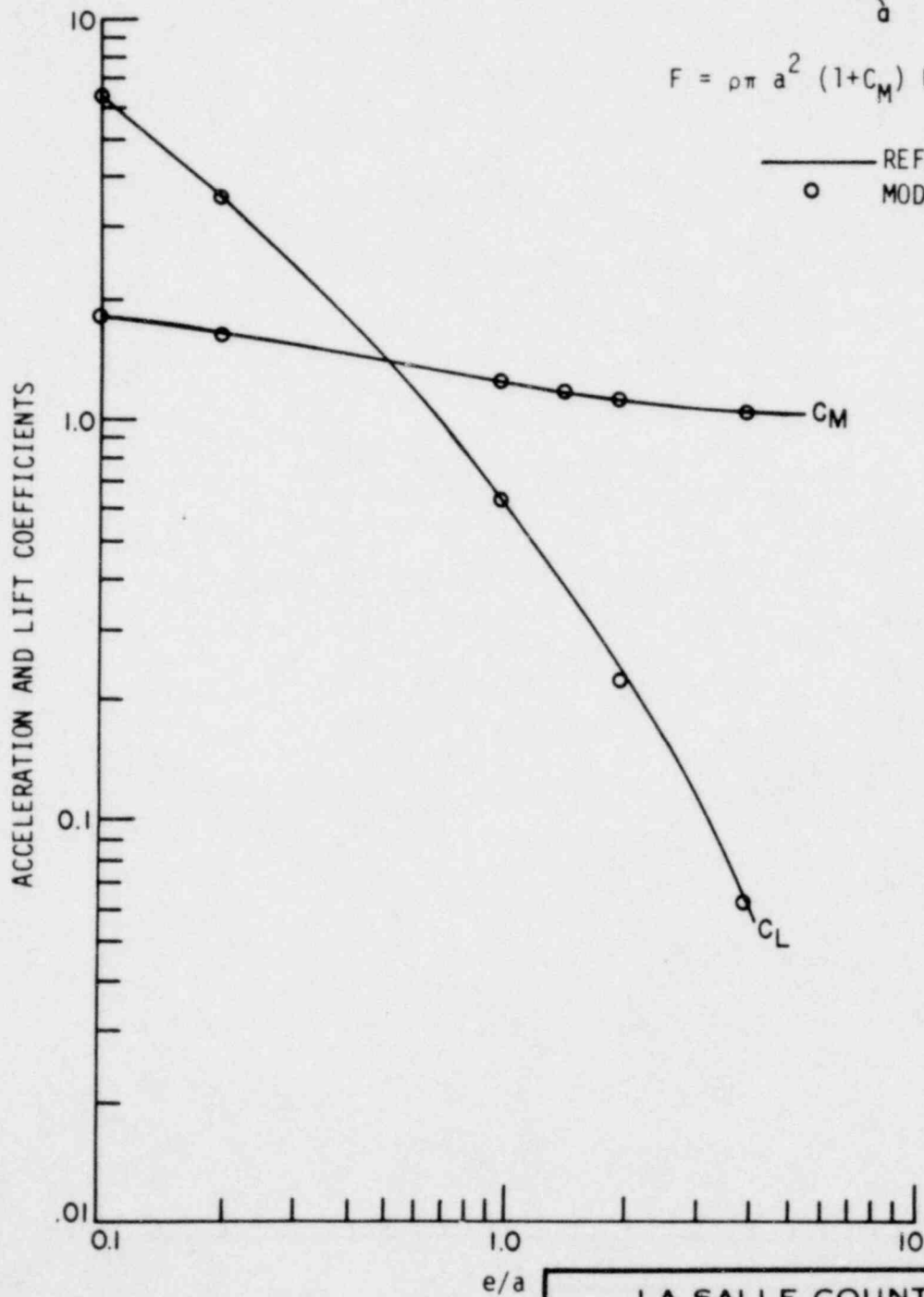
FIGURE C-4

SCHEMATIC VIEW OF SECTION A-A OF TYPICAL  
MARK II SUPPRESSION POOL



$$F = \rho \pi a^2 (1+C_M) U + p a C_L U^2$$

— REFERENCE 9  
 ○ MODEL

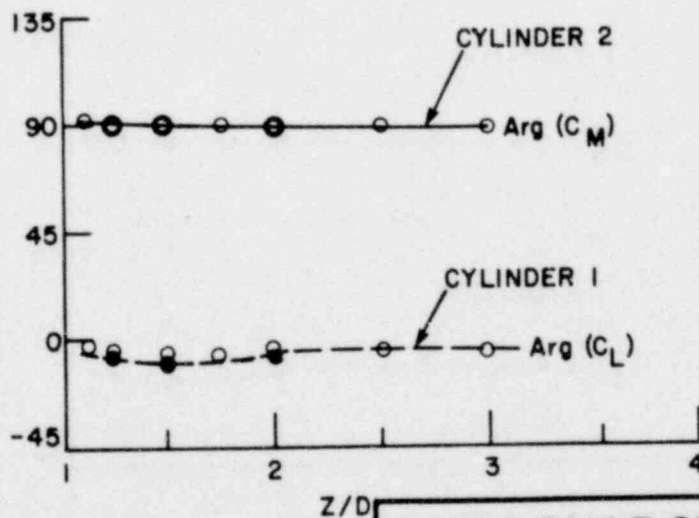
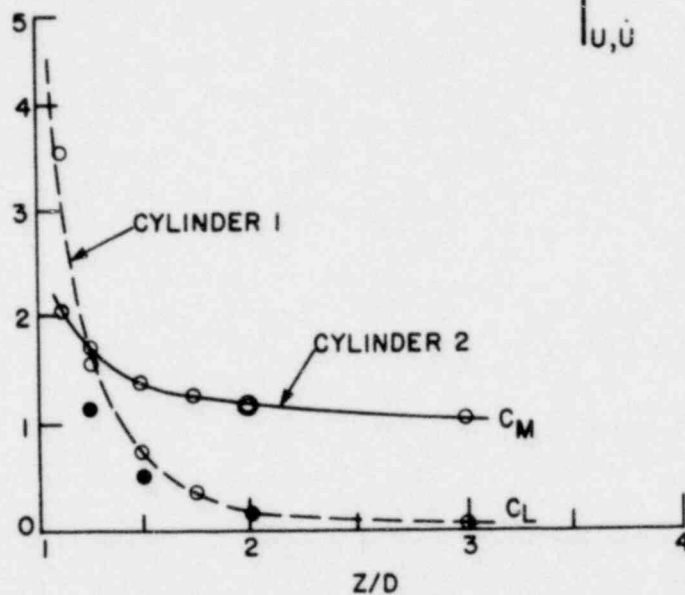
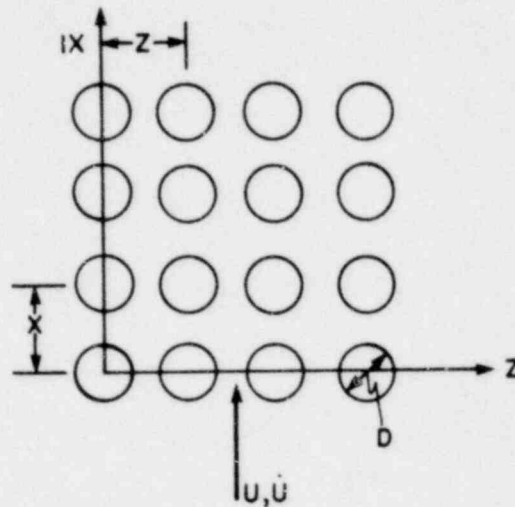


**LA SALLE COUNTY STATION**  
**MARK II DESIGN ASSESSMENT REPORT**  
  
 FIGURE C-5  
 MODEL/DATA COMPARISONS  
 (SHEET 1 of 4)

$$F = (1 + C_M) \rho \pi a^2 U + \rho a C_L U U$$

where  $a = D/2$

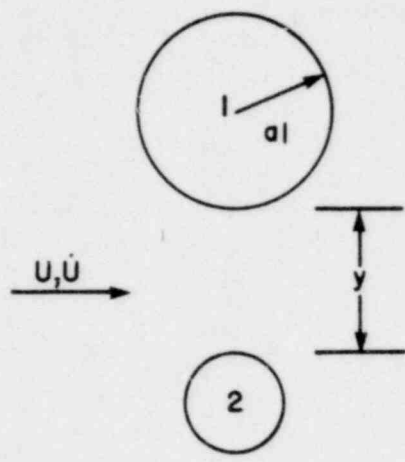
○, ●, —, - - - REFERENCE 10  
 ○ MODEL



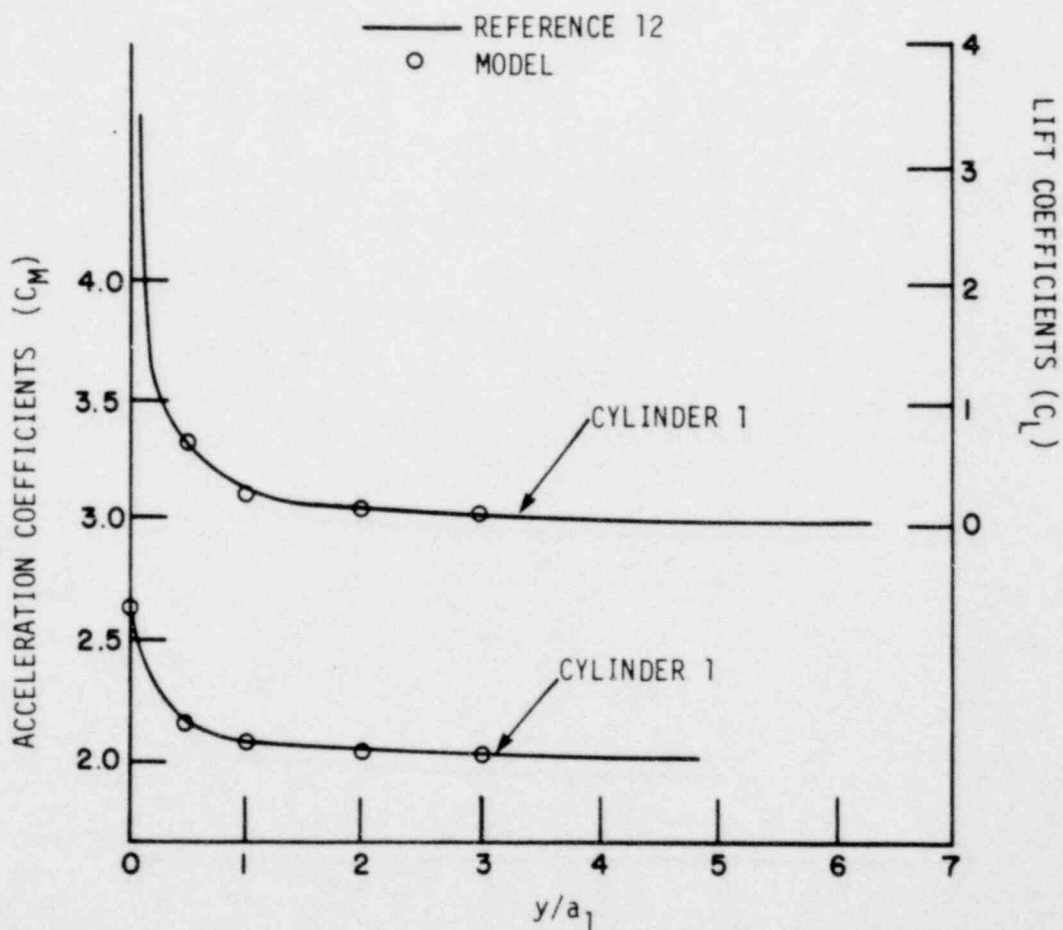
LA SALLE COUNTY STATION  
 MARK II DESIGN ASSESSMENT REPORT

---

FIGURE C-5  
 MODEL/DATA COMPARISONS  
 (SHEET 2 of 4)



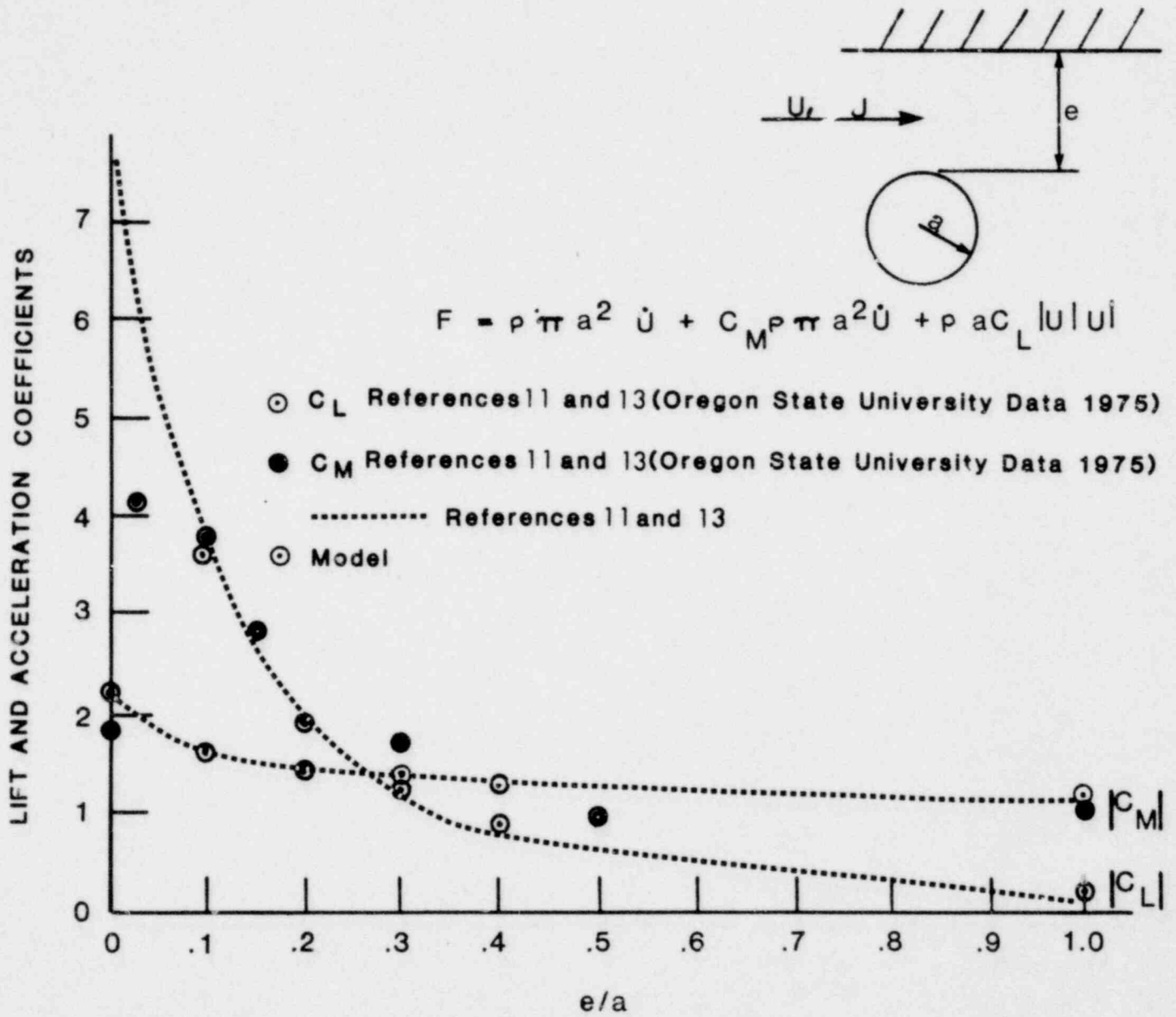
$$F = C_M \rho \pi a^2 \dot{U} + C_L \rho a U^2$$



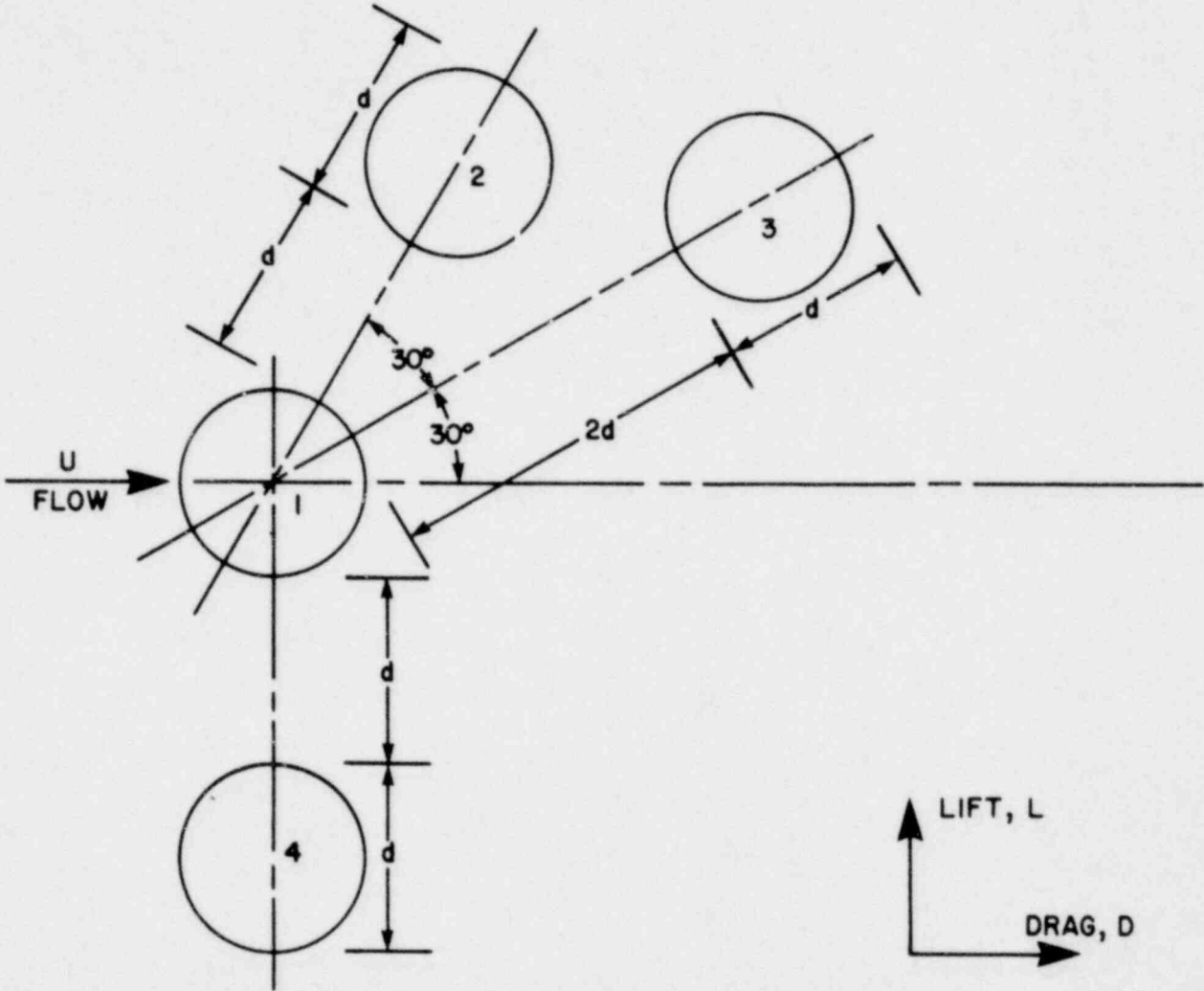
LA SALLE COUNTY STATION  
 MARK II DESIGN ASSESSMENT REPORT

---

FIGURE C-5  
 MODEL/DATA COMPARISONS  
 (SHEET 3 of 4)

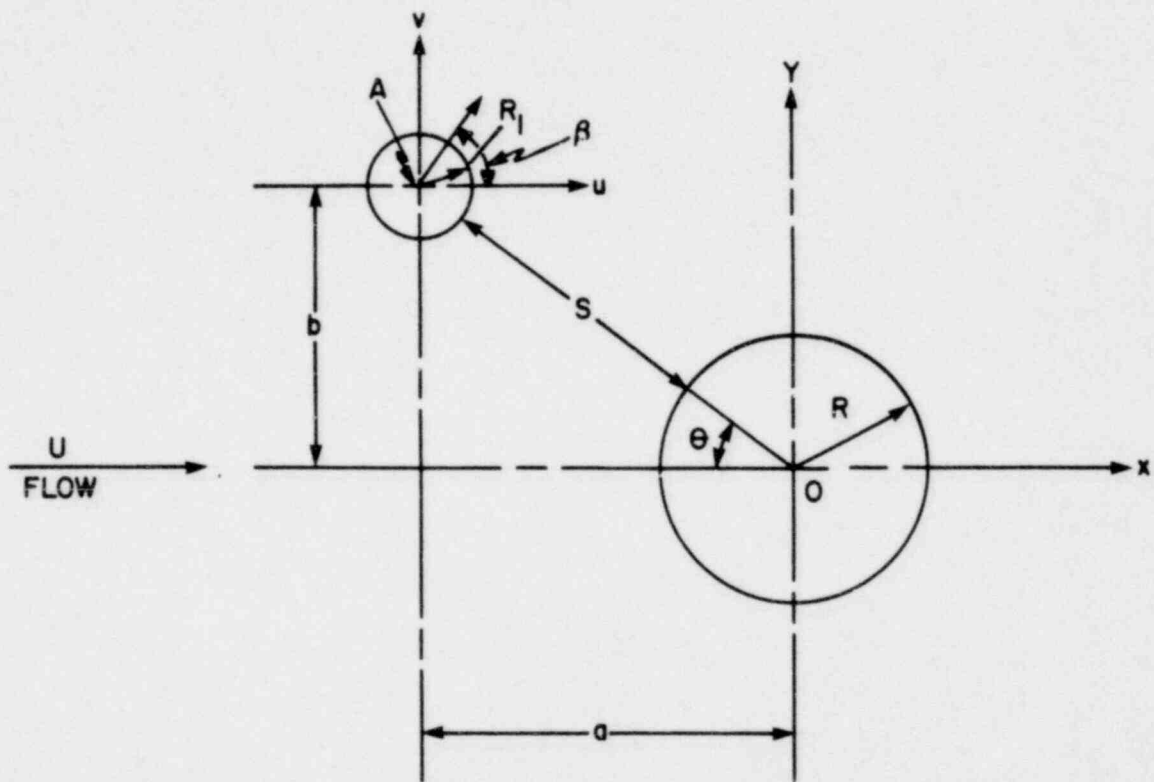


**LA SALLE COUNTY STATION**  
 MARK II DESIGN ASSESSMENT REPORT  
 FIGURE C-5  
 MODEL/DATA COMPARISONS  
 (SHEET 4 of 4)



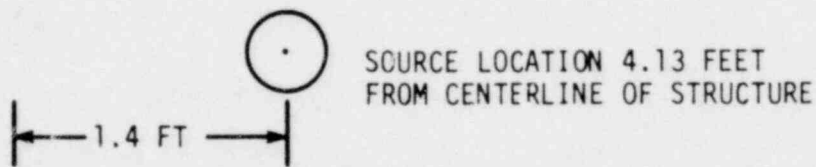
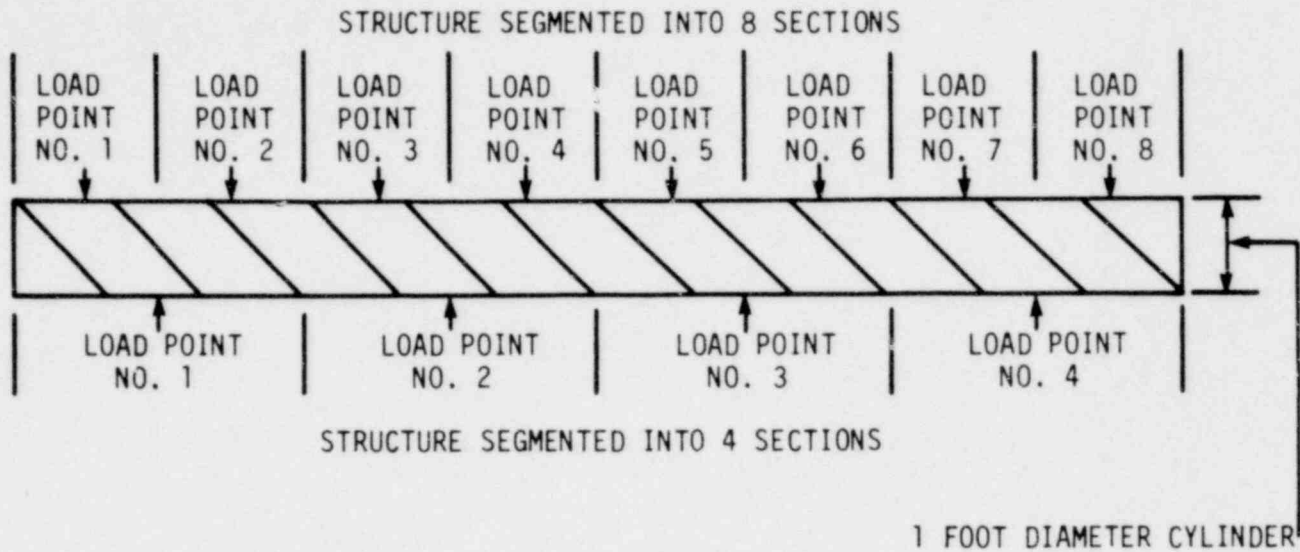
LA SALLE COUNTY STATION  
MARK II DESIGN ASSESSMENT REPORT

FIGURE C-6  
CYLINDER LOCATIONS

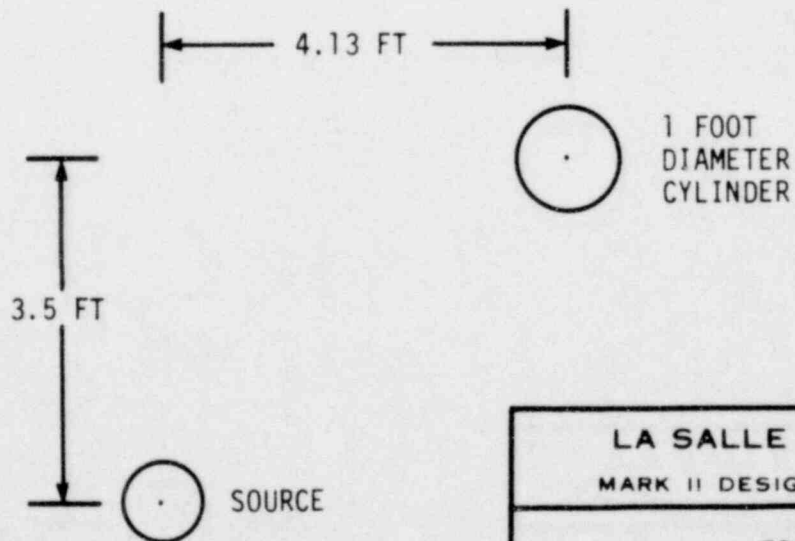


LA SALLE COUNTY STATION MARK II DESIGN ASSESSMENT REPORT
FIGURE C-7 FLOW AROUND UNEQUAL CYLINDERS

TOP VIEW OF STRUCTURE



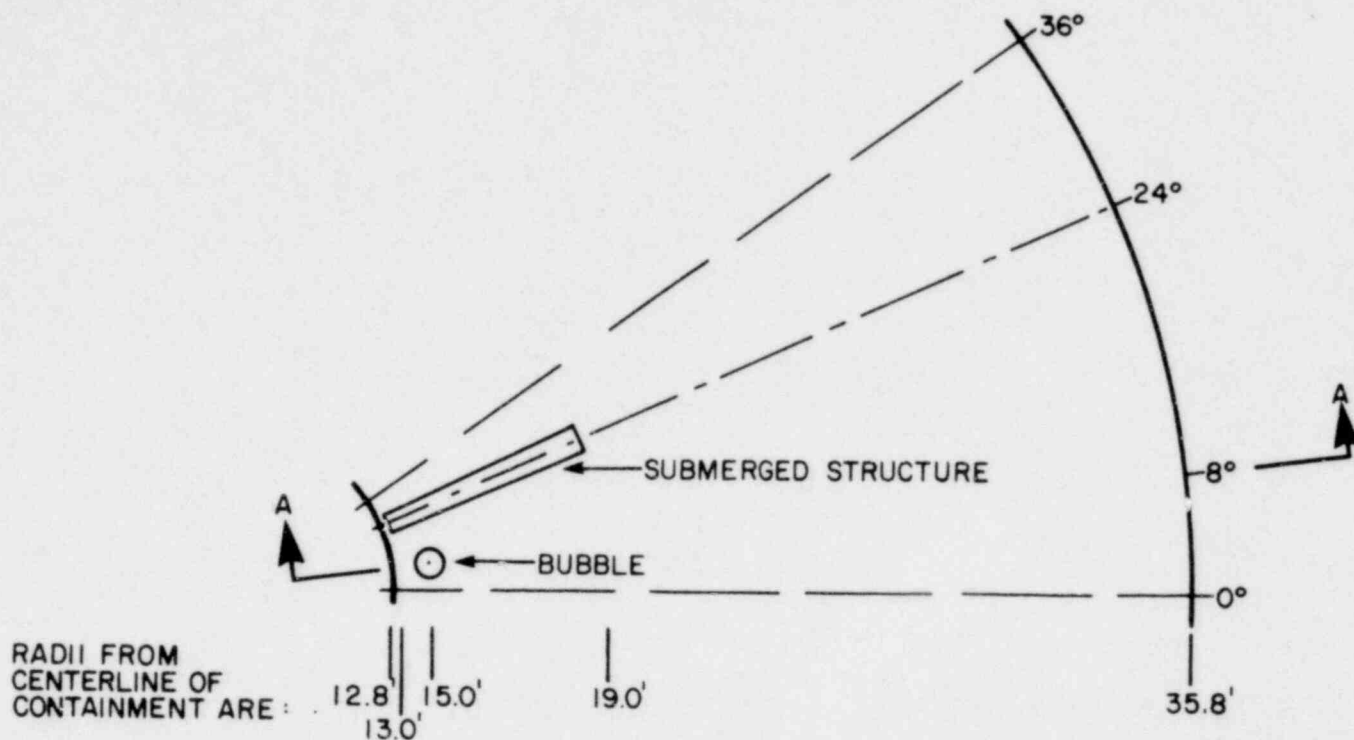
SIDE VIEW OF STRUCTURE



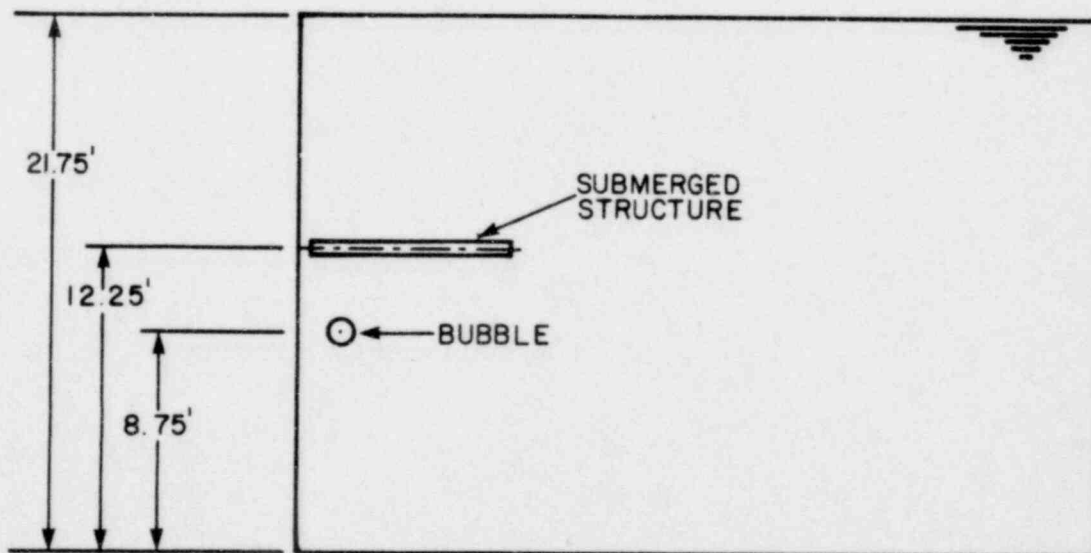
LA SALLE COUNTY STATION  
MARK II DESIGN ASSESSMENT REPORT

FIGURE C-8  
TOP AND SIDE VIEW OF STRUCTURE  
AND SOURCE LOCATIONS

TOP VIEW OF 36° SECTOR

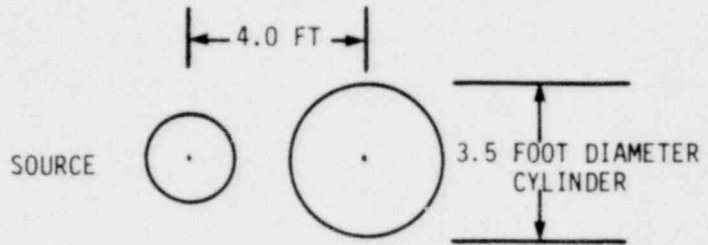


SIDE VIEW OF SECTION A-A



LA SALLE COUNTY STATION  
MARK II DESIGN ASSESSMENT REPORT

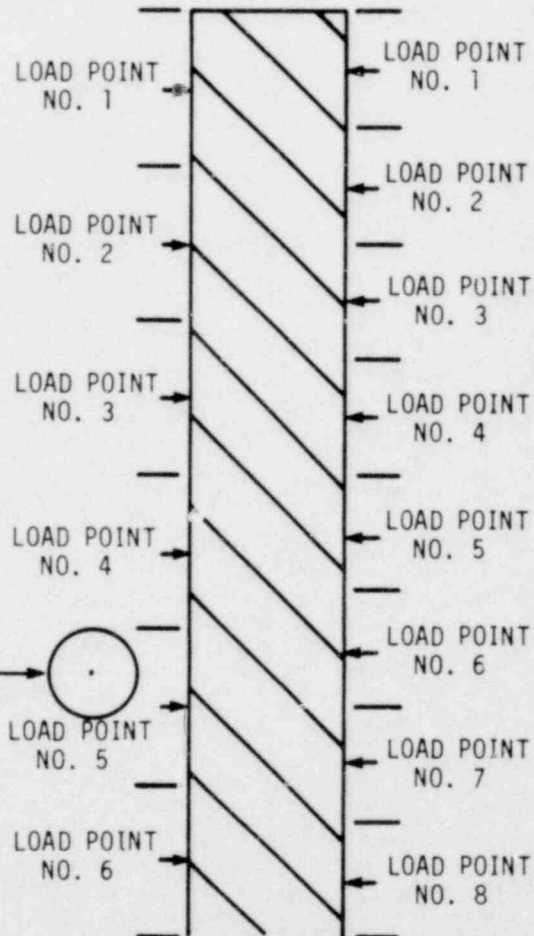
FIGURE C-9  
LOCATION OF HORIZONTAL SUBMERGED  
STRUCTURE IN THE SUPPRESSION POOL



SIDE VIEW OF STRUCTURE

A 21 FOOT VERTICAL  
STRUCTURE SEGMENTED  
INTO 6 AND 8 SECTIONS

SOURCE LOCATION  
4.0 FEET FROM  
CENTERLINE OF  
STRUCTURE

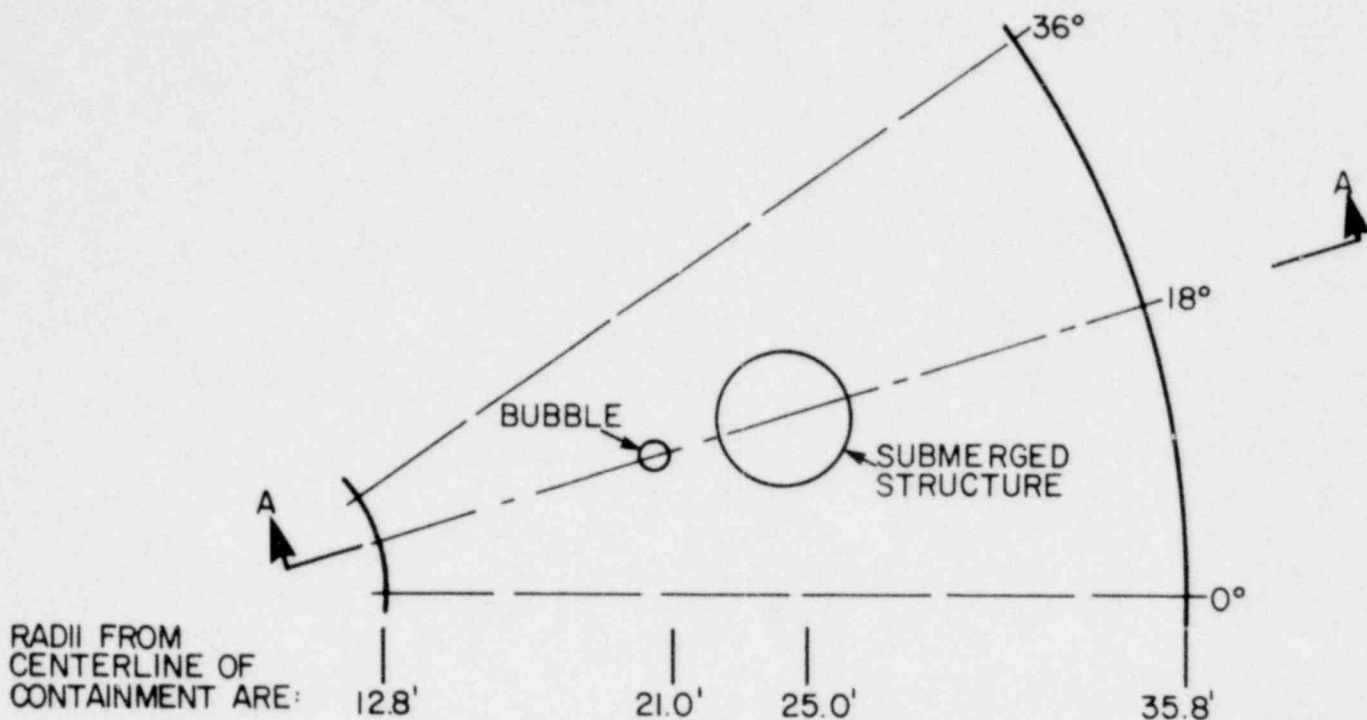


LA SALLE COUNTY STATION  
MARK II DESIGN ASSESSMENT REPORT

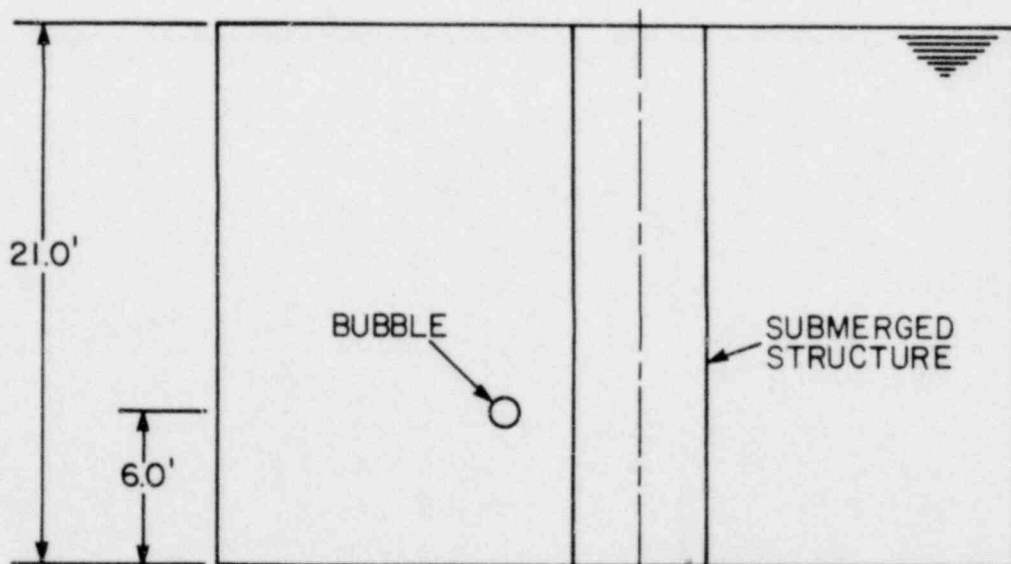
FIGURE C-10

TOP AND SIDE VIEW OF (SECOND)  
STRUCTURE AND SOURCE LOCATION

TOP VIEW OF 36° SECTOR



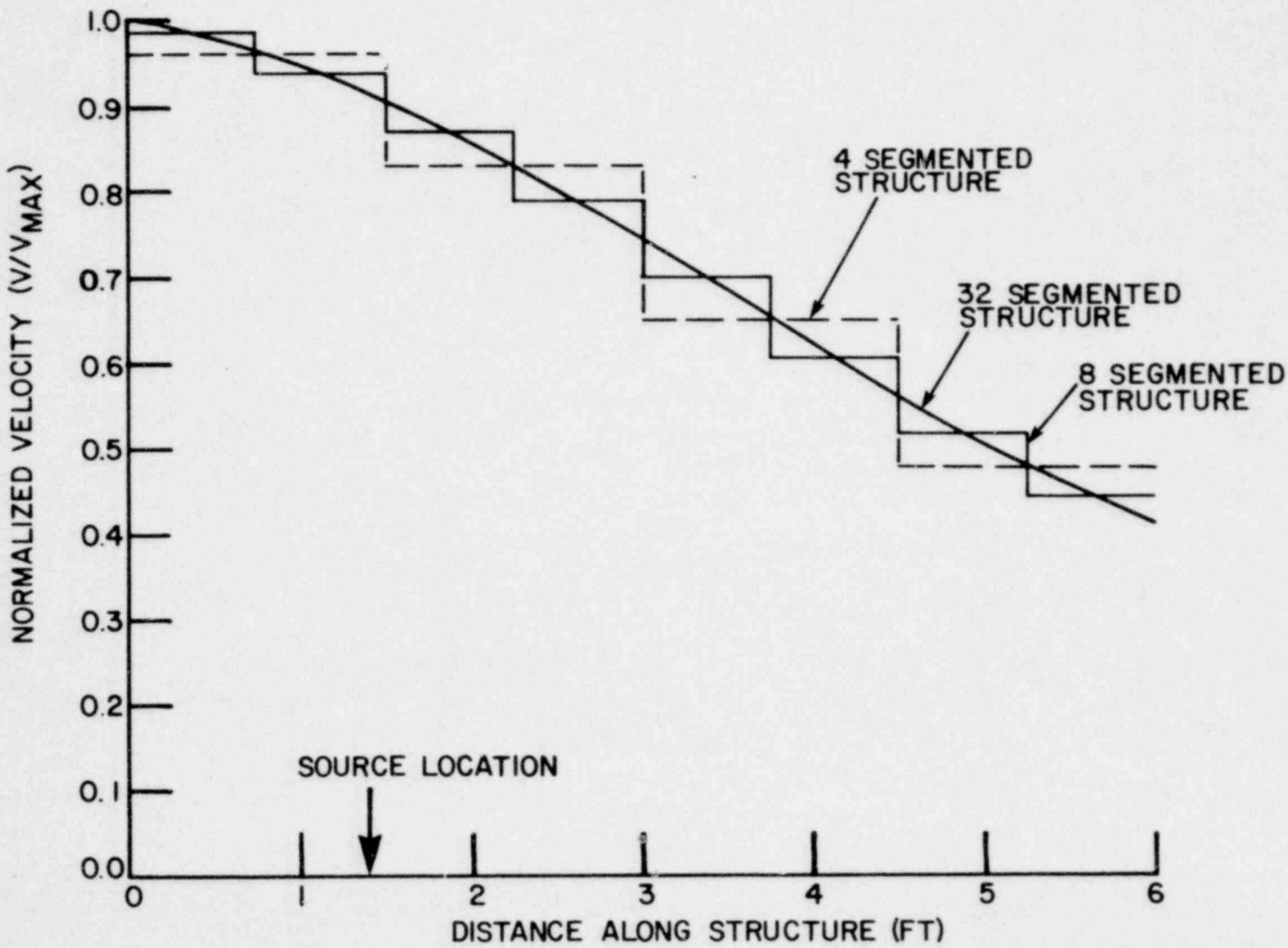
SIDE VIEW OF SECTION A-A



LA SALLE COUNTY STATION  
MARK II DESIGN ASSESSMENT REPORT

FIGURE C-11  
LOCATION OF VERTICAL SUBMERGED  
STRUCTURE IN THE SUPPRESSION POOL

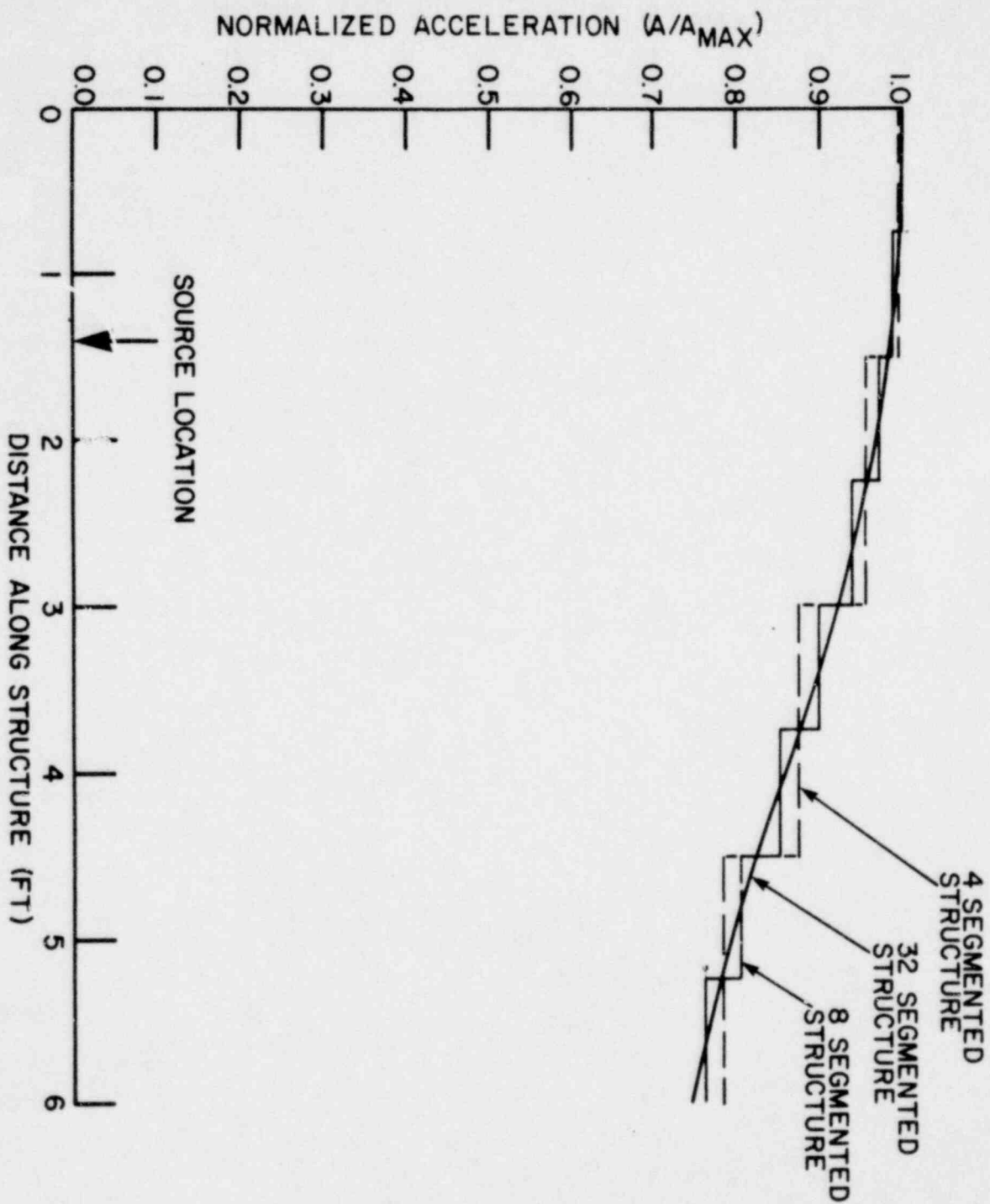
**LA SALLE COUNTY STATION**  
 MARK II DESIGN ASSESSMENT REPORT  
 FIGURE C-12  
 HORIZONTAL COMPONENT OF VELOCITY  
 ALONG A STRUCTURE SEGMENTED INTO  
 4, 8 AND 32 SECTIONS

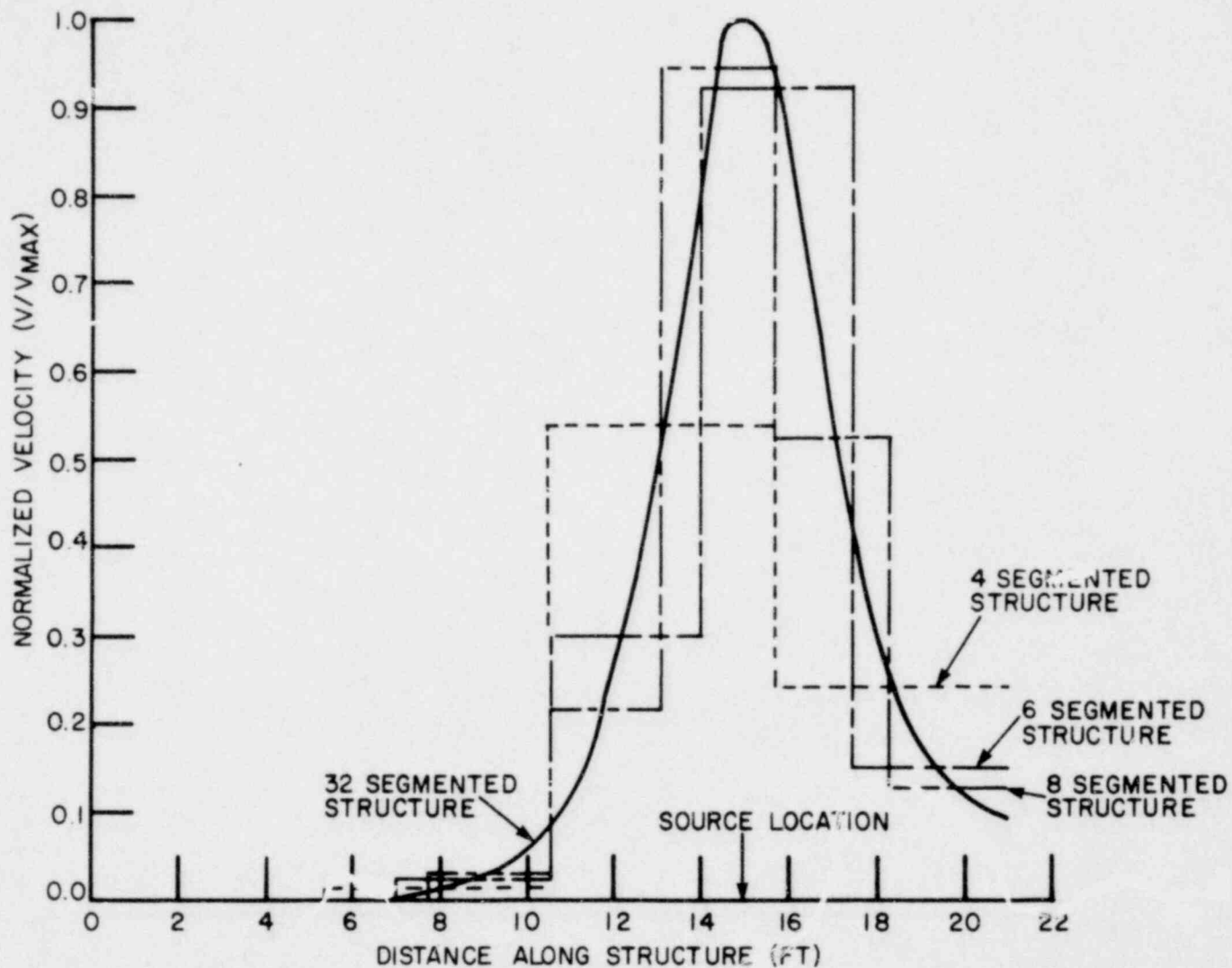


VERTICAL COMPONENT OF ACCELERATION  
ALONG A STRUCTURE SEGMENTED INTO  
4, 8 AND 32 SECTIONS

FIGURE C-13

LA SALLE COUNTY STATION  
MARK II DESIGN ASSESSMENT REPORT

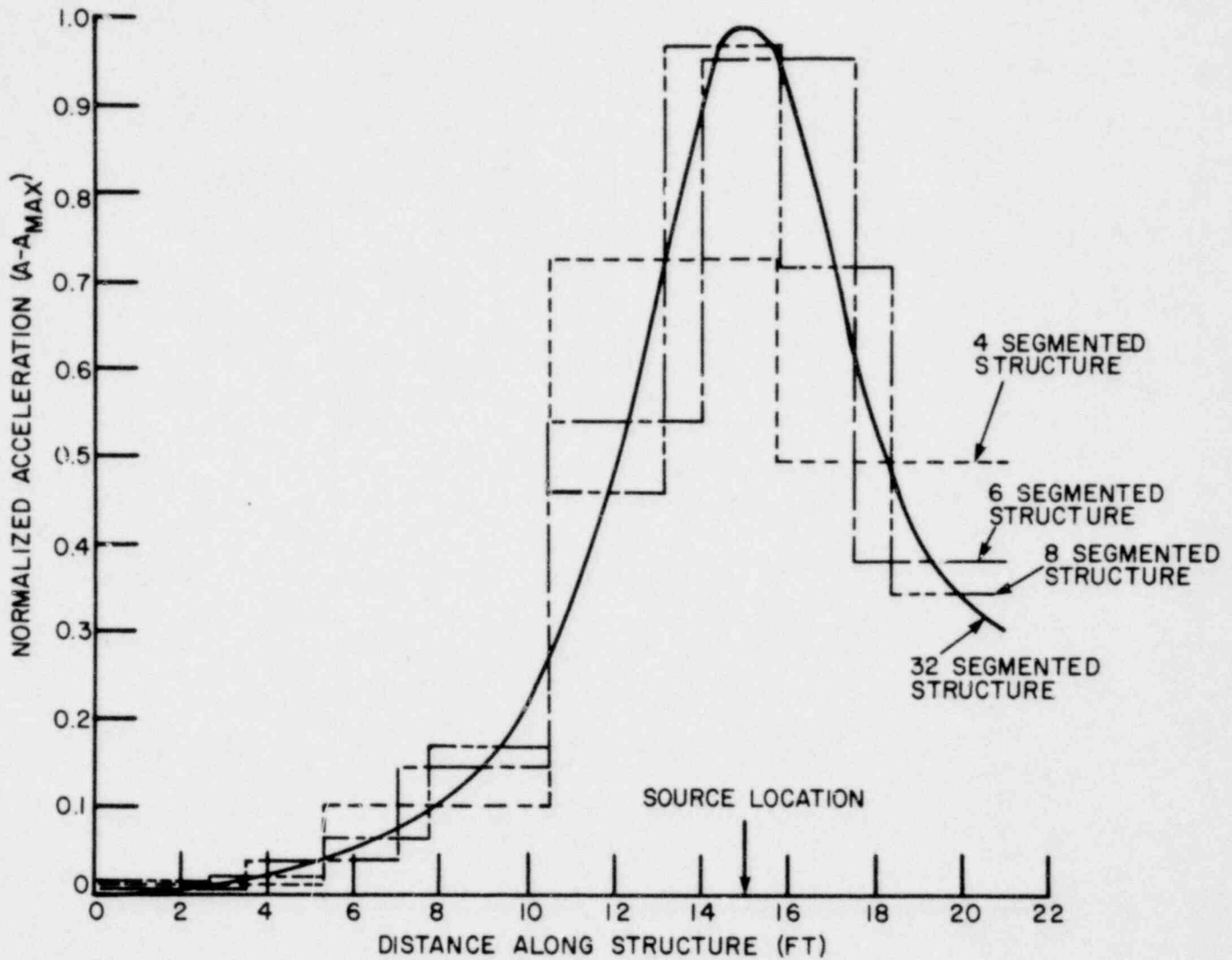




LA SALLE COUNTY STATION  
MARK II DESIGN ASSESSMENT REPORT

FIGURE C-14

RADIAL COMPONENT OF VELOCITY ALONG A  
STRUCTURE SEGMENTED INTO  
4, 6, 8 AND 32 SECTIONS



**LA SALLE COUNTY STATION**  
 MARK II DESIGN ASSESSMENT REPORT

---

FIGURE C-15

RADIAL COMPONENT OF ACCELERATION ALONG  
 A STRUCTURE SEGMENTED INTO  
 4, 6, 8 AND 32 SECTIONS

## APPENDIX D

NSSS OPERABILITY ASSURANCE

All active Class 1, 2, and 3 components are being evaluated for all transients associated with upset, emergency, and faulted plant conditions as identified in the DFFR Report (NEDO-21061).

All active components of the NSSS are being evaluated for the transients and load combinations identified in the DFFR (Section 6, Table 6-1) as well as the effects of annulus pressurization.

Qualification of Valves

The RCPS valves (Class 1, listed in FSAR Table 5.2-6) are qualified by functional tests, including the HPCS Injection valve and the SLC explosive valve. The other HPCS valves are also test qualified. The other Class 2, active valves and pumps, are qualified by analysis. The RCIC turbine and CRD hydraulic unit are not covered by the ASME code but are qualified for operability by a combination of test and analysis.

Qualification of Pumps

The essential NSSS pumps are qualified for operability by:

- a. Design analysis - an analysis is performed to determine:
  1. That the running clearances of selected parts within the pump internal do not effect operability of the pump during the abnormal conditions.

2. That the stresses caused by the combination of normal upset, emergency and faulted, operating loads will be limited to the material elastic limit as in FSAR Table 3.9-3. The average membrane stress ( $T_m$ ) for the faulted conditions loads is maintained at 1.25, or approximately 0.75  $T_y$  ( $T_y$ , yield stress) and the maximum stress in local fibers ( $T_m$  + bending stress ( $T_b$ )) will be limited to 1.85, or approximately 1.1 $T_y$ . The maximum seismic nozzle loads will also be considered in analysis of the pump supports and mounting bolting to assure that misalignment cannot occur.
- b. In-shop tests, including:
1. hydrostatic tests of pressure-retaining parts to 1.5 times the design pressure;
  2. seal leakage test; and
  3. performance tests while the pump is operated with flow to determine the total developed head at zero flow, minimum bypass flow, maximum allowable run out flow, and net positive suction head (NPSH) requirements. Also monitored during these operating tests are the vibration levels which will be shown to be below specified limit.
- d. After the pump is installed in the plant, it undergoes the cold hydro tests, functional tests, and the required periodic in-service inspection and operation. These tests demonstrate reliability of the pump for the design life of the plant.



APPENDIX ERPV INTERNALS LUMPED MASS MODEL ANALYSIS METHODS

The suppression pool dynamic loads, annulus pressurization, and seismic event impart primary loads on the containment structures and secondary accelerations on the reactor building equipment. The secondary accelerations on the equipment are based on structural system response data, developed using a composite soil-structure interaction model with a representation of the reactor pressure vessel. Resulting acceleration time histories are used for a local system analysis.

The local system analysis is based on a composite lumped mass model of the pedestal shield wall and a detailed representation of the reactor pressure vessel complex. The excitation inputs for this local system analysis are based on acceleration time histories for the suppression pool hydrodynamic forcing functions and seismic vibratory motions, and pressure time histories from annulus pressurization for postulated pipe breaks.

The local system analysis is conducted using the DYSEA (Dynamic and Seismic Analysis) computer program. This program is a General Electric proprietary program developed specifically for seismic and dynamic analysis of the reactor pressure vessel, internals and reactor building system. It calculates the dynamic response of linear structural systems by either temporal model superposition or response spectrum method. Fluid-structure interaction effect in the reactor pressure vessel is taken into account by way of hydrodynamic mass.

The DYSEA program was based on the SAP-IV program (see Appendix F) with added capability to handle the hydrodynamic mass effect. Structural stiffness and mass matrices are formulated

similar to SAP-IV. Solution is obtained in time domain by calculating the dynamic response mode by mode. Time integration is performed by using Newmark's method. Response spectrum solution is also available as an option.

#### Program Version and Computer

The DYSEA version now operating on the Honeywell 6000 computer of General Electric Nuclear Energy Systems Division, was developed by modifying the SAP-IV program. Capability was added to handle the hydrodynamic mass effect due to fluid-structure interaction in the reactor. It can handle 3-dimensional dynamic problems with beam, trusses and springs. Both acceleration time histories and response spectra may be used as input.

#### History of Use

The DYSEA Program was developed in the Summer of 1976. It has been adopted as a standard production program since 1977 and it has been used extensively in all dynamic and seismic analysis of the reactor pressure vessel supports and internal components.

#### Extent of Application

The current version of DYSEA has been used in all dynamic and seismic analysis since its development. Results from test problems were found to be in close agreement with those obtained from either verified programs or analytic solutions.

#### Test Problems

##### Problem 1:

The first test problem involves finding the eigenvalues and eigenvectors from the following characteristic equation:

$$(\omega^2 [M] - [K]) \{x\} = 0$$

where  $\omega$  is the circular frequency,  $x$  is the eigenvector, and  $[K]$  and  $[M]$  are the stiffness and the mass matrices given by:

$$[M] = \begin{bmatrix} 1 - \frac{4}{\pi^2} & \frac{4}{\pi^2} & -\frac{4}{q\pi^2} \\ & 1 - \frac{4}{q\pi^2} & \frac{4}{\pi^2} \\ \text{Symmetric} & & 1 - \frac{4}{25\pi^2} \end{bmatrix}$$

$$[K] = \begin{bmatrix} 1 + \frac{\pi^2}{4} & 3 & \frac{5}{q} \\ & 1 + \frac{q\pi^2}{4} & 15 \\ \text{Symmetric} & & 1 + \frac{25\pi^2}{4} \end{bmatrix}$$

The analytic solution and the solution from DYSEA are:

a) Eigenvalues  $\omega_i$ :

<u>i</u>	<u>DYSEA SOLUTION</u>	<u>ANALYTIC SOLUTION</u>
1	5.7835	5.7837
2	30.4889	30.4878
3	75.0493	75.0751

b) Eigenvectors  $\phi_i$ :

1. <u>DYSEA SOLUTION</u>	<u>ANALYTIC SOLUTION</u>
$\begin{bmatrix} 1.000 & 1.000 & 1.000 \\ -0.0319 & -1.5536 & -1.2105 \\ -0.0072 & -0.0666 & 2.0271 \end{bmatrix}$	$\begin{bmatrix} 1.000 & 1.000 & 1.000 \\ -0.0319 & -1.554 & -1.211 \\ -0.0072 & 0.0666 & 2.027 \end{bmatrix}$

Problem 2:

The second test problem compares the dynamic responses of the reactor pressure vessel, internals and reactor building subjected to earthquake ground motion.

The mathematical model of the reactor pressure vessel, internals and reactor building is given in Figure B-1. The input in the form of ground spectra are applied at the basemat level. Response spectrum analysis was used in the analysis.

Natural frequencies of the system and the maximum responses at key locations have been calculated by both DYSEA and SAMIS. Result comparisons are given in Tables E-1 and E-2. It can be seen that the results calculated by DYSEA agree closely with those obtained by SAMIS.

TABLE E-1

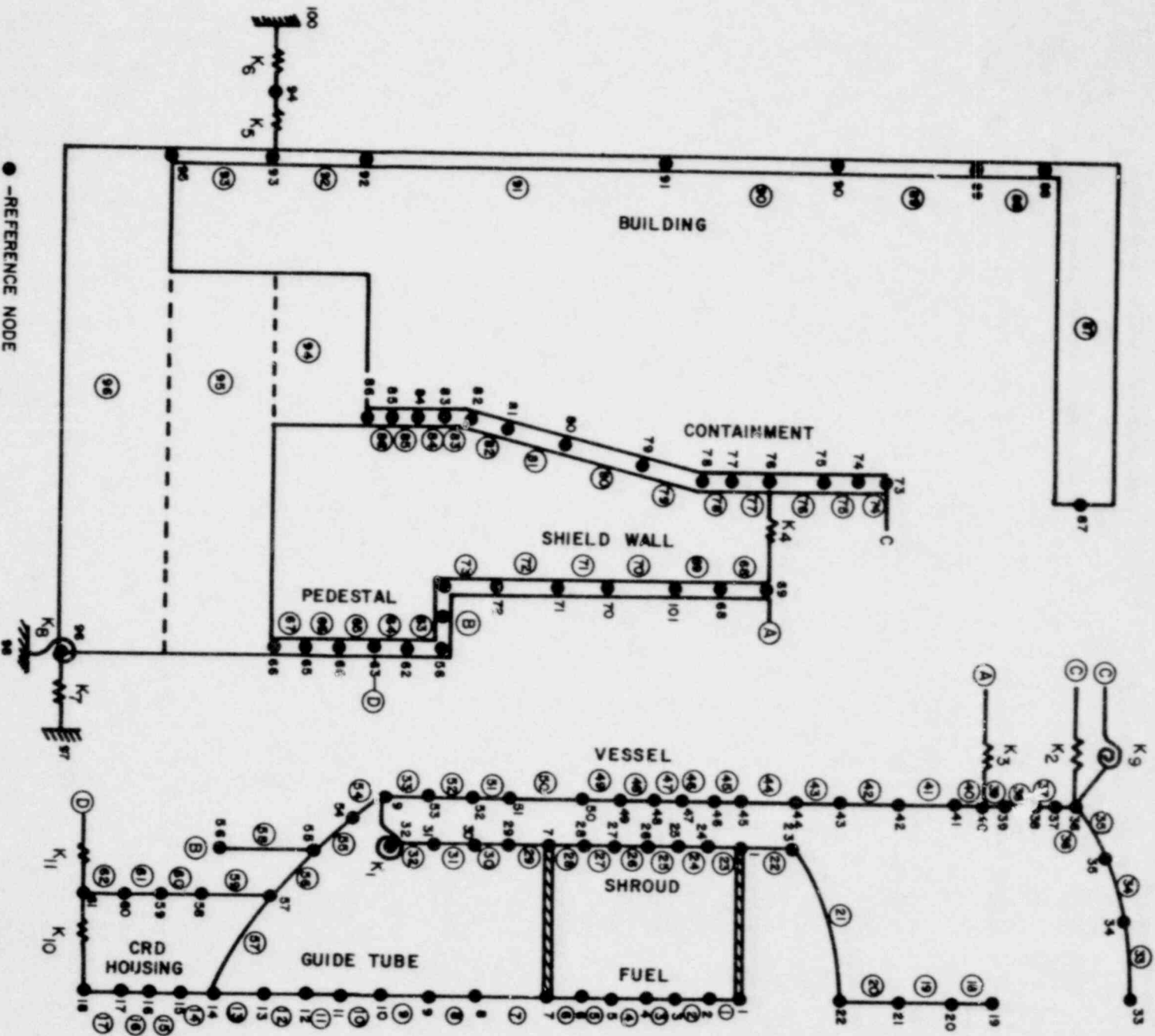
COMPARISON OF NATURAL FREQUENCIES OBTAINED BY DYSEA

<u>MODE</u>	<u>X-DIRECTION FREQUENCY</u>		<u>X-DIRECTION FREQUENCY</u>	
	<u>OLD ANALYSIS</u>	<u>DYSEA</u>	<u>OLD ANALYSIS</u>	<u>DYSEA</u>
1	2.810	2.727	2.678	2.649
2	3.000	2.999	2.810	2.728
3	3.764	3.763	3.762	3.758
4	3.791	3.781	3.771	3.769
5	4.588	4.576	4.578	4.531
6	5.041	5.044	5.040	5.039
7	5.776	5.791	5.486	5.431
8	6.071	6.047	6.069	6.025
9	8.731	8.625	8.598	8.524
10	10.950	11.270	9.614	9.824
11	12.796	12.800	12.563	12.760

TABLE E-2

COMPARISON OF MAXIMUM LOADS OBTAINED BY DYSEA

<u>STRUCTURAL COMPONENT</u>	<u>DYSEA SOLUTION</u>		<u>SAMIS SOLUTION</u>	
1. <u>RPV and Internals</u>				
Fuel Moment	17.11	(in-K)	18.64	(in-K)
Top Guide Shear	188	(K)	204	(K)
Shroud Head Shear	198	(K)	213	(K)
Shroud Head Moment	16,783	(in-K)	18,150	(in-K)
Shroud Support Shear	479.3	(K)	503.3	(K)
Shroud Support Moment	119,020	(in-K)	126,600	(in-K)
2. <u>Building</u>				
RPV Pedestal				
-Shear	602	(K)	575.9	(K)
-Moment	94,200	(in-K)	91,500	(in-K)
Containment				
-Shear	2,902	(K)	2,908	(K)
-Moment	1,413,000	(in-K)	1,434,000	(in-K)
Shield Building				
-Shear	34,037	(K)	38,060	(K)
-Moment	38,494,000	(in-K)	37,270,000	(in-K)



● -REFERENCE NODE  
○ -HINGE  
ZZZZ -RIGID MEMBER



LA SALLE COUNTY STATION  
MARK II DESIGN ASSESSMENT REPORT

FIGURE E-1

LUMPED MASS MODEL OF RPV, INTERNALS  
AND REACTOR BUILDING



APPENDIX FNSSS PIPING SYSTEMS ANALYSIS METHODS

General Electric analyzes the lumped mass models of the primary piping systems (main steam and recirculation), using a proprietary version of SAP-IV computer program. The procedures for preparing the structural system dynamic input responses are based on:

- a. For seismic vibratory motions and suppression pool structural system dynamic responses, an amplified response spectrum which envelopes the amplified response spectra for all attachment points within the piping system is constructed. Dynamic analyses are performed using the "envelope spectrum" as the uniform piping system excitation.
- b. For postulated pipe ruptures annulus pressurization dynamic responses on the unbroken piping system, the dynamic analysis of the piping system is performed using multiple acceleration time histories corresponding to amplified response spectra at each attachment point; i.e., distinct acceleration excitations are specified at each piping support and anchor points.

The input for multiple excitation time-history method is determined in one of two ways:

- a. Independent synthetic time histories conforming to the broadened response spectra are generated.
- b. The support point time histories are used directly. The time histories are time scaled to simulate response spectrum broadening.

If the results using the first method for seismic vibratory motions and suppression pool structural system responses cause unacceptable results for the piping or pipe mounted/connected equipment, then method 2 is used in a refined analysis to demonstrate NSSS piping and equipment adequacy.

#### SAP-IV Computer Program

This computer program was constructed from three earlier programs developed under the direction of Professor E. L. Wilson, Department of Civil Engineering, University of California at Berkeley. The element library and static analysis options were taken from the "SOLID/SAP" program, (Reference 1) the eigenvalue extraction algorithms were incorporated from coding that was originated by Dr. K. J. Bathe (Reference 2) and the forced vibration and response spectrum analyses were adapted from the original version of Professor Wilson's "SAP" program (Reference 3).

The method of analysis for this program version is presented in some detail in a recent report by Bathe (Reference 4).

Systems composed of large numbers of joints and members may be analyzed. The capacity of the program depends mainly on the total number of joints in the system. There is practically no restriction on the number of elements, number of static load cases, or the equation "bandwidth". Note that while the program has the capacity to analyze very large models, the system is relatively efficient in the solution of smaller problems.

#### Multiple Excitation Methods

The equations of motion used in the formulation of the multiple excitation methods conform to the fundamental laws of mechanics.

The theory is based on the same assumptions used for the uniform excitation methods, that is: small system damping, damping matrix orthogonal and applicable for linear systems. A general acceptance by the technical community has been made for the multiple excitation method. The procedure has briefly been described in textbooks and procedural details were presented in a General Electric publication at the Fourth SMIRT conference, August 1977. The use of the multiple excitation method was accepted by the NRC Staff on the GESSAR docket. Acceptance was also indicated on the memo L. C. Shao to R. R. MacCary, dated January 14, 1975, as shown in the following memo excerpt "General Electric proposed three methods for generating design time histories applicable as inputs to seismic analysis of multiple supported systems and components. They are (A) the time history of an envelope of the floor response spectra (for all cases analyzed) of all attachments points in a given input direction, (B) the time history of an envelope of the floor response spectra (for all cases analyzed) for each attachment point and (C) the worst time histories selected from all the cases analyzed on the basis of matching the first and second mode component frequencies with the peak spectral frequency of a given case study. After a lengthy discussion, the AEC Staff stated that the use of methods (A) and (B) above are acceptable, however, acceptance of method (C) requires further presentation of justification data from General Electric"

References

1. E. L. Wilson, "SOLID/SAP--A Static Analysis Program for Three Dimensional Solid Structures," Structures and Materials Research, Dept. of Civil Engrg. University of CA at Berkeley, Report SESMUC/7119, September 1971 (revised March 1972).
2. K. J. Bathe, "Solution Methods for Large Generalized Eigenvalue Problems in Structural Engineering," Structures and Materials Research, Dept. of Civil Engrg., University of Ca at Berkeley, Report UCSESM/7120, November 1971.
3. E. L. Wilson, "SAPA General Structural Analysis Program, : Structural Engrg. Lab, Report UCSESM/7020, University of CA at Berkeley, September 1970.
4. K. J. Bathe, E. L. Wilson, and F. E. Peterson, "SAP IV--A Structural Analysis Program for Static and Dynamic Response of Linear Systems" Earthquake Engrg. Research Center, University of CA at Berkeley, Report EERC 7311, June 1973.



APPENDIX GCALCULATION OF PRESSURE TIME HISTORIES IN THE ANNULUS

The pressure responses of the RPV-shield wall annulus to a postulated pipe rupture at the RPV nozzle safe-end to pipe weld for a recirculation suction line and a feedwater line were investigated using the RELAP4 computer code. A symmetric model consisting of 38 nodes and 86 flow paths was used in the analysis of the recirculation line break while a similar model using 33 nodes and 70 flow paths was developed for the analysis of the feedwater line break. Further description of these analytical models and detailed discussion of the analyses may be found in Subsection 6.2.1 of the La Salle County Final Safety Analysis Report.

The pressure histories generated by the RELAP4 code were in turn used to calculate the loads on the sacrificial shield wall and the reactor pressure vessel for each of the line breaks considered. The annulus was divided into several zones and a sixteenth order Fourier fit to the output pressure histories made for each zone to produce the Fourier coefficients required for the structural analysis of the shield wall. The specific loading data requested by GE for the NSSS adequacy evaluation for both postulated line breaks consisted of the time-pressure (psia) and time-force (lbf) histories for each node within the annulus. These time-force histories represent the resultant loads on the RPV for each node through its geometric center and were generated by taking the product of the node pressure and its 'effective' surface area,  $\eta_b$ , or more formally as:

$$\begin{aligned}
 F_{V_i} &= \int_{-\Delta\theta/2}^{+\Delta\theta/2} P_i \ell_i R_V \cos \theta d\theta - \sum_j P_j \frac{\pi D_j^2}{4} \\
 &= P_i 2 \ell_i R_V \sin (\Delta\theta/2) - P_i \sum_j \frac{\pi D_j^2}{4} \\
 &= P_i \eta_V
 \end{aligned}$$

where:

$F_{V_i}$  = Nodal Resultant Force on RPV (lbf)

$P_i$  = Node Absolute Pressure (psia)

$\ell_i$  = Node Height (inches)

$R_V$  = RPV Radius (inches)

$\Delta\theta$  = Azimuthal Width of Node (degrees)

$D_j$  = Pipe OD (inches)